



Milligan, Kathleen (1996) Cell cycle, growth and differentiation in *Trypanosoma brucei* and *Leishmania* species. PhD thesis

<http://theses.gla.ac.uk/7226/>

Copyright and moral rights for this thesis are retained by the author

A copy can be downloaded for personal non-commercial research or study, without prior permission or charge

This thesis cannot be reproduced or quoted extensively from without first obtaining permission in writing from the Author

The content must not be changed in any way or sold commercially in any format or medium without the formal permission of the Author

When referring to this work, full bibliographic details including the author, title, awarding institution and date of the thesis must be given

**Cell Cycle, Growth and Differentiation in
Trypanosoma brucei and *Leishmania* species**

Kathleen Milligan

**Parasitology Laboratory
Division of Infection and Immunity
University of Glasgow**

**This thesis is presented in submission for the
degree of Doctor of Philosophy in the Faculty of Science**

February, 1996

SUMMARY

Kinetoplastid protozoans have unusual cell cycles. Three unitary organelles need to be replicated and segregated to the daughter cells at each cell division; the nucleus, kinetoplast and basal body, associated with the flagellum. The replication and segregation of these organelles requires to be co-ordinated. In this study the timing of nuclear and kinetoplast cell cycle events was examined in two species of kinetoplastids, *Trypanosoma brucei* and *Leishmania mexicana*, which are major pathogens of humans, to ascertain the degree of co-ordination between the two organelles in the cell cycle. Particular attention was paid to three main features; the duration of S-phase for each organelle, the relative timing of mitosis and kinetoplast division and the lengths of the post-mitotic/division cytokinesis periods. Two life cycle stages were examined for each species i.e. procyclic and bloodstream forms of *T. brucei* and promastigote and amastigote forms of *L. mexicana*. The objectives of this study were to establish firstly whether a similar pattern of events occurs for both stages within each species examined and secondly, whether or not *T. brucei* and *L. mexicana* share common features to their cell cycles.

Studies of cell cycle events were conducted using immunofluorescent labelling to detect S-phase in both organelles, enabled by use of an anti-bromo-deoxyuridine (BrdU) antibody as an S-phase marker. Division of organelles was identified by staining the cells with DAPI, a DNA intercalating dye. Initial studies confirmed that the cell cycles of both species were consistent with the general pattern of events of the eukaryotic nuclear cycle. Also, as has been described previously in kinetoplastids, the kinetoplast DNA (containing mitochondrial DNA) has a pattern of discretely separated phases of replication and division analagous to the nuclear cycle. Analysis was made of the relative timing of S-phase, mitosis/division and cytokinesis for each life cycle stage, producing data which were statistically testable. For both life cycle stages of *T. brucei* a similar pattern of events was observed. Three populations of

BrdU labelled cells were identified; cells which were BrdU labelled in the nucleus only, labelled in the kinetoplast only and labelled for both organelles. These observations indicate that there was a non-co-ordinate start and finish to S-phase, with an overlap in the timing of the S-phase periods. Kinetoplast division was initiated and completed before the start of mitosis in the nucleus and an extended cytokinesis period for each organelle was identified, although of longer duration in the kinetoplast.

For both life cycle stages of *L. mexicana*, three populations of cells labelled with BrdU were observed as in *T. brucei*, again indicating that there was a non-co-ordinate start and finish to S-phase, with an overlap in the timing of both periods. The sequence of division for the organelles for both life cycle stages differed to that observed in *T. brucei*. The nucleus divided before the kinetoplast and there was a much shorter cytokinesis period for both organelles in comparison to *T. brucei*. These differences in the pattern of events may reflect either a difference in the control of cell cycle timing in each species or in the morphology of each cell type. Trypanosomes have to re-arrange their organelles, such that they occupy sites on either side of the division furrow, hence the extended cytokinesis phase. In *L. mexicana*, however, this requirement for organelle re-positioning is reduced or absent and therefore the cytokinesis periods are much shorter.

Antigenic variation is the key strategy which allows African trypanosomes to evade the effects of the host's immune response. The switching from expression of one variant surface glycoprotein (VSG) to that of another has been indirectly linked to the cell cycle, as bloodstream slender forms divide and undergo antigenic switching, whereas bloodstream stumpy forms are non-dividing and do not appear to switch. An attempt to examine directly the proposed link between antigenic switching and the cell cycle was made using cell cycle markers (anti-BrdU antibody as an S-phase marker and DAPI staining to determine the configurations of the organelles), as well as VAT-

specific antibodies against VSGs expressed in the cloned lines studied. Unfortunately, trypanosomes expressing two VSG coats simultaneously and therefore undergoing antigenic switch, could not be detected in any of the cloned lines examined. This unresolved difficulty was attributed to a deficiency in the detection system employed.

Differentiation in kinetoplastids is thought to be linked to the cell cycle, as progression through the life cycle involves transitions from proliferative to non-proliferative forms. The differentiation of *Leishmania major* promastigote forms, from dividing non-infective stages to non-dividing infective metacyclic forms, involves major molecular and morphological changes. Using three metacyclic-specific markers (non-agglutination by peanut agglutinin, a monoclonal antibody (3F12) against metacyclic-specific epitopes of the major surface molecule lipophosphoglycan (LPG) and a rabbit anti-serum (ab336) against a metacyclic-specific surface protein, the Gene B protein) metacyclic production in *in vitro* culture was examined. Observation of population growth curves suggests that differentiation is in part intrinsically programmed within the parasite but may also be inducible by environmental changes. Comparison of these data with mathematical models indicated that the promastigote population was likely to be heterogeneous, containing sub-populations that replicate and differentiate at different rates. Two major assumptions of the heterogeneous model are that metacyclic forms are both non-dividing and incapable of de-differentiation. These two possibilities were tested experimentally and indicated that metacyclic forms are indeed non-dividing, but are also capable of de-differentiation, albeit at a very low rate. Examination of metacyclic production at the cellular level also indicated that the event which causes commitment to differentiation occurs at least one cell division before symmetrical production of two daughter metacyclic forms.

It has been found that in the presence of a chronic infection the growth of a secondary infection is significantly inhibited (Turner *et al.*, 1996). The available data suggests

that there appears to be an overall down-regulation in the growth of the entire mixed population. The aim of this component of the project was to select for 'growth' mutant trypanosomes i.e. mutants which overcome growth inhibition. Bloodstream trypanosomes which had been mutagenised *in vitro* with ethyl methanesulphonate (EMS) were inoculated into mice in the presence of a pre-existing chronic infection. Populations of mutagenised trypanosomes which grew significantly in comparison to controls where only low rates of growth occurred, were selected by optical cloning. This rationale led to the generation of growth mutant clones which stably expressed the altered growth phenotype. These studies may permit the development of methods for the investigation of the regulation of growth and virulence in these parasites.

In conclusion, the analysis of the relative timing of cell cycle events in *T. brucei* and *L. mexicana* has highlighted both common and novel features to the cell cycles of these kinetoplastids. The study of metacyclic production in *L. major* has also revealed the intrinsic and extrinsic nature of regulation of differentiation in these parasites, as well as the commitment to differentiate at the cellular level. Furthermore, the generation of 'growth' mutant trypanosomes provides an additional tool for the future study of growth regulation in trypanosome infections.

LIST OF CONTENTS

	Page Number
TITLE PAGE	i
SUMMARY	ii
LIST OF CONTENTS	vi
LIST OF FIGURES	xi
LIST OF TABLES	xiv
LIST OF ABBREVIATIONS	xvi
DECLARATION	xix
ACKNOWLEDGEMENTS	xx
 CHAPTER 1	
GENERAL INTRODUCTION	1
1.1 LIFE CYCLE BIOLOGY	1
1.1.1 Taxonomy	1
<i>Trypanosoma brucei</i>	1
<i>Leishmania (L. mexicana, L. major)</i>	2
1.1.2 Development in the Vertebrate Host	3
<i>T. brucei</i>	3
Antigenic Variation	4
<i>Leishmania</i>	5
1.1.3 Development in the Invertebrate Host	6
<i>T. brucei</i>	6
<i>Leishmania</i>	7
1.2 THE CELL CYCLE	8
1.2.1 The Eukaryotic Cell Cycle	8
1.2.2 Timing of Cell Cycle Events	10
1.2.3 Cell Cycle of Kinetoplastids	11
1.2.4 Cell Cycle of <i>T. brucei</i>	13
1.3 CELL DIFFERENTIATION	15
1.3.1 Mechanisms of Differentiation	15
1.3.2 Differentiation of Trypanosomes and <i>Leishmania</i>	17
Trypanosome Differentiation	17
<i>Leishmania</i> Differentiation	21

1.4 GROWTH REGULATION OF KINETOPLASTID PROTOZOA	30
1.5 AIMS OF THE PROJECT	37
 CHAPTER 2	
DESCRIPTIONS OF THE CELL CYCLES OF <i>T. BRUCEI</i> AND <i>L. MEXICANA</i>	42
2.1 INTRODUCTION	42
2.2 MATERIALS AND METHODS	44
2.2.1 Culturing of <i>T. brucei</i> and <i>L. mexicana</i>	44
<i>T. brucei</i> Bloodstream Forms	44
<i>T. brucei</i> Procyclic Forms	45
<i>L. mexicana</i> Promastigote Forms	45
2.2.2 BrdU Labelling	46
2.2.3 Immunofluorescent Detection Using an Anti-BrdU Antibody	46
2.2.4 Growth Rate of Cultures	47
2.2.5 Cell Cycle Analysis	47
Periods of Division and Cytokinesis	47
G2-Phase	47
S-Phase	48
G1-Phase	48
2.2.6 Morphological Analyses	48
2.2.6.1 Effects of Air-Drying, Fixation and Storage of Smears on Organelle Morphology	48
2.2.6.2 Kinetoplast Lengths in <i>L. mexicana</i> Promastigote Forms	49
2.3 RESULTS	49
2.3.1 <i>T. brucei</i> Bloodstream Forms	49
2.3.1.1 Growth Rate of <i>T. brucei</i> Bloodstream Forms	49
2.3.1.2 BrdU Labelling	50
2.3.1.3 Cell Cycle Analysis	50
Periods of Division and Cytokinesis	50
G2-Phase	50
S-Phase	51
G1-Phase	51
2.3.1.4 Cell Cycle Maps	51
2.3.2 Morphological Analyses	52

2.4 DISCUSSION	56
 CHAPTER 3	
ANALYSIS OF THE RELATIVE TIMING OF CELL CYCLE EVENTS IN <i>T. BRUCEI</i> AND <i>L. MEXICANA</i>	70
3.1 INTRODUCTION	70
3.2 MATERIALS AND METHODS	72
3.2.1 Culturing of <i>T. brucei</i> and <i>L. mexicana</i>	72
<i>T. brucei</i> Procyclic and Bloodstream Forms and	
<i>L. mexicana</i> Promastigote Forms	72
<i>L. mexicana</i> Amastigote Forms	72
3.2.2 BrdU Incorporation and Immunofluorescent Detection of BrdU	73
3.2.3 Growth Rate of Cultures	73
3.2.4 Cell Cycle Analysis	73
3.2.4.1 S-Phase	73
3.2.4.2 Mitosis, Kinetoplast Division and Cytokinesis	74
3.3 RESULTS	76
3.3.1 Growth of <i>T. brucei</i> and <i>L. mexicana</i> Promastigotes	76
Growth of <i>L. mexicana</i> Amastigote Forms	76
3.3.2 Cell Cycle Analyses	77
3.3.2.1 Analysis of S-Phase	77
3.3.2.2 The Relative Timing of Mitosis and Kinetoplast Division	77
3.3.2.3 Mapping of Mitosis, Kinetoplast Division in the Cell Cycle	78
3.4 DISCUSSION	79
 CHAPTER 4	
IS ANTIGENIC SWITCHING LINKED TO THE CELL CYCLE?	100
4.1 INTRODUCTION	100
4.2 MATERIALS AND METHODS	102
4.2.1 Cloned Trypanosomes and VAT Analysis	102
4.2.2 Growth of Bloodstream Form Trypanosomes	103
4.2.3 Growth Rate of Cultures	103
4.2.4 BrdU Labelling	103
4.2.5 Immunofluorescent Detection of BrdU Incorporation	
and VAT Expression	104
BrdU Detection	104
VAT Detection	104

4.3 RESULTS	105
4.3.1 Growth of Bloodstream Cultures	105
4.3.2 VAT Labelling	105
4.4 DISCUSSION	106

CHAPTER 5

DIFFERENTIATION OF *L. MAJOR* PROMASTIGOTE TO METACYCLIC FORMS

5.1 INTRODUCTION	112
5.2 MATERIALS AND METHODS	114
5.2.1 Cultivation of <i>L. major</i> Promastigotes	114
5.2.2 Growth of <i>L. major</i> Promastigotes	114
5.2.3 Immunofluorescent Detection of Metacyclic Forms	115
5.2.4 Models for Replication, Growth and Differentiation	115
5.2.5 Agglutination of Promastigote Forms	117
5.2.6 BrdU Labelling	117
5.2.7 Immunofluorescent Detection of BrdU Incorporation	118
5.2.8 De-differentiation Studies	118
5.3 RESULTS	119
5.3.1 Metacyclic Production <i>In Vitro</i>	119
5.3.2 Are Metacyclics Non-Dividing Forms?	121
5.3.3 Do Metacyclics De-Differentiate to Promastigote Forms?	122
5.3.4 Models of Metacyclic Production	125
5.4 DISCUSSION	126

CHAPTER 6

GENERATION OF MUTANT TRYPANOSOME LINES WITH ALTERED GROWTH PHENOTYPE

6.1 INTRODUCTION	150
6.2 MATERIALS AND METHODS	151
6.2.1 Mutagenesis of Procyclic Forms <i>In Vitro</i>	151
6.2.2 Mutagenesis of Bloodstream Forms <i>In Vitro</i>	152
6.2.3 Challenge Infections with Mutagenised GUTat 7.2 Bloodstream Forms	152
6.2.4 Detection of GUTat 7.2 in A Mixed Infection	153
6.2.5 Calculating the Mutation Rate	153
6.2.6 Optical Cloning of Bloodstream Trypanosomes	154
6.2.7 Cryopreservation of Cloned and Unclassed Material	154

6.3	RESULTS	154
6.3.1	Growth of Mutagenised Procyclic Forms <i>In Vitro</i>	154
6.3.2	Growth of Mutagenised Bloodstream Forms <i>In Vivo</i>	155
6.3.3	Growth of Mutagenised GUTat 7.2 Bloodstream Forms In The Presence of A Chronic Infection	156
6.3.4	Stability of Growth Mutant Clones	157
6.4	DISCUSSION	160
 CHAPTER 7		
	GENERAL DISCUSSION	180
	 REFERENCES	 187

LIST OF FIGURES

	Page Number
1.1 Life Cycle of <i>T. brucei</i>	38
1.2 Life Cycle of <i>Leishmania</i>	39
1.3 Cell Cycle Control in Mammalian Cells	40
1.4 The Cell Cycle of <i>T. brucei</i> Procyclic Forms	41
2.1A Growth of GUTat 7.1 Bloodstream Forms	61
2.1B Growth of GUTat 7.1 Bloodstream Forms Incubated With BrdU	61
2.2 Cell Cycle Progression in <i>T. brucei</i> Bloodstream Forms	62
2.3A Kinetics of Appearance of BrdU Labelling in Dividing Nuclei	63
2.3B Kinetics of Appearance of BrdU Labelling in Dividing Kinetoplasts	63
2.4A Cell Cycle Map of <i>T. brucei</i> Bloodstream Forms	64
2.4B Cell Cycle Map of <i>T. brucei</i> Procyclic Forms	64
2.4C Cell Cycle Map of <i>L. mexicana</i> Promastigote Forms	64
2.5A Kinetoplasts of <i>T. brucei</i> Bloodstream Forms	65
2.5B Kinetoplasts of <i>T. brucei</i> Procyclic Forms	66
2.5C Kinetoplasts of <i>L. mexicana</i> Promastigote Forms	66
2.6 Frequency Histogram of Kinetoplast Lengths in Promastigote Forms	67
3.1 Models for the Relative Lengths and Timing of Nuclear and Kinetoplast S-Phase	85
3.2A Growth of <i>T. brucei</i> Procyclic Forms	86
3.2B Growth of <i>T. brucei</i> Procyclic Forms Incubated With BrdU	86
3.3A Growth of <i>T. brucei</i> Bloodstream Forms	87
3.3B Growth of <i>T. brucei</i> Bloodstream Forms Incubated With BrdU	87
3.4A Growth of <i>L. mexicana</i> Promastigote Forms	88
3.4B Growth of <i>L. mexicana</i> Promastigote Forms Incubated With BrdU	88
3.5A Growth of <i>L. mexicana</i> Amastigote Forms	89
3.5B Growth of <i>L. mexicana</i> Amastigote Forms Incubated With BrdU	89
3.6A <i>T. brucei</i> Procyclic Forms (Phase Contrast and DAPI Images)	90
3.6B <i>L. mexicana</i> Promastigote Forms (Phase Contrast and DAPI Images)	91
3.6C <i>L. mexicana</i> Amastigote Forms (Phase Contrast and DAPI Images)	91
3.7A The Relative Timing of the Periods of Division and Cytokinesis in <i>T. brucei</i> Procyclic Forms	92

3.7B The Relative Timing of the Periods of Division and Cytokinesis in <i>T. brucei</i> Bloodstream Forms	92
3.7C The Relative Timing of the Periods of Division and Cytokinesis in <i>L. mexicana</i> Promastigote Forms	93
3.7D The Relative Timing of the Periods of Division and Cytokinesis in <i>L. mexicana</i> Amastigote Forms	93
 4.1 Labelling of <i>T. brucei</i> Bloodstream Forms With VAT-Specific Antibodies	 108
 5.1 Model of <i>Leishmania</i> Replication, Growth and Differentiation	 133
5.2A Illustrative Solution to a Model of Replication and Differentiation in a Homogeneous Population	134
5.2 Illustrative Solutions to a Model of Replication and Differentiation B&C in a Heterogeneous Population	135
5.3A Growth of Friedlin VI Promastigote Forms and Production of Metacyclic Forms	136
5.3B Growth of RKK2 Promastigote Forms and Production of Metacyclic Forms	136
5.4A Exponential Phase of Growth of Friedlin VI Promastigote and Metacyclic Forms	137
5.4B Exponential Phase of Growth of RKK2 Promastigote and Metacyclic Forms	138
5.4C Exponential Phase of Growth of Friedlin VI Promastigote and Metacyclic Forms	139
5.5A Growth of PNA- and PNA+ Populations of Friedlin VI Culture Forms	140
5.5B Growth of PNA- and PNA+ Populations of RKK2 Culture Forms	140
5.6A Growth of Day 2 and Day 6 Culture Forms	141
5.6B Growth of PNA+ and PNA- Populations	141
5.7A Exponential Phase of Growth of Promastigotes of Day 2 and Day 6 Culture Forms	142
5.7B Exponential Phase of Growth of Promastigotes of PNA+ and PNA- Populations	142
5.8 Models of Metacyclic Production	143
5.9A Labelling of <i>L. major</i> Promastigote Forms with the ab336 Antibody	144

5.9B	Labelling of <i>L. major</i> Promastigote Forms with the 3F12 Antibody	145
5.9C	Double Labelling with the ab336 and 3F12 antibody	145
6.1	Growth of EMS Treated GUTat 7.2 Monomorphic Bloodstream Forms in Mice	165
6.2	Growth of EMS Treated GUTat 7.2 Pleomorphic Bloodstream Forms in Mice	165
6.3	Immunofluorescent Labelling of GUTat 7.2 Bloodstream Forms in a Mixed Infection	166
6.4	Percentage Prevalence of Mutagenised GUTat 7.2 in the Presence of a Pre-Existing Chronic Infection	167
6.5	Percentage Prevalence of Non-mutagenised GUTat 7.2 in the Presence of a Pre-Existing Chronic Infection	167
6.6A	Growth of GM1cl1 in the Presence of a Pre-Existing Chronic Infection	168
6.6B	Growth of GM2cl1 in the Presence of a Pre-Existing Chronic Infection	168
6.6C	Growth of GM1 Uncloned Population in the Presence of a Pre-Existing Chronic Infection	169
6.7	Percentage Prevalence of Re-Mutagenised GM1cl1 in the Presence of a Pre-Existing Chronic Infection	170
6.8A	Percentage Prevalence of R-mGM3 clones 1 and 2 in the Presence of a Pre-Existing Chronic Infection	171
6.8B	Percentage Prevalence of R-mGM13 clones 1 and 2 in the Presence of a Pre-Existing Chronic Infection	171
6.9A	Percentage Prevalence of R-mGM3 clones 1 and 2 Compared to Monomorphic GUTat 7.2	172
6.9B	Percentage Prevalence of R-mGM13 clones 1 and 2 Compared to Monomorphic GUTat 7.2	172
6.10	History of the Cloned Stock EATRO 2340 and Derivation of a Cloned Monomorphic Line GUTat 7.2	173
6.11	Derivation of a Cloned Pleomorphic Line GUTat 7.2	175
6.12	Generation of Growth Mutant Trypanosomes	176

LIST OF TABLES

	Page Number
2.1 Percentage Organelle Configurations in <i>T. brucei</i> Bloodstream Forms	68
2.2 Cell Cycle Timing in <i>T. brucei</i> Bloodstream Forms	68
2.3A Percentage Organelle Configurations of Bloodstream Forms Fixed/Treated Differently	69
2.3B Percentage Organelle Configurations of Bloodstream Forms Fixed/Treated Differently	69
3.1 Growth Statistics of Culture Forms	94
3.2A BrdU Labelling Counts	95
3.2B Statistical Analysis of the Relative Lengths of S-phase	95
3.3A Statistical Analysis of the Relative Timing of the Initiation of Mitosis and Kinetoplast Division	96
3.3B Statistical Analysis of the Relative Timing of the End of Mitosis and Kinetoplast Division	96
3.4 Percentage Organelle Configurations for the Nucleus and Kinetoplast	97
3.5A Duration of Nuclear Cell Cycle Events	98
3.5B Duration of Kinetoplast Cell Cycle Events	98
3.6 Lengths of Cytokinesis in the Nucleus and Kinetoplast	99
4.1 VAT Analysis of Cloned Trypanosome Lines	109
4.2 VAT Prevalence of Cloned Trypanosome Lines	110
4.3 Summary of Labelling Experiments	111
5.1A Percentage Prevalence of 3F12 and ab336 Labelling of Friedlin VI Promastigotes	146
5.1B Percentage Prevalence of Single and Double Labelling of Friedlin VI Promastigotes	146
5.2A Percentage BrdU Labelling of PNA+, PNA- and Stock Friedlin VI Culture Forms	147
5.2B Percentage BrdU Labelling of PNA+, PNA- and Stock RKK2 Culture Forms	147
5.3 Percentage Metacyclic Forms in PNA- Populations	147

5.4	Comparison of Calculated and Observed Numbers of Promastigotes at the Initiation of Culture	148
5.5A	Linear Regression Analysis of Growth Data of Day 2 and Day 6 Promastigote Forms	148
5.5B	Linear Regression Analysis of Growth Data of PNA+ and PNA- Promastigote Forms	148
5.6A	Prevalence of Promastigotes at t=0 in the Growth of Day 2 and Day 6 Culture Forms	149
5.6B	Prevalence of Promastigotes at t=0 in the Growth of PNA- and PNA+ Populations	149
6.1	Effect of Increasing Concentrations of EMS Upon the Growth of GUTat 7.2 Procyclic Forms <i>In Vitro</i>	177
6.2	Mutation Rates	178
6.3	Percentage Prevalence of Re-Mutagenised GM2cl1 in the Presence of a Pre-Existing Chronic Infection	179

LIST OF ABBREVIATIONS

A	Kinetoplast cytokinesis period
ADPRT	ADP-ribosyltransferase
ATP	Adenosine triphosphate
Balb/c	Inbred strain of mice
BrdU	Bromo-deoxyuridine
BSCM	Bloodstream culture medium
C	Nuclear cytokinesis period
cAMP	Cyclic adenosine monophosphate
Ca²⁺	Calcium ion
CBSS	Carter's balanced salt solution
<i>cdc</i>	Cell division cycle gene
CDK	Cyclin-dependent kinase
CFLP	Outbred strain of mice
CO₂	Carbon dioxide
D	Kinetoplast division
DABCO	1,4-Diazobicyclo-[2.2.2] octane
DAG	Diacylglycerol
DAPI	4,6,-Diamino-2-phenylindole
DMSO	Dimethyl sulphoxide
DNA	Deoxyribonucleic acid
EATRO	East African Trypanosomiasis Research Organisation
EGF	Epidermal growth factor
EMS	Ethyl methanesulphonate
<i>ESAG</i>	Expression-site-associated gene
FCS	Foetal calf serum
FITC	Fluorescein isothiocyanate
g	Acceleration due to gravity
G₀	Resting or quiescent phase
G1	Gap period before DNA synthesis
G2	Post-synthetic gap period
GIPL	Glycosylinositolphospholipids
GM1	Growth mutant population 1 (uncloned)
GM1cl1/2	Growth mutant population 1 clone 1/2
GM2	Growth mutant population 2 (uncloned)
GM2cl1/2	Growth mutant population 2 clone 1/2
GMC	Ganglion mother cell

GM-CFC	Granulocyte macrophage-colony-forming cells
GM-CSF	Granulocyte macrophage-colony stimulating factor
GPI	Glycosyl-phosphatidylinositol
GPS	Guinea pig serum
GTP	Guanosine triphosphate
GUP	Glasgow University Protozoology
GUTat	Glasgow University <i>Trypanozoon</i> antigen type
HCl	Hydrochloric acid
HDL	High-density lipoprotein
HIFCS	Heat-inactivated foetal calf serum
IFN-γ	Interferon γ
IL-2	Interleukin-2
ILTat	ILRAD <i>Trypanozoon</i> antigen type
LDL	Low-density lipoprotein
LPG	Lipophosphoglycan
M	Nuclear mitosis
M-CSF	Macrophage-colony stimulating factor
PARP	Procyclic acidic repetitive protein
PDGF	Platelet derived growth factor
PBS	Phosphate-buffered saline
PDT	Population doubling time
PNA	Peanut agglutinin
R-mGM	Re-mutagenised growth mutant population (uncloned)
R-mGM3	Re-mutagenised growth mutant population passaged through 3 mice
R-mGM13	Re-mutagenised growth mutant population passaged through 13 mice
R-mGM3cl1/2	R-mGM3 clone 1/2
R-mGM13cl1/2	R-mGM13 clone 1/2
RNA	Ribonucleic acid
SAPU	Scottish Antibody Production Unit
SDM-79	Semi-defined medium (1979)
SE	Standard error
S_k	Kinetoplast S-phase
S_n	Nuclear S-phase
STIB	Swiss Tropical Institute Basel
TFBP	Transferrin binding protein
TRITC	Tetramethylrhodamine isothiocyanate

VAT	Variant antigen type
VSG	Variant surface glycoprotein
WHO	World Health Organisation

DECLARATION

The results presented in this thesis are my own except where stated otherwise.

The mathematical models of replication, growth and differentiation described in chapter 5 are from Turner *et al.* (1995).

One of the growth inhibition experiments described in chapter 6 (Figure 6.5) was carried out by Nasreen Aslam (published in Turner *et al.*, 1996).

The work in chapter 3 has been published as a meeting abstract:

Milligan, K. & Turner, C.M.R. (1995) The relative timing of nuclear and kinetoplast cell cycle events in kinetoplastids *Transactions of the Royal Society of Tropical Medicine and Hygiene* **89**, 592

ACKNOWLEDGEMENTS

I would like to thank, first and foremost, Dr. Mike Turner for his invaluable help, advice and encouragement throughout my PhD. I would also like to thank Professor Graham Coombs for the use of facilities in his laboratory and acknowledge the financial support of the Biotechnology and Biological Sciences Research Council (BBSRC).

I am indebted to Dr. Debbie Smith, Imperial College, London for the provision of Friedlin VI strain *L. major* promastigote forms as well as the ab336 antibody and also to Dr. David Sacks, NIH, USA for the 3F12 antibody, used in the study of *Leishmania* differentiation (chapter 5).

There are also a number of people to whom I am extremely grateful for their kind help during my time in Glasgow:

to Nasreen Aslam, for introducing me to fluorescence microscopy;

to Dorothy Armstrong, for bringing some well needed order to my bench;

to the Parasitology staff and post-grads, especially Paul Appleton for his advice on microscopy and Kathryn Brown for the provision of axenic amastigotes;

to Caroline Morrison who rescued me many times from word-processing hiccups;

to Peter Rickus for photography;

to Isabel Thompson and Liz Denton for lending their expertise in Apple-Macing;

to everyone at the Joint Animal Facility (JAF) for their assistance in animal work, especially John Laurie;

to Alan Scott, for his help with figures and tables.

Finally, I wish to dedicate this thesis to my parents for their continual support and encouragement throughout my studies and research.

~~~~~

'What is the use of a book' thought Alice, 'without pictures and conversation?'

*Alice's Adventures in Wonderland*, **Lewis Carroll**

~~~~~

CHAPTER 1 GENERAL INTRODUCTION

1.1 Life cycle biology

1.1.1 Taxonomy

Trypanosoma brucei

The African trypanosomes are important parasites that cause sleeping sickness in humans and nagana in cattle. They have complex life cycles, consisting of several developmental stages in vector and mammalian hosts. An estimated 25,000 new cases of sleeping sickness are reported each year (WHO, 1986), all of which are inevitably fatal if untreated. However, the disease also has wider economic implications because of its dramatic effect upon domestic livestock, in terms of loss of production, wasting and infertility.

These parasites are flagellated protozoa which belong to the genus *Trypanosoma*, order Kinetoplastida. The genus is divided into several subgenera which are grouped into two sections, according to differences in the developmental cycle in the insect vector i.e. Stercoraria and Salivaria, the former group being transmitted through the insect's faeces and the latter group being transmitted through the saliva of the tsetse fly (reviewed by Vickerman, 1985). The salivarian trypanosomes encompass the species found in Africa. The main pathogenic species in Africa are *T. congolense*, *T. brucei*, *T. vivax* and *T. simiae*. *T. evansi* is also a salivarian trypanosome although no cyclical development occurs in the insect. Human sleeping sickness is caused by sub-species of *T. brucei*, *T. b. rhodesiense* and *T. b. gambiense*. The former causes the more acute East African illness and the latter the more chronic West African disease. Although another sub-species *T. b. brucei* is morphologically identical to these two sub-species at all stages of its life cycle, it does not infect humans, being confined to only wild and domestic animals (Vickerman *et al.*, 1991). Despite differences in regional occurrence, host specificity and severity of infection, all three sub-species share basically the same characteristic developmental cycle (Vickerman, 1985). The

three sub-species will therefore be referred to generally as *T. brucei* and will be the only species of trypanosome discussed here.

Leishmania (L. mexicana, L. major)

Leishmania is a genus of protozoan parasites also of the order Kinetoplastida responsible for a spectrum of diseases. Clinically, these diseases range from disfiguring cutaneous or mucocutaneous infections to life-threatening visceral infections (Marsden, 1984). Many species have been identified and classified taxonomically (reviewed by Lainson and Shaw, 1987). Although all *Leishmania* spp. exhibit similar morphology, they differ clinically, biologically and serologically (Schmidt and Roberts, 1989). These characteristics often overlap such that difficulties regarding the identification and classification of species have arisen in the past.

Leishmania spp. are grouped into two sections, according to differences in the developmental cycle in the sandfly vector i.e. Supracylaria and Peripylaria, the former section encompassing species that develop in the sandfly's midgut before moving anteriorly and the latter section being species that develop in the hindgut first (Molyneux and Killick-Kendrick, 1987). The two species discussed here (*L. mexicana* and *L. major*) are both suprapylarian species. The *Leishmania mexicana* complex, which encompasses a number of sub-species is responsible for mainly cutaneous leishmaniasis and occurs in the New World (Central and South America) (Chang *et al.*, 1985). Sandflies of the genus *Lutzomyia* are the vectors of *L. mexicana* infections. *L. major* is also mainly a cutaneous infection, although it has a different geographical distribution to the *L. mexicana* complex, occurring in the Old World (Africa, Middle East and Asia). Sandflies of the genus *Phlebotomus* are the intermediate hosts and vectors of *L. major* infections. Despite differences in regional occurrence and host specificity (both vector and mammal), both species share

essentially the same cycle of development (reviewed by Molyneux and Killick-Kendrick, 1987).

1.1.2 Development in the vertebrate host

An important premise underlying this study is that cell cycle and life cycle patterns of control are expected to be highly conserved in the kinetoplastids as a whole. In general, kinetoplastid life cycles alternate between dividing and non-dividing forms, the latter having functions in transmission between hosts (vector and mammal or vice versa) and/or migration, whereas the former establishes a population in a 'new' environment (see Figures 1.1 and 1.2). One exception to this general rule is differentiation from *Leishmania* amastigotes to promastigote forms which involves transformation from a dividing form to another dividing form. The amastigote form is an intracellular parasite adapted to life inside the macrophage and therefore removed from the extracellular environment of the host (reviewed by Bray and Alexander, 1987), a factor which may circumvent the requirement for an intermediate non-dividing stage before transmission to the sandfly vector.

T. brucei

The vector responsible for transmission is the tsetse fly, *Glossina* spp., which infects the vertebrate host with metacyclic forms. At the site of inoculation in the skin, metacyclic trypanosomes transform to slender forms, enter the draining lymphatics and arrive at the bloodstream. Slender forms divide by binary fission and are responsible for proliferation of the systemic infection (reviewed by Vickerman, 1985).

A proportion of the slender form population differentiate via intermediate forms to stumpy forms, which are biochemically and morphologically distinct from slender forms. Lacking mitochondrial cytochromes, long dividing slender forms rely exclusively on glycolysis for energy metabolism, whereas the short non-dividing stumpy forms have a partially activated mitochondrial system (Oppendoes, 1985). On

ingestion of a blood meal by the fly, stumpy forms have the capability of transforming to procyclic forms (see also section 1.3.2), the stage found in the fly midgut, suggesting that stumpy forms are pre-adapted for survival in the new environment of the vector.

During the course of a trypanosome infection, slender forms undergo antigenic variation, where each trypanosome repeatedly switches from expression of one variant surface glycoprotein (VSG) coat to that of another, thus evading the host's immune response. Antigenic variation appears to be an adaptation to the host environment that enables bloodstream trypanosomes to prolong the duration of an infection and thus promote cyclical transmission to the vector.

Antigenic variation

The interaction of a growing parasite population undergoing antigenic variation with VSG-specific immune responses on the part of the host gives rise to a characteristic fluctuating parasitaemia (reviewed by Barry and Turner, 1991). Each VSG is encoded by a separate gene and there is an estimated potential to express 1,000 VSG genes per trypanosome. Serologically, at least 101 variant antigen types (VATs) can be expressed in a clonal infection (Capburn *et al.*, 1977). Expression of VSGs is hierarchical and is not induced by host antibody production. During the course of an infection, a number of VATs can be expressed at any one time, although the proportions of each VAT will vary such that some are more common than others. An antibody response against the most commonly expressed VAT will lead to clearance of these trypanosomes from the circulation and hence a remission of infection. Once growth of another VAT is sustained, relapse occurs until another antibody response is generated. A distinct hierarchy of expression has been found such that some VATs are nearly always expressed in the early part of an infection while others occur much later. The various mechanisms regulating VSG expression have been investigated in

considerable detail, some of which have still to be fully determined (reviewed by Turner, 1992a and Pays *et al.*, 1994).

Switching rates have been measured in lines that were recently tsetse fly-transmitted, and a high rate of switching was observed - approximately 10^{-2} switches/cell/generation (Turner and Barry, 1989). This rate value was much higher than the previously estimated rate of approximately 10^{-6} switches/cell/generation in extensively syringe-passaged lines (Lamont *et al.*, 1986). Through this high frequency of switching, the course of an infection is sustained and transmission to the vector is promoted. Expression of two VSG coats on individual trypanosomes can be detected during the switching process in mice inoculated with metacyclic forms of *T. b. rhodesiense* using VAT-specific monoclonal antibodies (Esser and Schoenbechler, 1985). Stable co-expression of two VSG coats on the surface of *Trypanosoma equiperdum* has also been demonstrated in *in vitro* culture (Baltz *et al.*, 1986), although co-expression was rapidly lost *in vivo*.

It has been proposed that switching is linked to the cell cycle (Vickerman, 1985, Turner, 1990), as slender forms only are capable of division and undergo antigenic switching, whereas both metacyclic and stumpy forms do not divide (Shapiro, 1984) and do not appear to switch. Further indirect evidence of a link to the cell cycle was provided by a study of antigenic switching rates, where the *per capita* switch rate remained the same even when the growth rate was altered (Turner and Barry, 1989). There is no direct evidence, however, linking VAT switching and a particular phase of the cell cycle.

Leishmania

The vector responsible for *Leishmania* transmission is the female phlebotomine sandfly, which infects the host with metacyclic promastigote forms when taking a blood meal (reviewed by Molyneux and Killick-Kendrick, 1987). These forms are

then phagocytosed by macrophages, where *Leishmania* parasites exist as amastigote forms within the phagolysosome (Alexander and Vickerman, 1975). Amastigote forms are non-motile, non-flagellated forms, which have the ability to survive within the seemingly hostile environment of the macrophage (Bray and Alexander, 1987). Amastigotes are able to resist attack mechanisms such as enzymic, pH-dependent activity and the release of reactive oxygen species. Nitric oxide production is also a major killing mechanism employed by the macrophage (reviewed by Liew and Cox, 1991). The full extent of the *Leishmania* parasite's survival capacity has been investigated with considerable difficulty in the past, because of the complication of analysing an intracellular form. The more recent development of an axenic culture system for amastigote forms should provide an easier route to biochemical and molecular analysis (Bates *et al.*, 1992).

Amastigote division occurs by binary fission. Large numbers occupy the parasitophorous vacuole until the cell eventually bursts and further phagocytosis of amastigotes occurs. On ingestion of a blood meal by the fly, amastigotes undergo dramatic morphological and biochemical changes to promastigote forms in the midgut of the fly (Molyneux and Killick-Kendrick, 1987).

1.1.3 Development in the invertebrate host

T. brucei

The life cycle of *T. brucei* involves transitions from proliferating to non-proliferating forms (Figure 1.1). Differentiation of stumpy forms to the rapidly dividing procyclic forms is accompanied by significant biochemical and cellular changes. There is a switch from the utilisation of glucose, the main energy source for bloodstream forms, to the use of proline which is abundant in the fly. In procyclic forms, the mitochondrion is fully activated and the VSG coat of the bloodstream form is no longer present (Vickerman, 1985). Procyclic forms represent the main proliferative phase in the vector and can be successfully cultivated *in vitro*, with no apparent loss

of *in vivo* characteristics (Brun and Schonenberger, 1979). Established populations of dividing procyclic forms in the posterior midgut divide in both the ecto- and endoperitrophic spaces. Those found in the former site move forward to the proventriculus, where they differentiate to non-dividing proventricular forms capable of migrating to the salivary glands. Once in the salivary glands transformation to the proliferative epimastigote form occurs.

The epimastigote form undergoes division and is attached by its flagellum to the microvilli of the epithelium lining the salivary gland lumen. It is at this stage in the life cycle that differentiation to the metacyclic form occurs, the form infective to the vertebrate host (reviewed by Vickerman, 1985). Metacyclic forms are non-dividing, express VSG and transform to slender forms after infection of the mammalian host.

Leishmania

Both *L. mexicana* and *L. major* belong to the section Supracyclaria i.e. development occurs in the midgut and the foregut (Molyneux and Killick-Kendrick, 1987). Amastigote forms ingested in the blood meal are released from ruptured macrophages, which is thought to occur either through rupture in the feeding process, or damage caused in the ingestion process (Molyneux and Killick-Kendrick, 1987). There is some evidence of an early growth phase of amastigote forms in the midgut within 24 hours of ingestion, before transforming to short ovoid promastigote forms. The blood meal is encased by a peritrophic membrane in the abdominal midgut, within which nests of promastigotes undergo rapid division and transformation to long slender nectomonads 3-4 days post-feeding. Considerable heterogeneity of promastigote forms exists at this point in development. The membrane breaks up allowing free-swimming flagellated forms to escape, either through the membrane or anteriorly in the midgut. Rapid division takes place during the digestion of the blood meal, before migration to the thoracic midgut. Association between the flagella of promastigotes with the microvilli of midgut epithelial cells and the foregut is a

characteristic of Suprapylarian *Leishmania* infections (Molyneux and Killick-Kendrick, 1987, Pimenta *et al.*, 1992). Forward migration of promastigotes is accompanied by further transformation leading to short, slender, highly active metacyclic forms. It appears that sequential development from a non-infective promastigote form towards an infective metacyclic form occurs (Sacks and Perkins, 1985). Whether or not the heterogeneous population of promastigote forms identified in the sandfly midgut and also in *in vitro* culture of *L. mexicana* and *L. panamensis* (Brown *et al.*, 1994a, b) are distinct intermediate developmental forms necessary for metacyclics to be produced, has still to be fully clarified.

Dense infections of metacyclic forms are observed at the stomodeal valve from where they can also invade the foregut, including the pharynx, cibarium and proboscis. Development of an infective metacyclic form has been demonstrated, both *in vivo* and in axenic culture, in the case of *L. major* (reviewed by Sacks, 1989) and *L. mexicana* (Bates and Tetley, 1993). Metacyclogenesis, therefore parallels development in other hemoflagellates; differentiation of a replicating, non-infective form into a resting, infective stage which is pre-adapted for survival in the vertebrate host.

1.2 The cell cycle

1.2.1 The eukaryotic cell cycle

The eukaryotic cell cycle has already been well described for numerous organisms. It generally consists of four periods defined by nuclear activity (Howard and Pelc, 1953). Three of these periods belong to the classical interphase: G1-phase, the gap period before DNA synthesis occurs; S-phase, the period of DNA synthesis and G2-phase, the post-synthetic gap period. Mitosis and cell division form the fourth period. Mitochondrial DNA is dispersed between several mitochondria in eukaryotic cells, although the amount present depends upon growth conditions, ploidy and species involved (Lloyd *et al.*, 1982) and appears to be asynchronous with respect to the replication and division of mitochondrial DNA and mitochondria. However, an

average doubling of both mitochondria and mitochondrial DNA is required during the cell cycle (Clayton, 1982).

Two highly regulated transition points have been identified in the cell cycle: one termed START in G1-phase, when a cell decides to replicate its DNA and another point at the G2/M interface when a cell decides to initiate mitosis. The key regulators in these events are the well characterised cyclin-dependent kinases (CDKs) (reviewed by Murray and Kirschner, 1991 and Morgan, 1995, Figure 1.3). CDKs are heterodimeric proteins composed of a catalytic subunit, the protein kinase activity, which is dependent on association with the regulatory subunit or cyclin. CDKs were first recognised through genetic analysis of the cell cycle in yeasts. In *Schizosaccharomyces pombe* the main CDK is the *cdc2* kinase, whereas in *Saccharomyces cerevisiae* the major CDK is CD28. In humans a number of CDKs have been identified from CDK1 (CDC2) to CDK7. Each CDK interacts with a specific subset of cyclins, although the size of each subset varies. In addition to cyclin binding, CDK activation requires phosphorylation of a conserved threonine by the CDK-activating kinase. An active CDK-cyclin complex can be inhibited by phosphorylation of a conserved threonine-tyrosine pair or binding to CDK inhibitory subunits (Morgan, 1995). CDK activity is therefore tightly regulated to ensure successful progression through the cell cycle.

As progression through the cell cycle is critically important to the growth and development of both trypanosome and *leishmania* infections, its study is of particular relevance to a further understanding of the biology of these parasites and how they can be controlled. Recent work in identifying *cdc2*-like genes in *T. brucei* (Mottram, 1994, Mottram and Smith, 1995) and *L. mexicana* (Mottram *et al.*, 1993) as well as a cyclin homologue in *T. brucei* (Affranchino *et al.*, 1993) may provide the first insight into cell cycle control in kinetoplastid cell cycles.

1.2.2 Timing of cell cycle events

The timing of cell cycle events in a number of eukaryotic cells has been examined. Generally, a high proportion of mammalian cells are found in G1-phase and also in S-phase and a small proportion in G2- and M-phase. For example, the values for a V79 fibroblast cell line are respectively 42%, 46% and 12% (Fertig *et al.*, 1990). A mammalian cell in an asynchronous culture with a generation time of 16 hours, for example, would have G1=5hrs, S=7hrs, G2=3hrs and M=1hr (Prescott, 1976). In the cell cycle of *S. pombe* S-phase is very short and occurs near the beginning of the cell cycle simultaneous with cell separation. A protracted G2-phase follows, ending in nuclear division at 0.75 of a cell cycle. Mitosis is followed by a short G1-phase, ending with S-phase of the next cell cycle (Mitchison and Creanor, 1971). Cell division is indicated by formation of a septum across the middle of the cell followed by separation of two equally sized daughter cells. The type of cell division observed in *S. pombe* is more similar to that found in higher eukaryotes in comparison to the budding mode of division found in *S. cerevisiae* (Nurse *et al.*, 1976).

In most studies of the timing of cell cycle events, S-phase is long and mitosis occurs very rapidly. One notable exception to this is in embryonic cells, where mitosis lasts for about 40% of the total cell cycle time (Murray and Kirschner, 1991). The durations of mitosis and S-phase are relatively constant in cells of the same organism, whereas G1-phase is usually the most variable in length (Prescott, 1976, Basegra, 1989).

Cells can also be in a state of cell cycle arrest or quiescence, usually fixed in G1- or G₀-phase. Most non-proliferating cells in vertebrates are in G₀-phase, but are capable of re-entering the cell cycle in response to appropriate stimuli. Terminally differentiated cells e.g. cells circulating in the blood, are incapable of further division. While the difference between G1- and G₀-phase has been a matter of some controversy, it appears that certain growth-regulated genes are not expressed in G₀,

e.g. *c-fos* and *c-myc*. However, expression of several genes is induced when cells in G_0 are stimulated to re-enter the cell cycle (Basegra, 1989).

1.2.3 Cell cycle of kinetoplastids

How the durations of cell cycle events in kinetoplastids compare with other eukaryotes and how the timing of these events are controlled similarly to events in yeast and higher eukaryotes is of great interest. This is because kinetoplastids have a number of unusual features that set them apart from other eukaryotes and which have important implications for the regulation of the cell cycle and cell cycle dependent life cycle events such as differentiation and transformation. Three major organelles, the nucleus, the kinetoplast and the flagellum with associated basal body, are all present as single copies. The mitochondrial DNA in the single mitochondrion is collected in a single organelle at the base of the flagellum, termed the kinetoplast (reviewed by Simpson, 1972). Kinetoplast DNA has a discrete S-phase rather than KDNA synthesis occurring continuously throughout the cell cycle, as is the standard eukaryotic plan. Kinetoplastids have a single flagellum subtended by a mature basal body but also have a short pro-basal body in close proximity which forms the new flagellum during the cell cycle (Vickerman and Preston, 1976, Sherwin and Gull, 1989). During each cell division, replication and segregation must occur to ensure that a single copy of each organelle is distributed faithfully to each daughter cell and the simplest way in which it is envisaged that this co-ordination might be achieved is by control of the relative timing of one or more events in the cell cycle (Turner, 1992b).

In the study of the cell cycles of several species of Kinetoplastidae, a relationship between the timing of nuclear and kinetoplast division and also of nuclear and kinetoplast DNA synthesis was established. A close association between the initiation of S-phases for the nucleus and the kinetoplast was observed in *Trypanosoma mega* (Steinert and Steinert, 1962), *Crithidia luciliae* (Van Assel and Steinert, 1971),

Leishmania tarentolae (Simpson and Braly, 1970) and *Crithidia fasciculata* (Cosgrove and Skeen, 1970). It has been proposed that this synchrony is perhaps due to intracellular regulation of DNA synthesis and the availability of a common pool of deoxyribonucleotide substrates, occurring at only one point in the cell cycle (Cosgrove and Skeen, 1970). It appears to be quite a unique observation and unlike that found in other organisms, including *Tetrahymena* (Parsons, 1965, Parsons and Rustad, 1968) and *Physarum* (Evans, 1966) where mitochondrial DNA synthesis and nuclear DNA synthesis appear to occur independently of each other. However, the exact timing of S-phases was found to vary between species and growth conditions (Simpson, 1972).

The periods of division of nuclei and kinetoplasts were not clearly defined in these studies. It was generally found that kinetoplast division was initiated before mitosis in *C. fasciculata* grown at three different temperatures, in *T. mega* and *L. tarentolae*. In *C. luciliae*, mitosis was initiated before kinetoplast division. Observations of division sequences of *Leishmania* promastigote forms in the sandfly have described the initiation of mitosis occurring before kinetoplast division, although the opposite sequence has also been observed i.e. kinetoplast division before mitosis both *in vivo* and *in vitro* (Killick-Kendrick and Rioux, unpublished observations, cited in Molyneux and Killick-Kendrick, 1987, Christophers *et al.*, 1926, Adler, 1964, Walters, 1993).

In summary, these various studies have demonstrated that kinetoplast DNA is replicated in a discrete S-phase but the relative timing of organelle cell cycle events between the nucleus and kinetoplast remain unclear due, in the main, to the limitation of the techniques employed. The only study that has mapped the cell cycle of a kinetoplastid in any quantitative detail was conducted by Gull and colleagues (1990) in *T. brucei* procyclic forms.

1.2.4 Cell cycle of *T. brucei*.

The major morphological cell cycle events, from pro-basal body elongation (the event preceding initiation of a new flagellum) through to cytokinesis (the period that includes the post-mitotic period plus the actual period of cell cleavage), have been used as event markers in the study of the cell cycle of *T. brucei* (Sherwin and Gull, 1989). Quantitation of the timing of these events has been carried out only in procyclic forms, grown *in vitro* (Woodward and Gull, 1990). Using asynchronous cultures of a particular strain (427) with a population doubling time (PDT) of 8.65 hours, the durations of particular events within the cell cycle were determined. Immunofluorescence microscopy and staining with a DNA intercalating dye, DAPI, was used to ascertain the frequencies of cells with particular nuclear and kinetoplast configurations (single, dividing and post-division). Employing the method of analysis of Williams (1971), the durations of mitosis and cytokinesis for the nucleus and the corresponding periods of division and cytokinesis for the kinetoplast, were calculated. Incubating cells growing in culture with the thymidine analogue, bromo-deoxyuridine (BrdU) and then detecting BrdU incorporated into the sites of DNA replication with a BrdU-specific antibody, is a method by which cells specifically in S-phase can be visualised (Gratzner, 1982). Using this method, duration of S-phases for the nucleus and the kinetoplast were calculated from the frequencies of cells with labelled nuclei and kinetoplasts. The full calculations were made using the treatment derived by Stanners and Till (1960). The length of G2-phase was taken as the time for BrdU labelling to appear in an organelle classified as dividing (Woodward and Gull, 1990). G1-phase was calculated by adding together lengths of all other periods and subtracting these from the total cell cycle time.

From these analyses the complete cell cycle of *T. brucei* procyclic forms was mapped (Woodward and Gull, 1990) (Figure 1.4). It was shown that the start of S-phase for the nucleus and the kinetoplast approximately coincided. Basal body replication was also detected at this point in the cell cycle using an anti-basal body monoclonal

antibody. This co-incidence of timing suggested a possible link between two or more of the organelles. One aspect of this co-ordination which has been investigated further is the apparent link between the kinetoplast and the flagellar basal body. Direct linkage between these organelles was described, in which segregation of the kinetoplast DNA is dependent on a microtubule mediated separation of the new and old flagellar basal bodies during the cell cycle (Robinson and Gull, 1991).

In contrast to the synchrony of initiation of S-phase, the timing of termination of S-phase differed between the nucleus and the kinetoplast and the periods of division of these two organelles were also seen to differ significantly. An extended period of cytokinesis for both organelles was also observed.

From this analysis it can be seen that there is an apparent synchrony between the initiation of S-phase for the nucleus and the kinetoplast, a feature recognised in the study of other trypanosomatids (see section 1.2.3), indicating that a degree of inter-organellar regulation is in operation. After this point there appears to be asynchrony between organelles, particularly in their division periods. The timing of division seems to vary between species of trypanosomatids and may be a reflection of the morphology of a particular cell. A contrast is seen between *Crithidia* and *T. brucei*. *Crithidia* cells are rather rounded and after division therefore, cell cleavage is ensured by the production of a natural bilateral symmetry. For trypanosomes, which are long and thin, extensive rearrangement of the replicated organelles is required before cell cleavage along the longitudinal axis of the cell can occur and may also be the reason for the extended period of cytokinesis, readily defined in the cell cycle (Woodward and Gull, 1990).

In conclusion, there are two strong reasons why the cell cycles of kinetoplastids need detailed analysis. Firstly, to investigate the unusual features of the cell cycle imposed by the requirement to co-ordinate replication and segregation of three single copy

organelles. Second, to elucidate how the complex developmental cycles are regulated within the cell cycle context.

1.3 Cell Differentiation

1.3.1 Mechanisms of differentiation

Cell differentiation involves alterations to the gene expression of a cell, such that the new cell type differs from the parent by virtue of morphology, cell function and developmental potential (Newton and Ohta, 1990). The two cell types can normally be distinguished by phenotypic markers, either biochemically and/or morphologically. Cell differentiation can occur in response to changes in the external environment, but can also be intrinsically determined within the cell.

In mammalian cell differentiation, a cell is in a determined state when it is restricted in the type of differentiation it can undergo (Gurdon, 1992). Cells are thought to pass through several determined states, seen by the progressively restricted range of cell types, daughter cells are able to form. For example, pluripotent stem cells in the bone marrow and spleen give rise to committed stem cells of all types of cells circulating in the blood. Further down the lineage, however, haemopoietic stem cells can give rise to only one cell type, namely erythrocytes (Metcalf, 1989). Mammalian cell lineages involve differentiation steps initiated by a stem cell which will differentiate along a particular pathway, in response to a defined external stimulus provided by the microenvironment in which they find themselves. Stem cells and the precursor cells they produce, undergo rounds of proliferation and differentiation until the fully mature daughter cell is formed. This cell represents the end point of a particular lineage and does not divide. A change in the external environment can dramatically alter the route taken by differentiating cells. For example, incubation of granulocyte-macrophage colony-forming cells (GM-CFC) with GM-CSF or M-CSF induced irreversible commitment to granulocyte or macrophage production respectively within 24 hours of exposure (Metcalf and Burgess, 1982), although a large proportion of

GM-CFC were bi-responsive to both stimuli. Cell differentiation can also be induced by chemicals e.g. dimethylsulphoxide (DMSO) can induce differentiation of erythroleukemia cells (Orkin *et al.*, 1975) and leukemia cell line HL-60 (Tarella *et al.*, 1982).

In animal development, there are two main mechanisms by which differentiated cells arise; (1) asymmetric cell division, involving an unequal segregation of developmental potential and (2) the interaction between two different cell types, producing a third cell type (see review by Gurdon, 1992). In the *Drosophila* central nervous system, for example neural stem cells or neuroblasts divide asymmetrically into another neuroblast and a ganglion mother cell (GMC) (Vaessin *et al.*, 1991). A transcription factor, Prospero, is differentially segregated to GMCs from its site of synthesis in the neuroblast at mitosis (Hirata *et al.*, 1995). Asymmetric segregation of Prospero was also observed in the embryonic endoderm, suggesting that this type of differential gene regulation may be widespread in development. A membrane-associated protein, Numb, also exhibits asymmetric segregation during cell division. Furthermore, Numb co-localises with Prospero throughout mitosis, suggesting a common mechanism for asymmetric segregation (Knoblich *et al.*, 1995). There are also many examples of asymmetric divisions throughout nematode development, the pattern of which has been demonstrated to be important by the generation of mutations that lead to developmental defects (Horvitz and Herskovitz, 1992). A key mechanism observed in vertebrate development which involves cell interactions is embryonic induction, where one cell induces another (responding) cell to differentiate (Gurdon, 1992). Timing of development is therefore vital as cells can be limited in the way they respond to signals from other cells and their ability to respond or competence can also change rapidly.

The pattern of development in multi-cellular organisms is clearly complex and many questions remain unanswered, especially regarding the role of developmentally

regulated genes and gene products and also the influence of growth factors and other extracellular agents upon cell differentiation. Similar mechanisms of cell differentiation exist however, in lower eukaryotes and microbial organisms. Mating type switching in yeasts also involves asymmetric cell divisions, producing sisters of different developmental fates (Klar, 1992, Haber, 1992). This implies that control of production of different cell types is linked to the organism's cell cycle. In studies of the differentiation patterns of bacteria, evidence is also accumulating that the programmed sequence of differentiation is driven by cell cycle control. In *Caulobacter*, for example, there is a pattern of asymmetric cell division, producing one dividing form and one non-dividing form, which re-enters the cell cycle later in development. Analysis of *cdc* mutations has suggested that the timing and spatial organisation of many developmental events are linked to the cell cycle of *Caulobacter* (see review by Newton and Ohta, 1990). Other examples of prokaryotic differentiation e.g. heterocyst formation in *Anabaena*, sporulation in *Bacillus* and *Streptomyces* (see Newton and Ohta (1990) for references) also contain similarities to metazoan differentiation.

1.3.2 Differentiation of trypanosomes and *Leishmania*

Unlike most other systems of differentiation in multi-cellular eukaryotes which ultimately lead to a fully differentiated end-cell, there is no terminal differentiation in the life cycles of kinetoplastids as life cycle stages fixed in G₀/G₁-phase of the cell cycle always have the potential to re-enter the cell cycle. This ability to re-enter the cell cycle also applies to yeast mating type switching and the other examples of prokaryotic differentiation referred to in section 1.3.1.

Trypanosome differentiation

Each stage of the trypanosome life cycle is specifically adapted for survival in its immediate environment, be it host or vector. The non-proliferative forms-metacyclic, stumpy and proventricular-are also pre-adapted to survival in the next environment

and as such are responsible for the processes of transmission between vertebrate and vector hosts and for migration between sites in the tsetse fly (Vickerman, 1985). Most studies of trypanosome differentiation have focused upon two transitional stages of the trypanosome life cycle. One stage is the non-dividing metacyclic form which exists in the salivary glands of the tsetse fly and differentiates to the proliferating bloodstream form, on infection of the host (Vickerman, 1985). The other transitional stage, which ensures progression of the life cycle from host to vector, is differentiation from bloodstream to procyclic forms. Slender bloodstream forms differentiate to procyclic forms via the non-dividing stumpy form which is arrested in G₀/G₁-phase of the cell cycle (Shapiro *et al.*, 1984). This form is pre-adapted for survival in the tsetse fly, wherein it differentiates to the dividing procyclic form found in the insect's midgut. Progression to this stage of the life cycle involves dramatic changes in morphology and cellular metabolism.

One major alteration in gene expression is the exchange of VSG on the surface of the bloodstream form for a procyclic-specific coat protein, PARP/procyclin (Roditi *et al.*, 1989, Ziegelbauer *et al.*, 1990, 1993). This exchange of surface proteins is a synchronous event, which is co-incident with re-entry into the first cell cycle of the procyclic form. These markers have been used to analyse the differentiation step *in vitro* in order to elucidate the link between life cycle progression and the trypanosome cell cycle (Matthews and Gull, 1994a). Using a combination of cell cycle (antibody for detecting occurrence of S-phase) and differentiation markers (anti-VSG and anti-PARP antibodies), different populations of cells (populations predominately slender compared to populations predominately stumpy) were analysed for their ability to differentiate. While slender forms differentiated, the kinetics were slower than for populations that were predominately stumpy (Roditi *et al.*, 1989, Ziegelbauer *et al.*, 1990). These differences between the two populations are thought to be related to their respective positions in the cell cycle and their perception of the differentiation signal (Matthews and Gull, 1994a). Stumpy cells are within a 'window' to receive the

inductive signal (presumably in $G_0/G1$ -phase of the cell cycle) and are therefore irreversibly committed to differentiation, whereas slender forms are asynchronous with respect to their position in the cell cycle; a proportion of slender forms will be within the window and therefore be able to differentiate, while the majority are not and will either progress through the rest of the cell cycle until they reach the window or arrest and die. It has also been shown that while there is a clear link between the cell cycle and the commitment to differentiate, once differentiation has been initiated the two processes can be uncoupled (Matthews and Gull, 1994a). Bloodstream to procyclic differentiation and cell cycle progression therefore appear to be synchronous and co-incident processes. Piece by piece, a temporal map has been constructed for stumpy-cell differentiation through to the procyclic form, with its simultaneous re-entry into the cell cycle (reviewed by Matthews and Gull, 1994b).

One differentiation step which has been studied to a lesser degree is slender to stumpy differentiation. While the two previously discussed stages involve release from a cell cycle block with concomitant cellular differentiation, this step is the opposite, where slender forms become arrested in $G_0/G1$ -phase of the cell cycle, producing an irreversibly differentiated cell of altered cellular metabolism and morphology (reviewed by Vickerman, 1985). Slender to stumpy differentiation can also be observed in *in vitro* culture, believed to be characteristically similar to differentiation *in vivo* (Hamm *et al.*, 1990). Whether stumpy cell production is induced by external factors or intrinsically determined within the cell, is at present unclear, although a number of models are beginning to reveal possible mechanisms. At a single cell level, a slender form has a number of fates; either a slender form can divide asymmetrically producing one stumpy form and one slender form which can carry on dividing. Alternatively a slender form could become committed to differentiate and do so without further cell division, or a slender form could become committed to differentiate and then divide symmetrically producing two daughter stumpy forms (Matthews and Gull, 1994b). When slender forms become committed to differentiate

and whether intermediate forms (cells of intermediate morphology between slender and stumpy, Hoare, 1972) represent cells already destined to irreversible differentiation has yet to be elucidated.

Intrinsic production of stumpy forms has been demonstrated in a study of the prevalence of morphological types during *T. brucei* infections in mice (Balber, 1972). The change from slender forms predominating over stumpy forms during the growth phase to the converse at the peak of a parasitaemic wave was not caused by induction of stumpy form production but by a decrease in the number of slender forms. Intrinsic production of stumpy forms has also been observed in a study of slender form replication and differentiation (Turner *et al.*, 1995, described below). Contrasting evidence of induction of stumpy production has also been suggested, where slender to stumpy differentiation was controlled by host-derived growth factors which promote slender multiplication and inhibit differentiation (Black *et al.*, 1985). The depletion of an essential growth factor is suggested to be a trigger for a reduction in slender form replication and hence promote stumpy production. However, another study has suggested that depletion of a growth factor may not occur and that the reduction in slender forms is due to selective killing of slender forms at the peak of parasitaemic wave as shown by the markedly greater susceptibility of slender forms to complement-mediated lysis in comparison to stumpy forms (McLintock *et al.*, 1993). Induction of differentiation may therefore occur *in vivo*, but the evidence is as yet inconclusive.

While little information can be obtained regarding the mechanics of differentiation at the single cell level without suitable stumpy-specific markers, slender to stumpy differentiation can be more readily examined in terms of cell populations. In a study of how three different processes combine to determine growth of a trypanosome infection, namely slender form replication, differentiation from slender to stumpy forms and stumpy form mortality, theoretical models were constructed to which

experimental data were compared (Turner *et al.*, 1995). Two models were proposed; in the simple model, slender form populations grew exponentially, as did stumpy form populations and at similar rates. This model, however, did not accord with the experimental observation that the rate of increase of stumpy forms was lower than the rate of increase of slender forms. A second model, the heterogeneous model, was capable however of generating this experimental observation under some circumstances where the growing parasite population consisted of sub-populations of slender forms which replicated and differentiated at different rates. This model appeared to be a better explanation for the experimental data, where the rate of increase of stumpy forms was slower than the rate of increase of slender forms for a number of cloned stocks examined (Turner *et al.*, 1995).

***Leishmania* differentiation**

As in the trypanosome life cycle, *Leishmania* differentiation involves transitions from dividing to non-dividing forms. The most studied form, the promastigote form which is easily cultivated *in vitro* (Berens *et al.*, 1976), lives in the gut of the sandfly, wherein it migrates towards the oesophagus and pharynx, undergoing a number of significant biochemical and morphological changes. While it remains to be determined whether or not these changes represent distinct developmental stages, a vast body of evidence confirms that the end point of development in the sandfly is the metacyclic form, found predominately anteriorly and in the mouth parts of the sandfly, in the case of *L. major* and *L. mexicana* (reviewed by Sacks, 1989). This form is infective to the mammalian host and pre-adapted for survival in this new host environment. The period from feeding on an infected animal, until metacyclic production in *L. major* infections in sandflies has been demonstrated to take a minimum of 7 days (Davies *et al.*, 1990). Metacyclic forms are believed to be non-dividing (Sacks and Perkins, 1984, Bates, 1994) based on studies both *in vivo* and *in vitro*.

Metacyclic forms not only appear to be cell cycle arrested, but are also morphologically distinct from dividing promastigotes, having a much shorter cell body length and longer flagellum (Molyneux and Killick-Kendrick, 1987). Several studies have confirmed that metacyclic forms in *in vitro* culture are not only morphologically similar to their *in vivo* counterparts but are also infective of animals (Sacks and Perkins, 1984, Sacks and Perkins, 1985), in comparison to log-phase promastigotes or early midgut stages, which are relatively non-infective (reviewed by Sacks, 1989).

Significant biochemical changes also occur during the differentiation from promastigote forms to metacyclic forms, particularly to surface carbohydrates, determined by their ability to bind plant lectins (Sacks *et al.*, 1985). *L. major* metacyclic cells can be distinguished and even purified because they fail to be agglutinated by the lectin peanut agglutinin (PNA) at concentrations which agglutinate all non-infective promastigote forms. The relative virulence of stationary phase promastigote forms as determined by infectivity of mice, can be attributed to the number of non-agglutinated (PNA-) cells in the population. By use of decreased lectin binding as a marker for metacyclogenesis, it was demonstrated also that frequent subculturing led to a loss of virulence, as shown by a decrease in infectivity of mice and that metacyclogenesis did not appear to be a stable trait even for cloned lines of *Leishmania* (Da Silva and Sacks, 1987).

The major surface molecule, lipophosphoglycan (LPG), has been identified on promastigotes of all *Leishmania* species studied so far (Sacks, 1992). During metacyclogenesis the LPG molecule is modified extensively (reviewed by Sacks, 1992). In both log-phase promastigote and metacyclic forms, the LPG molecule is comprised of linear chains of phosphorylated oligosaccharide repeat units, anchored to the membrane via a glycosyl-phosphatidylinositol (GPI) glycolipid anchor (McConville *et al.*, 1990). During metacyclogenesis, there is an approximate doubling in the number of repeat units per molecule and a change in the terminal

sugar residue on the side branches from galactose to arabinose. This modification changes the binding preference of LPG, so it no longer binds PNA, a property observed in studies of *L. major* and *L. donovani* (Sacks, 1992). LPG expression has also been identified in *L. major* infections in sandflies, as well as the expression of other stage specific molecules e.g. the major surface metalloprotease GP63 (Davies *et al.*, 1990). LPG has been shown to inhibit antibody access to surface membrane proteins including GP63 (Karp *et al.*, 1991), therefore acts as a barrier to immunological attack after infection of the mammalian host.

It has been proposed that developmental modification of LPG causes metacyclic forms to be unable to interact with lectins present in the sandfly gut, would reduce the ability of cells to adhere to the midgut epithelium, encourage migration anteriorly and enhance the probability of regurgitation of these forms when the fly next takes a blood meal. Identification of lectin-like receptors in the sandfly midgut, that act like haemagglutinins could possibly be candidate receptors for LPG (see Jacobson, 1995), although this has still to be fully investigated. It is believed that changes to the LPG molecule also appear to have a modulatory effect on the binding of promastigotes to receptors on human macrophages (McConville *et al.*, 1992). The metacyclic-specific LPG promotes complement activation and C3 deposition in a non-lethal manner, such that opsonization of promastigotes leads to attachment and uptake via macrophage receptors (Sacks, 1992). This increased resistance to complement-mediated lysis, demonstrated by the binding of C5-9 to promastigote forms, resulted in cell lysis, while the complement complex was rapidly shed from the surface of metacyclic forms (Puentas *et al.*, 1991). This characteristic appears to be a key factor contributing to the increased infectivity of metacyclic forms. Metacyclic forms of *L. donovani* also display similar characteristics to *L. major* metacyclic forms, showing markedly increased infectivity, complement resistance and a lesser ability to bind PNA (Howard *et al.*, 1987).

Other studies of *Leishmania* biochemistry have focused upon the identification of genes expressed either exclusively or at increased levels in infective stages (Smith *et al.*, 1988, Coulson and Smith, 1990, Brodin *et al.*, 1992). A family of five genes located on a single chromosome has been characterised, four of which are exclusively expressed in the infective stages of *Leishmania* (Flinn and Smith, 1992). One member of this gene family, Gene B, has been studied in detail (Flinn *et al.*, 1994). This gene encodes a novel hydrophilic protein expressed on the surface of metacyclic forms, also detectable in amastigote forms, but not in log-phase promastigote forms. Co-capping experiments have revealed a close association between the Gene B protein and LPG (Pimenta *et al.*, 1994). The surface exposure of the Gene B protein is thought to be made possible by its hydrophilic and glycan binding properties, such that it interacts with the external surface of LPG and avoids being buried beneath the surface glycocalyx, therefore requiring to be attached to the membrane. This is in contrast to lipid anchored molecules such as GP63 which are buried beneath LPG and can only be exposed after capping and shedding of LPG (Pimenta *et al.*, 1994). Rapid capping and release of LPG (and Gene B protein) into the membrane of macrophages, may be related to increased survival within the host cell and increased parasite virulence (reviewed by Descoteaux and Turco, 1993).

There have been a number of studies addressing the question as to what causes metacyclogenesis. Most of these studies have exploited the fact that log-phase populations consist mainly of dividing promastigote forms equivalent to the *in vivo* midgut forms, whereas stationary phase populations contain a high proportion of infective metacyclic forms (Sacks and Perkins, 1984, Bates and Tetley, 1993). Metacyclogenesis has been shown to be induced by a change in environmental conditions. Cultivation of *L. mexicana* promastigote forms at pH 5.5 in Schneider's *Drosophila* medium, with 20% foetal calf serum, produced a homogeneous population of metacyclic-like forms (Bates and Tetley, 1993). These forms were demonstrated to be both morphologically and functionally similar to metacyclic forms,

both *in vivo* and *in vitro*. These findings suggested that metacyclic forms were pre-adapted for transformation to amastigote forms and therefore, also pre-adapted to survival at an acidic pH in the macrophage phagolysosome. Howard *et al.* (1987) have also shown that high numbers of metacyclic forms of *L. donovani* could be obtained using a modified Grace's medium and attributed this observation to cultivation at an acidic pH. Incubation of mid-log phase *L. major* promastigote forms in 'spent medium' resulted in a more rapid production of metacyclic forms (Mallinson and Coombs, 1989). The lower pH of the spent medium, has also been outlined as a significant factor in inducing differentiation (Bates and Tetley, 1993). The mechanism by which a lower pH induces differentiation is unknown, although it has been suggested that differentiation from promastigote to metacyclic forms may be a gradual process and may take a number of cell divisions before fully differentiated metacyclics are produced. One hypothesis has suggested that a drop in pH could be a density-dependent regulator of parasite numbers, thus promoting differentiation, either by selection or induction (Bates and Tetley, 1993) and that this phenomenon may occur *in vivo*, due to the high numbers of promastigote forms observed in sandflies (Lawyer *et al.*, 1987, Walters *et al.*, 1987). The pH value in the phlebotomus' midgut is unknown as yet, but is thought to be similar to that found in the mosquito (reported value > 8.5) (reviewed by Zilberstein and Shapira, 1994). Products of promastigote metabolism appear to lower pH (Marr, 1980), hence dense packaging of parasites in the sandfly midgut may reduce pH.

The effect of other possible factors which may regulate differentiation *in vivo* have been tested *in vitro*. *L. major* promastigotes cultured in the presence of haemoglobin, produced stationary phase cultures with predominately non-infective promastigote forms i.e. differentiation was inhibited (Schlein and Jacobson, 1994). The production of infective forms *in vivo* follows the digestion of the blood meal and the breakdown of the peritrophic membrane (Sacks and Perkins, 1985), a process thought to be aided by the release of chitinases by the parasites, enzymes which lyse the chitinous

framework of the membrane (Schlein *et al.*, 1991). It has been shown that the presence of haemoglobin or blood in the growth medium of *L. major* inhibits the secretion of chitinases and that this inhibition relates to the equivalent stage of development observed in the sandfly; as the blood meal is digested, the expression of chitinases and the subsequent breakdown of the peritrophic membrane leads to the release of promastigotes from the membrane and the development of infective forms (Schlein *et al.*, 1992).

In another study, salivary gland homogenates of *Lutzomyia longipalpis* inhibited the growth of promastigotes *in vitro* (Charlab and Ribeiro, 1993). This cell cycle arrest effect was thought to represent one way in which promastigotes were directed towards metacyclic differentiation. Sensitivity to saliva has also been shown to be related to the phase of growth *in vitro* (Charlab *et al.*, 1995). The effects of saliva and haemoglobin *in vitro* are thought to be reproduced *in vivo*, as part of the regulation of proliferation and differentiation pathways. Haemoglobin appears to hold promastigotes in the early stages of development in the intraperitrophic space. As the blood meal is digested and the peritrophic membrane is broken down, elongate nectomonad promastigote forms exit the blood meal, with most migrating towards the thoracic midgut (Walters, 1993). It is at this stage of development that parasites may encounter saliva along with sugar meals taken by the fly. The saliva may therefore direct differentiation towards the production of infective metacyclic forms (Charlab *et al.*, 1995). An increased level of glucose in cultures of *L. major* has also been shown to have an inhibitory effect upon the production of metacyclic forms, in comparison to control cultures (Smith and Ready, 1989). The full implications of these factors *in vivo*, however, remain to be fully investigated. Metacyclogenesis in the sandfly could be a process regulated by the change in the environment as multiplying promastigote forms migrate along the gut. As a blood meal is digested, levels of glucose and haemoglobin will decrease, which may induce promastigote populations to

differentiate. Lowering of pH may also create a suitable environment for metacyclogenesis to occur.

While evidence is accumulating that differentiation from promastigote to metacyclic forms can be induced, it remains to be determined whether differentiation can also be intrinsically determined within the cell. When the commitment to differentiate is made also needs to be ascertained and if so, when in the cell cycle this decision occurs.

The next stage of the life cycle, promastigote to amastigote differentiation, exposes *Leishmania* parasites to a dramatically different environment. Differentiation occurs during phagocytosis by host macrophages, wherein the amastigote lives inside the acidic environment of the phagolysosome (pH 4.5-6.0). This step not only involves re-entry into the cell cycle, but also significant changes to morphology and cellular metabolism. Intracellular amastigotes are highly adapted to life at both a lower pH and a higher temperature (Zilberstein and Shapira, 1994). The extreme changes in pH and temperature during the transmission from vector to host trigger changes in gene expression in the parasite. Heat shock related genes are abundantly expressed in *Leishmania* spp., similarly to many other eukaryotic organisms, induced by stress conditions (reviewed by Zilberstein and Shapira, 1994). Amastigote forms are of much smaller size (3-5µm), ovoid in shape and have non-emergent flagellum (Eperon and McMahon-Pratt, 1989). Amastigotes of *L. mexicana* and *L. amazonensis* also contain megasomes, unusual lysosomal organelles which are not found in promastigote forms (Alexander and Vickerman, 1975, Russell *et al.*, 1992). In a study of axenic cultivation and characterisation of *L. mexicana* amastigote forms, a temperature of 32-33°C was found to be the most favourable, consistent with the growth of *L. mexicana* resulting in cutaneous infections (Bates *et al.*, 1992). A pH of 5.5 was also required to retain amastigote morphology of the cultured parasites. This study also demonstrated that axenic amastigote forms were characteristically similar

to lesion amastigotes, in terms of ultrastructure, cysteine proteinase activity and infectivity.

Amastigote transformation to promastigote forms enables transmission from mammalian host to insect vector. This differentiation step can be easily mimicked *in vitro* by incubating amastigote forms in standard promastigote medium (e.g. Hart *et al.*, 1981b) at 27°C. The transformation of purified lesion amastigote forms of *L. mexicana* to promastigote forms has been examined in some detail, with particular attention paid to components of the *in vitro* system, found to be important in the transformation process and the effects of metabolic inhibitors and anti-protozoal drugs (Hart and Coombs, 1980, Hart *et al.*, 1981b). In these studies it was shown that the differentiation process involved three morphologically and biochemically distinct intermediates, including a division stage. The process was highly synchronous, with large numbers of amastigote forms transforming. By use of the DNA synthesis inhibitor hydroxyurea, it was also shown that cell division was necessary for transformation to proceed, contrary to previous reports of transformation studies of *L. donovani* (Simpson, 1968). Serum components, e.g. non-esterified fatty acids, were also demonstrated as being important in supporting a high rate of transformation. Transformation was inhibited however by a number of metabolic inhibitors including anti-leishmanial and anti-protozoal drugs. Changes in expression of the surface metalloprotease, GP63, have also been monitored during amastigote to promastigote transformation (Schneider *et al.*, 1992). Very little GP63 was found in the amastigote form, 300 times lower than corresponding levels of proteolytic activity found in promastigote forms. GP63 was expressed between 4 hours and 12 hours after the onset of the differentiation process, reaching a steady-state level before complete transformation to the motile extracellular promastigote form. It appears that the synthesis of GP63 preceded morphological changes to promastigote forms, as well as the appearance of promastigote-specific epitopes of LPG (Glaser *et al.*, 1991). In contrast, a family of mercaptoethanol-activated

proteases found in amastigote forms, was found to be down-regulated in promastigote forms (Schneider *et al.*, 1992).

Several studies have focused upon the early events controlling the onset of amastigote to promastigote differentiation. The role of ADP-ribosyltransferase (ADPRT) in the control of differentiation has been demonstrated in a wide range of eukaryotic organisms (reviewed by Williams and Johnstone, 1983). The presence of ADPRT has also been detected in a number of protozoa, including *T. brucei* (Farzaneh *et al.*, 1985), while the use of ADPRT antagonists inhibited differentiation in *T. cruzi* (Williams, 1983, 1984). In studies of transformation of *L. m. amazonensis* amastigotes to promastigotes, ADPRT antagonists such as 3-methoxybenzamide inhibited the early events of differentiation (Taylor and Williams, 1988). Four antagonists of ADPRT inhibited this differentiation step at concentrations which did not affect promastigote proliferation. Amastigote proliferation was also not affected suggesting that the inhibitors were directly acting upon a process specifically related to cell differentiation, rather than proliferation. Pre-incubation of amastigotes with the antagonists for 4-16 hours was necessary to produce this effect, suggesting that ADP-ribosylation of proteins is required for the initiation of differentiation. In the same study, the effects of inhibition of cell division upon the processes of differentiation were also assessed, by incubating amastigote forms with the DNA synthesis inhibitor, hydroxyurea. The transformation process was inhibited before the final stage of division to the fully mature promastigote form, such that a large number of intermediate forms accumulated. Similar observations were also made in *L. mexicana* (Hart *et al.*, 1981b). Taken together, these studies suggest that cell division is necessary for the completion of cell differentiation in these parasites and further demonstrates a link between the cell cycle and differentiation.

1.4 Growth regulation of Kinetoplastid protozoa

How cells receive and transduce signals from their external environment has been an area of considerable interest in recent years, particularly regarding the underlying mechanisms of growth regulation. In higher eukaryotes, these mechanisms often involve signal transduction pathways and regulatory enzymes. Cell surface receptors transduce signals to effectors such as adenylate cyclases, phospholipases and ion channels via guanine-nucleotide binding proteins (G-proteins) (reviewed by Bahouth and Malbon, 1994). Several hundred G-protein linked receptors have been identified, while the ligands which function via these receptors are chemically diverse, including amino acid derivatives, prostaglandins, peptides, polypeptides and multiple subunit glycoproteins. Another important class of cell surface receptors possess intrinsic tyrosine kinase activity, including molecules which bind to insulin, platelet derived growth factor (PDGF), colony stimulating factors and epidermal growth factor (EGF) (reviewed by Lund and Wiley, 1994). Ligand-receptor interactions involving growth factors such as these trigger a cascade of phosphorylation events which transduce changes at the nuclear level, hence altering the rate of cell division.

It is of interest therefore to ask whether similar intracellular signalling mechanisms operate in lower eukaryotes such as protozoan parasites. As kinetoplastids such as trypanosomes and *Leishmania* alternate between stages of growth and growth arrest throughout their life cycles, the reception and transduction of signals from the external environment necessitates tight regulation to ensure parasite survival and safe passage to the next life cycle stage. Also, the rate of growth of a parasite can reasonably be expected to act as an important determinant of the virulence of an infection as has been demonstrated in *T. brucei* (Turner *et al.*, 1995).

A number of studies have begun to unravel how growth is regulated in kinetoplastid parasites. Interactions between cytokines and protozoan parasites have been reported (reviewed by Barcinski and Costa-Moreira, 1994). T-cell supernatants had a direct

effect upon the growth of *L. amazonensis* promastigote forms (Mazingue *et al.*, 1989), an effect mainly attributed to interleukin-2 (IL-2). Another study showed that granulocyte macrophage colony-stimulating factor (GM-CSF) also acts as a growth factor for *L. amazonensis* promastigotes (Charlab *et al.*, 1990). GM-CSF also protected promastigotes from heat-induced death, thought to be important in protection of parasites exposed to higher temperatures, after infection of the mammalian host. An anti-GM-CSF antibody was also shown to decrease infectivity *in vivo* (Barcinski *et al.*, 1992), with the antibody possibly inhibiting the interaction at the site of infection, between the macrophage producing GM-CSF and the parasites. Another cytokine, interferon γ (IFN- γ), has also been shown to act as a growth factor for *T. brucei* bloodstream forms, an interaction which appears to play a role in the pathogenesis of the disease (Olsson *et al.*, 1991).

Receptors for host factors have also been identified in *T. brucei* which display similar characteristics and homology to those found in mammals. Antibodies to the mammalian EGF receptor recognised a 135kDa surface polypeptide in both procyclic and bloodstream forms of *T. brucei* (Hide *et al.*, 1989). This polypeptide was able to bind EGF and in trypanosome membrane fractions, EGF modified protein kinase activity. In addition, EGF stimulated the growth of procyclic forms *in vitro*. Similarly, mammalian EGF has been shown to promote growth of *T. brucei* bloodstream forms *in vitro* (Sternberg and McGuigan, 1994). In this paper the authors also suggest that EGF may have more influence upon trypanosome growth rate in tissues rather than in the bloodstream, due to low concentrations of EGF in the bloodstream compared to tissue and the comparatively high concentrations required to produce a mitogenic effect *in vitro*.

Trypanosomes also require serum lipoproteins and transferrin, obtaining these factors by receptor-mediated endocytosis (Coppens *et al.*, 1988, Webster and Grab, 1988). Receptors for both transferrin and host low-density lipoprotein have been identified in

the flagellar pocket region. The trypanosome LDL receptor shows significant cross-reactivity with the mammalian LDL receptor (Coppens *et al.*, 1992), while more recently a specific epitope defined by a monoclonal antibody has been identified on the extracellular domain of the trypanosome receptor (Bastin *et al.*, 1994). This epitope is accessible on living trypanosomes to antibodies and complement proteins, resulting in cell lysis. The receptor is also invariant in *T. b. brucei* (Coppens *et al.*, 1992), unlike the major VSG, a characteristic which has favoured the LDL-receptor as a possible candidate for vaccine development. Distinct binding sites of high-density lipoprotein (HDL) have also been detected in trypanosomes (Gillet and Owen, 1992). From these studies it appears that there may be two distinct types of binding sites for HDL. One type may be similar to mammalian HDL-receptors and play a role in cholesterol homeostasis, by allowing removal of cholesterol from the parasite. The other type exists in much greater numbers and may underlie the cytotoxic effect of human HDL upon trypanosomes (Hajduk *et al.*, 1989, reviewed by Lorenz *et al.*, 1995).

Transferrin uptake by trypanosomes has been studied using transferrin-colloidal gold complexes to identify parts of the endocytotic pathway (Webster and Grab, 1988). As well as a description of the organelles involved in the endocytotic process, this study also reported that VSG was co-internalized with the transferrin gold marker. Binding of transferrin-gold to the surface and the flagellar pocket was inhibited by the presence of excess free transferrin, suggesting that trypanosomes express transferrin receptors. A transferrin binding protein (TFBP) has been purified from bloodstream forms of *T. brucei* (Schell *et al.*, 1991). This protein is encoded by expression-site-associated genes (*ESAGs* 6 and 7, reviewed by Pays *et al.*, 1994), but is not found in procyclic forms, consistent with stage-specific expression of the multi-cistronic VSG transcription unit in bloodstream forms. TFBP is also modified by a C-terminal GPI-anchor and, like other glycoproteins, probably transported to the flagellar pocket in order to bind transferrin, before being internalized.

As well as receptors, evidence of receptor-associated proteins and intracellular signalling pathways in these parasites has also accumulated. G-proteins have been identified in plasma membrane preparations of *L. donovani* (Cassel *et al.*, 1991). *L. donovani* promastigotes possess high affinity GTP binding sites, as well as an endogenous GTPase activity in a fraction of these binding sites, thus providing further evidence of similarities with mammalian G-proteins. This study also showed that promastigotes possess a 38kDa protein (p38) which strongly reacts with an antiserum against a decapeptide containing the C-terminal sequence of transducin, the G-protein that mediates visual signal transduction. A similar antigen was also detected in two other *Leishmania* species, *L. major* and *L. mexicana*. The results suggest that a similar sequence to the C-terminal amino acids of the α -subunit of transducin is present in p38 and therefore may play a role in receptor-effector coupling.

Regulatory enzymes of cellular signalling such as protein kinases have also been found in kinetoplastids. Protein kinase activities detected in *T. brucei* bloodstream and procyclic forms, showed similar characteristics to mammalian protein kinase C (Keith *et al.*, 1990). Protein kinase C is a key enzyme in the cellular signalling pathway (Kuo *et al.*, 1980), which is activated by diacylglycerol (DAG), produced by the activation of phospholipase C and also by calcium. Three calcium/DAG-dependent protein kinase activities were separated from bloodstream trypanosomes, one of which showed substrate specificity for lysine-rich histone and protamine. This activity was also inhibited by the protein kinase C inhibitor, H7. A protein kinase assay of trypanosome homogenates *in situ* after separation by isoelectric focusing, revealed a greater number of kinases present in bloodstream forms, which differed from those in procyclic forms. A monoclonal antibody against mammalian protein kinase C also detected a specific polypeptide in bloodstream forms but not in procyclic forms. The occurrence of a protein kinase C like-activity in *T. cruzi* has similarly been described (Gomez *et al.*, 1989), as well as a soluble protein kinase activity in *L. donovani*

promastigotes (Banerjee and Sarkar, 1990). Both enzymes are postulated to play a role in growth and differentiation, although further characterisation is required.

More recently, protein kinases have been characterized which are capable of autophosphorylation (Hide *et al.*, 1994). Autophosphorylating protein kinases often play a regulatory role in other systems (Feder and Bishop, 1990). Two classes of autophosphorylating protein kinases were identified in *T. brucei*; one class which is dependent on ATP as a phosphate donor, while the other class is dependent upon GTP. Addition of mammalian EGF also stimulated autophosphorylation. The EGF receptor described previously (Hide *et al.*, 1989) also had a protein kinase activity. Again, further characterization is required to determine the full nature of the EGF-stimulated activity. An 89kDa serine-threonine protein kinase activity has also been identified in *T. brucei* (SPK89), which is regulated both in the life cycle as well as the cell cycle (Parsons *et al.*, 1993, Gale *et al.*, 1994). SPK89 activity was abundant in the proliferative slender and procyclic stages, whereas non-dividing stumpy forms and stationary phase procyclic forms exhibited minimal activity. Induction of SPK89 activity was also required for progression through S-phase shown by the correlation between inhibition of SPK89 activity and a concomitant block in the trypanosome cell cycle. As well as the study of serine-threonine protein kinase activity in *T. brucei*, Gale *et al.* (1994) also identified an increase in tyrosine phosphorylation after stimulation of serum-starved procyclic forms. This activity, however, was less dramatic than tyrosine phosphorylation in quiescent mammalian cells stimulated to re-enter the cell cycle (Cooper *et al.*, 1982).

Calcium plays a major role in cellular function (Orrenius and Bellomo, 1986). Ca^{2+} homeostasis is therefore critically important and has been examined in *T. brucei* (Moreno *et al.*, 1992) and *L. donovani* (Philosoph and Zilberstein, 1989). Evidence indicated that intracellular calcium levels in both parasites were regulated at low concentrations by mechanisms similar to those found in higher eukaryotes. The full

extent of the role of calcium as a second messenger, however, in response to the changing environment of these parasites remains to be fully determined.

Other studies have described the involvement of cyclic nucleotides such as cyclic AMP (cAMP) in the proliferation and differentiation of these parasites (Rolin *et al.*, 1993 and refs. therein). Activation of adenylate cyclase catalyses the conversion of ATP to cAMP. ESAG 4 and genes related to ESAG 4 (GRESAG 4) in *T. brucei* encode structurally distinct adenylate cyclases (Ross *et al.*, 1991, Paindavoine *et al.*, 1992). During synchronous differentiation of bloodstream forms to procyclic forms *in vitro* (see also section 1.3.2), transient stimulation of adenylate cyclase were observed (Rolin *et al.*, 1993). The first activity occurred 6-10 hours after differentiation was initiated following the release of VSG, while the second peak occurred after the first cell division, when the differentiated population began to proliferate. It appears that the first peak of activity was not responsible for triggering the differentiation process, but cAMP may be playing a role subsequent to the exchange of VSG for the major procyclic surface molecule, PARP. The authors also suggest that a link may exist between VSG release and adenylate cyclase activation and hypothesize that the ESAG 4 cyclase is inactivated by VSG, until a change in environmental conditions induces differentiation. This change in conditions triggers release of VSG, subsequent to which adenylate cyclase activity induces commitment to differentiate into procyclic forms.

The role of cAMP and adenylate cyclase has also been implicated in the differentiation of *T. cruzi* epimastigotes to infective metacyclic forms (Gonzalez-Perdomo *et al.*, 1988). The addition of cAMP and cAMP analogues, as well as adenylate cyclase activators and cAMP-phosphodiesterase inhibitors stimulated the transformation of epimastigotes to metacyclic trypomastigotes. Data obtained also indicated that adenylate cyclase might be activated by calmodulin and that G-proteins also appear to

be involved in adenylate cyclase activation. These studies suggest that cAMP is a key factor inducing differential gene expression and life cycle progression in *T. cruzi*.

Another molecular element similar to *c-myc* has been identified in *T. brucei* (Davis *et al.*, 1989). *c-myc* is involved in proliferation and apoptosis control in mammalian cells. Antibodies raised against a recombinant *myc* oncoprotein recognised a polypeptide in bloodstream and procyclic forms, suggesting a *myc* homologue occurs, which was further supported by Southern blot analysis.

Evidence of similarities between protozoan parasites and their host cells is therefore accumulating, in terms of molecular mechanisms of growth and differentiation. While at the biochemical and molecular level, intracellular signalling mechanisms in these parasites are becoming clearer, the relevance of these systems in terms of interactions between parasite and host *in vivo*, has yet to be fully determined.

One study has attempted to examine growth regulation of trypanosomes in chronic infections *in vivo* (Turner *et al.*, 1996). Trypanosome lines which were manipulated such that a population of cells all expressed the same VAT, were superimposed upon a chronic infection which expressed entirely different VATs. The fate of the secondary infection was then monitored using an antibody marker, in terms of its prevalence in the mixed infection. Results showed that growth of the secondary infection was significantly inhibited in the course of the chronic infection. This inhibition was neither specific to the line or VAT of trypanosomes used, nor specific to host. Accumulating evidence from this study suggests that trypanosomes in the secondary infection were not being killed by host immune responses. It appears that the inhibition of the secondary infection observed also occurred in the population as a whole and that slender form replication was down-regulated, rather than differentiation to stumpy forms up-regulated. Although the mechanism underlying

this inhibition remains to be determined, it is believed that this phenomenon may be a major determinant of virulence of trypanosome infections.

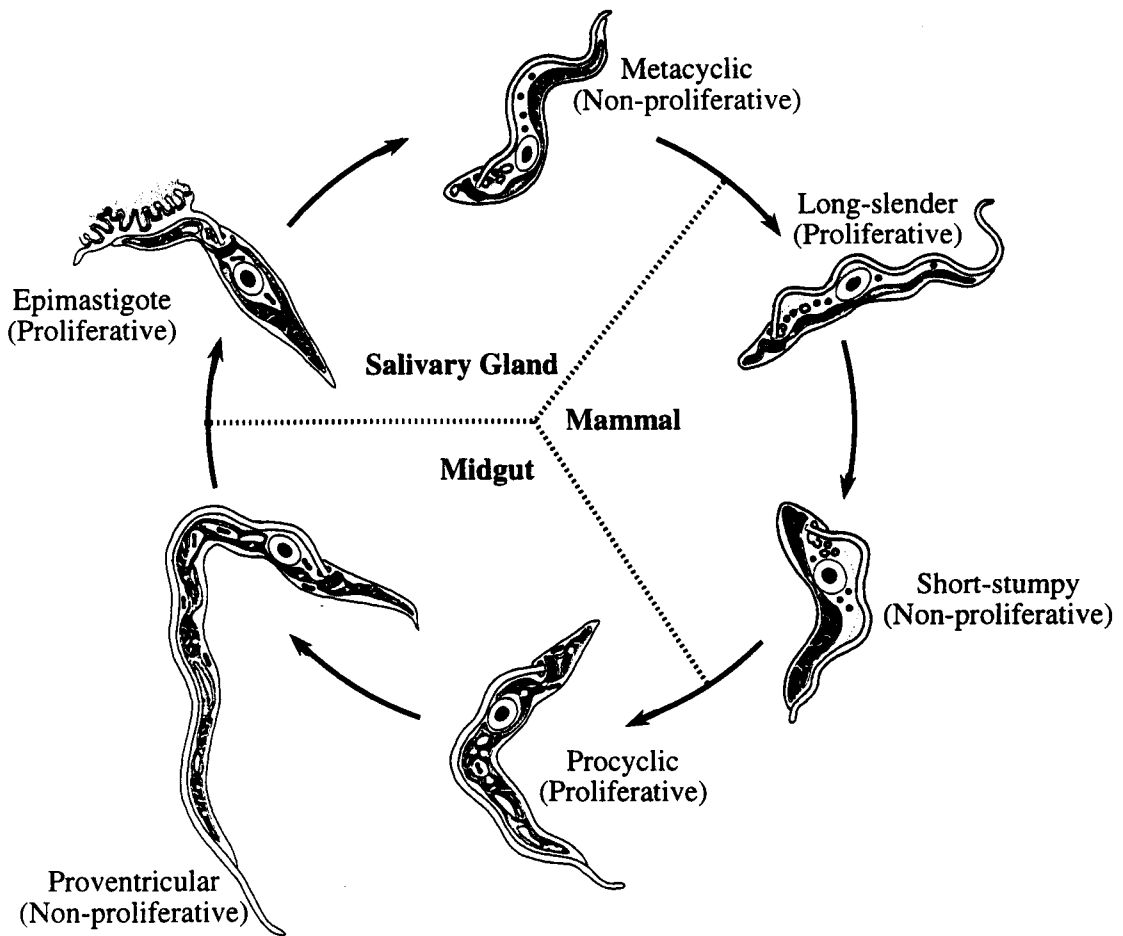
Much further work is required to fully understand the nature of growth of these parasites in their host environments, which is clearly complicated by a number of factors, including nutrition, host-derived regulators of growth and parasite/host genotype (Hide *et al.*, 1990).

1.5 Aims of the project

The general aims of this study were to investigate aspects of the cell biology, growth and differentiation in kinetoplastid parasites and links between the cell cycles and life cycles of these organisms. The work presented here can be considered as four separate stages:

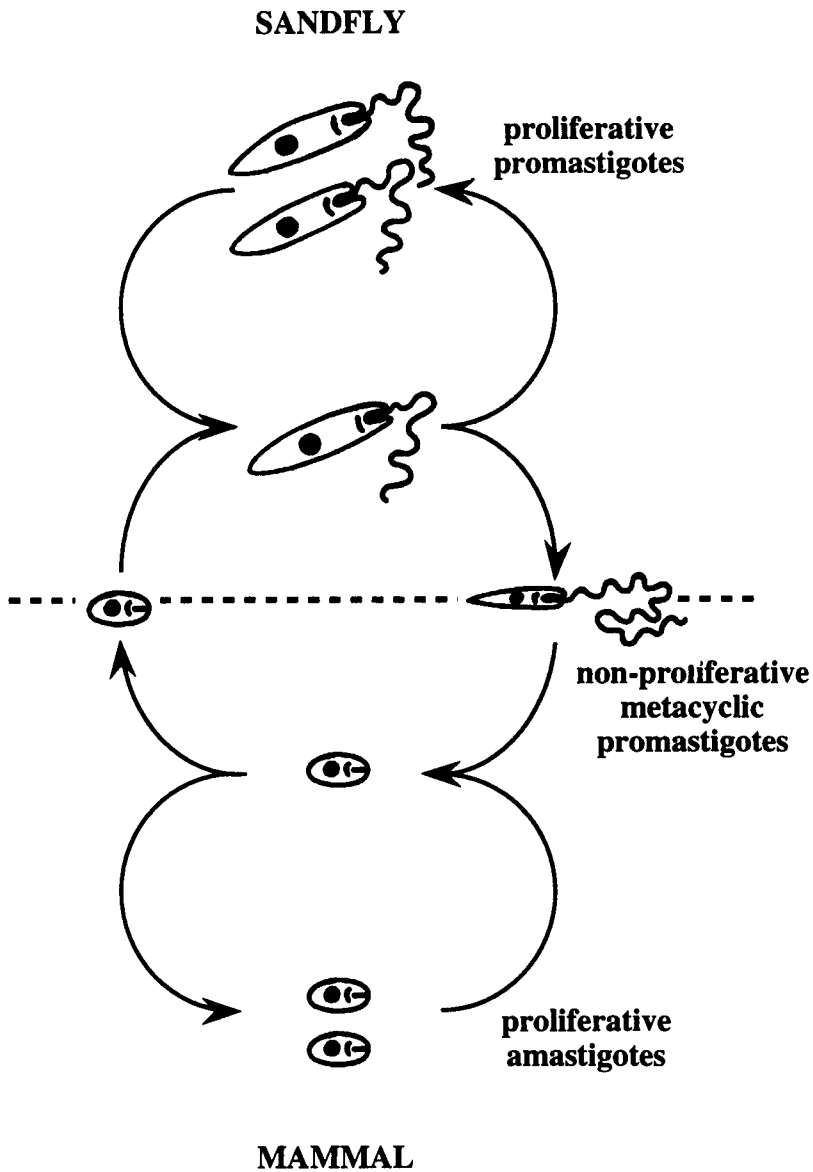
1. The analysis of the relative timing of cell cycle events in the nucleus and kinetoplast of *T. brucei* and *L. mexicana*. This study would allow comparison between life cycle stages, different morphological types of cells as well species (chapters 2 and 3).
2. Investigation of the proposed link between antigenic switching and the cell cycle of *T. brucei* bloodstream forms using both VAT-specific and cell cycle markers (chapter 4).
3. A study of the differentiation of promastigote to metacyclic forms in *L. major* using a number of metacyclic-specific markers to examine mechanisms of metacyclic production both at the population and cellular level (chapter 5).
4. The generation of 'growth' mutant trypanosomes which overcome growth inhibition in chronic infections (chapter 6).

Figure 1.1
Life Cycle of *T. brucei*



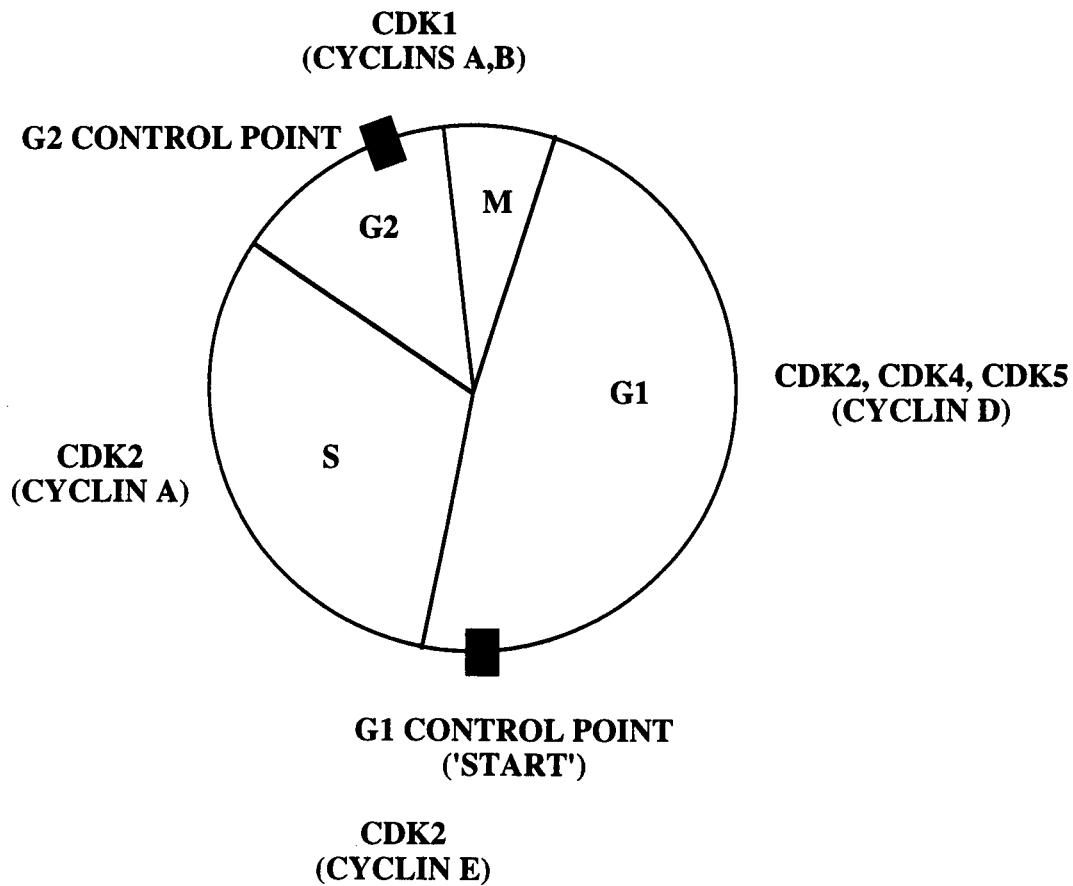
The life cycle of *T. brucei* consists of at least 6 distinct stages. It can be considered in terms of 3 different environments (tsetse salivary gland, mammalian host, and tsetse midgut) each of which contains two life cycle stages. In each environment, one life cycle stage undergoes proliferation thereby establishing a dense infection in the current environment. The other stage is non-dividing but is capable of migrating or being transmitted to a new environment, whereupon it changes morphology to a dividing form, capable of establishing a new infection (adapted from Vickerman, 1985).

Figure 1.2
Life Cycle of *Leishmania*



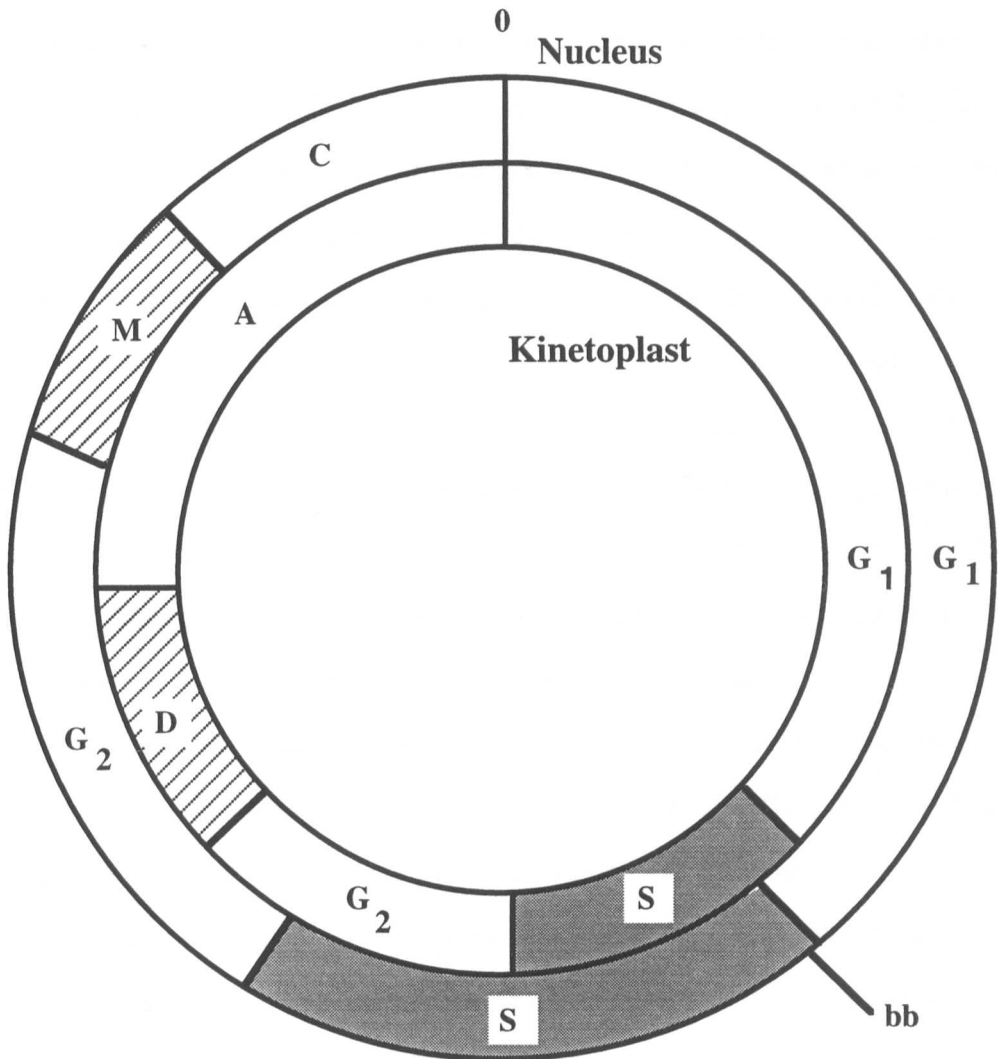
The life cycle of *leishmania* consists of at least three distinct stages. Proliferative promastigote forms are found in the midgut of the sand fly, establishing dense infections. Migration towards the foregut and mouth parts is accompanied by transformation to non-dividing metacyclic forms, which are infective to the mammalian host. After the initial infection these forms are phagocytosed by macrophages and exist as proliferative intracellular amastigote forms. On ingestion of a bloodmeal by the fly, amastigotes undergo transformation to proliferative promastigote forms (figure courtesy of P. Bates).

Figure 1.3
Cell Cycle Control in Mammalian Cells



A model for the action of CDK-cyclin complexes during the mammalian cell cycle. Cyclin D refers to all three D-type cyclins. New cyclins and CDKs continue to be identified such that this model is likely to be modified (adapted from model in *Molecular Cell Biology*, 1995).

Figure 1.4
Cell Cycle of *T.brucei* Procyclic Forms



The relative timing of cell cycle events in *T.brucei* procyclic forms (Woodward and Gull, 1990). The figure shows (1) the approximate synchrony of basal body (bb) replication and initiation of nuclear and kinetoplast S-phase, (2) the asynchrony of the termination of S-phase and of kinetoplast division (D) with nuclear mitosis (M) and (3) the extended phase of cytokinesis in both organelles (C and A) for the nucleus and kinetoplast respectively. The average cell cycle length was 8.5hrs (figure from Turner, 1992).

CHAPTER 2 DESCRIPTIONS OF THE CELL CYCLES OF *T. BRUCEI* AND *L. MEXICANA*

2.1 Introduction

Few studies have examined in detail the timing of cell cycle events in kinetoplastids. Timing is likely to be important because of the requirement to replicate and segregate each of three organelles; nucleus, kinetoplast and basal body subtending the flagellum, during the cell cycle. In most of the earlier work, little attention was paid to the exact timing of events, or to the morphological events associated with division. To visualise periods of DNA replication, these studies used autoradiographic detection of [³H]-thymidine incorporated into the DNA of the nucleus and the kinetoplast. The occurrence of a discrete period of DNA replication for the kinetoplast, as well as for the nucleus was identified. A close relationship between S-phases for the nucleus and kinetoplast was described, although slight differences between the timing of initiation of nuclear and kinetoplast S-phases were noted, depending upon species and culture conditions (reviewed by Simpson, 1972). Co-ordination in timing of the initiation of nuclear and kinetoplast S-phase was observed in *T. mega* (Steinert and Steinert, 1962), *C. luciliae* (Van Assel and Steinert, 1971) *L. tarentolae* (Simpson and Braly, 1970) and *C. fasciculata* (Cosgrove and Skeen, 1970). These observations contrast strongly with those observed in other organisms, such as *Tetrahymena* (Parsons, 1965, Parsons and Rustad, 1968), *Physarum* (Evans, 1966) and HeLa cells (Koch and Stokstad, 1967), where mitochondrial DNA synthesis occurs continuously throughout the cell cycle and is not linked to nuclear DNA replication or segregation.

A reservation with these older studies is that, due to the limitations of the techniques available, periods of organelle division could not be clearly defined. It was generally found that kinetoplast division occurred before mitosis, but this varied between species and culture conditions (Simpson, 1972). A period of cytokinesis was also not identified in any of these analyses as being a separate phase after mitosis and kinetoplast division.

The only detailed study to date of a cell cycle in a kinetoplastid has been the analysis of the timing of cell cycle events in *T. brucei* procyclic forms (Woodward and Gull, 1990). This analysis followed previous work which described the morphological events of the procyclic form cell cycle (Sherwin and Gull, 1989). Cells grown *in vitro*, were incubated with the thymidine analogue 5-bromo-deoxyuridine (BrdU), which is incorporated into the DNA of cells during S-phase of the cell cycle. The durations of S-phase for both nucleus and kinetoplast were ascertained using an anti-BrdU monoclonal antibody (Gratzner, 1982) detected by immunofluorescence microscopy. This technique is very sensitive and has been used to visualise periods of DNA replication in a variety of mammalian cell and tumour cell lines (Williamson, 1993). BrdU labelling *in vitro*, therefore, is an extremely useful method for monitoring cell proliferation rates as well as for analysing the timing of S-phase in the context of the other cell cycle events.

In the study of cell cycle events in *T. brucei* procyclic forms (Woodward and Gull, 1990), a close relationship between the initiation of nuclear and kinetoplast S-phase was observed, while no apparent synchrony was observed in the post S-phase events. Kinetoplast division was completed before the initiation of mitosis and an extended period of cytokinesis for the kinetoplast and the nucleus was also defined. Basal body replication, initiating generation of a new flagellum, was also described and was found to almost co-incide with the start of nuclear S-phase, marking the first cytological event of the cell cycle so far described. Initiation of paraflagellar rod synthesis was also identified. Thus a 'map' of cell cycle timing, as well as key morphological events was constructed.

Neither quantitative analysis, nor detailed examination of morphological events associated with the cell cycle has been conducted on any *Leishmania* species. The timing of events for the nucleus and kinetoplast, has been based so far upon observations of division sequences in promastigote forms in the sandfly and in *in vitro*

culture. In promastigote forms multiplying inside the sandfly midgut, outgrowth of a daughter flagellum marks the beginning of division, remaining shorter than the parent flagellum throughout the cell cycle (Killick-Kendrick, 1979). The nucleus was found to completely divide before the kinetoplast, a feature generally found for most *Leishmania* species, although the opposite sequence of events i.e kinetoplast division before mitosis is complete, has been observed in some culture forms (Christophers *et al.* 1926, Adler, 1964, Killick-Kendrick and Rioux, unpublished observations, cited in Molyneux and Killick-Kendrick, 1987). Once both organelles have divided, the body of the promastigote divides into two equal parts by a longitudinal cleft arising between the two flagella and continues posteriorly.

It was the aim of this current study to analyse the timing of cell cycle events in *T. brucei* bloodstream forms, using the BrdU labelling technique and compare results obtained from a similar analysis carried out in procyclic forms. This study would confirm whether or not the pattern of events is life cycle stage specific. Also, a study of cell cycle events in *L. mexicana* promastigote forms was carried out to ascertain whether or not a common pattern of cell cycle events exists between *L. mexicana* and *T. brucei* and between trypano- and promastigote forms of kinetoplastids.

2.2 Materials and Methods

2.2.1 Culturing of *T. brucei* and *L. mexicana*

***T. brucei* bloodstream forms**

Bloodstream culture medium (BSCM) used was based upon that described by Baltz *et al.*, (1985) and modified by Mhlanga and Shall (unpublished data). Incomplete medium contained :- Minimum Essential Medium with Earle's salt's (1 litre, Gibco), Non-essential Amino Acid Concentrate (x100) (10ml, Gibco), Hepes (6.0g), Glucose (1.0g), Sodium Bicarbonate (2.2g) and L-Glutamine (0.3g) (all chemicals from Sigma unless otherwise stated). This was made to a final volume of 1100ml with deionised double-distilled water and the pH was adjusted to 7.3. It was filtered sterilised

through a 0.22µm filter and stored for up to 3 months at 4°C. Before use the following supplements were added:- Thymidine (0.1mM), Hypoxanthine (0.016mM), Dithiothreitol (0.4mM), Sodium Pyruvate (2.0mM), Catalase (1.7µg/ml), Adenosine (0.04mM), Guanosine (0.02mM), and 20% non-heat inactivated Foetal Calf Serum (GIBCO).

T. brucei bloodstream forms (of a cloned line, GUTat 7.1) were harvested from a mouse (8 week old, female CFLP mice) with a parasitaemia in exponential growth and greater than 3×10^7 cells/ml by cardiac puncture, into a syringe containing 0.1ml heparin (500 units/ml) in Earle's balanced salts, under sterile conditions. The infected blood was then mixed with two volumes of complete BSCM and centrifuged at room temperature at 150g for 10 minutes. The resulting supernatant containing the trypanosomes, was then removed and diluted with complete BSCM to give a starting density of 1.5×10^5 cells/ml. Cultures were incubated at 37°C, in 5% CO₂.

***T. brucei* procyclic forms**

GUTat 7.1 bloodstream forms were grown in mice, harvested and transformed to procyclic forms in semi-defined medium (designated SDM-79, Brun and Schonenberger, 1979) supplemented with 10% heat-inactivated foetal calf serum (FCS) (Gibco) and 3mM cis-aconitate (Brun and Schonenberger, 1981). Transformed cells were cultivated in complete SDM-79 with 10% HI-FCS, at 27°C.

***L. mexicana* promastigote forms**

Promastigote forms, obtained by transformation of lesion amastigotes grown in mice, (Hart *et al.*, 1981a, b) were grown in modified Eagle's Minimal Essential Medium with Earle's salts (S-MEM) for hemoflagellates (designated HOMEM, Berens *et al.*, 1976) supplemented with 10% HI-FCS, at 26°C.

2.2.2 BrdU labelling

20mls of an exponentially growing culture was split into two 10ml flasks. To one flask was added 40 μ M of BrdU and an equimolar amount of 2-deoxycytidine. Both flasks were incubated at the stated temperatures for each culture form (section 2.2.1) and 0.5ml samples were taken from each culture at half-hourly intervals for a period of four hours. Cells were harvested by centrifugation (500g, room temp. for 10 minutes) and washed in cold phosphate buffered saline (PBS), pH 7.4. Thin smears were then made on slides, air-dried and fixed in 75% ethanol at 4°C for one hour. Slides were stored at -20°C, with silica gel, until processed for immunofluorescence analysis.

2.2.3 Immunofluorescent detection using an anti-BrdU antibody

Fixed cells were denatured in 1.5M HCl at room temp. for 20 mins., to allow the antibody access to the sites of DNA incorporation. Slides were washed approximately ten times in PBS (pH 8.0), to remove acid and then incubated for 70 mins. at room temperature in a humid chamber with an anti-BrdU antibody, supplied as a working strength solution (Amersham). After washing twice in PBS, the slides were incubated with a second antibody labelled with fluorescein isothiocyanate (FITC) (SAPU) diluted 1 in 50 with PBS for 45 mins in a humid chamber at room temp. The slides were washed briefly and stained with the DNA intercalating dye (4,6,-diamino-2-phenylindole (DAPI)) at 0.01 mg/ml as described by Woodward and Gull (1990), rinsed in PBS and then the slides mounted in Mowiol containing 1,4-Diazobicyclo-[2.2.2] octane (DABCO) as an anti-fading agent. Mowiol solution was made as described by Heimer and Taylor (1974). Two controls were used: one with the second antibody only and the other using cells that had not been cultured with BrdU.

2.2.4 Growth rate of cultures

Cell densities in BrdU labelling experiments and control cultures were counted each hour for 8 hours using an improved Neubauer haemocytometer and the growth rate, r , calculated by least squares regression analysis. The population doubling time (PDT) was calculated from $PDT = \log_e 2 / r$.

2.2.5 Cell cycle analysis**Periods of division and cytokinesis**

Frequencies of cells with the following nuclear and kinetoplast configurations, were determined for each organelle: (1) single organelle (2) dividing organelle (3) post-division. Organelles classified as dividing were those which were elongated or ovoid in shape. At least 500 cells were classified accordingly at each half-hourly interval. Using the analysis of Williams, (1971) the durations of mitosis (M) and cytokinesis (C) for the nucleus and the corresponding periods of division (D) and cytokinesis (A), for the kinetoplast, were determined as follows:

$$x = \frac{\log_e (1-y/2)}{-r}$$

where x is the cumulative time within the cell cycle taken to reach the end of the morphological stage in question, y is the cumulative % of cells up to and including the morphological stage in question, expressed as a fraction of one unit and r is as described in 2.2.4. This method of analysis requires that the following criteria are met: (1) that the position of a particular stage in the cell cycle is known, (2) the culture is truly asynchronous and (3) the generation time is constant.

G2-phase

As G2-phase is the period intermediate to S-phase and organelle division (either mitosis or kinetoplast division), the time taken for 50% of dividing organelles to

become labelled with BrdU was taken as the average G2-phase (Stanners and Till, 1960). A sample of 100 dividing organelles was counted at each time point.

S-phase

The duration of S-phase was calculated by counting 1,000 cells at individual time points and classifying them as labelled or unlabelled for each organelle. These frequencies were analysed using the treatment derived by Stanners and Till (1960). To calculate S-phase, the duration of the total post-S period is required as well as the percentage labelled cells for either organelle at a particular time point. S-phase could therefore be calculated using the equation;

$$S = 1/r \log_e[L + e^{r(z)}] - (z + t),$$

where r is as previously described, L is the percentage cells labelled for either nucleus or kinetoplast, z is the post S-period i.e. G2+M+C for the nucleus or G2+D+A for the kinetoplast and t is the duration of the labelling period.

G1-phase

The duration of G1-phase was calculated by the summation of all the other phases and subtraction from the total cell cycle time.

2.2.6 Morphological analyses

2.2.6.1 Effects of air-drying, fixation and storage of smears on organelle morphology

GUTat 7.1 bloodstream forms were harvested from a mouse as previously described (see section 2.2.1). Bloodstream forms were separated from blood by centrifugation in Carter's Balanced Salt Solution (CBSS, Fairlamb *et al.*, 1992) washed twice and then handled in the following ways;

1. Thin smears were made on slides, air-dried and then fixed in 75% ethanol for one hour at 4°C.
2. Cells were settled onto poly-L-lysine (M.W. 40,000, Sigma) coated slides in CBSS for 15 minutes, at 25°C in a moist chamber. The buffer plus any cells still in suspension were removed and replaced with 75% ethanol for one hour at 4°C.
3. Air-dried smears fixed in ethanol as described before, were again air-dried, post-fixation and stored overnight with silica gel at -20°C.
4. Air-dried smears were stored in 75% ethanol at 4°C overnight.

Cells were DAPI stained, as described previously and counts of organelle configuration conducted.

2.2.6.2 Kinetoplast length in *L. mexicana* promastigote forms

Lengths of kinetoplasts were determined by taking prints (Ilford HP5 400ASA) of sample populations of DAPI stained images at x1000 magnification and measuring lengths of kinetoplasts in two categories: cells with one kinetoplast and cells with two kinetoplasts. Widths of kinetoplasts were excluded from this analysis because they were observed to be very constant.

2.3 Results

2.3.1 *T. brucei* bloodstream forms

2.3.1.1 Growth rate of *T. brucei* bloodstream forms

Growth curves of the control culture and culture incubated with BrdU (Figures 2.1A and B respectively) indicated that the cells grew exponentially over the time course studied. The PDT for the control culture was calculated as 8.15 hrs ($r^2=0.93$) and for the BrdU containing culture was calculated as 8.25hrs ($r^2=0.97$). These data demonstrate that the BrdU had a negligible effect upon the growth rate and also indicate that the cultures grew exponentially, with a constant generation time.

2.3.1.2 BrdU labelling

Figure 2.2 shows progression through the cell cycle of *T. brucei* bloodstream forms. A-E are the phase contrast images, F-J the DAPI stained images of cells at progressive stages of the cell cycle and K-O, BrdU labelling of nuclei and kinetoplasts. F shows a cell in the early part of the cell cycle (G1-phase), with a single nucleus and kinetoplast. K indicates that the kinetoplast is in S-phase. The cell in G has an elongated kinetoplast and therefore in division. The corresponding FITC labelled image (L) indicates that the nucleus is now in S-phase. The nucleus elongates (H) and is therefore in mitosis. Kinetoplast division occurs before mitosis and the two daughter organelles segregate (I). After mitosis occurs, the daughter organelles are in a period of cytokinesis (J), before they re-assort themselves on either side of the division plane that divides the cell longitudinally.

2.3.1.3 Cell cycle analysis

Periods of division and cytokinesis

Frequencies of cells with single, dividing and post-division organelle configurations were ascertained (see Table 2.1). Examples of these configurations can be seen in the DAPI images of Figure 2.2. These frequencies were then used to calculate the lengths of mitosis (M) and cytokinesis (C) for the nucleus and the corresponding periods of division (D) and cytokinesis (A) for the kinetoplast (see Table 2.2).

G2-phase

The kinetics of appearance of BrdU label for each dividing organelle is shown in Figures 2.3A and B. The average duration of G2-phase was the time taken for 50% of the dividing organelles to become labelled. For the nucleus (Figure 2.3A) this was 0.92hrs and for the kinetoplast (Figure 2.3B) this was 1.00hr. A curve was fitted to the data using 'spline' fit (*Grafit* 3.0, Erithacus Software Ltd.,1992).

S-phase

The percentages of cells with either labelled nuclei or kinetoplasts were determined and, knowing the total post-S phase period calculated from the above data, the length of S-phase for each organelle was determined. This calculation was made for two different time points in the growth curve for each organelle: 1.0 and 1.5hrs for the kinetoplast and 2.0 and 2.5hrs for the nucleus. For each organelle, each time point produced similar results and the data from the two time-points were therefore combined to determine the average duration of S-phase, the values of which are given in Table 2.2.

G1-phase

The length of G1-phase was calculated by adding the durations of all the other phases and subtracting these from the total cell cycle time (Table 2.2).

2.3.1.4 Cell cycle maps

From the above calculations, the durations of each phase of the cell cycle were mapped (Figure 2.4A). This study of cell cycle events in *T. brucei* bloodstream forms shows that S-, G2- and M-phase in the kinetoplast (k) all start and end before the corresponding phases in the nucleus (n). Initiation of S_n and S_k occurs close together, suggesting that there may be a degree of co-ordination in timing between these two organelles at this point in the cell cycle. There is no apparent co-ordination in the timing of the post-S period and an extended period of cytokinesis for the nucleus and particularly the kinetoplast can be identified.

Cell cycle maps were also constructed for *T. brucei* procyclic forms and *L. mexicana* promastigote forms (Figure 2.4B and C), however, the data leading to their construction is not shown. In both cases, a similar pattern to that in *T. brucei* bloodstream forms was observed. S-, G2- and M-phase in the kinetoplast all start and end before corresponding events in the nucleus. However, no apparent synchrony

was observed in the timing of S-phase, nor in the post-S period. An extended cytokinesis period was identified for both organelles in both forms, particularly in the kinetoplast, although of much shorter duration in promastigote forms.

2.3.2 Morphological analyses

Upon examination of the cell cycle maps constructed, it was found that there were differences between the lengths of cell cycle phases for each form examined, in comparison to corresponding cell cycle events for procyclic forms, previously described (Woodward and Gull, 1990). As a proportion of the total cell cycle time, the lengths of S-phase for the nucleus and the kinetoplast were less than half the value for the corresponding events in procyclic forms. More strikingly, however, were the differences between the lengths of the periods of division; values calculated for the lengths of mitosis and kinetoplast division in all three forms were found in this study to be approximately three times that of corresponding values in procyclic forms observed by Woodward and Gull (1990). The value for the length of mitosis is also considerably greater than equivalent values in a range of organisms (see for example: *S. pombe* <10% (Mitchison and Creanor, 1971); mammalian cells in culture, e.g. fibroblast cell line 12% (Fertig *et al.*, 1990). To investigate these differences, the effects of air-drying of smears compared to cells settled onto poly-lysine coated slides were assessed in order to ascertain whether or not the treatment of cells affected the subsequent classification of organelles. In addition, the way in which smears were fixed and stored before being processed for immunofluorescence was also assessed, to determine the possibility of artefacts of organelle morphology arising and therefore contributing towards misclassification of the organelles.

Another possibility considered, was the introduction of a systematic bias into the data from too many organelles being classified as dividing. This bias, if present, would have led to longer periods of mitosis and kinetoplast division being calculated. To assess this possibility, an 'independent' score of organelle configurations was carried

out, in order to ascertain whether or not a bias had been introduced into my own classification criteria.

Cells were DAPI stained, as described previously, before counts of organelle configurations were conducted. Frequencies of cells with single, dividing and post-dividing organelles were determined for each of the four treatments and are given in Table 2.3A. To determine whether the method of air-drying, fixing or storing smears was affecting the results, the frequencies of cells with particular organelle configurations were compared.

To determine whether any systematic bias was apparent in the classification of organelle configurations, slides from each of the four treatments were analysed 'blind' by an independent observer, Dr. Mike Turner, (Table 2.3B) and the results of the two observers compared.

Results shown in Table 2.3A demonstrate that there were few differences between percentages of organelle configurations for the four treatments and therefore seems to indicate that the treatment of the cells had little effect upon the classification criteria. These results are comparable to the organelle configurations used to calculate the durations of the periods of division and cytokinesis for the nucleus and kinetoplast (see Table 2.1 and Figure 2.4A). Upon comparison with results in Table 2.3B, however, notable differences could be seen between the two sets of counts. Of most significance, were the differences between percentages of single and dividing nuclei and kinetoplasts; under my classification (Table 2.3A) the number of dividing organelles identified were approximately three times those classified as dividing in Table 2.3B. This, in turn, resulted in lower numbers of single organelles being identified. These counts seem to indicate that there was a bias in the classification of nuclei and kinetoplasts and that too many organelles were classified as dividing. Using these data to calculate the lengths of mitosis and kinetoplast division resulted in

an approximately three fold increase in the lengths of these cell cycle periods. Furthermore, the methods of calculation employed will also have resulted in potential errors in determining the duration of G2-phase for each organelle.

While carrying out a similar cell cycle analysis (see section 2.2.5) for *T. brucei* procyclic forms and *L. mexicana* promastigote forms (data not shown), a number of difficulties were encountered, which could in part explain the bias in the data and therefore the misclassification of organelles. The major problem for each of the three stages examined, was the failure to identify accurately dividing organelles. In comparison to nuclei and kinetoplasts round in shape and therefore classified as single, organelles which were ovoid were all classified as dividing. Another problem was the difficulty in identifying mitotic spindles at the resolution of the light microscope, which are formed during mitosis and have been demonstrated by electron microscopy (reviewed by Vickerman and Preston, 1976). The presence of the mitotic spindle would have provided a further marker for identifying dividing nuclei (Woodward and Gull, 1990), but their preservation is noted as being unpredictable on fixation (Vickerman and Preston, 1976).

A particular problem encountered in classifying dividing kinetoplasts of *T. brucei* bloodstream and procyclic forms, was the close proximity with which two post-divided kinetoplasts were positioned with respect to one another (Figures 2.5A and B). On first examination, it appeared that the kinetoplasts were bilobed and therefore still dividing, a factor which may also have contributed to a greater number classified as dividing.

Kinetoplasts of *L. mexicana* promastigote forms posed an extra difficulty with regard to interpretation, because a large number of them were elongate rather than round (Figure 2.5C). To investigate further whether pre-division kinetoplasts were all round or perhaps elongate, a frequency distribution of kinetoplast length was constructed to

compare lengths of kinetoplasts in cells with one kinetoplast to cells with two kinetoplasts. Figure 2.6 is a frequency histogram of the measurements. Cells with two kinetoplasts represent daughter cells of the next generation, hence the lengths of these kinetoplasts would be representative of kinetoplasts before initiation of elongation and division. For the histogram of post-division kinetoplasts, kinetoplasts with lengths $0.7\mu\text{m}$ and $0.9\mu\text{m}$ were each calculated as a proportion of the number with length $0.5\mu\text{m}$. I then assumed that the proportion of kinetoplasts in the different length classes for non-dividing kinetoplasts in cells with only one kinetoplast per cell should be similar. These calculations result in the 'predicted' values indicated in Figure 2.6. The differences between observed and predicted numbers for the lengths of kinetoplasts in cells with only one kinetoplast should approximately correspond to the numbers of dividing kinetoplasts.

Approximately 42.7% of kinetoplasts according to these calculations were elongate, a value extremely close to that for the number of kinetoplasts classified as dividing (43%) by the classification of organelles (see section 2.2.5) and represented in the cell cycle map (Figure 2.4C). From Figure 2.6, a high number of cells (34% of total) with one kinetoplast were measured as being $0.9\mu\text{m}$ in length. One interpretation of these data is that kinetoplast division is indeed unusually protracted. I would, however, view this as being highly unlikely and that a proportion of these kinetoplasts must have been representative of single, non-dividing kinetoplasts. This variation in length of kinetoplasts, therefore casts some doubt over using a frequency method of this kind to ascertain the true number of dividing cells; it seems likely that a bias introduced into the data could explain the high number of kinetoplasts classified as dividing and that carrying out a frequency analysis only illustrated the length variation, rather than give a true figure for kinetoplasts undergoing division.

2.4 Discussion

This study represents the first description of the cell cycle in *Leishmania mexicana*, as well as being the first description of the mitochondrial DNA cycle in both *T. brucei* bloodstream forms and *L. mexicana*. From this description of cell cycle events in *T. brucei* and *L. mexicana*, a number of features have been identified; S-, G2- and D-phases in the kinetoplast, started and ended before corresponding events in the nucleus. In bloodstream forms, initiation of S-phase was close together, suggesting possible synchrony of this event between the two organelles. This is similar to the situation in other kinetoplastids previously examined (Simpson, 1972, Woodward and Gull, 1990). There was, however, no apparent synchrony observed in the timing of S-phase in procyclic and promastigote forms. There was also no apparent synchrony in the post-S period in all three forms examined and an extended cytokinesis period particularly in the kinetoplast, was identified, although of shorter duration in *L. mexicana*.

In comparison to cell cycle events examined in *T. brucei* procyclic forms (Woodward and Gull, 1990), a number of differences can be observed. In that study, initiation of S-phases for the nucleus and kinetoplast occurred very close together and each S-phase was of longer proportional duration than was observed in the current investigation (see Table 2.2). Kinetoplast division was completed before mitosis was initiated in the Woodward and Gull (1990) study whereas an overlap in the timing of these two events was calculated for all three forms (see Figures 2.4A-C). The lengths of division calculated in the previous study, were also much shorter, with kinetoplast division and mitosis each occupying approximately 10% of the total cell cycle time, whereas I have calculated values for these periods of division and mitosis as being approximately three times longer. While the construction of cell cycle maps enabled comparisons to be made between the timing of nuclear cell cycle events with respect to kinetoplast events as well as cell cycle timing between the two species, dramatic differences between the present and previous study (Woodward and Gull, 1990) led

to an investigation of the potential difficulties in identifying dividing organelles. Upon closer examination of the classification criteria adopted in this study (see section 2.3.2), it was found that a bias was likely to have been introduced into the data and that this led to the calculation of longer periods of kinetoplast division and mitosis. It seems unlikely that the way in which the cells were treated before organelle classification was conducted, contributed towards this bias (see also section 2.3.2).

In terms of cell cycle timing, the vast majority of studies of eukaryotic cell lines, including mammalian cells, describe mitosis as being relatively short in comparison to the other cell cycle phases and is on average only 10% of the total cell cycle time (see section 1.2.2). One exception of this is embryonic cells which are in mitosis for about 40% of the total cell cycle (Murray and Kirschner, 1991). It seems unlikely, therefore, that protozoan parasites would have a protracted mitotic phase.

An unfortunate effect arising from the errors in classifying dividing organelles is that the lengths of other periods of the cell cycle were also affected in the analysis. To estimate the duration of their respective G2-phases, labelled mitotic nuclei and labelled dividing kinetoplasts were identified over a time course (see section 2.2.5). From analyses of the increases in proportions of labelled organelles with time, the average G2-phase was estimated as the time taken for 50% of the organelles to become labelled in bloodstream forms (see Figures 2.3A and B). Upon examination of the curves constructed for bloodstream forms, it can be seen that experimental points lie below the fitted theoretical curve at the top of the peak. This was similarly the case for procyclic and promastigote forms (data not shown). The graphs constructed were probably a result of a misclassification of labelled dividing organelles (Steel, 1986). A bias towards too many organelles being classified as dividing and labelled would therefore introduce error into the length of G2-phase calculated. An alternative method of calculating the duration of G2-phase can be made from the peak of the differential or 'rate of change' of the original curves

(Stanners and Till, 1960). Values obtained from this second method were similar to those determined as the times when 50% of dividing organelle were labelled (data not shown), although the misclassification of organelles would also contribute towards the same error in the calculation of G2-phase. As a result, the lengths of G2-phase were shorter in comparison to corresponding lengths in procyclic forms (see Table 2.2 and Woodward and Gull, 1990); a bias towards organelles classified as dividing would lead to the 50% point being reached in a shorter time period.

To calculate the lengths of S-phase, the total post-S-phase period is required i.e. G2+M+C for the nucleus and G2+D+A for the kinetoplast (Stanners and Till, 1960). Misclassification of the organelles would affect the lengths of the post S-phase periods, particularly G2-phase and the periods of division and in turn affect the lengths of S-phase calculated. As a result, the durations of S-phase calculated for both organelles in bloodstream forms (Table 2.2 and Figure 2.4A), as well as procyclic and promastigote forms (Figures 2.4B and C) were shorter in comparison to those determined for procyclic forms (Woodward and Gull, 1990).

This study of *T. brucei* and *L. mexicana* confirms that the kinetoplastid cell cycle consists of the same general features of eukaryotic cell division, as first described by Howard and Pelc (1953). Kinetoplastids uniquely have two cell cycles in one; the nucleus and kinetoplast go through a similar pattern of events, most notably, DNA replication, mitosis/division and cytokinesis. Initiation of nuclear and kinetoplast DNA replication appears to be co-ordinated, while subsequent events are asynchronous in timing. The close timing of initiation of nuclear and kinetoplast S-phase, may be a feature of intracellular regulation and the availability of substrates to both organelles at only one part of the cell cycle (Simpson, 1972). This is unlike the situation in other eukaryotes, which can contain quite large numbers of mitochondria and undergo DNA synthesis continuously throughout the cell cycle, as seen in *Physarum* (Evans, 1966), *Tetrahymena* (Parsons, 1965, Parsons and Rustad, 1968)

and mouse L cells (Bogenhagen and Clayton, 1977). Kinetoplastids are also different from other eukaryotes in that they only contain a single mitochondrion and its DNA is concentrated in an associated organelle, the kinetoplast.

There is no evidence of a link between the nucleus and kinetoplast, in terms of which organelle initiates DNA replication first and whether or not this event is under inter-organelle control. While two major cell cycle check-points have been identified in yeast and higher eukaryotes, one in G1-phase prior to entry into S-phase at a point called 'START', when the cell is committed to DNA replication and the other in G2-phase before entry into mitosis (Nurse, 1990, Morgan, 1995), it is as yet unclear whether or not the same check-points exist in the cell cycles of kinetoplastids. The identification of cdc2-related protein kinases in trypanosomatids (reviewed by Mottram, 1994) provide some evidence of similarities in cell cycle control between kinetoplastids, yeast and higher organisms. Whether or not these molecules play a part in check-point control, however, needs to be established.

While the initiation of nuclear and kinetoplast S-phase appears synchronous, the post-S-phase periods are non-co-ordinated in timing. In *T. brucei* procyclic forms, a daughter flagellum elongates on the newly matured basal body (Sherwin and Gull, 1989). The flagellum emerges from the flagellar pocket with detection of the paraflagellar rod. Both basal body replication and paraflagellar rod synthesis have been identified and are completed before the end of DNA replication (Woodward and Gull, 1990). After the completion of DNA replication, the organelles are re-arranged to well defined positions, before the division plane is formed. The kinetoplast divides first into two daughter organelles, which are re-positioned with their associated basal bodies, parallel to the division plane (Sherwin and Gull, 1989). A direct link between the kinetoplast and flagellar basal body has been described, in which segregation of the kinetoplast DNA is dependent on a microtubule mediated separation of the new and old flagellar basal bodies during the cell cycle (Robinson and Gull, 1991). The

basal bodies move apart before the daughter flagellum has reached its full length. The kinetoplast therefore has an extended period of cytokinesis, a feature also noted in this study, before nuclear division occurs. Mitosis occurs within the nucleus (the nuclear membrane doesn't degrade during mitosis) and the two resulting daughter nuclei are also re-positioned to ensure partitioning of the cell. Neither basal body replication nor daughter flagellar growth was investigated in this study but it is assumed that a similar pattern of events occurs in bloodstream forms and *L. mexicana* promastigote forms.

While this study concentrated on the timing of cell cycle events for the nucleus and the kinetoplast, similarities between *T. brucei* procyclic forms and bloodstream forms can certainly be identified. Unfortunately, due to a bias in the classification of dividing organelles a true description of how the daughter organelles are re-positioned before cell cleavage takes place, was not made for bloodstream forms.

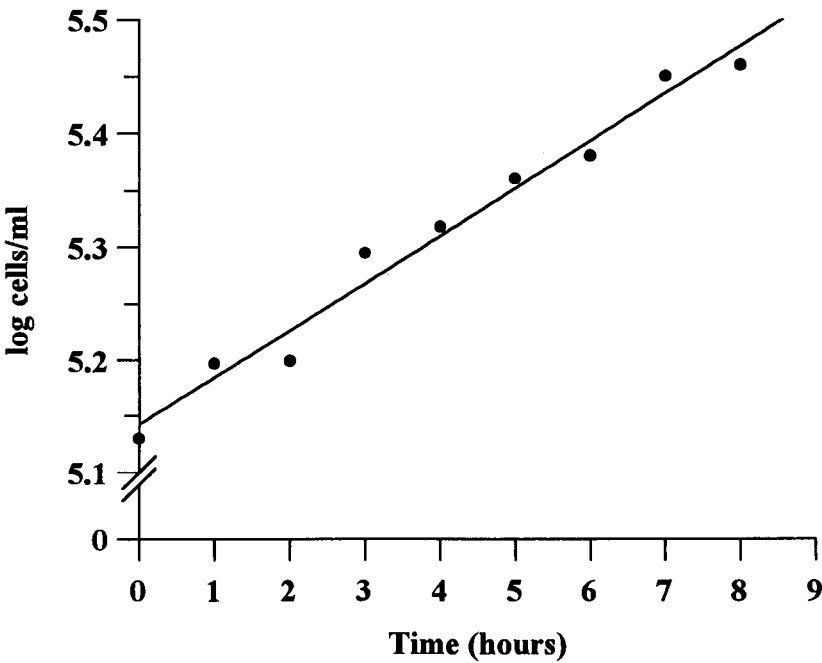


Figure 2.1A Growth of GUTat 7.1 bloodstream forms.

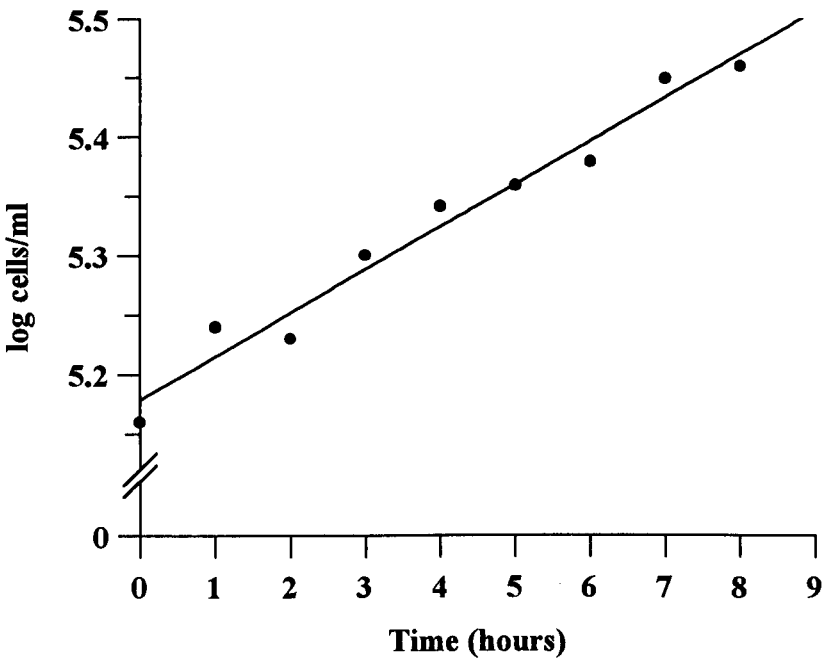
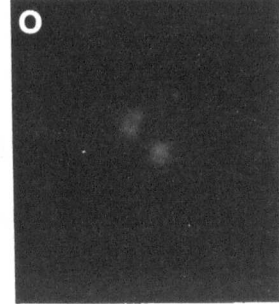
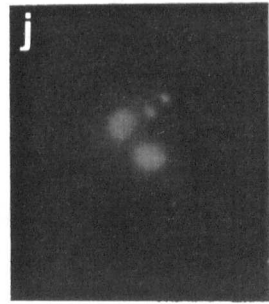
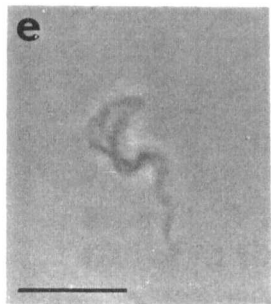
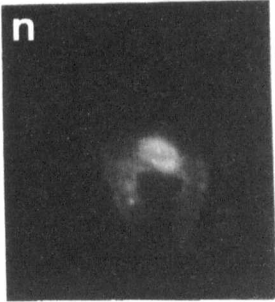
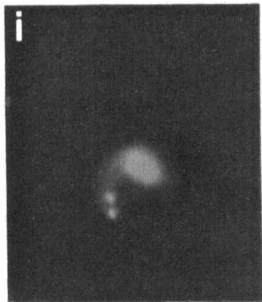
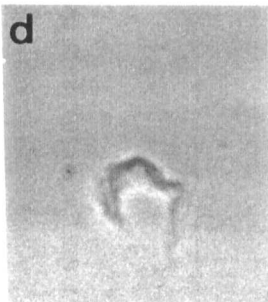
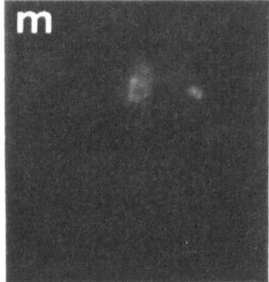
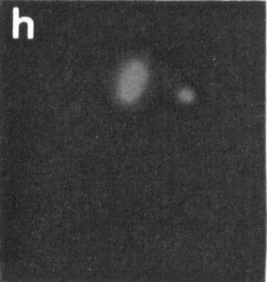
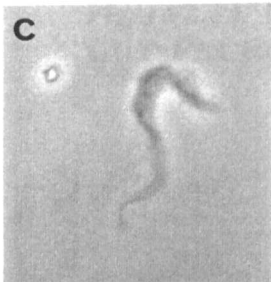
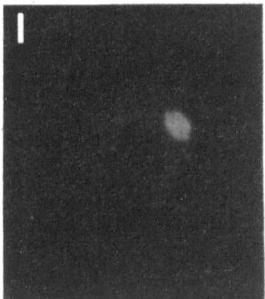
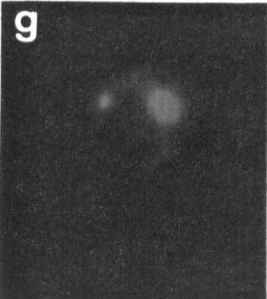
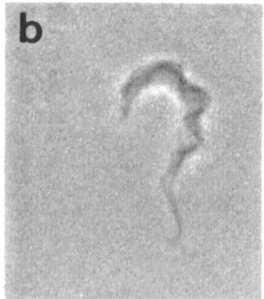
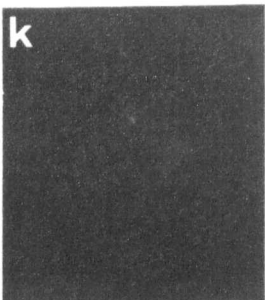
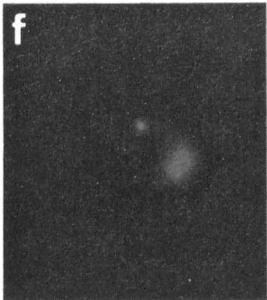
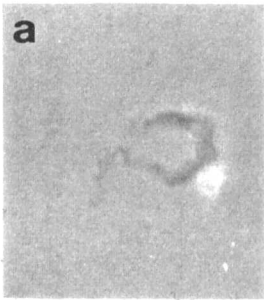


Figure 2.1B Growth of GUTat 7.1 incubated with BrdU.

Figure 2.2 Cell cycle progression in *T. brucei* bloodstream forms. BrdU labelled nuclei and kinetoplasts were detected using an anti-BrdU antibody and visualised by immunofluorescence microscopy. Cells were also counterstained with the DNA intercalating dye, DAPI. DAPI staining indicates cells at progressive stages in the *T. brucei* cell cycle. Initially the kinetoplast elongates (g) and the daughter organelles segregate before nuclear division is complete (i). The nucleus elongates (h) and after mitosis occurs (j) the divided organelles are in a period of cytokinesis before they re-assort themselves on either side of the division plane before cell cleavage takes place. k-o shows BrdU incorporation in the nuclei and kinetoplasts of the dividing cells. The proportion of cells BrdU labelled in the nucleus and kinetoplast was used to calculate the durations of nuclear and kinetoplast S-phase in the cell cycle, respectively (section 2.2.5). Scale bar=10µm.



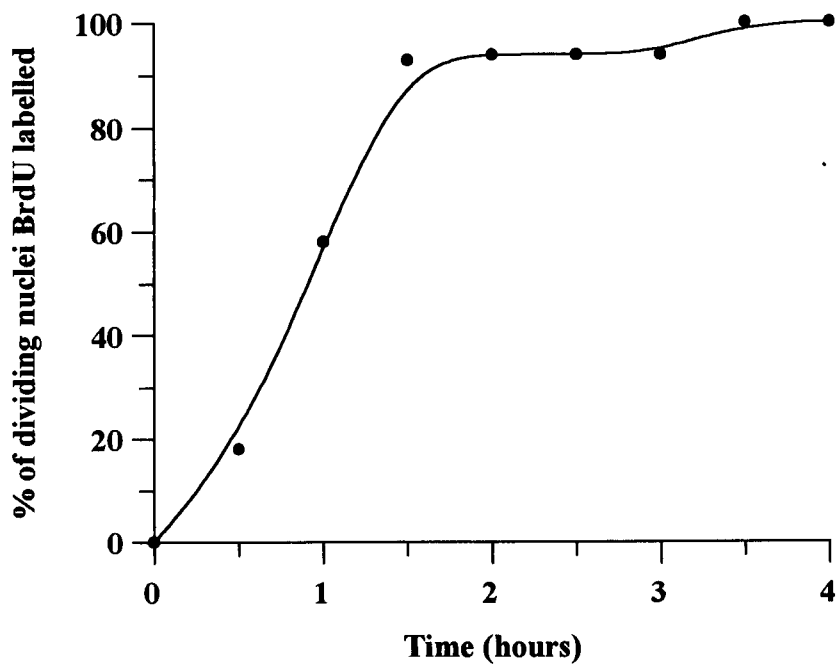


Figure 2.3A Kinetics of appearance of BrdU label in dividing nuclei of GUTat 7.1 bloodstream forms.

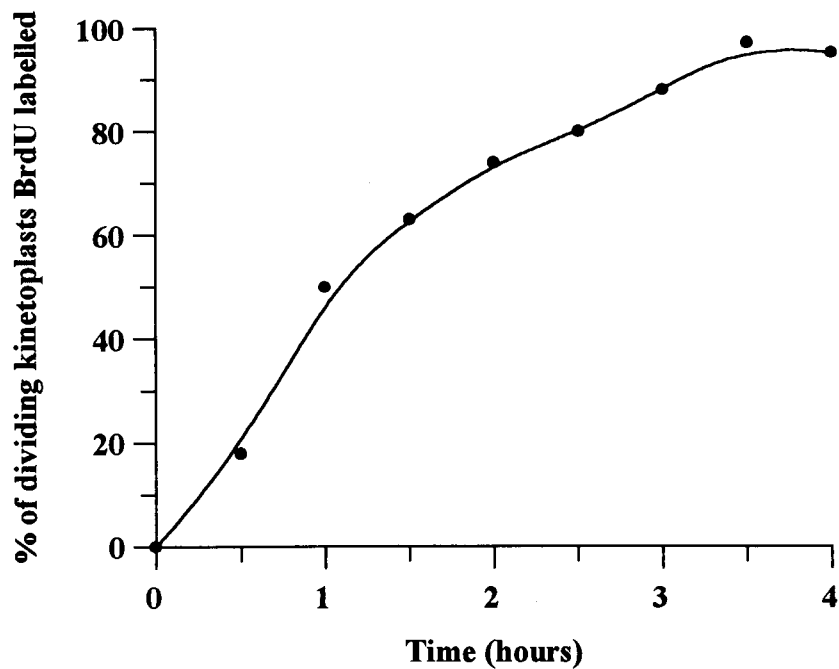


Figure 2.3B Kinetics of appearance of BrdU label in dividing kinetoplasts of GUTat 7.1 bloodstream forms.

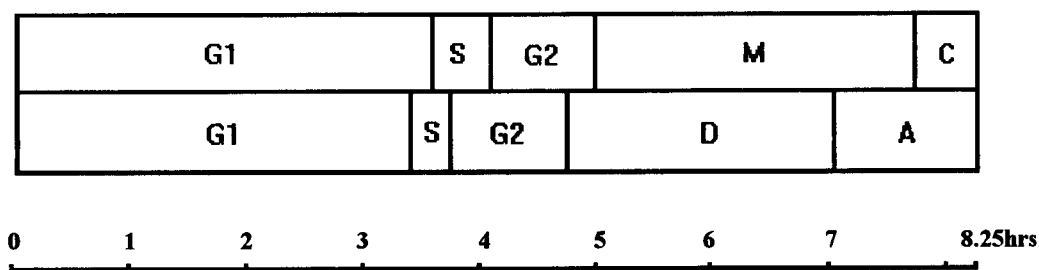


Figure 2.4A Cell cycle map of *T. brucei* bloodstream forms.

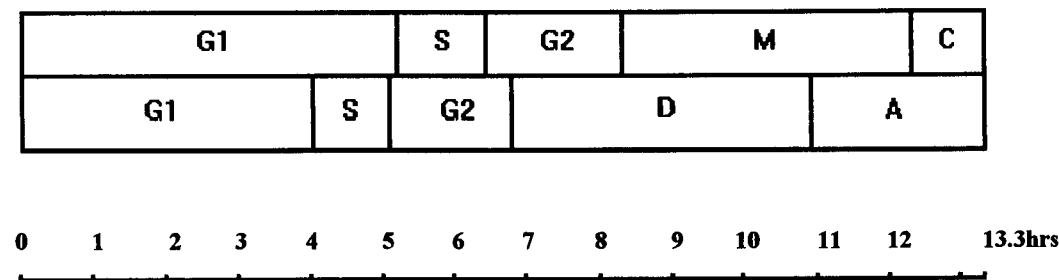


Figure 2.4B Cell cycle map of *T. brucei* procyclic forms.

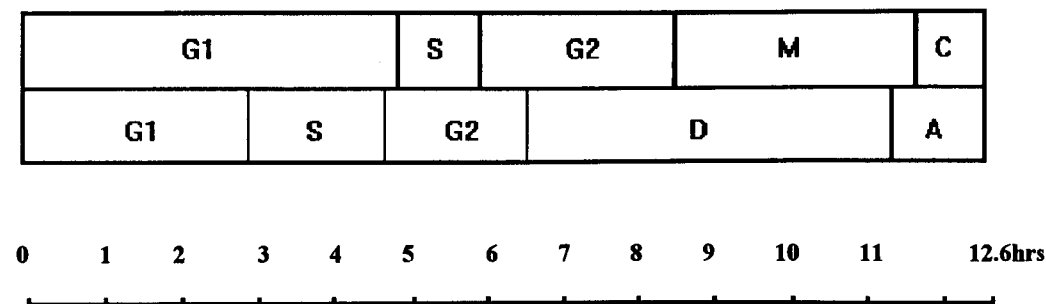


Figure 2.4C Cell cycle map of *L. mexicana* promastigote forms.

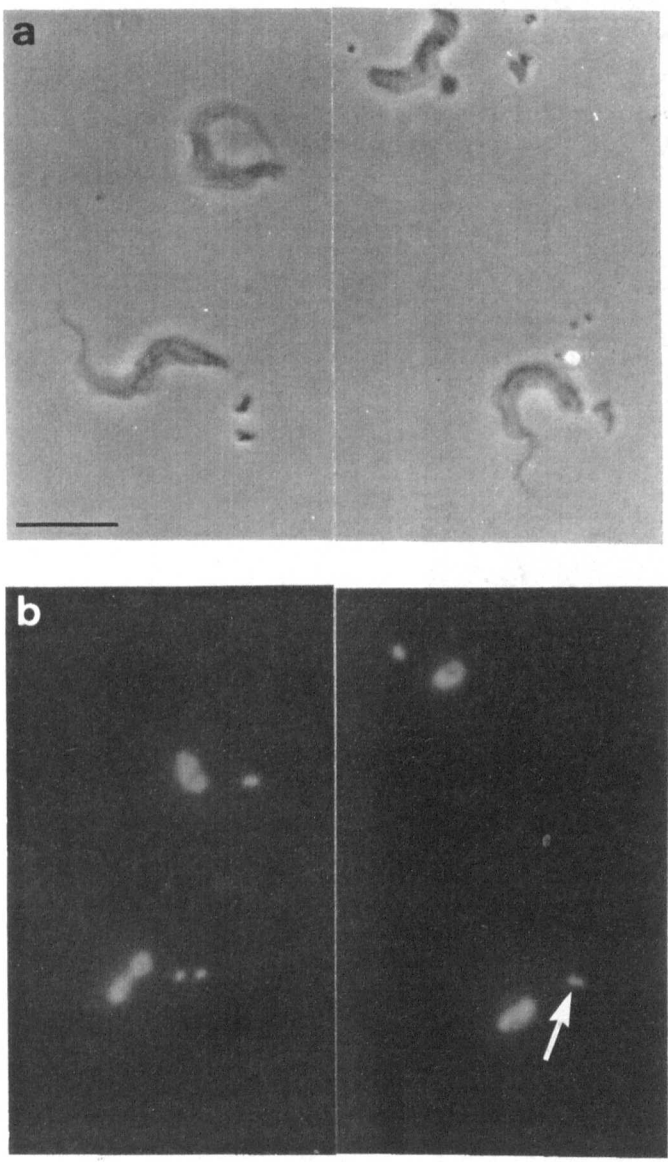


Figure 2.5A *T. brucei* bloodstream forms. (a) is the phase contrast image of GUTat 7.1 bloodstream culture forms and (b) the corresponding DAPI image. Arrow indicates the close proximity of the post-divided kinetoplasts (scale bar=10μm).

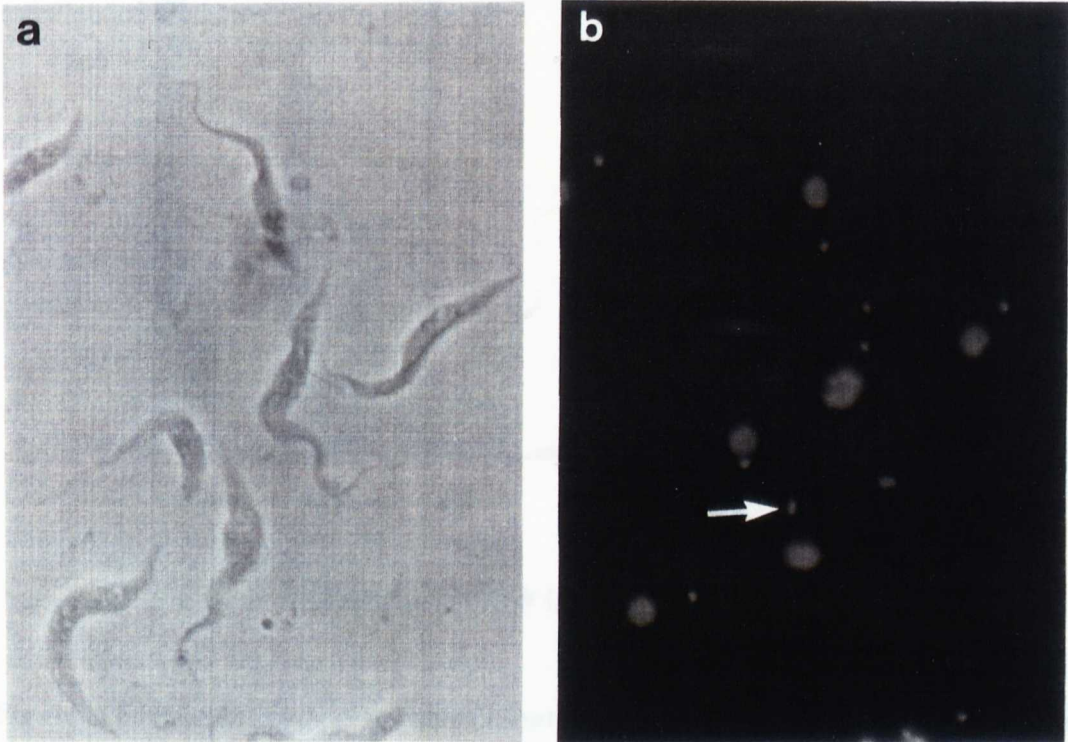


Figure 2.5B *T. brucei* procyclic forms. (a) is the phase contrast image of GUTat 7.1 procyclic culture forms and (b) the corresponding DAPI image. Arrow indicates the close proximity of the post-divided kinetoplasts.

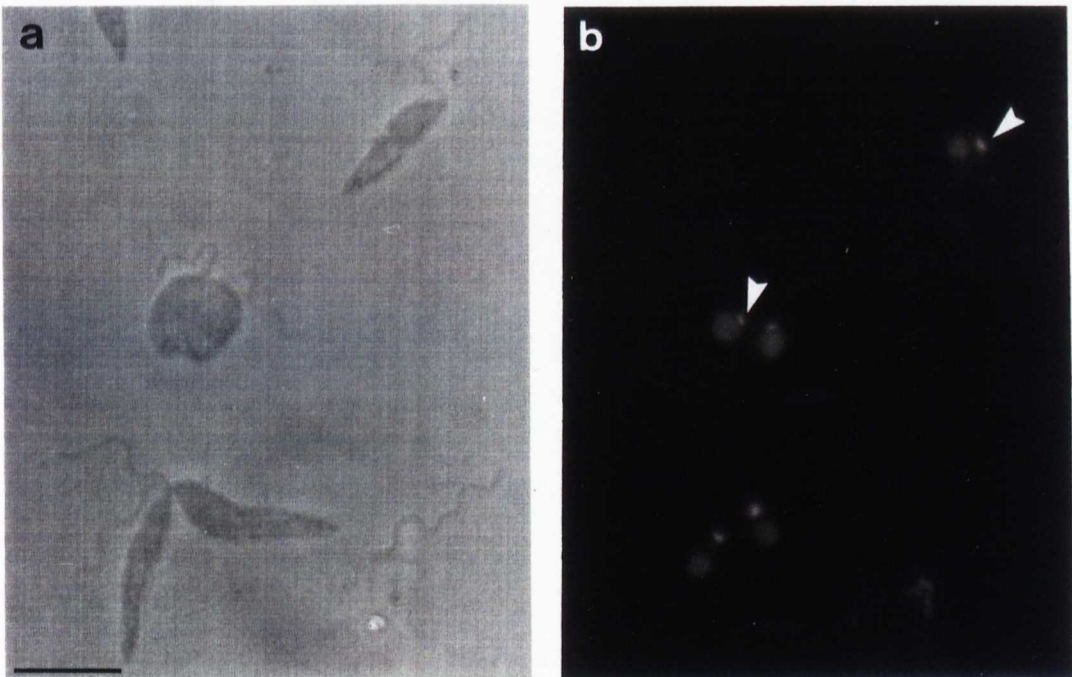


Figure 2.5C *L. mexicana* promastigote forms. (a) is the phase contrast image of *in vitro* promastigote forms and (b) the corresponding DAPI image. Arrow heads indicate elongate (rod-shaped) kinetoplasts observed in these cell types (scale bar for both figures = 10 μ m).

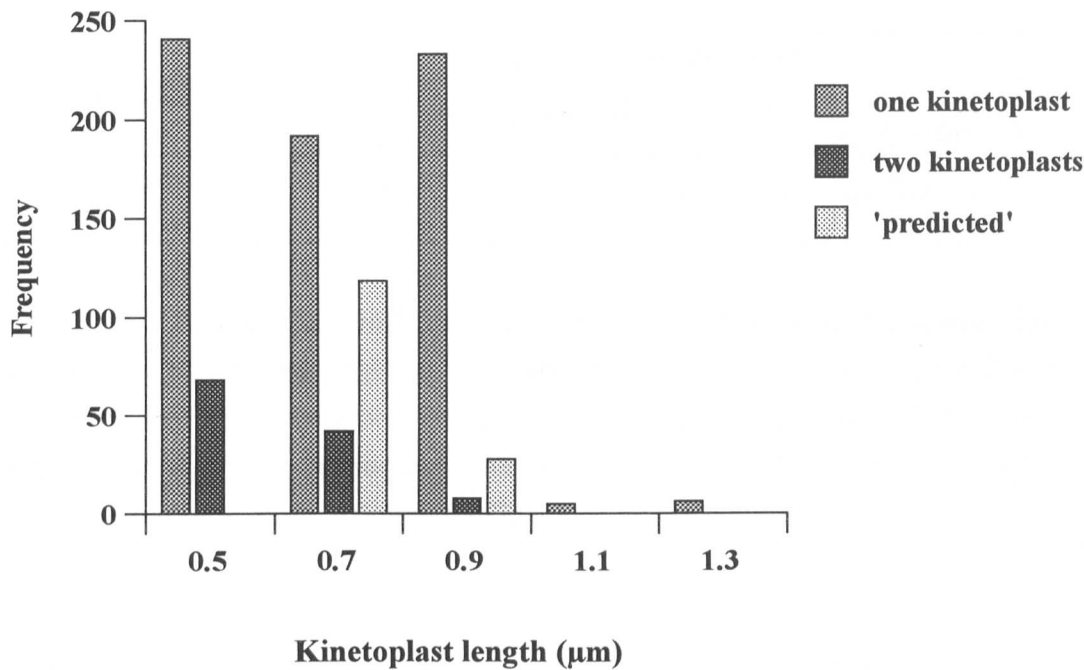


Figure 2.6 Frequency histogram of kinetoplast lengths in promastigote forms in cells with one kinetoplast and cells with two kinetoplasts. The predicted values were calculated as described in section 2.3.2. Length categories represent approximate measurements calculated from photographic prints.

Organelle	Organelle configuration		
	single	dividing	post-division
nucleus	68.6±0.01	27.0±0.01	4.2±0.01
kinetoplast	65.4±0.01	23.7±0.01	11.0±0.01

Table 2.1 Percentage configurations for the nucleus and the kinetoplast in GUTat 7.1 bloodstream forms. At least 500 cells were classified at half-hourly intervals and these values were used to estimate the periods of division and cytokinesis for each organelle. The 95% confidence limits of each mean are shown (Snedecor and Cochran, 1967).

Cell cycle stage	Proportion of cell cycle time		Duration	
	n	k	n	k
G1	0.43	0.41	3.57hrs	3.41hrs
S	0.06	0.04	0.52hrs	0.31hrs
G2	0.11	0.12	0.91hrs	1.00hrs
M/D	0.33	0.28	2.74hrs	2.31hrs
C/A	0.06	0.15	0.51hrs	1.23hrs

Table 2.2 The durations of each phase of the cell cycle for GUTat 7.1 bloodstream forms. Each cell cycle phase is also shown as a proportion of the total cell cycle time (=8.25hrs).

Table 2.3A Percentage configurations for the nucleus and the kinetoplast in GUTat 7.1 bloodstream forms (n=500), determined from smears which were treated differently. The four treatments were as described in section 2.2.6.1:

- 1. Smears were air-dried and fixed in ethanol for one hour at 4°C.**
- 2. Cells were settled onto poly-L-lysine coated slides for 10 mins. in CBSS, before being fixed in ethanol.**
- 3. Smears which had been air-dried, fixed and then stored at -20°C, were taken from the freezer, warmed to room temperature and then configurations analysed by DAPI staining.**
- 4. Smears which were air-dried and then fixed in ethanol at 4°C overnight before being examined.**

Table 2.3B Percentage configurations for the nucleus and kinetoplast of GUTat 7.1 bloodstream forms from smears treated differently as described above. At least 300 cells were classified for each treatment under 'blind score' conditions, using the same slides for values determined in Table 2.3A. This 'blind' score was carried out by Dr. Mike Turner.

Treatment	Organelle	Organelle configuration		
		single	dividing	post-division
1	nucleus	75.8	20.8	3.4
	kinetoplast	67.8	21.0	11.2
2	nucleus	76.2	21.0	2.8
	kinetoplast	66.4	20.6	13.0
3	nucleus	73.0	21.8	5.2
	kinetoplast	63.8	23.0	13.2
4	nucleus	75.0	21.0	4.0
	kinetoplast	70.0	17.8	12.2

Table 2.3A

Treatment	Organelle	Organelle configuration		
		single	dividing	post-division
1	nucleus	92.2	3.8	4.0
	kinetoplast	77.5	11.4	11.1
2	nucleus	86.0	8.5	5.5
	kinetoplast	79.0	9.2	11.8
3	nucleus	80.7	14.6	4.7
	kinetoplast	86.5	5.5	8.0
4	nucleus	90.3	5.6	4.1
	kinetoplast	77.5	12.9	9.6

Table 2.3B

CHAPTER 3 ANALYSIS OF THE RELATIVE TIMING OF CELL CYCLE EVENTS OF *T. BRUCEI* AND *L. MEXICANA*

3.1 Introduction

The timing of cell cycle events of kinetoplastids has not been studied in great detail until relatively recently, when a full map of cell cycle events for *T. brucei* procyclic forms was constructed (Woodward and Gull, 1990). This study related the timing of events to the morphogenesis of trypanosomes (Sherwin and Gull, 1989) and the division and re-positioning of organelles within the microtubule corset before cell cleavage takes place (Gull *et al.*, 1990). Co-ordination of cell cycle events is required to ensure that single copies of each organelle are inherited into each daughter cell at the end of division.

While examining the map of events for *T. brucei* procyclic forms (see Figure 1.4), there appear to be three key features that distinguish the cell cycle in these organisms from the customary eukaryotic plan and may also indicate how the organellar cycles of the kinetoplast and nucleus are co-ordinated. These three features are: (1) the initiation of S-phase which appears to be similar in the two organelles, (2) the relative timing of mitosis and kinetoplast division (the latter occurs before the former) and (3) the extended phase of cytokinesis for both organelles. These first two features are of particular interest because they may equate to the two main cell cycle checkpoints that have been identified in yeast and higher eukaryotes: the transition through a point called 'START' in late G1-phase, which cells have to pass through in order to proceed through the rest of the cell cycle and the G2/M transition. Both points are controlled by a single group of molecules, the cyclin-dependent kinases (CDKs) (reviewed by Morgan, 1995, Figure 1.3). Given the apparently high degree of conservation of CDKs through eukaryotic evolution and the identification of structural *cdc2* homologues in *T. brucei* and *L. mexicana* (Mottram *et al.*, 1993, Mottram, 1994, Mottram and Smith, 1995), it seems reasonable to presume that such checkpoints are

also present in the kinetoplastid cell cycle. Furthermore, progression through either or both checkpoints can potentially control the co-ordination of cycles between the two organelles. Following these lines of argument, it has been proposed that the apparent synchrony of the start of S-phase indicates that this time point controls co-ordination of the two organelles and that the difference in timing between mitosis and kinetoplast division suggests some degree of intraorganellar modification of this co-ordination (Woodward and Gull, 1990, Turner, 1992b). The difficulty with these views is that they are bound in production of cell cycle maps for each organelle which do not permit quantitative comparison of the timing of events between organelles (chapter 2). A further aspect of cell cycle co-ordination that has not yet been addressed is that the requirements for co-ordination should apply to the vast majority of kinetoplastids - all those with a single flagellum and unitary kinetoplast. A comparison of cell cycle events in different species, different life cycle stages and of different morphological types of kinetoplastids could inform as to which cell cycle features that have been identified in *T. brucei* procyclic forms are general to the group as a whole.

The two overall aims of this study were to develop and use a method for quantitatively comparing the timing of cell cycle events in the nucleus and kinetoplast and establish which features are likely to be general features of kinetoplastids rather than specific to a particular species, life cycle stage and/or morphological type of cell. To achieve these aims, I examined the relative timing of nuclear and kinetoplast events in procyclic and bloodstream trypomastigotes of *T. brucei* and promastigotes and amastigotes of *L. mexicana*, to ascertain the degree of co-ordination between the two organelles in the cell cycle. Particular attention was paid to three main features; the relative durations of S-phase for each organelle, the relative timing of mitosis and kinetoplast division and the lengths of the cytokinesis periods.

To analyse the relative timing of cell cycle events in each cell type an approach was used that directly and quantitatively compared the timing of events in the nucleus and kinetoplast and did not require a full map of the cell cycle to be constructed for each species and life cycle stage studied. In this analysis, these key questions could be addressed relating to the timing of the three main features of the cell cycle :

1. Is the start or end of S-phase co-incident in timing and what are the relative lengths of the S-phase periods?
2. What is the relative timing of the start and end of mitosis and kinetoplast division?
3. Is there an extended phase of post-mitotic cytokinesis?

The first question was addressed by using the BrdU labelling technique and analysing numbers of labelled nuclei versus labelled kinetoplasts, while questions two and three were addressed by analysing organelle configurations by DAPI staining. These results were then analysed statistically to test the validity of the data.

3.2 Materials and Methods

3.2.1 Culturing of *T. brucei* and *L. mexicana*

***T. brucei* procyclic and bloodstream forms and *L. mexicana* promastigote forms**

GUTat 7.1 procyclic and bloodstream forms were each cultivated as described in section 2.2.1, as were *L. mexicana* (MNYC/BZ/62/M379) promastigote forms.

***L. mexicana* amastigote forms**

Cultivation of axenic amastigote forms (MNYC/BZ/62/M379) was essentially as described by Bates *et al.*, (1992). Purified amastigotes from lesions were provided by Miss K.G. Brown and used to establish *in vitro* cultures. Axenic cultures of amastigotes were routinely sub-cultured in Schneider's *Drosophila* Medium (Gibco) supplemented with 20% foetal calf serum (Gibco) at pH 5.5. Cultures were maintained at 32-33°C with 5% CO₂ and subpassaged every 5-6 days by passing the cells through a needle to break up any large clumps and initiated at a new density of

1-5x10⁵cells/ml. Amastigote forms were less than 10 passages in culture from purification from lesion.

3.2.2 BrdU incorporation and immunofluorescent detection of BrdU

This was carried out essentially as described in sections 2.2.2 and 2.2.3.

3.2.3 Growth rate of cultures

Cell densities were counted every 1-2 hours for 8-10 hours using an improved Neubauer haemocytometer and the growth rate (r) calculated by least squares regression analysis. The population doubling time (PDT) was calculated from $PDT = \log_e 2/r$.

3.2.4 Cell cycle analysis

3.2.4.1 S-phase

To determine the relative lengths and degree of overlap in S-phases of nuclei and kinetoplasts, cells were classified as those with labelled nuclei only, those with labelled kinetoplasts only and those labelled for both organelles. 500 cells were counted at each of two time points (after 2 and 4 hours incubation). No proportional difference in the results were observed between the two time points (analyses not shown) and so these counts were combined and then analysed by Chi-square.

To determine whether or not the start or end of the S-phase periods were co-incident in timing, six possible models were considered (see Figure 3.1). Neither the start nor the end of the S-phase periods could have been co-incident, with either kinetoplast S-phase first (Figure 3.1A) or nuclear S-phase initiated first (Figure 3.1B). On the other hand, the start of the S-phase periods could have been co-incident in timing while the end was not (Figure 3.1C), or vice versa (Figure 3.1D). In addition, a further two models could be considered where kinetoplast S-phase both starts and ends at some point during the occurrence of nuclear S-phase (Figure 3.1E) or vice versa (Figure

3.1F). Analysis of frequencies of cells with only one organelle labelled (either nucleus or kinetoplast) would therefore discriminate between the various models. The observation of populations of cells with both singly labelled kinetoplasts and nuclei would suggest, for instance, that models C-F were all incorrect but would not discriminate between models A and B.

To determine the relative lengths of nuclear and kinetoplast S-phase, the numbers of BrdU labelled nuclei and kinetoplasts were compared. The null hypothesis employed was that the lengths of S-phase were the same in the kinetoplast (a+b) as in the nucleus (b+c) (see Figure 3.1) and therefore that the expected number of labelled kinetoplasts should equal the observed number of labelled nuclei. The expected and observed numbers of labelled kinetoplasts were compared by Chi-square analysis.

3.2.4.2 Mitosis, kinetoplast division and cytokinesis

To investigate the relative timing of mitosis and kinetoplast division cells were classified into categories as follows:-

1. Cells with one nucleus and a dividing/two kinetoplasts (1n, d/2k).
2. Cells with one kinetoplast and a dividing/two nuclei (1k, d/2n).
3. Cells with two nuclei and one/dividing kinetoplast (2n, 1/dk).
4. Cells with two kinetoplasts and one/dividing nucleus (2k, 1/dn).

Comparison of the numbers of cells in categories 1 and 2 indicated whether initiation of mitosis preceded initiation of kinetoplast division or vice versa or whether the two were co-incident. The null hypothesis employed was that the initiation of kinetoplast division and mitosis co-incident and that an expected value was calculated as the number of cells in category 1 added to the number of cells in category 2, divided by two, i.e. $E = (\text{category 1} + \text{category 2})/2$. Comparison of the numbers of cells in categories 3 and 4 provided equivalent information on the end of mitosis and kinetoplast division. The null hypothesis employed was that the end of kinetoplast division and mitosis co-incident and that an expected value was calculated as the

number of cells in category 3 added to the number of cells in category 4, divided by two, i.e. $E = (\text{category 3} + \text{category 4})/2$. For each comparison 500 cells were counted at each time point (at 2 and 4 hours). These counts were combined and then analysed by Chi-square.

Dividing organelles were only classified as such if they appeared either truly bilobed or very elongated in each life cycle stage examined. Particular attention was paid to *L. mexicana* kinetoplasts as well as care in discriminating between dividing and post-division kinetoplasts in *T. brucei* (see section 2.3.2).

To investigate further the relative timing of mitosis and kinetoplast division and determine the duration of cytokinesis for each organelle, cell cycle maps for the later part of the cell cycle were calculated as described previously in section 2.2.5. Frequencies of cells with the following nuclear and kinetoplast configurations, were determined for each organelle: (1) single organelle (2) dividing organelle (3) post-division. At least 1,000 cells were classified accordingly at each time point (at 2 and 4 hours). Using the analysis of Williams, (1971) the durations of mitosis (M) and cytokinesis (C) for the nucleus and the corresponding periods of division (D) and cytokinesis (A), for the kinetoplast, were determined as follows:

$$x = \frac{\log_e (1-y/2)}{-r}$$

where x is the cumulative time within the cell cycle taken to reach the end of the morphological stage in question, y is the cumulative % of cells up to and including the morphological stage in question, expressed as a fraction of one unit and r is the specific growth rate.

3.3 Results

3.3.1 Growth of *T. brucei* and *L. mexicana* promastigotes

Growth curves of the control culture and culture incubated with BrdU for *T. brucei* procyclic forms (Figures 3.2A and B respectively), *T. brucei* bloodstream forms (Figures 3.3A and 3.3B) and *L. mexicana* promastigote forms (Figures 3.4A and 3.4B) indicated that the cells grew exponentially over the time course studied. The calculated population doubling times for each curve shown in Table 3.1 demonstrate that the BrdU had a negligible effect upon the growth rate and also indicate that the cultures grew exponentially with a constant generation time.

Growth of *L. mexicana* amastigote forms

Growth curves of the control culture and culture incubated with BrdU (Figs. 3.5A and 3.5B respectively) indicated that the cells grew exponentially over the time course studied. PDT for the control was calculated as 10.8 hrs ($r^2=0.92$) and PDT for the BrdU culture was calculated as 13.6hrs ($r^2=0.88$) (see Table 3.1). Due to the difference in PDTs for both cultures, the BrdU may have been having an effect upon cell growth. However this seems unlikely as the concentration of BrdU used (40 μ M) had no effect upon the other culture forms examined (see Table 3.1), or indeed upon any other growth curves constructed (data not shown). It seems more likely that this difference was due to difficulties in sampling from the cultures as a result of amastigotes clumping which would also explain the slightly lower r^2 value observed with amastigote forms compared to the other three types of cells.

These data show: (1) cells analysed at 2 and 4 hours will have had only one opportunity to enter S-phase because 4 hours is less than the cell cycle time: this is important to S-phase analysis. (2) S-phase data are not affected by BrdU cytotoxicity. (3) exponential growth indicates that the mapping method is acceptable.

3.3.2 Cell cycle analysis

3.3.2.1 Analysis of S-phase

For all cell types examined, three types of BrdU labelled cells were identified: cells with only the nucleus labelled, cells with only the kinetoplast labelled and cells with both the nucleus and kinetoplast labelled (Tables 3.2A). These observations therefore indicated that four of the proposed models could be rejected (Figures 3.1C-3.1F), while either one of the other two could be correct (Figures 3.1A and 3.1B). Unfortunately, it was not possible to resolve from the data which of these two models was correct. From the analysis, however, it was clear that there was a non-coincident start and end to S-phase for the nucleus and the kinetoplast, with a period of overlap in between, confirmed by the observation that both organelles were labelled in a sub-population of cells.

The frequencies of cells labelled were analysed by Chi-square, to determine the relative lengths of nuclear and kinetoplast S-phase. Table 3.2B demonstrates that in all forms examined the length of nuclear S-phase was significantly longer than the length of kinetoplast S-phase, except in the case of amastigote forms, wherein the lengths of nuclear and kinetoplast S-phase were similar, at $p < 0.01$.

3.3.2.2 The relative timing of mitosis and kinetoplast division

Figures 2.2 and 3.6 shows phase contrast images of each life cycle stage and their corresponding DAPI images, illustrating typical organelle configurations of each population studied. The frequencies of cells categorised as described in section 3.2.4.2 are shown in Table 3.3A and B, as well as the Chi-square results. For *T. brucei* procyclic forms and bloodstream forms a similar pattern was observed. For both life cycle stages, kinetoplast division started and ended before mitosis was initiated, with differences between cell categories significant at $p < 0.01$. This pattern of division can be observed in Figures 2.2 for bloodstream forms and 3.6A for procyclic forms.

In *L. mexicana*, a different pattern was observed from *T. brucei*. In both life cycle stages of *L. mexicana*, the nucleus divided before the kinetoplast, with differences between cell categories significant at $p < 0.01$. A small proportion of cells (0.3%) were also identified as having both a dividing nucleus and dividing kinetoplast. This appears to indicate that there was an overlap in the timing of the division phases for the nucleus and the kinetoplast. In promastigote forms, a very small percentage of cells were identified, wherein the kinetoplast divided before mitosis. Despite this fact, overall analysis indicated that mitosis occurred before kinetoplast division in both life cycle stages. This pattern of division can be observed in Figures 3.6B and C for promastigotes and amastigotes, respectively.

3.3.2.3 Mapping of mitosis, kinetoplast division and cytokinesis in the cell cycle

Nuclear and kinetoplast configurations of each life cycle stage were classified as single, dividing and post-division (Table 3.4). These data were then analysed using the method of Williams (1971) to calculate the durations of mitosis (M) and cytokinesis (C) for the nucleus, as well as kinetoplast division (D) and cytokinesis (A) (Tables 3.5A and B). The lengths of these phases are represented in Figure 3.7. In both forms of *T. brucei*, kinetoplast division occurred before mitosis, with an extended phase of cytokinesis for both organelles, but of longer duration in the kinetoplast. In bloodstream forms, the calculations of the lengths of mitosis and kinetoplast division led to a greater gap in timing between the end of kinetoplast division and the initiation of mitosis, in comparison to procyclic forms (Figures 3.7A and B).

In both forms of *L. mexicana*, mitosis occurred first, closely followed by kinetoplast division (Figures 3.7C and D). An overlap in the timing of mitosis and kinetoplast division was observed. A period of cytokinesis was identified for both organelles, although of much shorter duration than the equivalent periods in *T. brucei*. For each stage examined, the proportion of the total cell cycle time with two nuclei or two

kinetoplasts is shown in Table 3.6. Bloodstream forms had the longest nuclear and kinetoplast cytokinesis periods whereas amastigote forms had the shortest.

3.4 Discussion

In this study of the relative timing of cell cycle events in *T. brucei* and *L. mexicana*, a number of features have been identified. From the analysis of BrdU labelled organelles, a non-co-incident start and end to S-phase, with an overlap in the timing of S-phase for the nucleus and kinetoplast, was identified in all the life cycle stages examined. Nuclear S-phase was also significantly longer than kinetoplast S-phase, except in the case of *L. mexicana* amastigote forms, wherein both phases were of similar duration. While it appears reasonable that nuclear S-phase should be longer in three of the forms studied possibly due to a greater amount of DNA requiring to be replicated, it is not certain why amastigotes should be different.

The relative timing and the durations of the periods of division and cytokinesis were also identified. In both *T. brucei* life cycle stages, kinetoplast division was completed before the initiation of mitosis. An extended cytokinesis period was also identified, although of much longer duration in the kinetoplast. In both forms of *L. mexicana*, the converse situation to that observed in *T. brucei* occurred: mitosis was first, closely followed by kinetoplast division. The periods of cytokinesis were of much shorter duration in comparison to *T. brucei*, the shortest being in amastigote forms.

These analyses illustrate a number of important points regarding the co-ordination of cell cycle timing. For each form studied, nuclear and kinetoplast S-phase appear to be almost synchronous in timing, supported by the observation that some cells were labelled in both the nucleus and kinetoplast, although there was a non-co-incident start and end to S-phase. This is similar to findings in other studies of kinetoplastid cell cycle timing (Steinert and Steinert, 1962, Simpson and Braly, 1970, Cosgrove and Skeen, 1970, Van Assel and Steinert, 1971). Unfortunately, whether or not

nuclear or kinetoplast S-phase was initiated first cannot be resolved from this data. As to which organelle appears to initiate S-phase first, seems to vary between species (Steinert and Steinert, 1962, Simpson and Braly, 1970, Cosgrove and Skeen, 1970, Van Assel and Steinert, 1971). In the study of *T. brucei* procyclic forms, kinetoplast S-phase was initiated first, closely followed by nuclear S-phase (Woodward and Gull, 1990). The apparent proximity of these two events has led to the suggestion that, S-phase was co-incident indicating that synchronization of organellar cycles was likely to occur at the G1/S transition (Turner, 1992b). The Woodward and Gull (1990) study involved mapping the full cell cycle, starting from the end events i.e. division and cytokinesis and working back to the start i.e. G1-phase. This method lacks sufficient precision to compare the relative timing of events in the two organelles. Whether the nucleus receives signals from the kinetoplast to start DNA replication, or vice versa, is still unclear. It seems likely, however, that there is some intra-organelle control of the termination of S-phase, to prevent the re-replication of DNA throughout the remainder of the cell cycle (Woodward and Gull, 1990).

While S-phase appears to be at least partly synchronous in timing, there are differences in the post-S-phase periods between species. In *T. brucei*, mitosis and kinetoplast division were completely non-co-incident with the latter occurring before the former. In *L. mexicana* mitosis was initiated before kinetoplast division but an overlap in the two phases was also observed. The differences between the two species may represent differences in cell cycle control. The pattern and duration of the division and cytokinesis periods, however, seems more likely to be associated with differences in cell morphology between trypanosomes and *Leishmania*. In trypanosome cell division, the divided organelles re-locate to either side of the division plane, before cell cleavage takes place. The kinetoplast divides first, the daughter organelles then move apart to either side of the division plane, after which the nucleus divides between the daughter kinetoplasts and re-locates to a position posterior to the kinetoplast in each daughter cell. Hence, there is a protracted

cytokinesis period in the kinetoplast, while the cell undergoes mitosis and re-positions its newly divided nuclei. This pattern of division was also observed in previous studies of the procyclic cell cycle (Sherwin and Gull, 1989, Woodward and Gull, 1990).

This pattern of division contrasts with that observed in *Leishmania*. The nucleus divides first, either laterally or longitudinally with most pairs of divided nuclei arranged longitudinally in the cell. The kinetoplast then divides across the cell, by which time the divided nuclei have re-positioned themselves on either side of the division plane. A division cleft then arises such that the daughter cells are clearly separated. This pattern of division in *Leishmania* has been described before (Molyneux and Killick-Kendrick, 1987, Christophers *et al.*, 1926, Adler, 1964, Walters, 1993), but the durations of the division and cytokinesis periods have not been accurately described nor measured. In *L. mexicana* the requirement for organelle re-arrangement to new sites is reduced or absent and therefore the cytokinesis periods are much shorter in comparison to *T. brucei*.

The clear separation in time between the end of kinetoplast division and the initiation of mitosis in *T. brucei*, contrasts also with the observation of cells with a dividing kinetoplast and dividing nucleus in *L. mexicana* (Table 3.3B), under the classification criteria adopted. The calculation of the durations of the division and cytokinesis periods in *L. mexicana* also produced an overlap in the timing of kinetoplast division and mitosis (Figures 3.7C and D). The periods of division were also much shorter than the equivalent periods in *T. brucei*, as were the cytokinesis periods.

Leishmania differ from trypanosomes, in that the nucleus divides before the kinetoplast, however, it has been also noted that promastigote nuclear division is before flagellar replication in the gut of the sandfly (Walters *et al.*, 1989). Although appearance of the new daughter flagellum was not quantified in this study, it was

observed that emergence of the new daughter flagellum, which remains much shorter than the parent flagellum throughout the remaining cell cycle, occurred before organelle division, a feature also observed previously (Molyneux and Killick-Kendrick, 1987). In *T. brucei*, initiation of growth of the new flagellum occurs before organelle division (Sherwin and Gull, 1989). The first major cell cycle event is pro-basal body elongation, which occupies a posterior position within the cell, when it initiates growth of the new flagellum. Pro-basal body duplication occurs, almost coincident with the initiation of nuclear S-phase (Woodward and Gull, 1990). Extension of the new flagellum, as well as the paraflagellar rod continues throughout a major portion of the cell cycle. Production of the new flagellum is therefore, before kinetoplast division as well as mitosis in the nucleus. Although the *Leishmania* cell cycle has not been studied in great detail, it seems likely that growth of the new flagellum and duplication of the basal bodies would occur similarly to that in *T. brucei*, but this remains to be confirmed.

The amastigote form represents the 'simplest' form with respect to morphology of the four cell types studied here. Its ovoid shape and small size (3-5 μ m on the major axis, Bates *et. al*, 1992) means that extensive organelle rearrangement is not required. Cell cleavage could therefore occur almost as soon as organelle division is complete, a feature demonstrated by the very short cytokinesis periods measured.

Within a log-phase population of promastigotes *in vitro* a number of morphological types are observed (Molyneux and Killick-Kendrick, 1987). In early log-phase, shorter, rounded flagellated forms (Type '1' forms) appear to predominate (Brown *et al.*, 1994a, b). These 'haptomonad' forms (Molyneux and Killick-Kendrick, 1987, Walters, 1993) are found attached in the midgut of the sandfly. In mid to late log-phase *in vitro*, relatively long elongate forms (Type '2' forms) predominate (Brown *et al.*, 1994a, b). These 'nectomonad' type cells (Killick-Kendrick, 1987, Walters, 1993) are free-swimming in the midgut of the sandfly. Another morphological type, the

non-dividing metacyclic form, is found mainly in stationary phase (Sack and Perkins, 1984, Bates and Tetley, 1993). These forms, which have short cell bodies and long flagella, are fast, free-swimming cells found in the pharynx, oesophagus and thoracic midgut and are infective to the mammalian host (Davies *et al.*, 1990). It still remains to be fully determined, however, as to whether or not these forms follow a particular sequence of development *in vivo* and *in vitro*.

The vast majority of cells examined in this study were mid log-phase cells and therefore, predominantly of the nectomonad type (Figure. 3.6B). The two main types found in log-phase (haptomonad and nectomonad) were not distinguished in this study of cell cycle timing, although the pattern of division described here appeared to hold for both types (no data shown). Metacyclic forms were not identified in the population of cells examined and therefore presumed not to have affected the data in any way. Metacyclic forms are difficult to identify reliably from promastigote forms but are normally only a small percentage of a log-phase population (Bates and Tetley, 1993).

The trypanosome represents the most 'complex' form of the four morphological types studied here, wherein extensive re-arrangement is required, after organelle division, in order for cell cleavage to take place. Its shape and form is maintained by a cytoskeleton of subpellicular microtubules. The microtubules of *T. brucei* have been studied in considerable detail (Sherwin *et al.*, 1987). Tyrosinolated α -tubulin, detected by antibody, has a distinct localisation within individual microtubules and organelles, a localisation which is modulated throughout the cell cycle. Such a marker has been used to detect newly formed microtubules, through the cell cycle. It is essential that cell cycle decisions integrate with cell growth progression. The microtubular network plays an important role in the organisation of the cytoplasm, as well as ensuring organelle segregation and fidelity of cell division (Tournier and Bornens, 1994). It remains to be seen whether or not differences exist in

microtubular organisation between trypanosomes and *Leishmania*. The differing pattern of division between the two species may involve different mechanisms of microtubular control of organelle segregation and flagellar outgrowth.

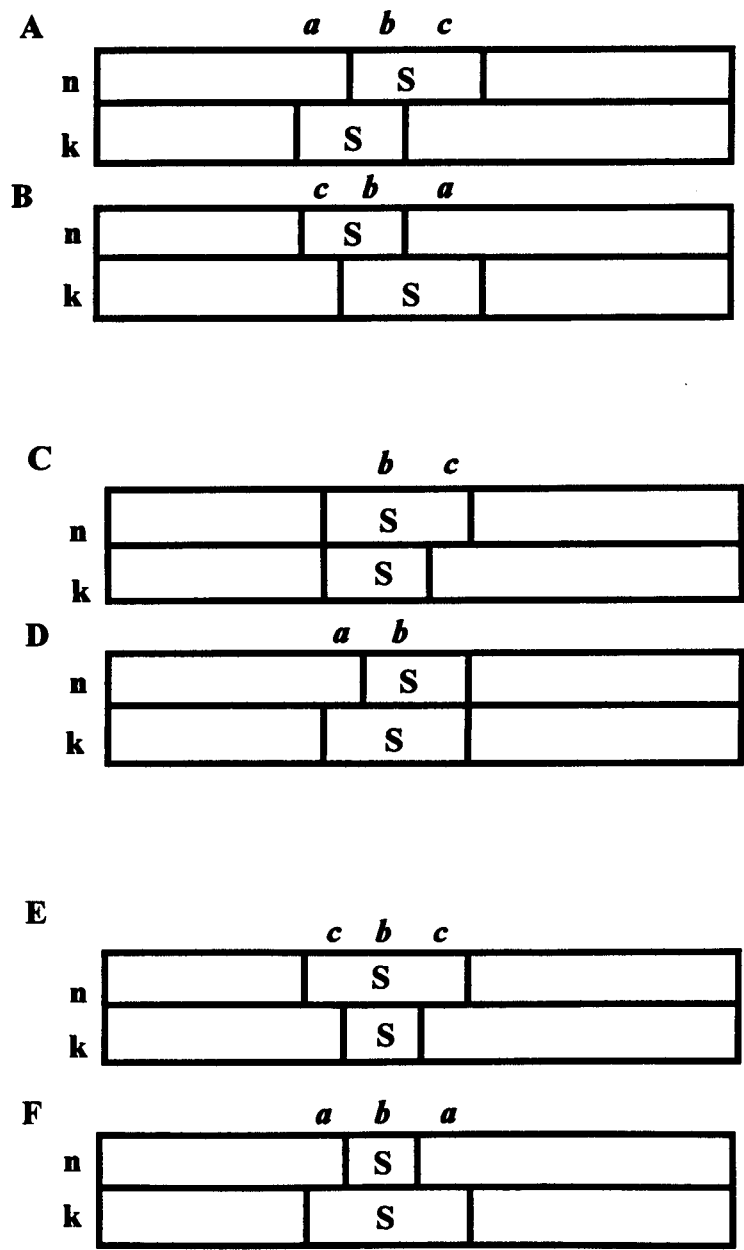


Figure 3.1 Stylised cell cycle maps showing all possible theoretical models for the relative lengths and timing of nuclear and kinetoplast S-phase, where *a* represents cells which are labelled in the kinetoplast only, *b*, cells labelled in both organelles and *c*, cells labelled only in the nucleus.

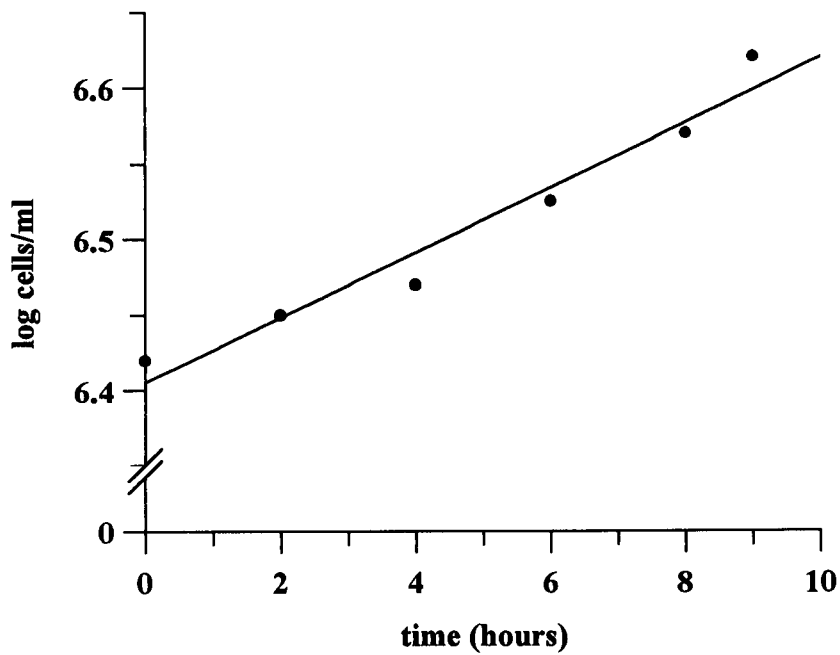


Figure 3.2A Growth of procyclic forms (control culture).

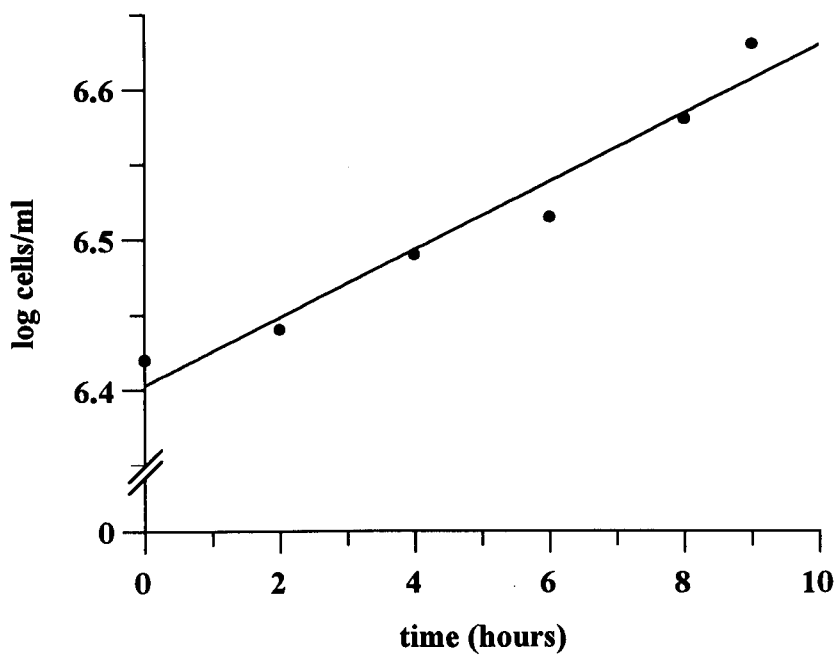


Figure 3.2B Growth of procyclic forms incubated with BrdU.

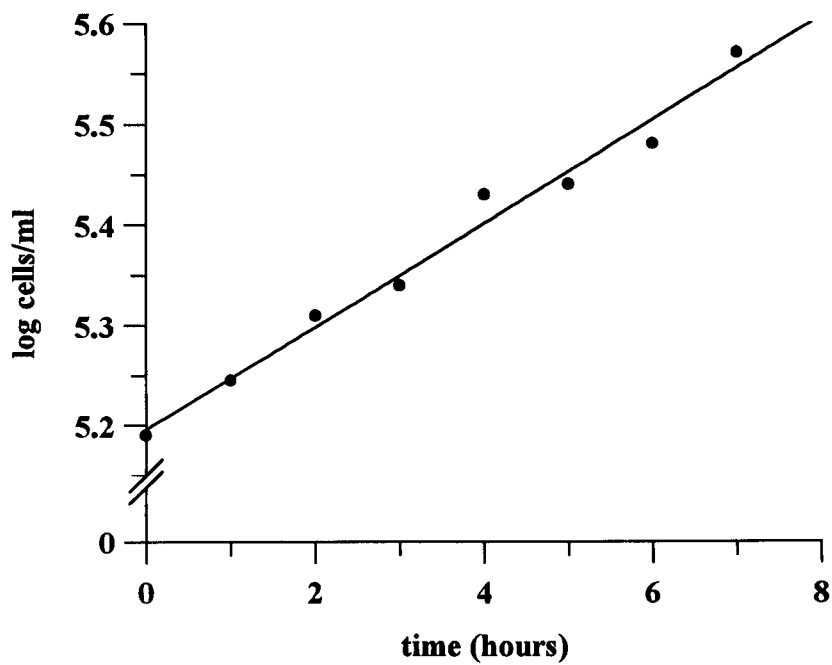


Figure 3.3A Growth of bloodstream forms (control culture).

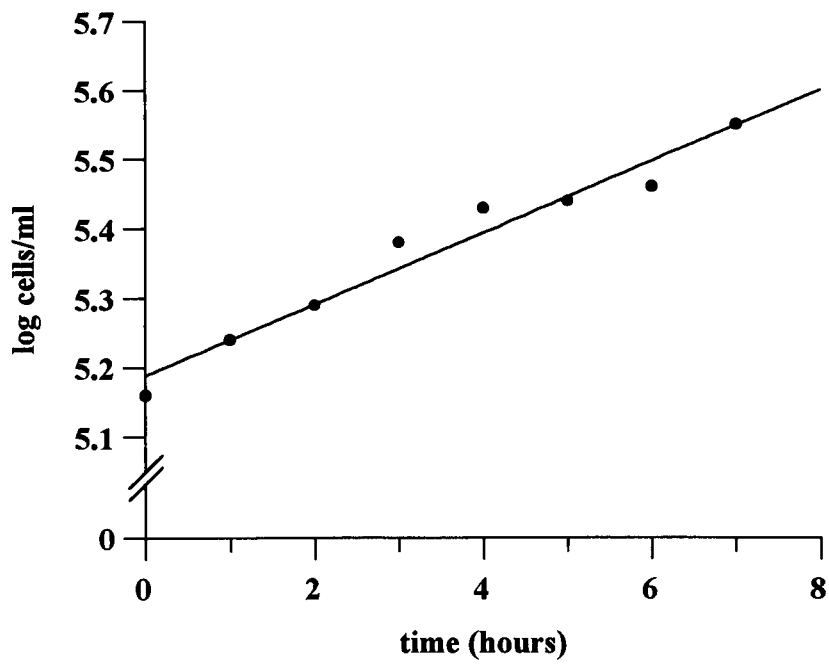


Figure 3.3B Growth of bloodstream forms incubated with BrdU.

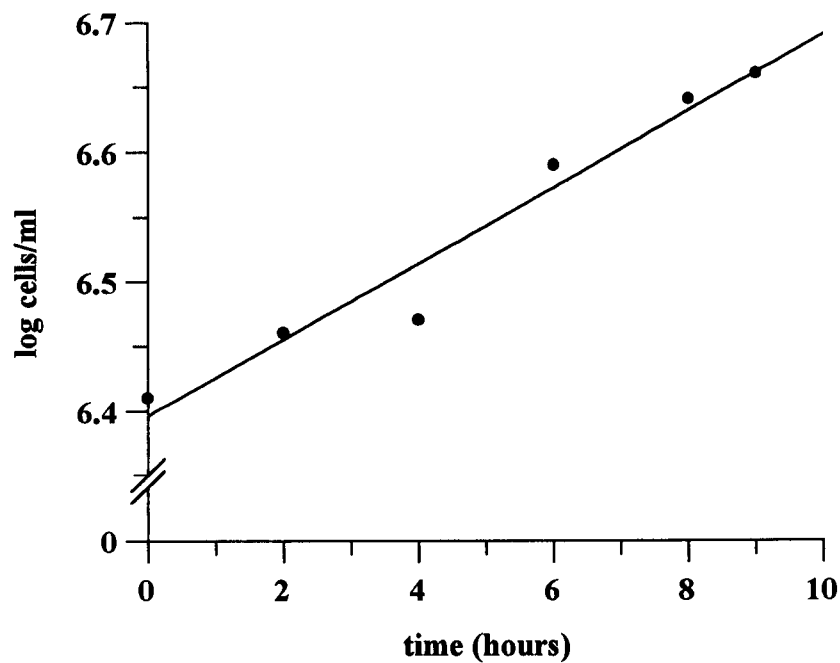


Fig. 3.4A Growth of promastigote forms (control culture).

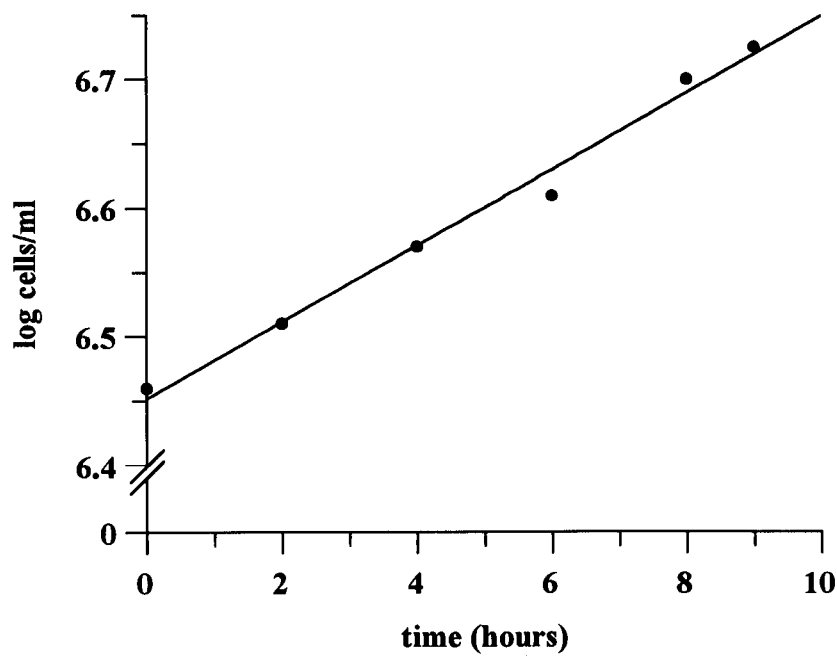


Fig. 3.4B Growth of promastigote forms incubated with BrdU.

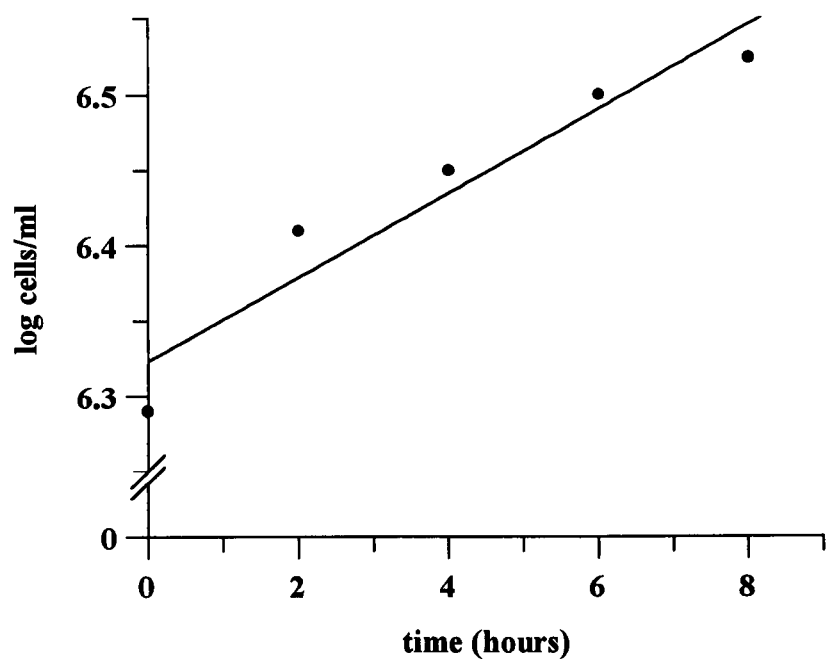


Figure 3.5A Growth of amastigote forms (control culture).

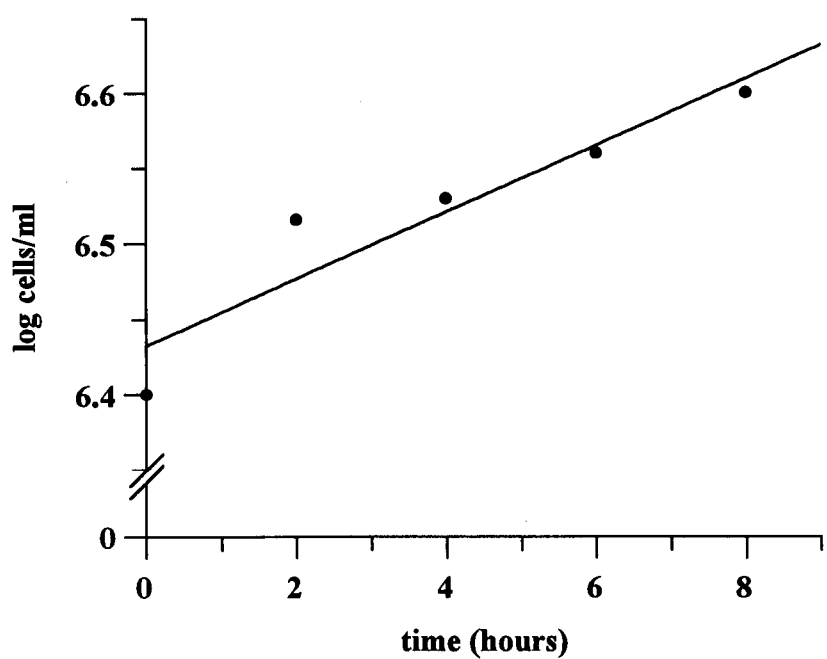


Figure 3.5B Growth of amastigote forms incubated with BrdU.

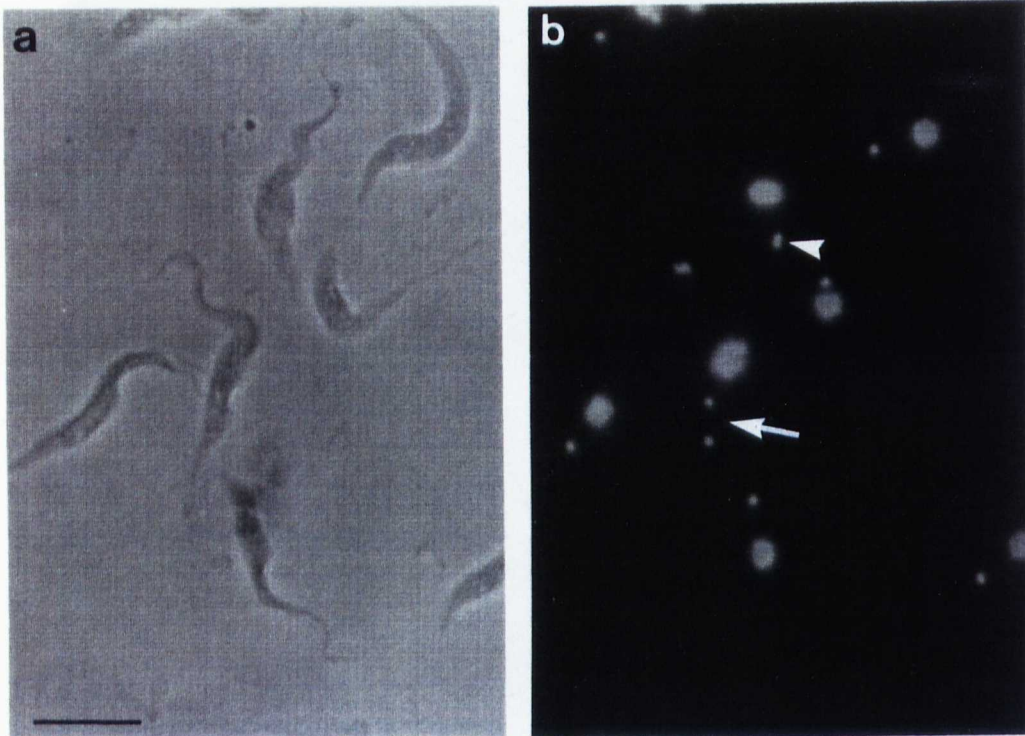
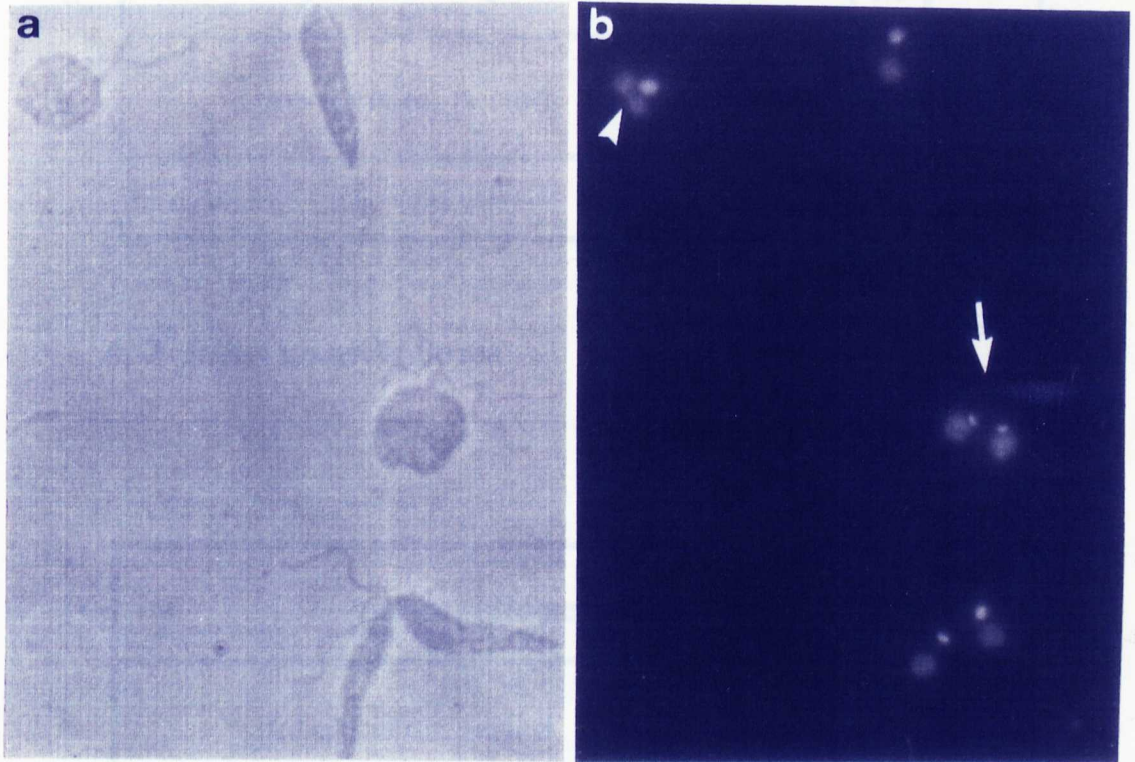


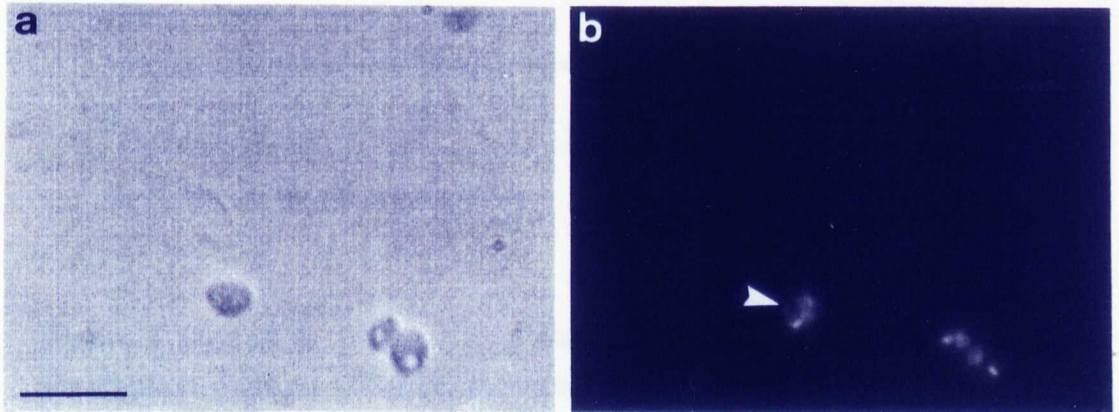
Figure 3.6A *T. brucei* procyclic forms. (a) is the phase contrast image and (b) the corresponding DAPI image of *in vitro* culture forms. A similar pattern of events was observed in both life cycle stages of *T. brucei* (see Figure 2.2 for cell cycle progression in bloodstream forms). Arrow head indicates that kinetoplast division was initiated and completed before mitosis in the nucleus (arrow indicates fully segregated kinetoplasts). An extended period of cytokinesis was identified in both organelles, although of longer duration in the kinetoplast (see Table 3.6). Scale bar=10 μ m.

Figure 3.6B and C. *L. smithi* promastigote and amastigote forms. (a) is the phase contrast image and (b) the corresponding DAPI image of *in vitro* culture forms. In both life cycle stages, the nucleus divided before the kinetoplast (indicated by arrow heads) and there was a short period of cytokinesis in both organelles before cell cleavage occurred. Arrow in B indicates a promastigote form just prior to cell cleavage. The promastigotes in B were a sample population from a mid-log phase culture and consisted mainly of long slender non-inflamed (type '2') promastigotes (see section 3.4). Scale bar=10 μ m.

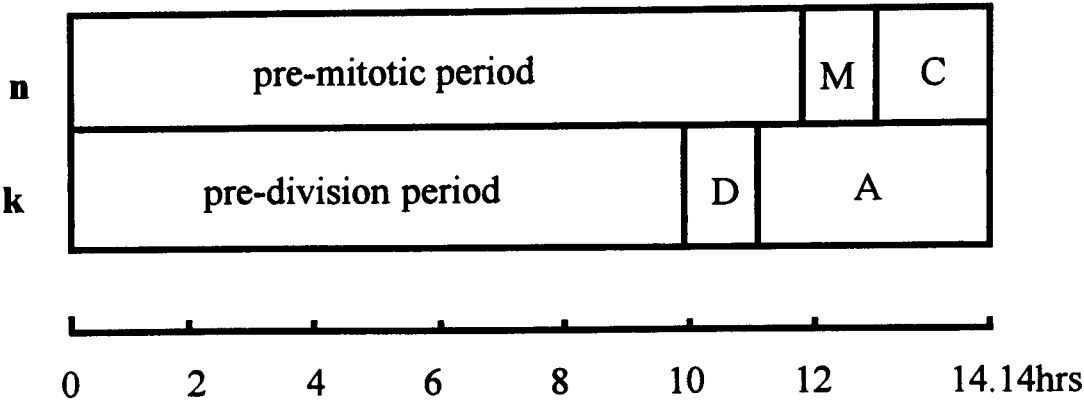
(B)



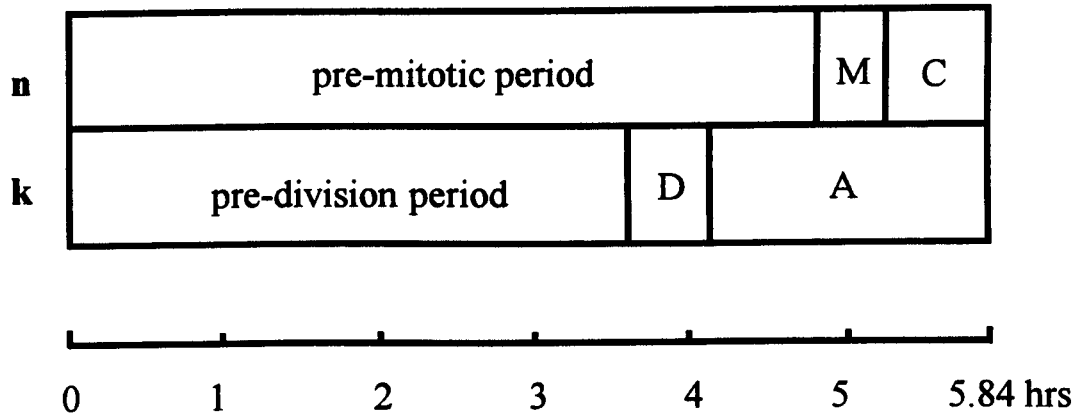
(C)



Figures 3.6B and C *L. mexicana* promastigote and amastigote forms. (a) is the phase contrast image and (b) the corresponding DAPI image of *in vitro* culture forms. In both life cycle stages, the nucleus divided before the kinetoplast (indicated by arrow heads) and there was a short period of cytokinesis in both organelles before cell cleavage occurred. Arrow in B indicates a promastigote form just prior to cell cleavage. The promastigotes in B were a sample population from a mid-log phase culture and consisted mainly of long slender nectomonad (type '2') promastigotes (see section 3.4). Scale bar=10 μ m.

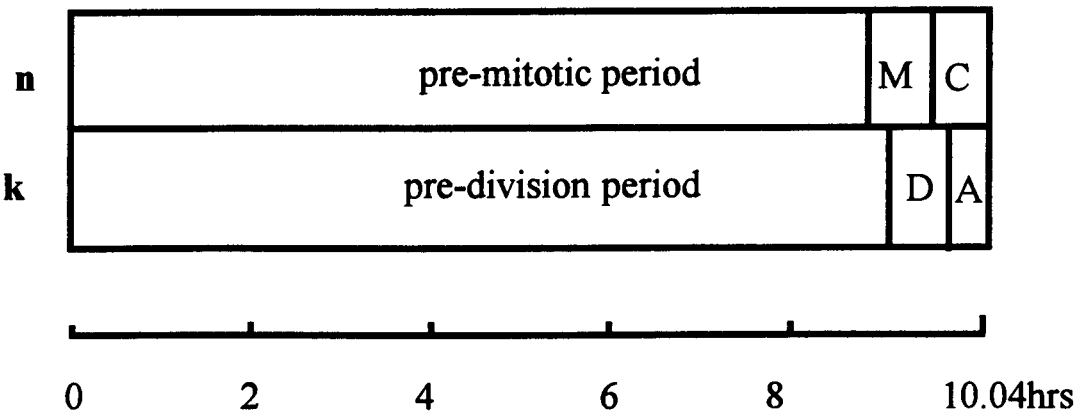


A *T. brucei* procyclic forms

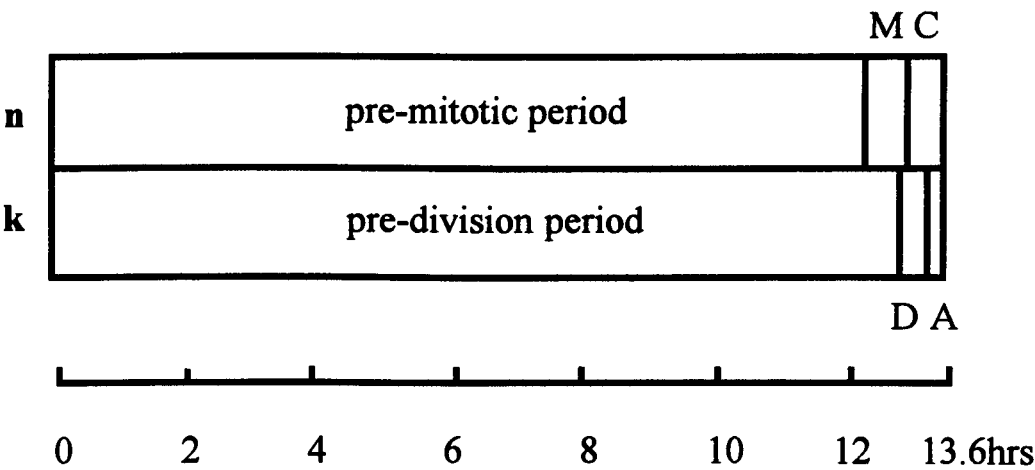


B *T. brucei* bloodstream forms

Figure 3.7A and B The relative timing of mitosis in the nucleus (M), kinetoplast division (D) and the cytokinesis periods (C and A for the nucleus and kinetoplast, respectively) in *T. brucei* procyclic and bloodstream forms.



C *L. mexicana* promastigote forms



D *L. mexicana* amastigote forms

Figure 3.7C and D The relative timing of mitosis in the nucleus (M), kinetoplast division (D) and the cytokinesis periods (C and A for the nucleus and kinetoplast respectively) in *L. mexicana* promastigote and amastigote forms.

Life cycle stage	Culture	PDT (hrs)	Growth rate (r)	r ²
<i>T. brucei</i> procyclic forms	Control	14.9hrs	0.047	0.98
	BrdU	14.1hrs	0.049	0.98
<i>T. brucei</i> bloodstream forms	Control	6.5hrs	0.107	0.97
	BrdU	5.8hrs	0.119	0.96
<i>L. mexicana</i> promastigote forms	Control	10.3hrs	0.067	0.96
	BrdU	10.0hrs	0.069	0.99
<i>L. mexicana</i> amastigote forms	Control	10.8hrs	0.064	0.92
	BrdU	13.6hrs	0.051	0.88

Table 3.1 Growth statistics of culture forms.

Cell type	Cell categories		
	Labelled kinetoplast only (a)	Labelled nucleus and kinetoplast (b)	Labelled nucleus only (c)
<i>T. brucei</i> procyclic forms	23	53	161
<i>T. brucei</i> bloodstream forms	20	489	302
<i>L. mexicana</i> promastigote forms	33	359	158
<i>L. mexicana</i> amastigote forms	82	222	54

Table 3.2A The total number of labelled organelles for two counts conducted after 2 and 4 hours BrdU incubation. The results indicated that there was a non-co-incident start and end to S-phase in the nucleus and kinetoplast, with an overlap in the timing of both periods in all cell types examined. This data was also used in Chi-squares analysis to determine the relative lengths of S-phase (see Table 3.2B).

Cell type	a+b	b+c	χ^2
<i>T. brucei</i> procyclic forms	76	214	89.0
<i>T. brucei</i> bloodstream forms	509	791	100.5
<i>L. mexicana</i> promastigote forms	392	517	30.2
<i>L. mexicana</i> amastigote forms	304	276	2.8*

Table 3.2B Comparing the relative lengths of S-phase. Differences between paired populations significant , df=1, P<0.01, except*.

Cell type	1n, d/2k	1k, d/2n	χ^2
<i>T. brucei</i> procyclic forms	109	1	106.5
<i>T. brucei</i> bloodstream forms	193	0	96.5
<i>L. mexicana</i> promastigote forms	7	32	16.0
<i>L. mexicana</i> amastigote forms	0	36	36.0

Table 3.3A The relative timing of the initiation of mitosis and kinetoplast division. Cells in categories 1 and 2 described in section 3.2.5.2 were analysed by Chi-squares analysis. Differences between paired populations significant, $df=1$, $P<0.01$.

Cell type	2n, 1/dk	2k, 1/dn	*dn/dk	χ^2
<i>T. brucei</i> procyclic forms	1	87	-	84.0
<i>T. brucei</i> bloodstream forms	0	157	-	78.5
<i>L. mexicana</i> promastigote forms	24	1	3	21.2
<i>L. mexicana</i> amastigote forms	29	0	3	29.0

Table 3.3B: The relative timing of the end of mitosis and kinetoplast division. Cells in categories 3 and 4 described in section 3.2.5.2 were analysed by Chi-squares analysis. Differences between paired populations significant, $df=1$, $P<0.01$. In addition, cells with both a dividing nucleus and kinetoplast under the classification criteria adopted were identified in both life-cycle stages of *L. mexicana*, but not *T. brucei**.

Life-cycle stage	Organelle	Organelle configuration		
		single	dividing	post-division
<i>T. brucei</i> procyclic forms	nucleus	87.6	6.5	6.0
	kinetoplast	77.7	7.1	15.2
<i>T. brucei</i> bloodstream forms	nucleus	86.4	6.3	7.3
	kinetoplast	69.5	6.8	23.9
<i>L. mexicana</i> promastigotes	nucleus	92.4	3.1	4.6
	kinetoplast	93.5	3.8	2.8
<i>L. mexicana</i> amastigotes	nucleus	95.4	2.5	2.2
	kinetoplast	97.5	1.9	0.6

Table 3.4 Percentage organelle configurations for the nucleus and the kinetoplast in each of the four stages examined. The 95% confidence limits of each mean were calculated (Snedecor and Cochran, 1967) and were less than 0.06% in all cases.

Life cycle stage	Cell cycle phase	Proportion of the cell cycle (%)	Hours
<i>T. brucei</i> procyclic forms	Pre-mitosis	83.1	11.75
	Mitosis (M)	8.6	1.21
	Cytokinesis (C)	8.3	1.18
<i>T. brucei</i> bloodstream forms	Pre-mitosis	81.6	4.76
	Mitosis (M)	8.2	0.48
	Cytokinesis (C)	10.2	0.6
<i>L. mexicana</i> promastigote forms	Pre-mitosis	89.4	8.98
	Mitosis (M)	4.2	0.42
	Cytokinesis (C)	6.4	0.64
<i>L. mexicana</i> amastigote forms	Pre-mitosis	93.5	12.68
	Mitosis (M)	3.6	0.48
	Cytokinesis (C)	2.9	0.4

Table 3.5A Duration of cell cycle events with respect to nuclear events for each of the stages studied.

Life cycle stage	Cell cycle phase	Proportion of the cell cycle	Hours
<i>T. brucei</i> procyclic forms	Pre-division	70.0	10.03
	Division (D)	8.6	1.22
	Cytokinesis (A)	20.4	2.89
<i>T. brucei</i> bloodstream forms	Pre-division	61.5	3.59
	Division (D)	7.7	0.45
	Cytokinesis (A)	30.8	1.8
<i>L. mexicana</i> promastigote forms	Pre-division	90.9	9.13
	Division (D)	5.1	0.51
	Cytokinesis (A)	4.0	0.4
<i>L. mexicana</i> amastigote forms	Pre-mitosis	96.5	13.08
	Division (D)	2.7	0.37
	Cytokinesis (A)	0.8	0.11

Table 3.5B Duration of cell cycle events with respect to kinetoplast events for each of the stages studied.

Life cycle stage	Proportion of the cell cycle	
	2n	2k
<i>T. brucei</i> procyclic forms	8.3%	20.4%
<i>T. brucei</i> bloodstream forms	10.2%	30.8%
<i>L. mexicana</i> promastigote forms	6.4%	4.0%
<i>L. mexicana</i> amastigote forms	2.9%	0.8%

Table 3.6 The lengths of cytokinesis for the nucleus (2n) and the kinetoplast (2k), as a percentage of the total cell cycle time for each stage studied.

CHAPTER 4 IS ANTIGENIC SWITCHING LINKED TO THE CELL CYCLE?

4.1 Introduction

Antigenic variation is the key strategy which allows African trypanosomes to evade the effects of the host immune response. This strategy involves the switching from expression of one variant surface glycoprotein (VSG) to that of another, an event which occurs at a high rate with almost one in every hundred trypanosomes per generation undergoing switch (Turner and Barry, 1989). The repertoire of VSG genes a trypanosome can express during the course of an infection is very large ($\approx 1,000$ VSG genes) but a hierarchy of expression exists such that particular VSGs are expressed early in infection, while others are expressed later (reviewed by Turner, 1992a).

A VSG gene is always transcribed in a telomeric expression site, with only one expression site being active at any one time (Pays *et al.*, 1994). Two main mechanisms can lead to a change in VSG expression; (1) *in situ* activation of an alternative expression site allows a different VSG gene to be expressed without DNA rearrangements. VSG genes expressed in the early stages of an infection most commonly employ this mechanism. (2) VSG genes replace each other in a given expression site through DNA rearrangements. In this mechanism a gene from the unexpressed repertoire is duplicated and transposed to an expression site where the active gene is displaced, therefore allowing the new gene to be transcribed. The genes located internally in chromosomes (the vast majority) are expressed via this mechanism (reviewed by Turner, 1992a and Pays *et al.*, 1994). The mechanism of duplicative transposition is still unresolved but it may be mediated by a gene conversion (duplex break repair) mechanism (Borst and Rudenko, 1994). Other mechanisms of antigenic variation have been described but only very infrequently. Of these, partial replacements or even point mutations in VSG genes, observed in the

very late stages of infection may be particularly important as they can lead to greater genetic diversity (Borst and Rudenko, 1994).

Approximately 10^7 molecules of VSG are arranged at the surface of each trypanosome, tightly packed in a single layer of homodimers (Jackson *et al.*, 1985). Each VSG is anchored in the plasma membrane by covalent linkage to a glycosyl phosphatidylinositol (GPI) anchor (Ferguson and Homans, 1989). The time required for the trypanosome to synthesize and express a VSG molecule on the cell surface has been estimated to be about 40 minutes (McConnell *et al.*, 1983). When a trypanosome switches expression of one VSG to another, the new molecules intermix with the old ones over the surface of the cell (Esser and Schoenbecher, 1985). This result requires lateral diffusion, as VSG is only exocytosed from a discrete part of the plasma membrane lining the flagellar pocket (Bülow *et al.*, 1988). It is necessary that the new VSG expresses different exposed epitopes from the old VSG and that the mixed coat folds together tightly (Borst and Rudenko, 1994). Stable co-expression of two VSG coats has been observed only once, in *T. equiperdum* in *in vitro* culture (Baltz *et al.*, 1986).

A number of authors have suggested that antigenic variation is linked to the cell cycle (Vickerman, 1985, Turner, 1990, Matthews and Gull, 1994b), but evidence for this link is extremely weak. Non-dividing stumpy forms in the bloodstream are fixed in G₀/G1-phase of the cell cycle (Shapiro *et al.*, 1984) and switching in these forms has not been reported. Metacyclic forms are also fixed in G₀/G1-phase of the cell cycle (Shapiro *et al.*, 1984) and acquire VSG expression at the final stages of development in the fly's salivary glands. Co-expression of two VATs on metacyclic forms was not observed (Tetley *et al.*, 1987). Metacyclic forms are capable of expressing only a small subset of VATs of the parasite's complete repertoire (≤ 27 M-VATs in *T. b. rhodesiense*, Turner *et al.*, 1988) by a stage specific expression mechanism which differs from mechanisms of switching in bloodstream forms (reviewed by Pays *et al.*,

1994). After infection of the mammalian host the first trypanosomes to appear in the bloodstream are bloodstream form parasites expressing M-VATs and undergo rapid switching from one M-VAT to another. Expression of bloodstream VATs occurs during the initial phase of parasitaemia, one of the first being the 'I-VAT', the VAT originally ingested by the tsetse fly (Hajduk and Vickerman, 1981). One study has examined the switching from an M-VAT to three different bloodstream VATs during the initial parasitaemia (Esser and Schoenbechler, 1985). Co-expression of two VSGs was not observed in metacyclic forms from tsetse flies, further evidence that these non-dividing forms do not switch.

While this evidence seems to suggest that antigenic switching could be linked to the cell cycle, no direct evidence linking switching to a particular phase of the cell cycle exists. It was the aim of this study to determine whether such a link exists, using an immunofluorescence technique to detect cells which co-express two VSGs and are therefore undergoing antigenic switching. Cell cycle markers were also used, DAPI staining to determine organelle configurations and therefore the relative stage of the cell cycle for each cell and also an anti-BrdU antibody as an S-phase marker. Correlating cells undergoing antigenic switching with a particular phase of the cell cycle would indicate whether or not such a link exists and might lead to the identification of a single point in the cell cycle where commitment events, leading to antigenic switching events, occur.

4.2 Materials and Methods

4.2.1 Cloned trypanosomes and VAT analysis

The cloned populations used in this study were of the ILTat (ILRAD *Trypanozoon* antigen type) series, derived from the cloned stock EATRO (East African Trypanosomiasis Research Organization) 795. These lines are relatively antigenically homogeneous, can be transmitted through flies and display high rates of antigenic switching (Turner and Barry, 1989). Each line examined is named as shown in Table

4.1, as well as their serological equivalents (isoVATs) of the GUTat (Glasgow University *Trypanozoon* antigen type) 7 series and GUP (Glasgow University Protozoology) (stabilate) numbers, from which infections in mice were established. Each clone was $\geq 98\%$ homogeneous for expression of its designated VAT at the time of stabilisation (Turner and Barry, unpublished results). Also shown are the VATs examined in each population, both 'major' and 'minor' VATs.

4.2.2 Growth of bloodstream form trypanosomes

Trypanosomes were grown from stabilate in Balb/c mice for 3 to 6 days before harvesting and transfer of parasites to *in vitro* culture. *T. brucei* bloodstream forms were cultivated essentially as described in section 2.2.1 using the short-term culture system described by Baltz *et al.* (1985) and modified by Mhlanga and Shall (unpublished data). In summary, trypanosomes were harvested from mice during exponential growth and incubated axenically at a starting density of approximately 1×10^5 cells/ml at 37°C, in 5% CO₂. For each cloned line used in this study, blood smears were also made before cultivation *in vitro*, for the purposes of determining VAT prevalence *in vivo* at the point of harvest. Thin blood smears were made on slides, air-dried and then fixed in 75% ethanol for one hour. Slides were stored at -20°C with silica gel, until processed for immunofluorescence analysis.

4.2.3 Growth rate of cultures

Cell densities were counted each hour for 8-10 hours as described in section 2.2.4.

4.2.4 BrdU Labelling

BrdU labelling was essentially as described in section 2.2.2. In summary, 20mls of an exponentially growing culture was split into two 10ml flasks, one incubated with BrdU and one without (control culture). 0.5ml samples were taken from each flask every hour for 8-10 hours, cells harvested and thin smears made also as described previously.

4.2.5 Immunofluorescent detection of BrdU incorporation and VAT expression

BrdU detection

BrdU incorporation was detected using an anti-BrdU monoclonal antibody by immunofluorescence as described in section 2.2.3.

VAT detection

For each cloned line examined, VAT detection was enabled by use of rabbit anti-sera, rat anti-sera or murine monoclonal antibodies produced from previous studies of antigenic switching in these cloned lines (Turner *et al.*, 1988, Turner and Barry, 1989). Prevalences of the major VAT and minor VAT(s) were determined from the blood smears made before harvesting cells from mice and/or from the smears made from cells cultivated axenically. To detect cells co-expressing two antigens, double labelling was carried out and counts made of cells labelled only with the major VAT antibody, cells labelled only with the minor VAT (s) antibodies and cells which were labelled with both. Indirect immunofluorescence was carried out essentially as described by Van Meirvenne *et al.* (1975), using appropriately diluted anti-sera, ascitic fluid or undiluted monoclonal *in vitro* culture supernatant fractions. To detect two or more antigens, fixed cells were incubated with primary antibodies sequentially, with cells washed in PBS, pH 8.0 between antibody incubations for 10 minutes. Positive cells were detected using mixtures of corresponding conjugates, usually FITC (donkey anti-rabbit IgG, or sheep anti-mouse IgG, SAPU) and TRITC (goat anti-rabbit IgG, Sigma) or Texas Red (goat anti-rabbit or goat anti-mouse, Seralab) all at a dilution of 1 in 50. One VAT was labelled with an anti-immunogold antibody (5nm, Auoprobe, Amersham) using the protocol described by De Waele *et al.* (1986), with Auoprobe used at 1 in 20 and silver enhancement (Amersham) for 10 minutes. 200-400 cells were counted to determine VAT prevalence in each experiment.

4.3 Results

4.3.1 Growth of bloodstream cultures

Growth curves of the control culture and culture incubated with BrdU indicated that the cells grew exponentially over the time course studied and that the BrdU had a negligible effect upon the growth rate (Figures 2.1 and 2.2, 3.3A and B).

4.3.2 VAT labelling

For each cloned line examined, VAT prevalence was determined using the available VAT-specific antibodies described in Tables 4.1. VAT prevalence counts are shown in Table 4.2. In each experiment one major and one or more minor VATs were detected. However, cells co-expressing two VATs and therefore undergoing antigenic switching could not be detected in any of the lines examined. In order to try and explain the discrepancy between these observations and previous reports of co-expression in bloodstream forms (Esser and Schoenbechler, 1985) various control experiments were conducted, to ascertain whether or not failure to detect double expressors was perhaps due to technical limitations. Conjugated antibodies were tested on selected VATs using control blood smears made from populations of cells homogeneous for that particular VAT. In all cases, each conjugate tested proved to be specific for the selected VATs, as indicated in Table 4.3. For the line expressing ILTat 1.64a, double labelling with BrdU and VAT-specific antibodies was achieved but labelling of two VATs simultaneously using FITC, TRITC and immunogold conjugates for detection was unsuccessful. Likewise, for the lines expressing GUTat 7.1 and ILTat 1.61c double labelling with BrdU and VAT-specific antibodies was successful but labelling of cells which co-expressed two VATs was unsuccessful. This was the case for both blood smears made of populations before harvesting cells from mice (*in vivo*), as well as smears made from axenic culture (*in vitro*).

Both Texas Red and TRITC conjugated secondary antibodies (emission spectra 615nm and 580nm, respectively) were compared to ascertain whether any differences

between these two fluorochromes using filter set 487900 (a filter more suitable for Texas Red labelling: excitation filter, BP530-585; mirror, FT600; barrier filter, LP615) on a Zeiss Axioskop fluorescence microscope (Carl Zeiss Inc., New York) had compromised the detection of double expressors. No difference was found between the two conjugated antibodies and still no double expressors were detected. Another filter, filter set 487915 (suitable for rhodamine labelling: excitation filter, BP546/12; mirror, FT580; barrier filter, LP590) was also used in an attempt to detect double expressors of 1.61 and 7.2 in an ILTat 1.61c population, but proved again to be unsuccessful. Figure 4.1 shows labelling of 1.61 with FITC, the major VAT of 1.61c and labelling of 7.2 a minor VAT using Texas Red, to illustrate that positive labelling of single VAT expressing cells was achieved, but co-expressing cells were not detected. Table 4.3 summarises the labelling experiments conducted.

4.4 Discussion

The question as to whether antigenic switching was linked to the cell cycle could not be properly addressed, due to failure to detect double expressors in the cloned lines examined. Labelling techniques were investigated to ascertain whether or not limitations in the detection system contributed to this failure. As each experiment was successful in that single labelled cells could be detected, it seems unlikely that the conjugates tested were at fault. TRITC labelling was compared to Texas Red with little difference found between them in the brightness of the fluorescence. Two different filters, a rhodamine and Texas Red filter were also compared and again no difference was found between them in terms of resolving Texas Red labelled cells, whereas double expressors were still not detected. In a separate study (chapter 5), double labelling of single cells was achieved using antibodies against two surface antigens of *Leishmania major* (a rabbit anti-serum, ab336, against the Gene B protein and a mouse monoclonal antibody, 3F12, against a metacyclic-specific epitope of LPG) using anti-mouse FITC and anti-rabbit Texas Red conjugates, as well as the corresponding filters (see Fig 5.9C). As double labelling was achieved in the case of

L. major, it seems probable that other factors were responsible for the failure to detect co-expressing trypanosomes in this study.

It is possible that antigenic switching was occurring at a low rate, below the level of detection because only small numbers (hundreds) of cells were observed. This possibility would however contradict predictions from switching rates measured in these same populations (Turner and Barry, 1989). Two estimates of overall switching rate for one of the lines examined in this study, ILTat 1.64a, are relatively high, 2.2×10^{-2} switches/cell/generation and 1.6×10^{-3} switches/cell/generation (Turner, unpublished results). It is also possible that double expressors could not be detected due to co-expressing parasites being killed by antibodies against the antigen expressed first, *in vivo*. Double expressors, however, have been detected *in vivo* using other lines, with up to 2.7% of the population undergoing switch at any one time (Esser and Schoenbecker, 1985). Trypanosomes undergoing switch from an M-VAT to a B-VAT in that study, were observed as having weaker reactivity for the rhodamine label (antibody to the M-VAT) than with the fluorescein label (antibody to the B-VAT), although degrees of reactivity varied between individual cells.

The most straightforward explanation for the inability to detect double-expressors in the present study would be that the weaker levels of labelling expected on double-labelled cells fall below the limits of detection of the optical system employed. The use of a 100W mercury vapour source (a 50W mercury vapour lamp was used in this study) as well as the use of low-light video microscopy or equipment which is capable of digitally enhancing images may improve the ability to detect double expressors. The use of other immunocytochemistry or fluorescence techniques e.g. biotin/avidin labelling, gold/silver amplification methods may also improve the likelihood of detecting low-level labelling.

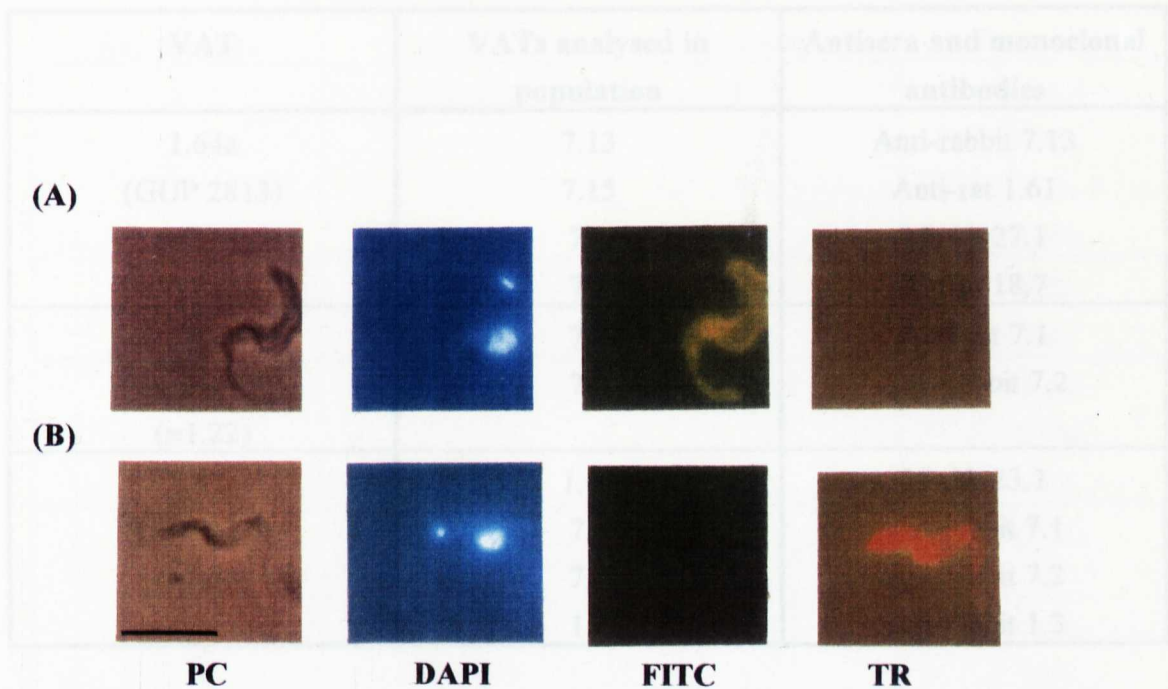


Figure 4.1 Labelling of ILTat 1.61c *T. brucei* bloodstream forms with VAT-specific antibodies (Table 4.2, experiment 5). (A) shows labelling with an anti-1.61 monoclonal antibody, detected with an anti-mouse FITC conjugate. (B) shows labelling with an anti-7.2 rabbit serum, detected with an anti-rabbit Texas Red conjugate. Co-expressing cells were not detected. Both cells were photographed from the same slide. PC=phase contrast, DAPI=DAPI labelling, FITC=fluorescein labelling, TR=Texas Red labelling. Scale bar=10µm.

VAT	VATs analysed in population	Antisera and monoclonal antibodies
1.64a (GUP 2813) (\equiv 7.13)	7.13	Anti-rabbit 7.13
	7.15	Anti-rat 1.61
	7.1	McAb 27.1
	7.2	McAb 18.7
7.1 (GUP 4007) (\equiv 1.22)	7.1	Anti-rat 7.1
	7.2	Anti-rabbit 7.2
1.61c (GUP 2812) (\equiv 7.15)	1.61	McAb 23.1
	7.1	anti-rabbit 7.1
	7.2	anti-rabbit 7.2
	1.3	anti-rabbit 1.3

Table 4.1 Cloned trypanosome populations; VAT, isoVAT and stabilate designations of these lines and VATs analysed.

Experiment	Line	VATs analysed	Prevalence
1	ILTat 1.64a	7.13	39.9%
		7.15	5.0%
		7.1	5.0%
		7.2	0.5%
2	GUTat 7.1	7.1	ND
		7.2	ND
3	ILTat 1.61c	1.61	65.5%
		7.1	0.5%
		7.2	1.5%
4	ILTat 1.61c	1.61	62.5%
		7.1	0
		7.2	1.25%
		1.3	ND
5	ILTat 1.61c	1.61	46.5%
		7.2	0.5%
6	ILTat 1.61c	1.61	48.5%
		7.2	0.5%

Table 4.2 VAT prevalence of each cloned line analysed (ND=not determined).

Experiment	Type of labelling	Summary
1	7.13+TRITC, 7.15+Immunogold & BrdU+FITC; 7.13+TRITC & 7.1+FITC; 7.13+TRITC & 7.2+FITC	Positive labelling of each VAT Double labelling of BrdU and 7.15 No DEs detected
2	7.1+Immunogold & 7.2+TRITC & BrdU+FITC	Positive labelling of each VAT and BrdU No DEs detected
3	1.61+FITC & 7.1+TRITC; 1.61+FITC & 7.2+TRITC; 7.2+TRITC & BrdU+FITC	Positive labelling of each VAT and BrdU No DEs detected
4	1.61+FITC & 7.1+TRITC; 1.61+FITC & 7.2+TRITC; 1.61+FITC & 1.3+TRITC	Positive labelling of each VAT (except 7.1) No DEs detected
5 Using filter 00 (Texas Red)	1.61+FITC & 7.2+Texas Red	Positive labelling of each VAT No DEs detected
6 Using filter 15 (Rhodamine)	1.61+FITC & 7.2+Texas Red	Positive labelling of each VAT No DEs detected

Table 4.3 A summary of the labelling experiments outlined in Table 4.2.
DE=Double Expressor.

CHAPTER 5 DIFFERENTIATION OF *L. MAJOR* PROMASTIGOTES TO METACYCLIC FORMS

5.1 Introduction

Leishmania parasites undergo a series of differentiation steps during their migration within the alimentary tract of the sand fly vector (reviewed by Molyneux and Killick-Kendrick, 1987; Walters, 1993). Procyclic promastigote forms develop from the intracellular amastigote stage soon after ingestion of a blood meal (18-24 hrs). These short ovoid forms divide rapidly in the abdominal midgut and transform to long slender nectomonad forms. Forward migration towards the thoracic midgut (4-5 days post-feeding) is accompanied by morphological transformation to other promastigote forms, including the short slender highly motile metacyclic form, found predominantly at the stomodeal valve and in the foregut. Metacyclic forms appear to be non-dividing and are highly infective to the mammalian host (Sacks and Perkins, 1984). Although different morphological types appear sequentially *in vivo* and in *in vitro* culture (Molyneux and Killick-Kendrick, 1987; Brown *et al.*, 1994a, b), the most distinct differentiation step is from dividing cells with various morphologies to metacyclic forms. Metacyclics have short slender cell bodies and long flagella and are readily distinguishable from other forms, particularly in stationary phase in *in vitro* cultures (Bates and Tetley, 1993). These forms are highly virulent, shown by a marked increase in infectivity of experimental animals in comparison to their log-phase counterparts (Da Silva and Sacks, 1987) and are also more resistant to intracellular killing by macrophages and extracellular killing by complement (reviewed by Sacks, 1992).

Increased virulence of metacyclic forms is thought to be attributable, at least in part, to biochemical modifications to the major surface molecule of *Leishmania*, the lipophosphoglycan (LPG), during metacyclogenesis (Sacks, 1992). During this differentiation step, an elongation of the molecule occurs, due to an approximate

doubling in the number of phosphorylated oligosaccharide units as well as a down-regulation in the number of sidechain substitutions expressing a terminal galactose residue in favour of terminal arabinopyranose residues. As a result of these changes to their surface carbohydrates, metacyclics exhibit a loss in binding by peanut lectin agglutinin (PNA) and as such can be separated from log-phase promastigote forms. This characteristic has been observed in two species of *Leishmania*; *L. major* and *L. donovani* (Sacks *et al.*, 1985, Howard *et al.*, 1987).

Changes in expression of another molecule also occurs during metacyclogenesis. Gene B protein is a hydrophilic protein expressed on the surface of metacyclic forms but not in log-phase promastigotes (Flinn *et al.*, 1994). This protein associates with LPG on the cell surface, as shown by membrane capping (Pimenta *et al.*, 1994). The protein is characterised by an unusual amino acid repeat motif related to the peptidoglycan binding domain of protein A from *Staphylococcus aureus* strongly suggesting that the Gene B protein interacts with LPG and/or GIPLs via this domain in order to attach to the cell (Bates, 1995).

The aim of this study was to examine metacyclic production in *in vitro* cultures of *L. major* using three metacyclic specific markers: a monoclonal antibody (3F12) against arabinose containing oligosaccharide repeat units upregulated in metacyclic specific LPG (Sacks and Da Silva, 1987, Kelleher *et al.*, 1994), a rabbit anti-serum (ab336) against Gene B protein (Flinn *et al.*, 1994) and non-agglutination by PNA (Sacks and Da Silva, 1987). These markers could be used to establish the generality of the observations made for differentiation in trypanosomes by comparing the data from that organism (Turner *et al.*, 1995) with equivalent data in another (much more tractable) system. Because studying differentiation in *Leishmania* is more tractable, due to the availability of suitable stage-specific markers, it is also possible to extend studies of differentiation to address one question that cannot as yet be addressed in *T.*

brucei; to investigate how commitment to differentiation relates to the cell cycle.

Four key questions regarding metacyclogenesis could therefore be addressed:

1. Is metacyclogenesis intrinsically programmed within the cell or induced by environmental changes?
2. Does metacyclogenesis fit a simple or a heterogeneous model of differentiation (Turner *et al.*, 1995)?
3. Is commitment irreversible or can metacyclic forms de-differentiate to promastigote forms?
4. Does the commitment to differentiation arise before or after cell division?

5.2 Materials and Methods

5.2.1 Cultivation of *L. major* promastigotes

L. major promastigotes were routinely cultivated in HOMEM medium (Berens *et al.*, 1976) plus 10% heat-inactivated foetal calf serum (Labtech). Two strains of *L. major* were used throughout the study; HMOM/SA/83/RKK2, hereinafter termed RKK2, and another strain, NIH/Friedlin clone VI (MHOM/IL/80/Friedlin), hereinafter termed Friedlin VI. RKK2 promastigotes were originally transformed from lesion amastigote forms and cryopreserved as stabiliates in 5% DMSO in liquid nitrogen as stabilate GUP 3579. Friedlin VI promastigotes were provided by Dr. D.F. Smith, Imperial College, London after transformation from amastigotes and 4 sub-passages in culture. They were cryopreserved in 7% glycerol as stabiliates GUP 4141. All growth experiments were conducted using cultures which had been sub-passaged less than 10-12 times, because of loss of metacyclic production *in vitro* through extensive sub-passaging (Da Silva and Sacks, 1987).

5.2.2 Growth of *L. major* promastigotes

Growth studies were routinely carried out by seeding 3 cultures at a starting density of 10^5 cells/ml and counting cell densities every 12 hours. Also, 0.5 ml samples were

taken from each culture at each time point, cells pelleted and washed in PBS pH 7.2 before smears were made onto slides, air-dried and fixed in 75% ethanol at 4°C.

5.2.3 Immunofluorescent detection of metacyclic forms

Immunofluorescence was essentially as described by Van Meirvenne *et al.* (1975). Two antibodies were used to detect metacyclic-specific antigens; an affinity purified rabbit anti-serum, ab336, a gift from Dr. D.F. Smith, Imperial College, London and a monoclonal antibody, 3F12, a gift from Dr. D.L. Sacks, NIH, USA. Briefly, fixed cells on smears were incubated with the primary antibody at an appropriate dilution (1:100 for ab336 and 1:20 for 3F12) for 30 minutes in a humid chamber. After washing twice in PBS pH 8.0 for 10 minutes, cells were incubated with appropriate FITC conjugated antibodies (SAPU) at a concentration of 1:50 for 15 minutes. The smears were then washed briefly in PBS, counterstained with DAPI, 0.01mg/ml, and mounted in Mowiol solution containing 2.5% DABCO as an anti-fading agent. The percentage of metacyclic forms was determined for the three cultures at each time point. At least 400 cells per smear per culture were counted.

5.2.4 Models for replication, growth and differentiation

The simplest possible model of *Leishmania* parasites growing in culture without limit is shown in Figure 5.1, derived from an equivalent model for slender to stumpy differentiation in *T. brucei* (Turner *et al.*, 1995). A promastigote population (X) replicates by binary fission at rate r and differentiates to a non-dividing metacyclic population (Y) at rate f . m is the mortality rate of metacyclics. This model can be described as a pair of coupled differential equations:

$$\frac{dX(t)}{dt} = (r-f)X(t) \quad (1)$$

$$\frac{dY(t)}{dt} = fX(t) - mY(t) \quad (2)$$

This system has analytical solutions (equations (3) and (4)) and an illustrative solution is shown in Figure 5.2A.

$$X(t) = X(0)e^{(r-f)t} \quad (3)$$

$$Y(t) = \frac{fX(0)}{r-f+m} (e^{(r-f)t} - e^{-mt}) \quad (4)$$

The key feature of this model is that it predicts the metacyclic population to grow at a rate approximately equal to or greater than that of the promastigote population. Experimental data (presented below) shows this model to be unrealistic in that the growth rate of the metacyclic population is lower than that of the promastigote population. One possibility which could explain the apparent difference between the predicted outcome of the model and the experimental data is that the dividing promastigote population is heterogeneous, consisting of promastigote forms which replicate and differentiate at different rates. To obtain this new model equations (1) and (2) are extended:

$$\frac{dX_i(t)}{dt} = (r_i - f_i)X_i(t) \quad (5)$$

$$\frac{dY_i(t)}{dt} = f_iX_i(t) - mY_i(t) \quad (6)$$

where subscript i refers to a particular type of parasite with characteristic replication and differentiation rates r_i and f_i . These equations have analytical solutions (equations (7) and (8))

$$X(t) = \sum_{i=1}^n X_i(t) = \sum_{i=1}^n X_i(0) e^{(r_i - f_i)t} \quad (7)$$

$$Y(t) = \sum_{i=1}^n Y_i(t) = \sum_{i=1}^n \frac{f_i X_i(0)}{r_i - f_i + m} \left(e^{(r_i - f_i)t} - e^{-mt} \right) \quad (8)$$

and illustrative solutions, assuming there are two kinds of parasite, shown in Figure 5.2B and C. These solutions show populations growing with two particular sets of parameter values and demonstrates that, at least under some circumstances, growth rates of the metacyclic populations can be slower than those of the promastigote populations.

5.2.5 Agglutination of promastigote forms

Cells were grown to a density of $1-2 \times 10^7$ cells/ml (day 4/5 of culture), at which point cells were usually in stationary phase. Promastigote forms were then separated from metacyclic forms using peanut lectin agglutinin (PNA, Sigma) using a procedure modified from that described by Sacks and Da Silva (1987). Cells were pelleted by centrifugation at 500g for 10 minutes, resuspended in incomplete HOMEM at a density of 5×10^8 cells/ml and incubated with $100 \mu\text{g/ml}$ of PNA at room temperature for 30 minutes. Non-agglutinated cells (PNA- population) present in the supernatant were then separated from agglutinated cells (PNA+ population). The PNA+ population was passed through a needle several times in order to separate cell clumps. Smears were made from each of the enriched populations for immunofluorescence analysis to assess the degree of enrichment. Growth of PNA+ and PNA- populations was examined by seeding new cultures at 10^6 cells/ml, in comparison to control cultures of cells which had not undergone agglutination with PNA.

5.2.6 BrdU labelling

BrdU labelling was as described previously in section 2.2.2. In summary, three cultures (PNA+, PNA- and control cells not treated with PNA) were incubated with

50µM BrdU and an equimolar solution of 2-deoxycytidine. 0.5 ml samples were taken from each culture after 2 and 4 hours incubation, cells pelleted and washed in PBS pH 7.2 and smears made onto slides, air-dried and fixed in 75% ethanol at 4°C for 1 hour.

5.2.7 Immunofluorescent detection of BrdU incorporation

Immunofluorescence using an anti-BrdU monoclonal antibody was essentially as described in section 2.2.3. Numbers of cells labelled in the nucleus only, kinetoplast only, as well as those labelled for both organelles were counted at each time point. 500 cells were scored at each time point, for each culture.

5.2.8 De-differentiation studies

To determine whether metacyclic forms de-differentiate to log-phase promastigote forms, two experiments were conducted. In the first experiment, promastigote forms were grown for 2 days (mid-log phase) and for 6 days (stationary phase). Cells from each of these populations were seeded into new cultures at 10^6 cells/ml. A third set of cultures were seeded at the same density but with a 50:50 ratio of Day 2 and Day 6 culture forms. The growth of each culture was subsequently monitored by counting total cell densities every 12 hours. At each time point smears of cells were made to ascertain the number of metacyclics present using the ab336 antibody marker. Percentages of promastigotes present were calculated by subtracting the number of metacyclic forms from the total population. Exponential regression analysis of the promastigote data was conducted in order to determine the equation of the line $y=cxe^{mx}$, where c is the intercept of the y -axis and hence the 'calculated' number of promastigotes at $t=0$. The calculated number of promastigote forms at $t=0$ represented the actively dividing population and was compared to the 'observed' numbers of promastigote forms at $t=0$ as determined by prevalence counts using the antibody marker.

The second experiment was similar in design, except in this case populations of cells separated by agglutination were employed as starting materials. PNA- cells were separated from PNA+ cells and each seeded at a density of 10^6 cells/ml, together with cultures initiated with a 50:50 ratio of PNA- and PNA+ cells. Growth of each population was monitored as in the previous experiment, with the percentages of metacyclics and promastigotes determined at each time point. Regression analysis of the promastigote data was conducted in order to determine the calculated number of promastigotes at $t=0$. The calculated number of promastigote forms at $t=0$ was compared to the observed numbers of promastigote forms at $t=0$ as determined by prevalence counts using the antibody marker.

5.3 Results

5.3.1 Metacyclic production *in vitro*

To determine whether differentiation is programmed and/or induced, growth of promastigotes was examined every 12 hours *in vitro*. The number of 3F12 positively labelled cells was ascertained at each time interval, giving the percentage of metacyclics present. Figure 5.3A and B shows the production of metacyclic forms in cultures of Friedlin VI and RKK2 cells, respectively. For both strains the number of metacyclics increased during logarithmic phase, indicating that differentiation is in part intrinsically programmed. As the total population reached stationary phase an increase in the rate of production of metacyclic forms was observed (50-80 hrs after initiation of cultures), suggesting that at this point in the growth curve, differentiation was induced.

In the study of metacyclic production in Friedlin VI culture forms, cells positively labelled with the ab336 antibody were counted at selected time points in the growth curve. Prevalence counts with this antibody correlated well with counts of 3F12 positive cells at these time points (Table 5.1A). Similarly, cells which were double labelled with both antibodies also correlated well with these prevalence counts,

although a small proportion of cells were identified as being single labelled for either antibody (Table 5.1B). A decline in the percentage of metacyclic forms during the exponential phase of growth was also observed, until stationary phase was reached and the percentage of metacyclic forms started to increase again (Tables 5.1A and B). The decline in percentage prevalence of metacyclic forms during the exponential phase of growth did, however, convert to an increase in the absolute abundance of metacyclics (see Figures 5.4A and B).

Differences in the staining pattern of the two antibodies were also observed which may account for slight differences in their respective prevalence counts. Ab336 labelling can be observed in the flagellar pocket region of some cells identified as logarithmic-phase promastigotes under morphological criteria (Flinn *et al.*, 1994). Cells identified as metacyclic forms, however, were labelled over the entire cell surface, including the flagellum. Only cells which were labelled over the entire cell surface were classified as a positively labelled cell in this study. 3F12 shows a slightly different pattern of labelling. An 'internal' stain can be observed on a proportion of cells morphologically identified as log-phase cells, whereas cells which are morphologically metacyclic show complete cell surface labelling, including the flagellum (Saraiva *et al.*, in press). Cells which were labelled over the entire cell surface as well as cells displaying a strong internal stain were classified as positively labelled cells in this study. Immunostaining was originally compared to both positive and negative controls to verify the specificity of both antibodies (data not shown).

The exponential phase of growth of these data were examined in further detail. Figures 5.4 A and B show the rate of increase in the numbers of metacyclic forms compared to the increase in promastigote forms for Friedlin VI and RKK2 cells, respectively. In each case, the growth rate of metacyclic forms was significantly lower than the growth rate of promastigote forms. This contrasts with a second study of metacyclic production in Friedlin VI strain promastigote forms. In this case there

was no significant difference in the rates of increase of metacyclic forms and promastigote forms (Figure 5.4C). Low numbers of metacyclic forms were produced during growth of these cells, reaching a total of 3.2% prevalence in stationary phase (after 84 hrs growth), in contrast to 9-14% at an equivalent time point in the other two experiments, which increased thereafter to 17.5-21.0% in the time course examined (120 hrs growth). The ability of cultured promastigote populations to produce metacyclic forms appeared to vary even from one passage to the next (data not shown) and is especially noticeable after extensive sub-passaging (Da Silva and Sacks, 1987).

The growth data shown in Figures 5.4 A-C was compared with the mathematical models described in section 5.2.4. The simple homogeneous model illustrated in Figure 5.2A could explain the relative growth rates of the metacyclic and promastigote population measured in one experiment (Figure 5.4C) but would not be able to account for the data in two other experiments (Figure 5.4A and B). In contrast, the heterogeneous model illustrated in Figure 5.2B and C could account for all three sets of data, where sub-populations exist which replicate and differentiate at different rates. The heterogeneous model may still be deficient, however, in terms of an adequate representation of *Leishmania* biology. It assumes (1) that metacyclic forms do not divide and (2) that they are incapable of de-differentiating to promastigotes. Each of these two possibilities has been tested experimentally.

5.3.2 Are metacyclics non-dividing forms?

The models described in section 5.2.4 assumes that metacyclics are non-dividing forms. To specifically address the question as to whether this assumption is valid in *Leishmania*, a marker for cell cycle progression, bromo-deoxyuridine (BrdU) described in chapters 2 and 3, was used to determine whether metacyclics progress through the cell cycle or are indeed cell cycle arrested. By agglutination with PNA, two populations of cells were separated; cells which were PNA⁺ (mainly

promastigote forms) and cells which were PNA- (mainly metacyclic forms). After 2 and 4 hours incubation with BrdU, a greater number of promastigote forms were labelled in comparison to metacyclic forms for both Friedlin VI and RKK2 culture forms (Tables 5.2A and 5.2B, respectively). In each study, however, a proportion of the PNA- population was labelled with the anti-BrdU antibody which could have been attributed to either a proportion of metacyclics in the PNA- population undergoing growth, or log-phase cells contaminating this population. Examination of the percentage of metacyclic forms in the PNA- population (Table 5.3), indicated that some promastigote forms had contaminated the population and were likely to be responsible for the BrdU labelling observed in this population.

Growth of PNA- populations was also monitored in comparison to PNA+ cells and a control stock culture for both Friedlin VI and RKK2 strain culture forms (Figure 5.5A and B). PNA- cells of Friedlin VI culture forms did not recover growth until after 25 hours, resuming a similar rate of growth to PNA+ cells and stock culture forms. In RKK2 culture forms, PNA- cells did not recover growth until after 40 hours growth, subsequently growing at a slower rate compared to PNA+ cells and stock culture forms. The observation of growth of cultures from PNA- populations in both experiments could be attributed either to the contaminating log-phase cells, or metacyclic forms which had de-differentiated. In summary, this evidence, as well as observations from other studies (Sacks and Perkins, 1984, Molyneux and Killick-Kendrick, 1987), suggest, but cannot conclusively demonstrate, that metacyclic forms are indeed non-dividing forms.

5.3.3 Do metacyclics de-differentiate to promastigote forms?

A question related to that of the non-dividing status of metacyclic forms concerns whether these cell types are capable of de-differentiating to promastigote forms or not. The formal models (section 5.2.4) assume that de-differentiation does not occur. To address this question of ability to de-differentiate, growth of RKK2 cells from a

day 2 culture was compared to growth of cells from a day 6 culture, as well as to growth of a culture containing a 50:50 ratio of cells from both populations (Figure 5.6A). Day 2 cells were an actively dividing population and as such grew without limit until reaching stationary phase after approximately 50 hours growth. Day 6 cells, a stationary phase population, lagged for approximately 20 hours, before exponential growth was restored. The 50:50 ratio population was intermediate to growth of the day 2 and day 6 populations. At each 12 hourly interval the prevalence of metacyclic forms was determined by ab336 labelling to obtain the number of promastigote forms present (total population minus metacyclic population). From the numbers of promastigote forms calculated, regression analysis of the period of exponential growth for each culture was made, such that the growth rate r , population doubling time (PDT) and intercept of the y -axis, c , was determined. The intercept c represents the estimated number of promastigote forms at the initiation of each culture ($t=0$) capable of growth.

This calculated number of promastigote forms capable of growth was compared to the observed number of promastigote forms determined by the absence of ab336 labelling at the start of the experiment ($t=0$). By comparing these two figures three possibilities can be considered (Table 5.4). Firstly, if the the observed number of promastigote forms was significantly greater than the calculated number of promastigote forms capable of growth, then this would indicate that a proportion of the ab336 unlabelled (promastigote) population was not actually growing (interpretation A). Secondly, if the number of observed promastigote forms was lower than the calculated number then this would suggest that metacyclic forms had de-differentiated to dividing promastigote forms (B). Thirdly, if observed and calculated numbers were equal then this would suggest that all promastigote forms grew while metacyclic forms did not (C) or that the number of metacyclic forms which de-differentiated equalled the number of promastigote forms which did not grow (D).

Figure 5.7A shows logarithmic growth of each population examined. This growth data was used in regression analysis, the results of which are shown in Table 5.5A. In the day 2 population, the observed number of promastigote forms approximately equalled the calculated number of promastigote forms (Table 5.6A), suggesting that interpretation (C) or (D) is correct (Table 5.4). In the 50:50 ratio population of day 2 and day 6 cells, the observed number of promastigote forms was higher than the calculated number, suggesting that a proportion of promastigote forms was not growing (A). Finally in the day 6 population, the prevalence of observed promastigote forms was significantly higher than the calculated number, indicating that a large proportion of promastigotes did not grow, but also remained undifferentiated (A).

In a second experiment, metacyclic forms were separated from promastigote forms by agglutination and growth of each population monitored, as well as a population containing 50:50 ratio of PNA⁺ and PNA⁻ cells (Figure 5.6B). Growth of the PNA⁺ population lagged for approximately 20hrs before growth was restored. The 50:50 ratio population lagged for a longer period (approx. 30hrs) before resuming growth at a rate similar to the PNA⁺ population. The PNA⁻ population, however, decreased in cell density until approximately 40hrs, indicating that a proportion of the population died within this period. After 40hrs the population appeared to resume growth but with a growth rate slower than that of PNA⁺ population. The resulting curve also appeared more variable, a result attributed to cells clumping and therefore giving less accurate cell counts.

Figure 5.7B shows logarithmic growth of each population examined. This growth data was used in linear regression analysis, the results of which are shown in Table 5.5B. In the PNA⁺ population, the observed number of promastigote forms was greater than the calculated number, suggesting that interpretation (A) is correct (Table 5.6B). In the 50:50 ratio population the observed number of promastigote

forms was also higher than the calculated number of promastigote forms growing, suggesting also that in this case (A) was correct. In the PNA- population, however, the observed number of promastigote forms was significantly lower than the calculated number, suggesting that a proportion of the metacyclic population had in fact de-differentiated. This de-differentiation was likely to have occurred at a low rate, indicated by the difference in the slopes for the PNA- population in comparison to the PNA+ population (Figure 5.7B) and the extended PDT calculated for the PNA- population (Table 5.5B).

5.3.4 Models of metacyclic production

A number of models of metacyclic production can be considered, depending upon whether the commitment to differentiate is before or after cell division (Figure 5.8). In the first model (A), a promastigote divides to two daughter promastigote forms, one of which is committed to differentiate without further cell division, while the other continues to divide and may become committed at some point afterwards. In the second model (B), a promastigote is committed to differentiate and divides asymmetrically into a promastigote and metacyclic form. Finally, in model (C) a promastigote becomes committed and divides symmetrically into two daughter metacyclic forms (models adapted from Matthews and Gull, 1994b). To investigate which of these models might prove correct, immunostaining with both the ab336 and 3F12 antibodies was examined at the cellular level. Observations of cells labelled with the two metacyclic specific antibody markers have indicated that model (C) of Figure 5.8 appears to be correct. Figure 5.9 shows a number of examples of positively labelled cells late in the cell cycle immediately prior to cell cleavage, indicating symmetrical production of two daughter metacyclic forms. Models A and B would not be expected to generate patterns of labelling such as those shown in Figure 5.9.

5.4 Discussion

This study of metacyclic production in *in vitro* culture demonstrated two main features; differentiation from promastigote to metacyclic forms is intrinsically programmed within the parasite, indicated by the increase in metacyclic forms through time in culture (Figures 5.3A and B) and that differentiation can also be induced by a change in environmental conditions, shown by the increase in the rate of metacyclic production as the total population reached stationary phase. Intrinsic programming of differentiation has been observed in a study of slender to stumpy differentiation in *T. brucei* infections *in vivo* (Turner *et al.*, 1995). How induction of differentiation occurred in this study was not examined in detail, in terms of analysing the role of putative induction factors. Induction of metacyclogenesis has been observed in other studies (see also section 1.3.2). Growth of *L. mexicana* promastigote forms at an acidic pH (pH 5.5) induced metacyclogenesis (Bates and Tetley, 1993). A decrease in pH during growth in culture could be a density-dependent regulator of parasite numbers by promoting differentiation, either by selection or induction. Regulation of parasite numbers may occur *in vivo* by lowering pH, as products of promastigote metabolism appear to decrease pH (Marr, 1980).

Incubation of log-phase *L. major* promastigotes in 'spent' medium from stationary phase cultures has been shown to produce infective organisms in 4-6 hours (Sacks and Perkins, 1985), a result similarly observed in another study of *L. major* (Mallinson and Coombs, 1989). These observations suggest that a soluble factor is capable of inducing differentiation. Induction of slender to stumpy differentiation by conditioned medium has also been demonstrated in an *in vitro* culture system of *T. brucei* bloodstream forms (M. Boshart, pers. comm.) although unequivocal evidence for induction of differentiation has so far not been observed in trypanosome infections *in vivo*. Induction of stumpy production has been suggested in one study, where the reduction in slender form replication results from the depletion of a host-derived factor and hence promotes stumpy production (Black *et al.*, 1985). However,

another study has suggested that depletion of a growth factor may not occur and that the reduction in slender forms is due to selective killing of slender forms at the peak of parasitaemic wave by immune effector responses (McLintock *et al.*, 1993). Induction of differentiation from epimastigote forms to metacyclic trypomastigote forms of *T. cruzi* has also been demonstrated, where the incubation of culture-derived epimastigote forms in chambers implanted subcutaneously in mice, induced differentiation to trypomastigote forms (Sher and Snary, 1982). Induction was blocked by a monoclonal antibody specific for a surface glycoprotein found only on the surface of epimastigotes and metacyclic trypomastigotes. This induction regime, however, was considered to be rather different from the situation in the wild, where lectins in the digestive tract of the insect vector are likely to play an important role in the control of *T. cruzi* differentiation (Williams, 1985).

Examination of the exponential phase of growth of each strain indicated that in two of three experiments the rate of increase of metacyclic forms was significantly slower than the rate of increase of promastigote forms (Figure 5.4A and B). While one experiment (Figure 5.4C) confirmed the predictions of the simple homogeneous model (Figure 5.2A), where the replication rate is equal to the differentiation rate, the other two experiments proved this model to be unrealistic and that the heterogeneous model (Figures 5.2B and C) could provide an explanation for all three sets of data. The heterogeneous model indicates that the promastigote population consists of sub-populations which replicate and differentiate at different rates and recovers the biological reality that is missing from the simple homogeneous model whereby the metacyclic population can, under some circumstances, grow more slowly than the promastigote population. These circumstances depend on details of parameter values. Other models might reasonably explain the experimental data but the heterogeneous model has the advantage over these others in that it is both a simple and testable model. Experimental data has similarly been obtained in a study of slender to stumpy differentiation in trypanosome infections *in vivo*, indicating that the total population

consists of sub-populations which replicate and differentiate at different rates (Turner *et al.*, 1995). The heterogeneous model may provide therefore a reasonable explanation for kinetoplastid replication and differentiation in general, but would not rule out other possible models.

Numbers of metacyclic forms produced in culture (17.5-25.0% on day 6) were comparable to published figures. Da Silva and Sacks (1987) reported a maximum of 25% metacyclics by non-agglutination of *L. major* V121 promastigotes on days 6 and 7 of culture. Bates and Tetley (1993) reported approximately 25% metacyclics by morphological criteria on day 6 of growth of *L. mexicana* *in vitro*. The percentage of metacyclic forms during the exponential phase of growth in both Friedlin VI (Table 5.1A and B) and RKK2 (data not shown) promastigotes also declined until stationary phase was reached, when the percentage of metacyclic forms increased again. The percentage of metacyclics which decreased during the exponential phase of growth, however, did represent an increase in absolute abundance (Figures 5.4A and B). Very low numbers of metacyclics were produced in stationary phase in one experiment of metacyclic production in Friedlin VI strain promastigote forms, despite being a culture of low passage number (5 passages) (Figure 5.4C), indicating that in this case the total population had reached stationary phase without metacyclogenesis occurring (data not shown). No induction of differentiation was observed either (data not shown). Frequent subculturing has been shown to produce a dramatic decrease in infective forms (Giannini, 1974, Da Silva and Sacks, 1987) and the data presented here would suggest that metacyclogenesis can be highly unstable even for cloned lines.

This study has also provided evidence that metacyclic forms are non-dividing. Populations separated by agglutination and incubated with BrdU indicated that a lower percentage of the PNA- population (mainly metacyclic forms) was labelled in comparison to the PNA+ population (mainly promastigote forms) (Tables 5.2A and

B). Metacyclic forms have been identified as non-dividing in other studies (Sacks and Perkins, 1984, Molyneux and Killick-Kendrick, 1987) and are presumably fixed in G₀/G₁-phase of the cell cycle. Examination of DNA content of metacyclic forms would confirm whether or not they are fixed at this point in the cell cycle, as is the case in metacyclic forms of *T. brucei* (Shapiro *et al.*, 1984). BrdU labelling of the PNA- population was attributed to log-phase cells contaminating the population. Generally, separation of populations of cells by agglutination yielded 73.0-98.0% metacyclic forms, either by 3F12, ab336 or double labelling, numbers comparable to published yields (Ready and Smith, 1988). Why a difference between the number of 3F12 and ab336 labelled cells was observed in agglutination of Friedlin VI culture forms (Table 5.3) is unclear but could be attributed to the different labelling pattern of the antibodies, as described in section 5.3.1. Prevalence counts of 3F12 labelled cells included a proportion of cells displaying a strong 'internal' stain, forms recently identified as promastigote forms under morphological criteria (Saraiva *et al.*, in press). Ab336 labelled cells were only classified as positive if labelled over the entire cell surface and would therefore account for the greater number of cells designated metacyclics by 3F12 labelling in comparison to ab336 labelling.

Throughout the entire study, cells were characterised as metacyclic forms by labelling of the two metacyclic-specific markers in comparison to positive and negative controls and not by morphological criteria. Another strain of *L. major*, LV39, was originally tested for 3F12 and ab336 labelling. While this strain could be positively labelled with the ab336 antibody and expresses high levels of the Gene B protein (D.F. Smith, pers. comm.) it remained unlabelled with the 3F12 antibody. LV39 appears not to express the 3F12-specific epitope, which is arabinose containing oligosaccharide repeat units (S. Cilmi, pers. comm.).

To determine whether metacyclic forms de-differentiate to promastigote forms, the growth of populations from different days in culture (day 2 compared to day 6) as

well as populations separated by agglutination were analysed. By regression analysis of the exponential growth phase of each population, the number of culture forms capable of growth at $t=0$ could be calculated and compared to the prevalence of promastigote forms at this point as determined by absence of labelling with the ab336 antibody (Tables 5.6A and B). Table 5.4 describes the situations under which metacyclic forms would/would not differentiate. Comparison of observed promastigote prevalence to the number of growing promastigotes suggested that a stationary phase population (day 6 of culture) consisted of populations of cells which did not grow, but also remained undifferentiated. 74.5% of the population were promastigotes in this culture while only 10% of this population were capable of growth. Promastigote forms could become growth arrested either through nutrient or growth factor depletion, or the presence of a growth inhibitor. A further implication of this study is that stationary phase populations are not a reliable source of metacyclic forms and that care should be taken to distinguish between cells which are neither dividing nor differentiated to non-dividing metacyclic forms. A stationary phase population which is heterogeneous with respect to the growth status of its sub-populations as well as their capacity to differentiate, provides further evidence that the heterogeneous model could provide a reasonable explanation for promastigote replication and differentiation.

Examination of populations separated by agglutination indicated that the PNA-population (mainly metacyclic forms) contained metacyclic forms which de-differentiated to promastigote forms. Only 1.75% of the PNA- population were promastigote forms, however, almost 20.0% were capable of growth suggesting that a proportion of the 98% pure metacyclic population had de-differentiated to dividing promastigote forms. This observation bears comparison to transformation in *T. brucei*, where stumpy forms differentiate to procyclic forms preferentially, synchronously and co-incidentally through their first post-arrest cell cycle (Matthews and Gull, 1994a), in that metacyclic to promastigote de-differentiation would also

involve re-entry into the cell cycle. Whether or not this differentiation step is synchronous was not determined in this study, but metacyclic forms are likely to be in a receptive cell cycle 'window' in order to receive signals to de-differentiate as suggested for stumpy forms (Matthews and Gull, 1994a). The formation of stumpy forms and metacyclic forms is analogous because both forms are pre-adapted for life in a new environment on transmission from mammalian host to vector in the case of stumpy forms or the reverse for metacyclic forms. Metacyclic forms do re-enter the cell cycle when differentiating to the intracellular amastigote stage in the mammalian host, but how the two processes of cell division and differentiation are linked is as yet unknown.

It may take several cycles of division for complete loss of expression of metacyclic specific genes such as the Gene B protein during de-differentiation of metacyclic to promastigote forms. De-differentiation was observed as occurring at a low rate as indicated by the slow growth rate and extended PDT of the PNA- population (Table 5.5B). Further investigation is required to determine the extent of this de-differentiation and how it may affect the model of promastigote replication and differentiation (Figure 5.1).

The availability of two specific antibody markers for *L. major* metacyclic forms has enabled the examination of metacyclogenesis *in vitro*, both at the cellular and population level. Although the markers recognise completely different surface antigens, an association between LPG and the Gene B protein has been established (Pimenta *et al.*, 1994). Modifications to LPG molecule have been implicated in the anterior migration of metacyclic forms in the sandfly vector promoted by the inability to attach to midgut epithelial cells (Pimenta *et al.*, 1992), as well as the increased infectivity and virulence, demonstrated by resistance to host attack mechanisms (Sacks, 1992). No function has so far been ascribed to the Gene B protein, but

considering its close proximity and association to LPG, it could also be involved in one or more of these functions *in vivo* (Flinn *et al.*, 1994).

Examination of individual Friedlin VI or RKK2 cells labelled for either marker indicated that the commitment to differentiate occurred prior to mitosis/kinetoplast division, with symmetrical production of two daughter metacyclic forms (Figure 5.9). Symmetrical differentiation of *L. major* differs from differentiation observed in other systems, where development is essentially asymmetric. Asymmetric divisions have been observed in cell differentiation in a wide range of organisms (including vertebrates, plants and nematodes) and in mating type switching of yeasts (reviewed by Wolpert, 1988, Gurdon, 1992). Asymmetric divisions have also been observed in bacteria e.g. *Caulobacter* (Newton and Ohta, 1990). The mechanisms which give rise to asymmetry may be intrinsic or extrinsic, e.g. the specification of mating types in yeast is generated intrinsically (Wolpert, 1988). Whether symmetrical production of metacyclic forms is controlled both intrinsically and extrinsically is as yet unknown. At which phase of the cell cycle the commitment to differentiate occurs could not be ascertained from this study either. The use of cell cycle phase inhibitors e.g. aphidicolin (a nuclear DNA synthesis inhibitor) might indicate more clearly the extent to which metacyclogenesis is linked to the cell cycle.

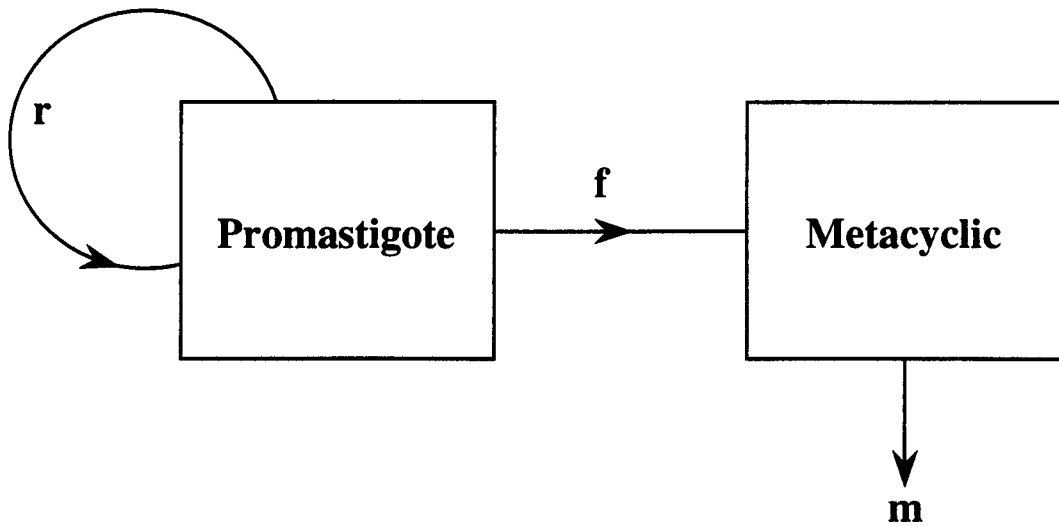


Figure 5.1 A model of *Leishmania* promastigote replication and differentiation. A promastigote population replicates by binary fission at rate r and differentiates to a non-dividing metacyclic population at a rate f . m is the mortality rate of the metacyclics (adapted from model given by Turner *et al.*, 1995).

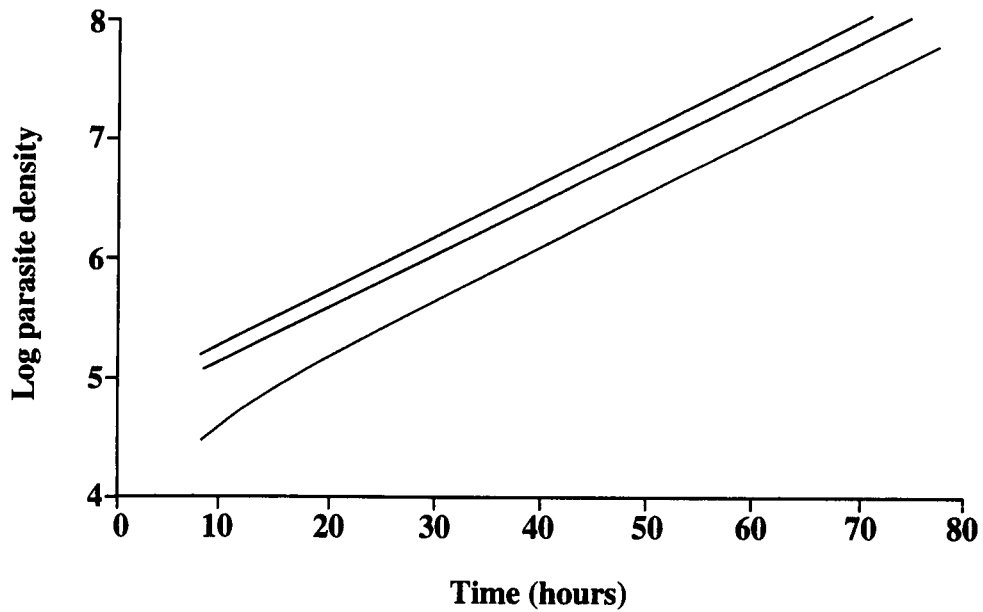
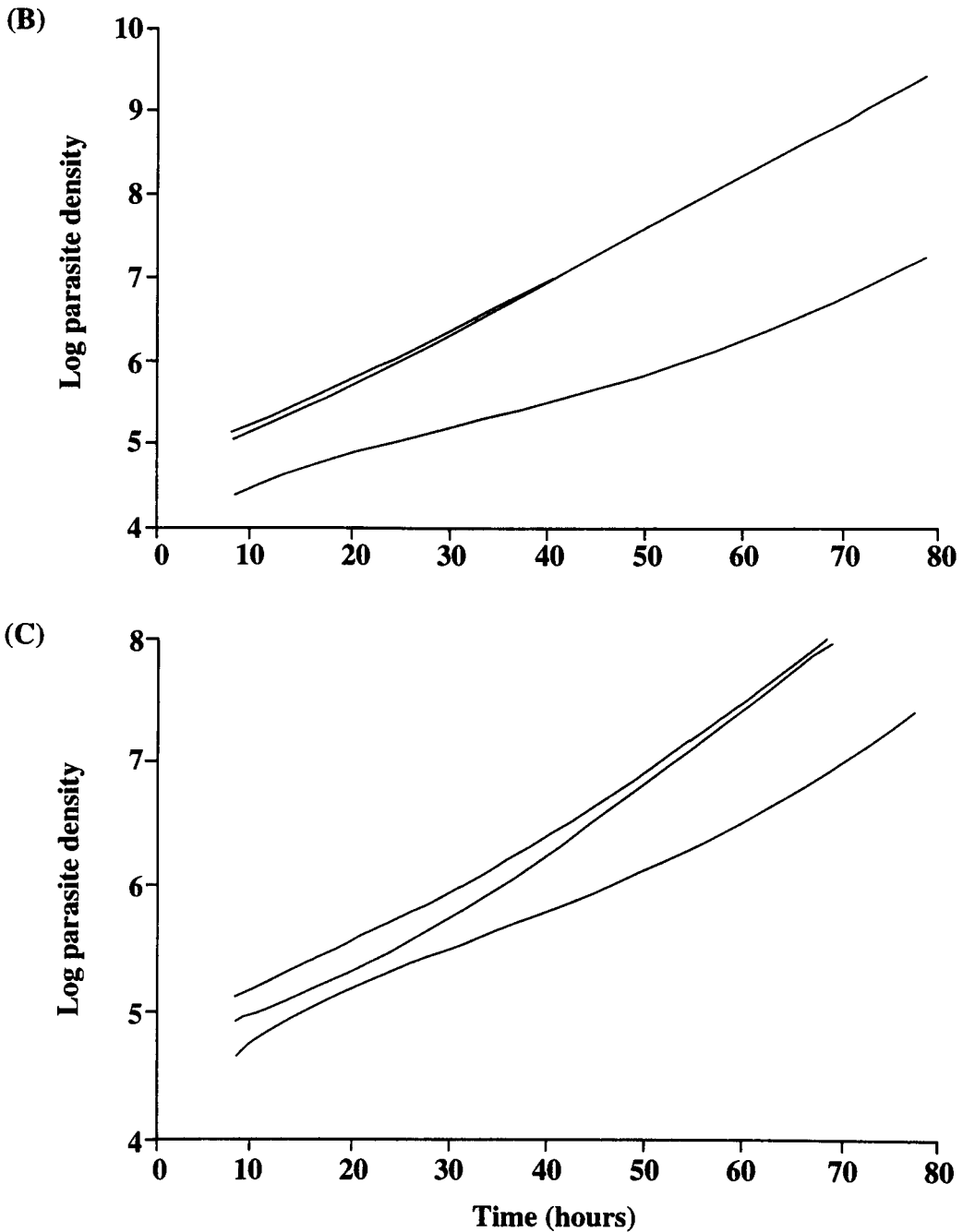


Figure 5.2A Illustrative solution to a model of replication and differentiation in a homogeneous population. The upper line is $\log_{10}(X+Y)$ - the whole population, the middle line is $\log_{10}X$ - promastigotes and the lower line is $\log_{10}Y$ - metacyclics. Parameter values (rates/h): $r=0.15$, $f=0.05$, $m=0.01$.



Figures 5.2B and C Illustrative solutions to a model of replication and differentiation in a heterogeneous population with two kinds of parasites; very low differentiation rate in type 1 parasites (B) and a large proportion of type 2 parasites at outset (C). Parameter values in (B) $r_1=r_2=0.15$, $d_1=0.001$, $d_2=0.01$, $m=0.01$, proportion of initial inoculum consisting of type 2 parasites, $p=0.5$. (C) as for (B) except $d_1=0.01$, $p=0.9$.

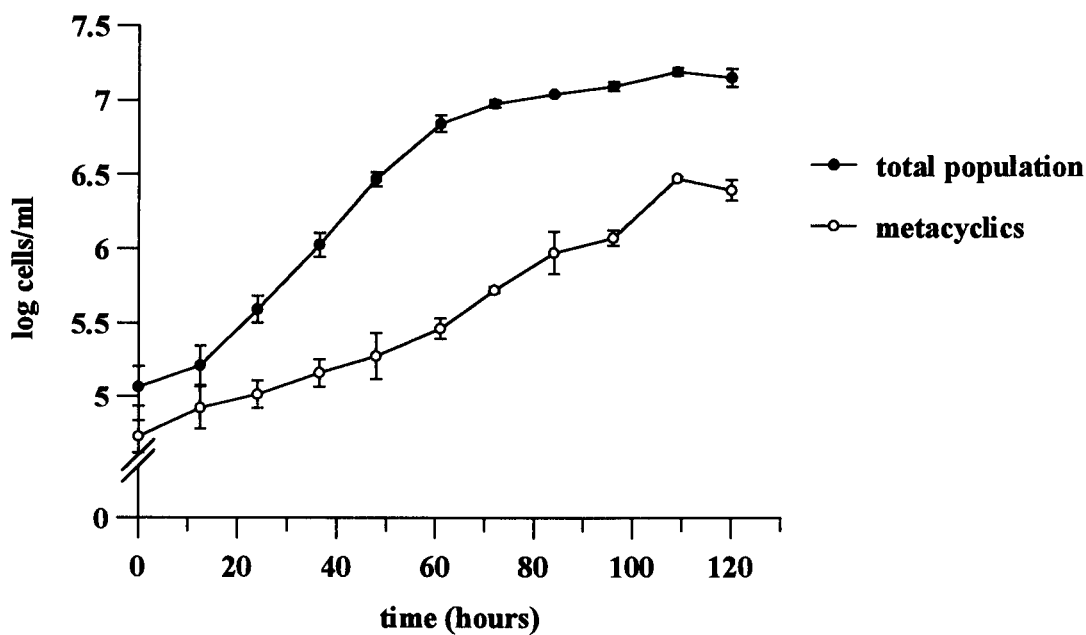


Figure 5.3A Growth of Friedlin VI strain promastigotes and the production of metacyclic forms.

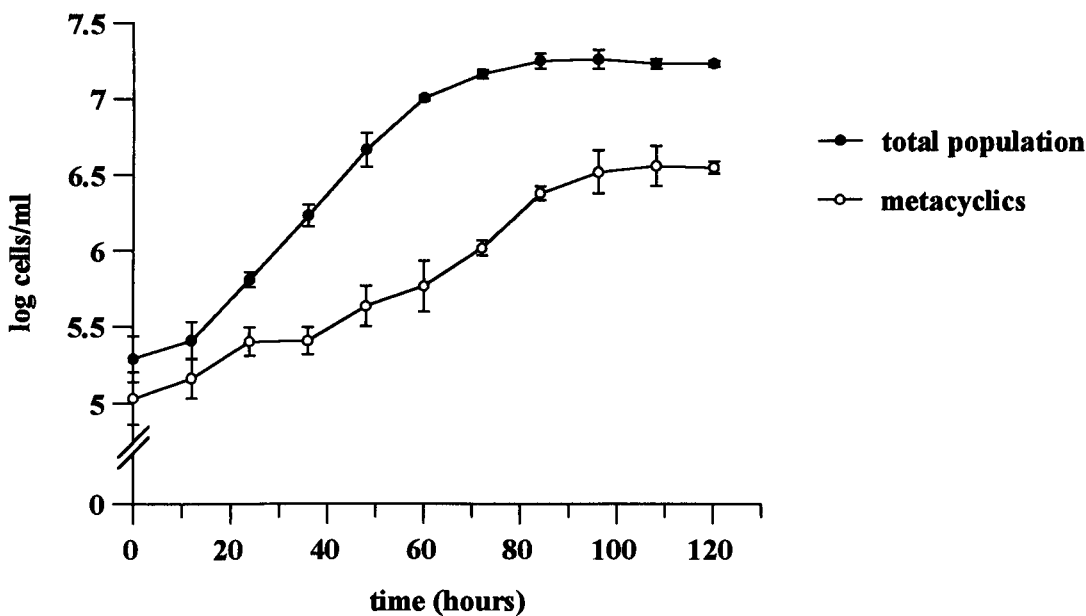


Figure 5.3B Growth of RKK2 strain promastigotes and the production of metacyclic forms. Population sizes in both experiments are geometric means \pm 2SE, $n=3$.

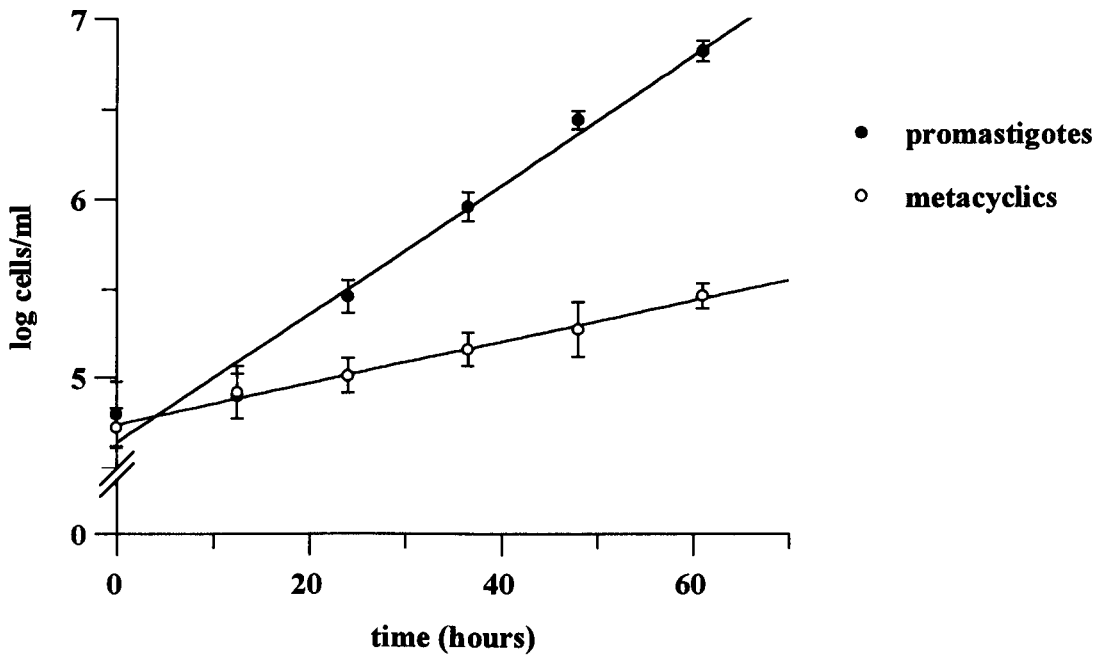


Figure 5.4A Exponential phase of growth of Friedlin VI promastigote and metacyclic forms. Data are shown as geometric means of absolute abundance \pm 2SE, $n=3$. The growth rates of the promastigote and metacyclic populations were calculated by exponential regression and compared by ANCOVA ($F_{1,32}=173.32$, $p<0.001$).

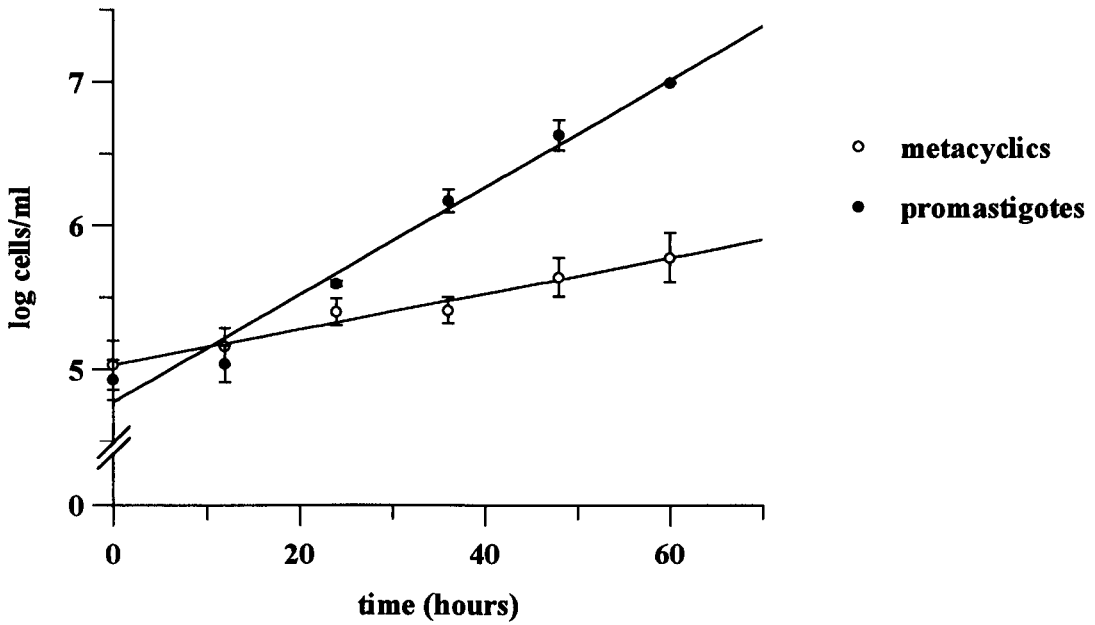


Figure 5.4B Exponential phase of growth of RKK2 promastigote and metacyclic forms. Data are shown as geometric means of absolute abundance $\pm 2SE$, $n=3$. The growth rates of the promastigote and metacyclic populations were calculated by exponential regression and compared by ANCOVA ($F_{1,32}=151.03$, $p<0.001$).

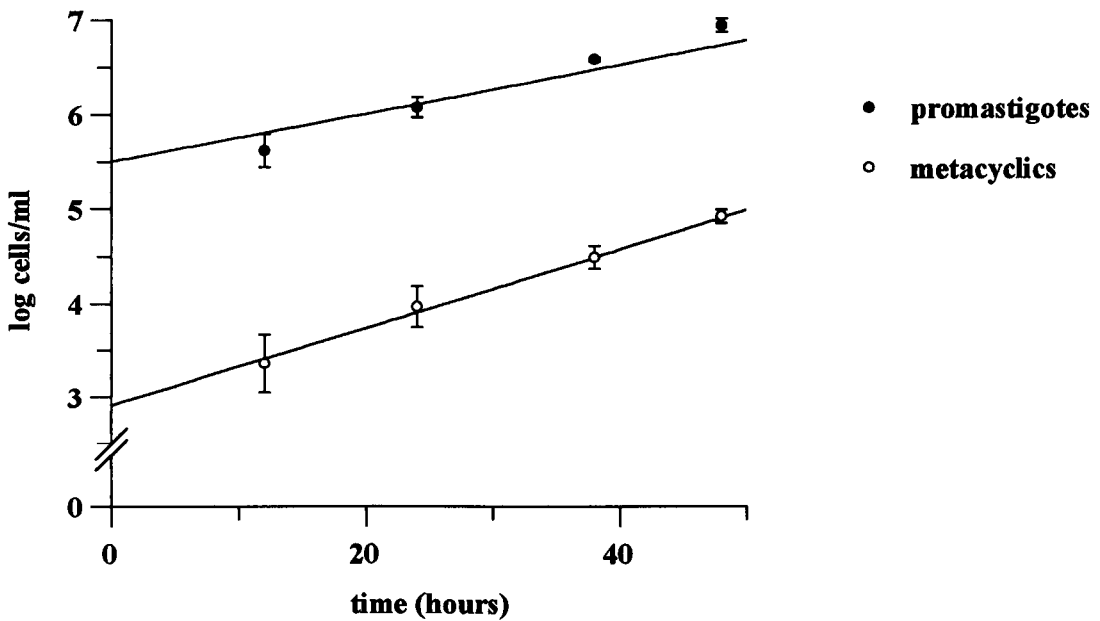


Figure 5.4C Exponential phase of growth of Friedlin VI promastigote forms and metacyclic forms. Data are shown as geometric means of absolute abundance $\pm 2SE$, $n=3$. The growth rates of the promastigote and metacyclic populations were calculated by exponential regression and compared by ANCOVA ($F_{1,20}=2.56$, $p=0.125$).

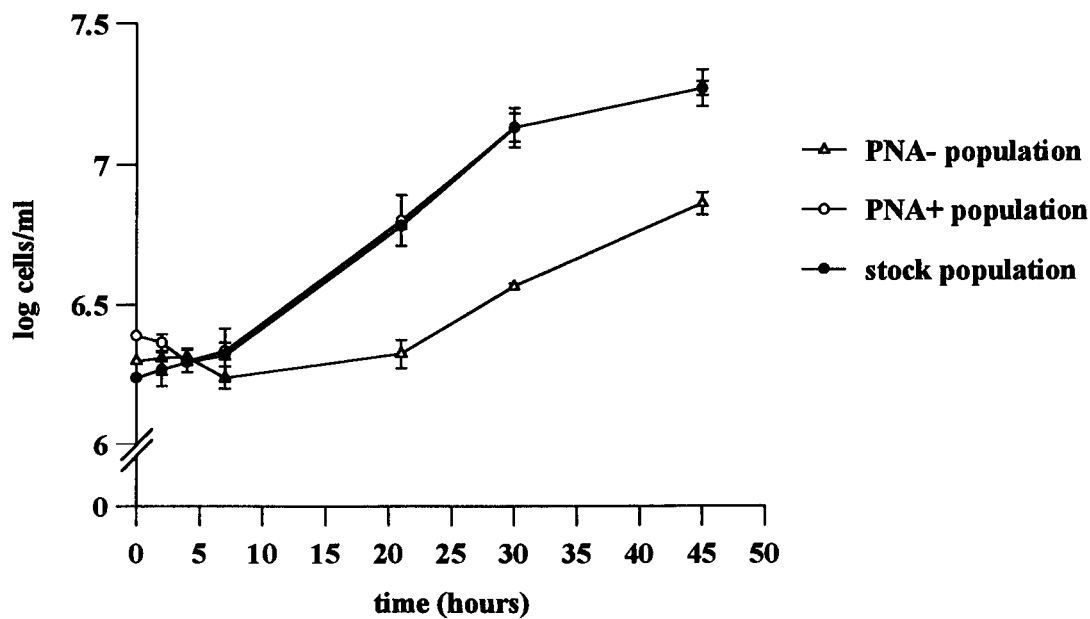


Figure 5.5A Growth of stock culture, PNA- and PNA+ populations separated after agglutination of Friedlin VI strain culture forms.

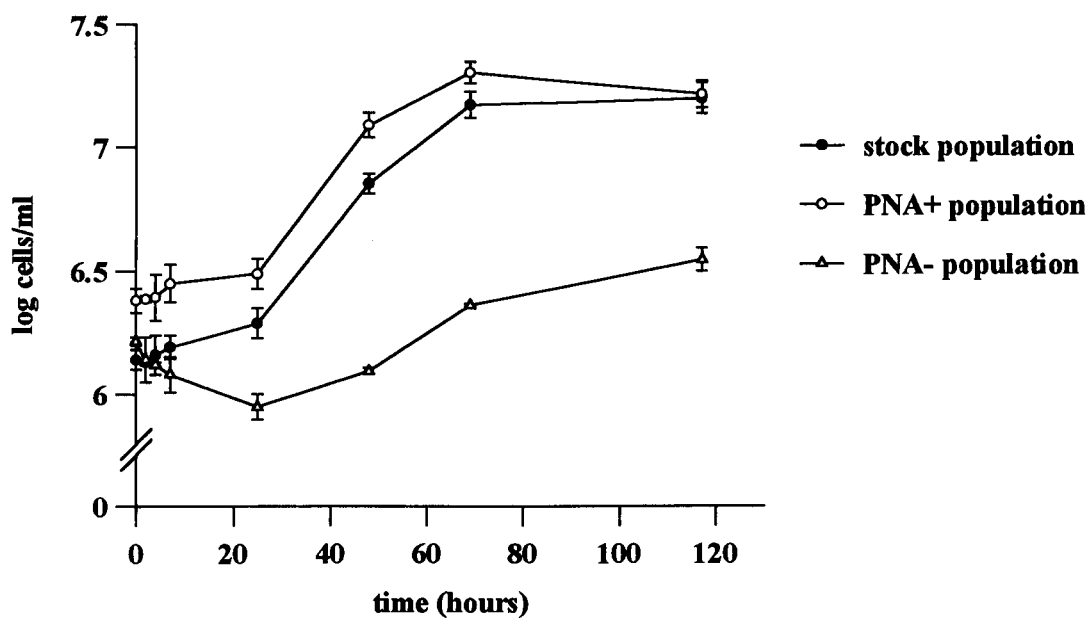


Figure 5.5B Growth of stock culture, PNA- and PNA+ populations separated after agglutination of RKK2 strain culture forms. Population sizes in both experiments are geometric means \pm 2SE, n=3.

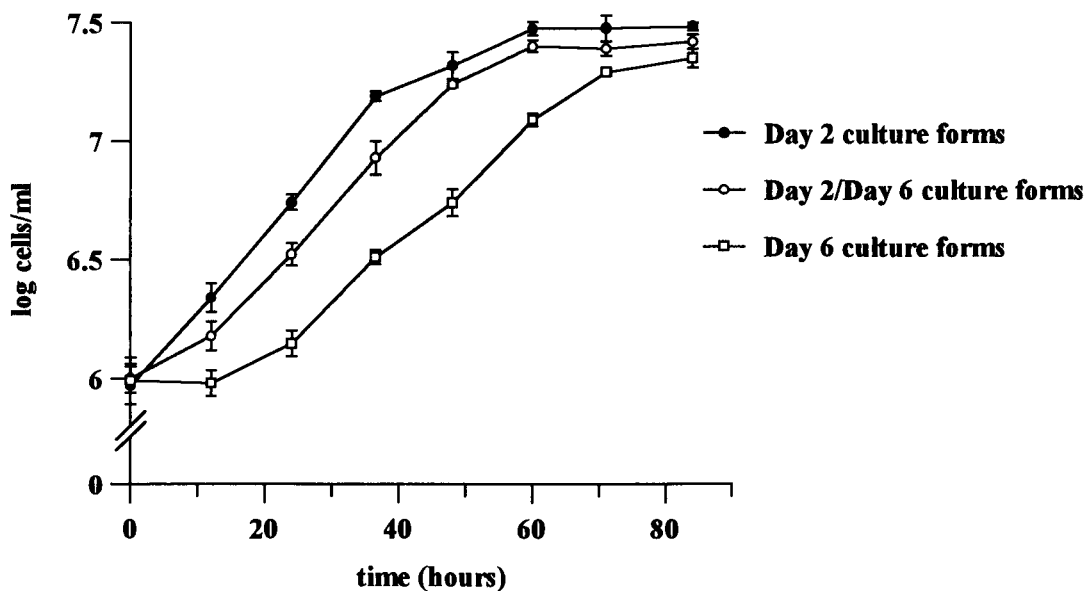


Figure 5.6A Growth of day 2, day 6 and day2/day 6 culture forms.

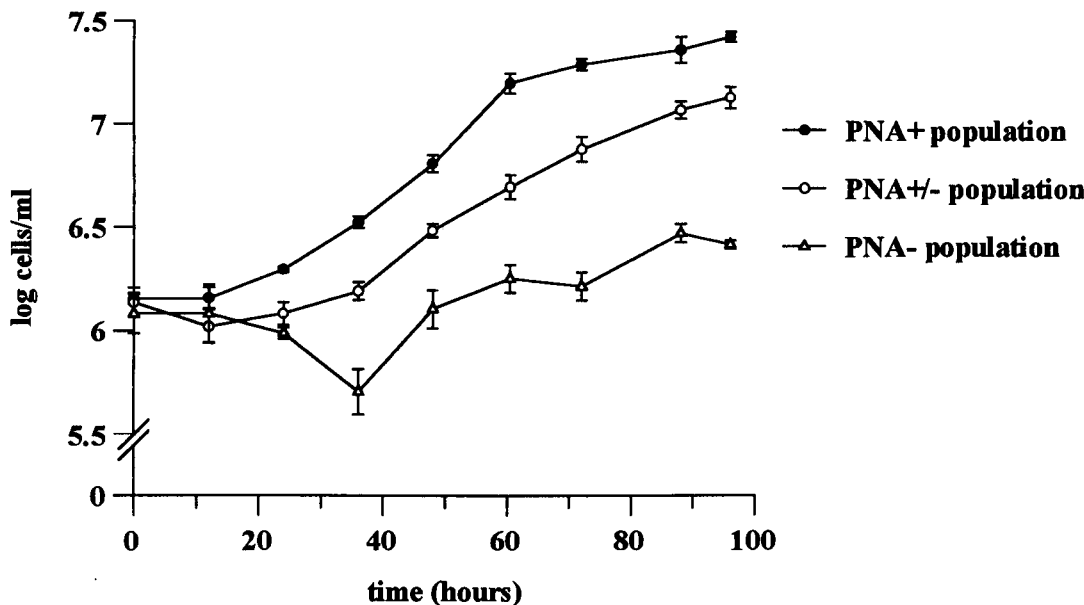


Figure 5.6B Growth of PNA+, PNA- and PNA+/PNA- populations. Population sizes are geometric means \pm 2SE, n=3.

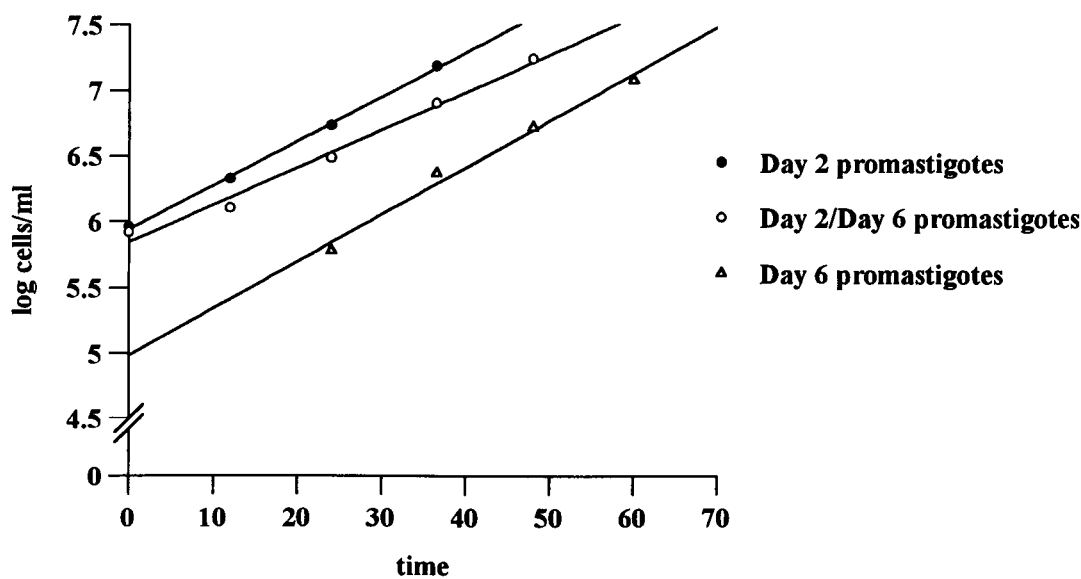


Figure 5.7A Exponential growth of promastigote forms of day 2, day 6 and day 2/6 shown in Figure 5.6A.

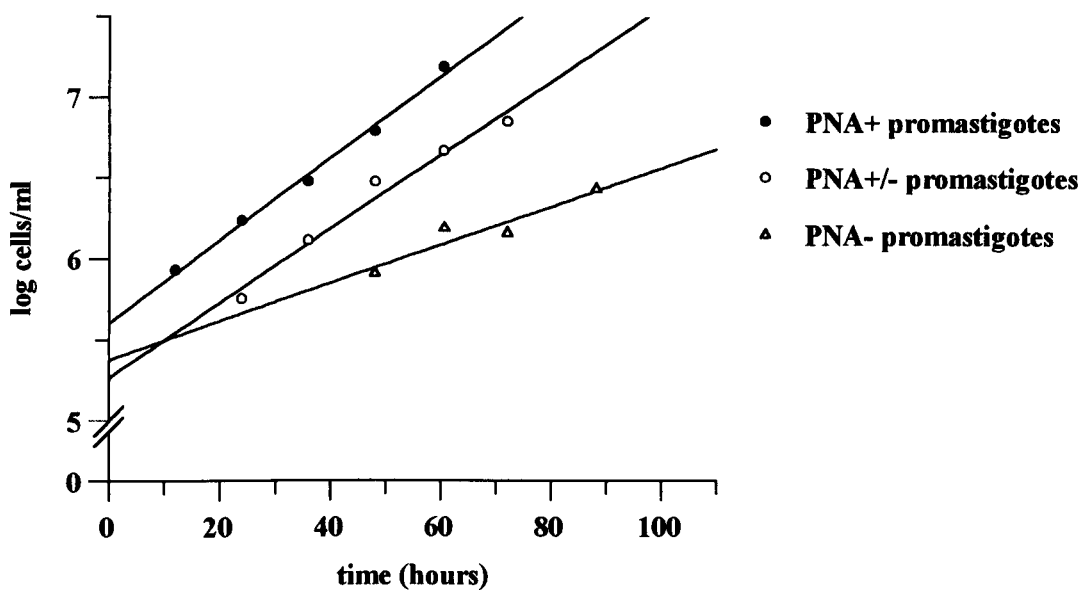


Figure 5.7B Exponential phase of growth of promastigotes of PNA+, PNA- and PNA+/PNA- shown in Figure 5.6B.

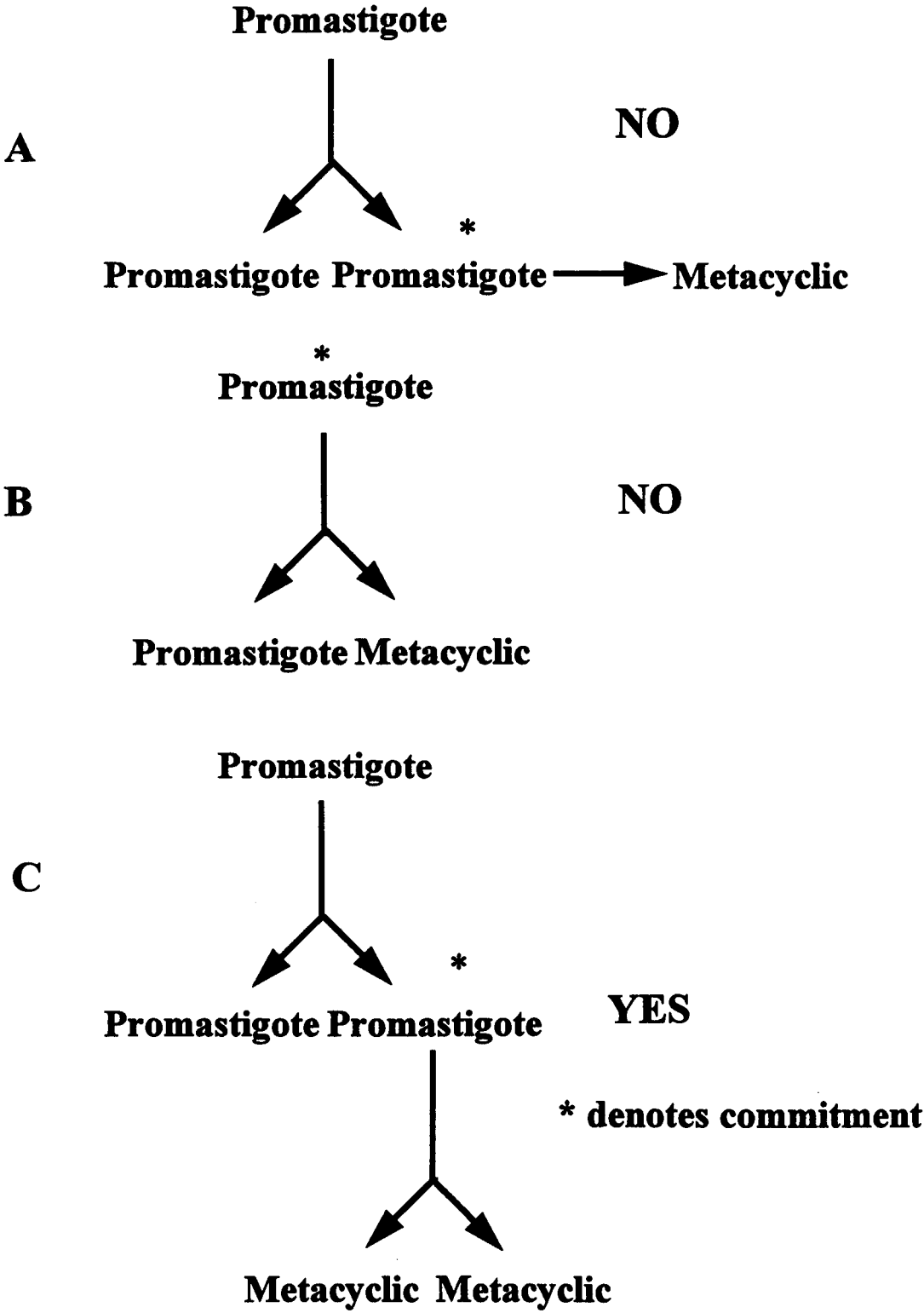
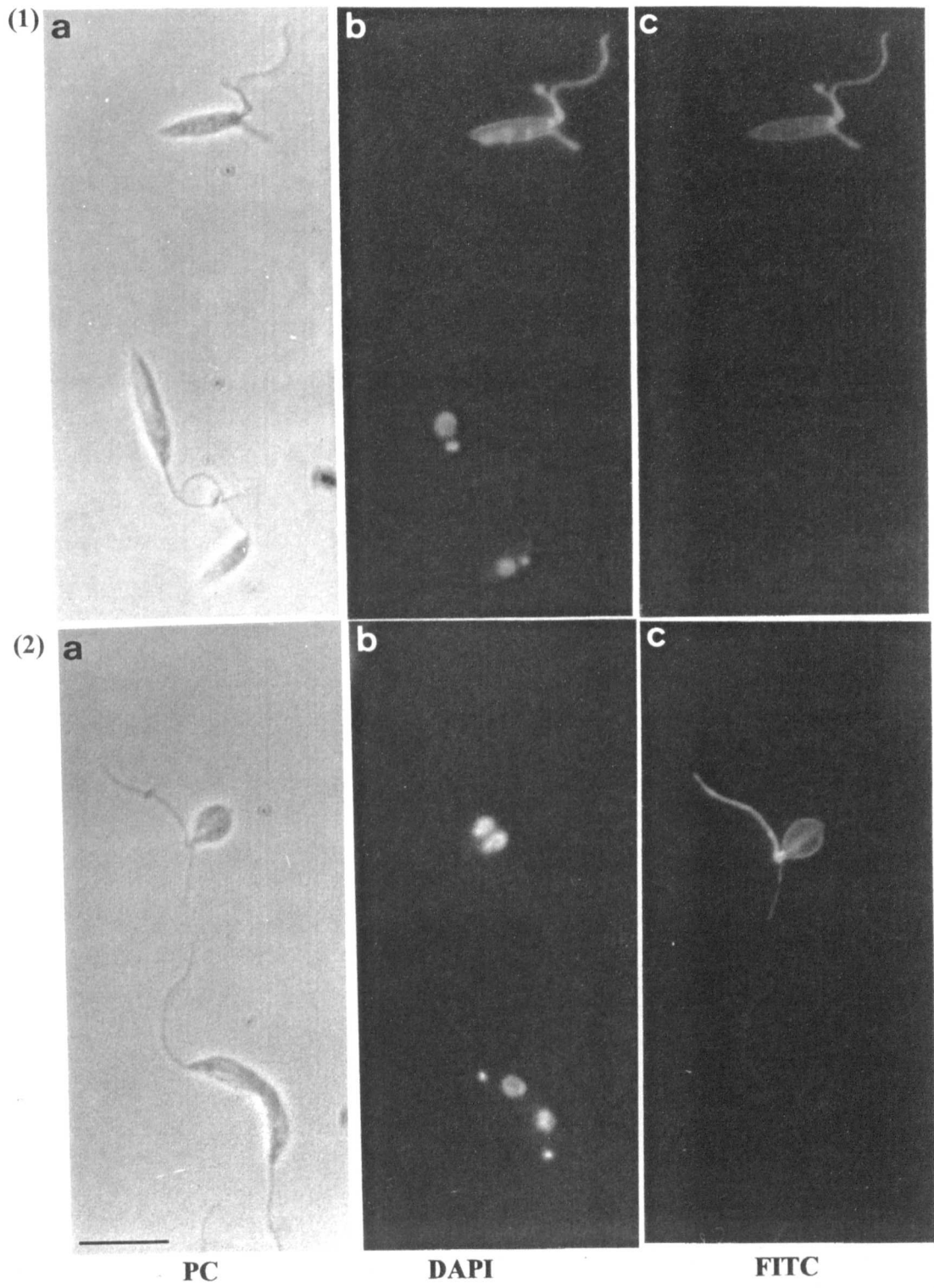


Figure 5.8 Models of metacyclic production.

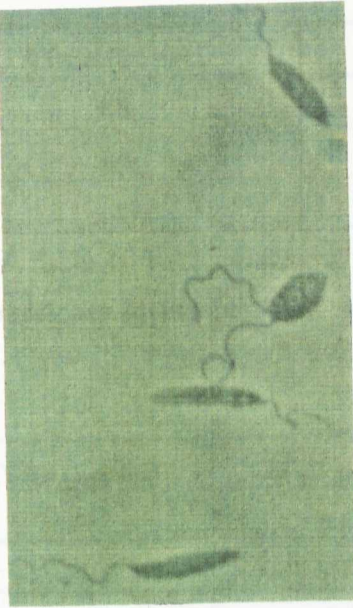
Figure 5.9A Labelling of *L. major* promastigotes with the ab336 antibody. (1) shows positive labelling of a dividing cell with two nuclei, one kinetoplast and a secondary daughter flagellum. Whole cell body staining in b is due to ab336 labelling and not DAPI staining. (2) shows positive labelling of a cell just prior to cell cleavage, as indicated by the status of the post-division organelles and the cleavage furrow. These observations of labelled cells comply with model C in Figure 5.8 i.e. the commitment to differentiate is at least one cell division before symmetrical production of two daughter metacyclic forms. PC=Phase contrast, DAPI=DAPI labelling, FITC=Fluorescein labelling. Scale bar=10µm.



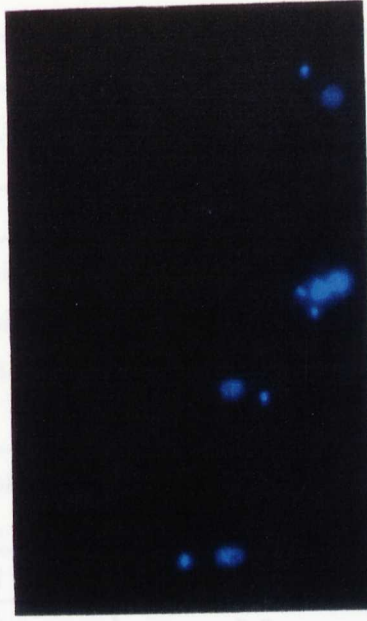
5.9B Labelling of *L. major* promastigote forms with the 3F12 antibody. The FITC image shows positive labelling of a cell in the final stages of division, with two nuclei, two kinetoplasts and secondary daughter flagellum.

5.9C Double labelling of *L. major* promastigote forms with 3F12 and ab336 antibodies. The FITC image shows positive labelling of a dividing form with the 3F12 antibody. Texas red (TR) image shows labelling of the same cell with the ab336 antibody. Observations in both figures comply with model C in Figure 5.8 i.e. the commitment to differentiate is at least one cell division before symmetrical production of two daughter metacyclic forms. Scale bar=10µm.

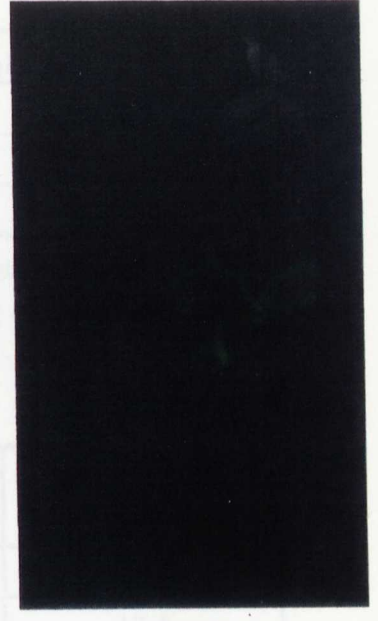
(B)



PC



DAPI

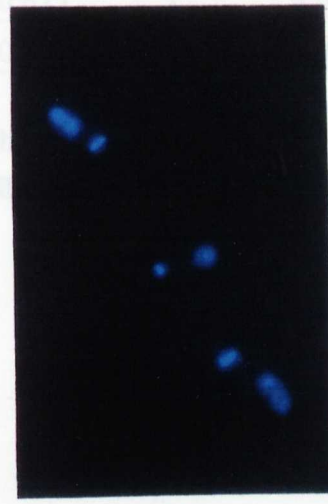


FITC

(C)



PC



DAPI



FITC



TR

Time (hours)	3F12 labelling	ab336 labelling
48	6.6 ± 2.2	9.9 ± 3.5
84	8.8 ± 2.7	5.5 ± 2.1
120	17.6 ± 1.0	19.0 ± 0.8

Table 5.1A % prevalence of 3F12 and ab336 labelling of Friedlin VI promastigote forms (n=400). Values shown are the means of two/three counts ± 2SE. Growth of Friedlin VI is shown in Figure 5.3A

Time (hours)	3F12 positive only	ab336 positive only	Double labelled (3F12+336)
24	0.75	3.0	22.3
36	0.75	2.0	17.5
60	1.625	0.625	4.6
96	0.875	0.625	7.8

Table 5.1B % prevalence of 3F12 and ab336 labelling of Friedlin VI promastigote forms when cells were double labelled for both antibodies (n=400). Growth of Friedlin VI is shown in Figure 5.3A.

Population	Time (hours)	Total % BrdU Labelling
Stock	2	9.6
PNA+	2	7.3
PNA-	2	2.0
Stock	4	31.1
PNA+	4	37.1
PNA-	4	10.4

Table 5.2A % BrdU labelling after 2 and 4 hours incubation of stock Friedlin VI culture forms, PNA+ and PNA- populations separated after agglutination (n=1,000).

Population	Time (hours)	Total % BrdU Labelling
Stock	2	8.9
PNA+	2	7.4
PNA-	2	2.2
Stock	4	26.1
PNA+	4	18.7
PNA-	4	10.3

Table 5.2B % BrdU labelling after 2 and 4 hours incubation of stock RKK2 culture forms, PNA+ and PNA- populations separated after agglutination (n=1,000).

Strain	3F12 only labelling	ab336 only labelling	3F12+ab336 double labelling
Friedlin VI	87.6%	73.0	ND
RKK2	1.6%	0	83.4%

Table 5.3 % metacyclic forms in the PNA- population determined by 3F12 and ab336 labelling (n=500).

Observed value	Calculated value	Interpretation
High	Low	(A) Some unlabelled cells (promastigotes) are not capable of growth
Low	High	(B) (Some) metacyclics are capable of de-differentiation
Equal	Equal	(C) All promastigotes grow and all metacyclics do not or (D) the effects of (A) and (B) counterbalance each other

Table 5.4 A comparison of calculated and observed numbers of promastigotes at the initiation of cultures: possible interpretations. The observed numbers were determined by absence of ab336 labelling and the calculated number is the intercept value derived from fitting the data for the growing population to an exponential regression. These interpretations all assume that metacyclics are non-dividing (section 5.3.2).

Linear regression	Day 2 population	Day 2:Day 6 50:50 ratio	Day 6 population
Growth rate (r)	0.08	0.07	0.08
PDT (hrs)	8.94	10.55	8.56
r ²	0.99	0.99	0.98
log ₁₀ intercept value, c	5.94	5.84	4.99

Table 5.5A Linear regression analysis of growth data shown in Figure 5.7A.

Linear regression	PNA+ population	PNA+/PNA- 50:50 ratio	PNA- population
Growth rate (r)	0.06	0.05	0.03
PDT (hrs)	11.8	13.1	25.2
r ²	0.99	0.97	0.90
log ₁₀ intercept value, c	5.6	5.27	5.4

Table 5.5B Linear regression analysis of growth data shown in Figure 5.7B.

Population	Observed percentage	Calculated percentage
Day 2	98.75%	94.0%
Day 2:Day 6	83.0%	69.8%
Day 6	74.5%	10.0%

Table 5.6A The observed percentage of promastigote forms at $t=0$ determined from counts of ab336 positive cells (total population-metacyclic population) compared to the calculated percentage of promastigote forms capable of growth at $t=0$. These results were compared to the possible interpretations described in Table 5.4.

Population	Observed percentage	Calculated percentage
PNA+	48.0%	28.1%
PNA+:PNA-	23.25%	13.6%
PNA-	1.75%	19.6%

Table 5.6B The observed percentage of promastigote forms at $t=0$ determined from counts of ab336 positive cells (total population-metacyclic population) compared to the percentage of promastigote forms capable of growth at $t=0$. These results were compared to the possible interpretations described in Table 5.4.

CHAPTER 6 GENERATION OF MUTANT TRYPANOSOME LINES WITH ALTERED GROWTH PHENOTYPE

6.1 Introduction

T. brucei infections produce fluctuating parasitaemias as parasite populations undergo antigenic variation (Barry and Turner, 1991). While the switching of one VSG to that of another greatly influences the outcome of a trypanosome infection, other aspects of the interaction between parasite and host are also major determining factors. The potential for growth regulation of parasites by host factors has been demonstrated, receptors for epidermal growth factor (EGF), low-density lipoprotein (LDL) and transferrin have been identified in *T. brucei* (reviewed by Turco, 1995), while the addition of EGF and IFN- γ promotes growth *in vitro* (reviewed by Barcinski and Costa-Moreira, 1994). The elucidation of intracellular signalling pathways in parasites has also provided information regarding the transduction of external signals which ultimately lead to cell proliferation (Turco, 1995). While evidence of extracellular and intracellular regulation is accumulating, its importance in determining the course of trypanosome infections *in vivo* remains to be fully determined.

Only one study has examined regulation of growth rates of trypanosome infections *in vivo* in chronic infections (Turner *et al.*, 1996). Mice harbouring a primary chronic infection (a cloned stock; EATRO 2340) were challenged with a secondary infection which the population homogeneously expressed one VAT (GUTat 7.2), a VAT not expressed by cells in the primary infection. The fate of trypanosomes in the secondary inocula could therefore be discriminated from parasites of the primary infection using the VAT as a marker and their fate determined. In the presence of a pre-existing chronic infection, growth of the secondary infection was significantly inhibited in comparison to control experiments. A similar result was observed using a different stock (STIB 247) as the primary infection, although onset of inhibition was slower. Growth inhibition was also observed in sheep and was therefore not a species-specific

phenomenon. The growth rate of the secondary infection was much slower in the presence of a chronic infection, giving a Population Doubling Time (PDT) of approximately 2.8 days compared to a normal PDT of approximately 4.5 hours. No significant difference was found between the prevalence of slender forms in both primary and secondary infections, suggesting that the entire mixed population was inhibited in its growth and that this negative growth regulation may be a means of sustaining the infection in the mammal (Turner *et al.*, 1996).

These observations represent the first record of growth regulation by a protozoan parasite *in vivo* and as such raise a number of questions as to the mechanism of the control of growth, the nature of the external regulatory factor and how the external modifying signal is transduced within the parasite. A number of approaches are available to address these questions of which one of the most powerful (by analogy with other systems) would be to generate growth mutant lines of parasites which can be compared to wild-type lines. Clearly, a key technical development to underly this line of work would be the generation of growth mutant trypanosomes i.e. cloned mutant populations which overcome growth inhibition. This chapter describes attempts to generate growth mutant cell lines. A chemical mutagen, ethyl methanesulphonate (EMS) which induces point mutations (Zoeller and Raetz, 1992) was used to mutagenise GUTat 7.2 parasites *in vitro*. These mutagenised parasites were then inoculated as secondary infections into mice harbouring primary infections of EATRO 2340. Infections were subsequently monitored for mutant populations which were not inhibited in their growth.

6.2 Materials and Methods

6.2.1 Mutagenesis of procyclic forms *in vitro*

Some preliminary mutagenization experiments were conducted in procyclic forms. Procyclics used in this study were GUTat 7.2 culture forms, originally transformed from GUTat 7.2 bloodstream forms and routinely cultivated in SDM-79 medium plus

10% heat inactivated FCS (Brun and Schonenberger, 1979). The chemical mutagen selected for use was ethyl methanesulphonate (EMS, Sigma). The effect of increasing concentrations of EMS upon the growth of procyclic forms was assessed in order to determine an optimal concentration which (a) induced mutations and (b) allowed a proportion of cells to survive the treatment. The range of concentrations tested was comparable to concentrations in published mutagenesis protocols (Esko and Raetz, 1978, Hughes *et al.*, 1982, Zoeller and Raetz, 1992). A stock solution of 1.2mg/ml of EMS in complete SDM-79 medium was made. EMS is an oil at room temperature and required gentle swirling over a 10 minute period to allow complete dispersion. The presence of foetal calf serum in the medium also aided in the solubilization of EMS (Zoeller and Raetz, 1992).

GUTat 7.2 procyclic forms were incubated with 0-600µg/ml of EMS for 2 hours, after which cells were pelleted by centrifugation at 500g for 10 minutes and re-suspended in fresh medium at a density of 10^6 cells/ml. The proportions of cells dead were determined (n=300). Growth was then monitored every 24 hours until control cultures reached stationary phase ($1-2 \times 10^7$ cells/ml).

6.2.2 Mutagenesis of bloodstream forms *in vitro*

Bloodstream culture medium (BSCM) was made as described in section 2.2.1. *T. brucei* bloodstream forms were harvested from mice, separated from blood cells and diluted with BSCM plus 10% FCS to give a starting density of approximately 1×10^5 cells/ml in axenic culture. GUTat 7.2 bloodstream forms were mutagenised *in vitro* with EMS for 2 hours, after which cells were pelleted, resuspended in fresh medium and inoculated into mice.

6.2.3 Challenge infections with mutagenised GUTat 7.2 bloodstream forms

Balb/c mice were infected with 10^6 cells/ml of a cloned trypanosome line EATRO 2340, which produces chronic infections in mice (Turner *et al.*, 1996). The same

mice harbouring chronic infections were challenged with an inoculum of, usually, 10^6 cells/ml of mutagenised GUTat 7.2 bloodstream forms, at least 10 days after inoculation with the primary 2340 infection. The prevalence of GUTat 7.2 in mixed infections was then monitored for a further 10 days.

6.2.4 Detection of GUTat 7.2 in a mixed infection

GUTat 7.2 trypanosomes were detected by indirect immunofluorescence. Blood smears were made from tail bleeds of chronically infected mice, air-dried and fixed in methanol for two minutes at room temperature. Indirect immunofluorescence was as described by Van Meirvenne *et al.* (1975). In summary, fixed cells were incubated with a rabbit anti-serum against GUTat 7.2 at a concentration of 1:200 diluted in PBS pH 8.0, in a humid chamber at room temperature for 30 mins. Smears were then washed in PBS for a period of 10 minutes (twice) and incubated with an anti-rabbit FITC conjugate for 15 minutes in a humid chamber. Cells were finally counterstained with DAPI 0.01mg/ml and mounted in Mowiol solution containing 2.5% DABCO as an anti-fadant. Smears were screened by immunofluorescence microscopy and the prevalence of positively labelled GUTat 7.2 bloodstream forms determined (n=200).

6.2.5 Calculating the mutation rate

The number of mutant populations in each experiment was used to calculate the mutation rate, after the method described by Luria and Delbruck (1943). The mutation rate/cell/generation was calculated as follows:

$$\omega = 0.693 (-\log_e P_0)/N,$$

where N is the number of cells inoculated per mouse and P_0 is the proportion of mice in a group in which mutant populations were not observed.

6.2.6 Optical cloning of bloodstream trypanosomes

Optical cloning was carried out as previously described (McLintock, 1990). In brief, a drop of infected blood was suspended in approximately 100-200µl of guinea pig serum (GPS). Using a fine pin a small drop from the mixture was spotted into each well of a humidified Terasaki tissue culture plate in a cold room (approx. 10°C), as a means of preventing evaporation of the small drops. The wells were examined using an inverted microscope for the presence of single trypanosomes: 10µl of GPS was added immediately to any wells containing single trypanosomes, mixed with CBSS in an eppendorf tube and injected into the peritoneum of a mouse. Mice were monitored for 10 days for the appearance of an infection. Most clonal infections appeared between 6-10 days post-infection with an approximate 20-30% success rate. Smears were made from tail bleeds of infected mice to test if positive for GUTat 7.2 by immunofluorescence and GUTat 7.2 positive clones were cryopreserved.

6.2.7 Cryopreservation of cloned and uncloned material

0.75-1ml of infected blood was harvested from mice by cardiac puncture, cryopreserved with 7.5% DMSO in CBSS containing heparin at a concentration of 100U/ml and stored as stablates in liquid nitrogen. Each stablate was assigned a Glasgow University Protozoology (GUP) number.

6.3 Results

6.3.1 Growth of mutagenised procyclic forms *in vitro*

The effect of a concentration range of EMS upon the growth of GUTat 7.2 procyclic forms was assessed *in vitro*. After 2 hours incubation, 7.5 and 15µg/ml of EMS had no effect upon procyclic growth, populations subsequently growing at a rate similar to that of a control culture not exposed to EMS (Table 6.1). With higher concentrations of EMS (30-600µg/ml) a proportion of the population was killed after 2 hours incubation. However, 48 hours after initial exposure to EMS, growth was observed only in cultures having contained concentrations up to 150µg/ml; beyond this

concentration (300-600µg/ml) growth was significantly inhibited. Based on the results from this experiment, a concentration of 150µg/ml was selected for the mutagenesis of bloodstream forms. This concentration appeared to induce mutations as indicated by the high percentage of dead cells after 2 hours exposure, but also allowed a population of cells to survive exposure and as such should allow selection of mutants.

6.3.2 Growth of mutagenised bloodstream forms *in vivo*

GUTat 7.2 bloodstream forms were mutagenised with 150µg/ml of EMS in *in vitro* culture for 2 hours. Two groups of mice were inoculated with bloodstream forms at a density of 10^6 cells/ml; one group with mutagenised bloodstream forms and another control group with bloodstream forms not exposed to EMS. Growth of mutagenised monomorphic GUTat 7.2 bloodstream forms was significantly inhibited in comparison to control infections (Figure 6.1), but recovered growth at a similar rate to trypanosomes in control mice after day 2 of infection. Monomorphic lines produce unresolving infections in mice, killing their hosts at the first peak of parasitaemia (Turner, 1990). As the infection reached a density equal to or greater than antilog 9.0 trypanosomes/ml, mice were therefore withdrawn from the experiment. At this density, bloodstream trypanosomes compete for host glucose resulting in severe hypoglycaemia and inevitable death of the host (Herbert *et al.*, 1975).

Growth of mutagenised pleomorphic GUTat 7.2 trypanosomes was also examined *in vivo* (Figure 6.2). As with monomorphic GUTat 7.2, mutagenised pleomorphic trypanosomes were significantly inhibited in growth in comparison to control infections, but recovered growth at a similar rate to control trypanosomes after day 2 of infection. The peak of parasitaemia reached by the EMS treated cells was also lower than that reached by the control infection. Both experiments indicate that a concentration of 150µg/ml of EMS was effective in inducing mutations, indicated by the initial inhibition of growth probably caused by EMS inducing lethal mutations, as

well as allowing a population of cells to survive the treatment, thereby enabling the selection of mutants.

6.3.3 Growth of mutagenised GUTat 7.2 bloodstream forms in the presence of a chronic infection

A group of 10 mice harbouring EATRO 2340 infections were challenged with mutagenised GUTat 7.2 pleomorphic bloodstream forms. The prevalence of GUTat 7.2 within the subsequent mixed infection was ascertained on each day for a period of 10 days post-challenge. Figure 6.3 shows positively labelled GUTat 7.2 bloodstream forms within a mixed infection, by immunofluorescence microscopy. Percentage prevalence of GUTat 7.2 for three combined experiments (30 mice in total) is shown in Figure 6.4. In 27 of these mice growth of GUTat 7.2 bloodstream forms was significantly inhibited, similar to control experiments conducted in previous studies with challenge infections of non-mutagenised GUTat 7.2 bloodstream forms (Figure 6.5, Turner *et al.*, 1996). A population of GUTat 7.2 forms which were not inhibited in growth, however, was detected in the remaining three mice; one population reached a prevalence of 94.0% on day 9 post-challenge, named 'Growth' Mutant Population 1 (GM1), another population reached a prevalence of 44.0% on day 7 post-challenge but subsequently decreased to 20.0% on day 10 while another population increased to a much lower level of 18.0% on day 10 post-challenge named GM2, although this was significantly different to mean values for control experiments (Figure 6.5).

In another experiment, mice harbouring EATRO 2340 infections were challenged with a higher inoculum (5×10^6 cells/ml) of mutagenised GUTat 7.2 bloodstream forms, in order to increase the probability of obtaining a growth mutant. In this case, no mutants were obtained (data not shown).

The mutation rates for each experiment were calculated and are shown in Table 6.2. Results indicated that the mutation rate/cell/generation occurred at a low rate (8.24×10^{-7} - 2.37×10^{-8}).

6.3.4 Stability of growth mutant clones

By optical cloning two clones from each growth mutant population were obtained, GM1cl1 and GM1cl2 from GM1 and GM2cl1 and GM2cl2 from GM2. Each clone homogeneously expressed 7.2. Clone 1 from each GM population was tested for their respective ability to overcome growth inhibition in the presence of a chronic infection. Groups of 3 mice harbouring EATRO 2340 infections were infected with 10^6 cells/ml of a particular clone and the prevalence of each clone subsequently monitored in mixed infections in comparison to a control group of chronically infected mice challenged with wild-type GUTat 7.2. Although no positively labelled GUTat 7.2 trypanosomes were detected in the control group on all days examined post-challenge (data not shown), positively labelled GUTat 7.2 forms were detected in the experimental groups of chronically infected mice challenged with the GM clones. Considerable variation was observed, however, between mice within a group (Figure 6.6A and B). In some mice, significant growth of the clones was observed in comparison to controls, but in other mice infected with the same clone, no significant growth was observed e.g. mouse 1 compared to mouse 2 infected with GM2cl1 (Figure 6.6B). A group of mice challenged with the uncloned population GM1 also showed similar variation between mice (Figure 6.6C). In repeat experiments the GM clones gave similarly variable results (data not shown).

In order to obtain more stable mutants, another approach was taken. Two clones (GM1cl1 and GM2cl1) both of which demonstrated an ability to overcome growth inhibition, albeit with a highly unstable phenotype (Figures 6.6A and B), were re-mutagenised with EMS, the rationale being that two mutations were perhaps required to produce a stable phenotype.

A group of mice harbouring a chronic infection was challenged with re-mutagenised GM2c11 (Table 6.3). Of a total of 20 mice, significant prevalence levels compared to control values (Figure 6.5) were only observed in two mice, mouse A5 and mouse D4, increasing to levels of 17.0 and 20.0% on day 10 post-challenge in each mouse respectively. These populations, however, consisted of a high proportion of stumpy forms and were therefore not used in further experiments.

Another group of 20 mice harbouring a chronic infection was challenged with re-mutagenised GM1c11 (Figure 6.7). In 17 mice, growth of re-mutagenised GM1c11 was significantly inhibited as observed in control experiments (Figure 6.5). In two other mice, populations reached peak prevalences of 35.0% and 64.0% respectively on day 5 post-challenge, but subsequently decreased below the levels of detection. Another population was however detected on day 6 at 5.0% which subsequently increased to 64% on day 10 post-challenge. This uncloned population, termed R-mGM was cryopreserved.

In addition, R-mGM was passaged in mice several times with the aim of producing a more stable population which would overcome growth inhibition. An uncloned population of Rm-GM was cryopreserved after passaging through 3 mice for a total period of 11 days, termed Rm-GM3. The prevalence of GUTat 7.2 in this population was 94%. The uncloned population of Rm-GM was also passaged for a longer period, through 13 mice for a total period of 47 days, termed Rm-GM13 before being cryopreserved when the prevalence of Rm-GM in the mixed population was 85.0%. 4 clones were obtained from Rm-GM3 and 3 clones from the Rm-GM13.

Growth of 2 clones of each of RmGM3 and RmGM13 was examined in comparison to controls of wild-type pleomorphic GUTat 7.2 bloodstream forms passaged for the same period (47 days) as the Rm-GM13 population, in the presence of a chronic

infection. No significant difference was observed between the prevalences of the passaged wild-type control and two clones of Rm-GM3 (Figure 6.8A). Passaging of wild-type GUTat 7.2 bloodstream forms, caused growth inhibition to be partially overcome when compared to growth of a non-passaged population (compare figures 6.5 and 6.8A and B). In contrast, two clones of Rm-GM13 increased to a peak prevalence of almost 100% and a total parasitaemia of antilog 9.0 trypanosomes/ml in all mice infected, such that mice had to be withdrawn from the experiment (Figure 6.8B). This ability to overcome growth inhibition was considerably greater than that for the passaged wild-type control. Note in particular that parasitaemias in mice challenged with the passaged wild-type control did not reach levels such that mice had to be withdrawn from the study.

In a second group of experiments, growth of these same clones was examined in comparison to that of a monomorphic line of GUTat 7.2, which had been passaged more than 30 times through mice (Figures 6.9A and B). The derivation of monomorphic GUTat 7.2 from the stock EATRO 2340 is shown in Figure 6.10, as well as the derivation of pleomorphic GUTat 7.2 (Figure 6.11). Monomorphic and pleomorphic GUTat 7.2 both homogeneously express the same VAT (7.2), a VAT not expressed in the line of EATRO 2340 (p13, see Figure 6.10) used in the chronic infection studies (Turner *et al.*, 1996). The single copy gene encoding GUTat 7.2 in the original stock was spontaneously deleted in multiple cyclical transmissions (Turner and Barry, unpublished results). Rapid syringe-passaging produces monomorphic trypanosome lines which kill mice within a week of inoculation and the rate of stumpy production is reduced such that only slender forms are observed in the population (Turner, 1990). Monomorphic GUTat 7.2 reached a peak prevalence of nearly 100% and a total parasitaemia of antilog 9.0 trypanosomes/ml in all mice infected, such that mice had to be withdrawn from the experiment on day 5/6 post-challenge (Figures 6.9A and B). This monomorphic line's ability to overcome growth inhibition was similar to R-mGM13cl1 and 2, but not to R-mGM3cl1 and cl2, which only showed

partial ability in overcoming growth inhibition. This monomorphic line appeared to share the same phenotype as growth mutants which overcome growth inhibition. Figure 6.12 is a summary of the production of growth mutant populations in this study.

6.4 Discussion

This study has demonstrated that by use of a chemical mutagen to induce point mutations, mutant trypanosomes were generated such that an alteration in the phenotype of trypanosome growth occurred *in vivo*. 'Growth' mutants were produced by manipulation of a method used to examine growth in *T. brucei* infections, where a secondary infection could be discriminated from a pre-existing chronic infection by virtue of its VAT expression (Turner *et al.*, 1996). This method indicated that the secondary infection was significantly inhibited in its rate of growth. In the present study, mutagenesis of trypanosomes of the secondary infection, allowed selection of growth mutants that could overcome growth inhibition.

Growth inhibition was demonstrated as being neither a trypanosome stock- nor host species-specific phenomenon (Turner *et al.*, 1996). Inhibition was also probably mediated by a decrease in the replication rate of slender forms rather than an increase in the differentiation rate of slender to stumpy forms, as both slender and stumpy forms were present in the secondary infection, as well as the primary infection. Data also indicated that a down-regulation in the replication rate of the entire mixed population occurred, rather than just of the secondary infection. Inhibition required the presence of an active infection and was unlikely to be a result of preferential killing of the secondary infection by host immune responses (Turner *et al.*, 1996, Turner and Aslam, unpublished results).

Growth inhibition could be caused by limitation of a growth factor, lack of an essential nutrient or the production of a growth inhibitor (Turner *et al.*, 1996). The

generation of growth mutant populations that overcame growth inhibition suggests that interaction between parasite and host environment and/or the intracellular transduction of external signals could be a major factor determining growth inhibition in chronic infections.

Mutations occur spontaneously at a characteristic rate or background level for a particular organism, but on average occur at a frequency of approximately 10^{-6} per cell per generation (Zoeller and Raetz, 1992). Chemical mutagenesis can increase this frequency by 100-fold, therefore introducing a wider variety of genetic lesions for selection. EMS typically yields point mutations, thus limiting the lesion to one or a small number of base pairs. The mutation would therefore result in a genetic alteration to a single gene or allele. In the first set of three mutagenesis experiments, the mutation rates were calculated as occurring at a low rate (Table 6.2), less than one mutation per cell in an inoculum of 3×10^5 cells per mouse. These low rates suggest that only one mutation was likely to have led to the phenotypic change responsible for overcoming growth inhibition. However, clones of the mutant populations GM1 and GM2 displayed a highly unstable phenotype (Figure 6.6A and B). It is therefore possible that the mutagenesis procedure was not effective in inducing a genetic lesion, but instead had a 'phenocopy' effect, where a phenotypic modification occurred without any genetic alteration, as can occur when organisms are exposed to chemicals or different environmental conditions (Russell, 1992). The mutagenesis protocol employed was based upon a concentration of EMS within a range used in published protocols (see section 6.2.1) as well as length of exposure time. The concentration of EMS used in this study ($150 \mu\text{g/ml}$) appeared to be optimal under the parameters examined; this concentration induced lethal mutations indicated by the death of cells and the lag in growth (Table 6.1, Figures 6.1 and 6.2), as well as allowing the survival of a population of cells and any mutant alleles to segregate. Whether this concentration specifically induced genetic mutations was not examined. An attempt to grow *T.*

brucei procyclic forms as colonies on agar plates was made, to ascertain the optimal conditions under which mutant colonies were produced. However, growth conditions on agar were too variable for this to be determined. It can therefore only be speculated at this stage that the change in phenotype was caused by a genetic alteration.

Another approach was taken to produce growth mutants which displayed a more stable phenotype, based upon the rationale that a further mutation was perhaps required to induce stable recovery from inhibition. Clones of GM1 and GM2 were therefore re-mutagenised and any mutant populations that could overcome growth inhibition selected. Only one population was successfully recovered from the re-mutagenesis of GM1c11, a population termed Rm-GM. The mutation rate for this experiment was also calculated as occurring at a low rate (Table 6.2). Two successive rounds of mutagenesis, therefore led to the selection of a population with two mutations responsible for recovery from inhibition.

In addition, Rm-GM was rapidly passaged through mice in order to increase stability of the phenotype. Clones of the passaged populations were then tested for stability of phenotype in the presence of a pre-existing chronic infection, in comparison to a wild-type pleomorphic line of GUTat 7.2 which also had been syringe passaged (Figures 6.8A and 6.8B). Rapid-syringe passaging clearly led to a more stable phenotype of recovery from growth inhibition, with the Rm-GM13 clones displaying the most effective recovery, reaching a peak prevalence of almost 100%. However, passaging of the wild-type line produced populations displaying partial recovery from growth inhibition, although neither this control nor the Rm-GM3 clones reached prevalence levels close to those reached by the Rm-GM13 clones (Figures 6.8A and 6.8B). Growth of the R-mGM13 clones also reached very high parasitaemias such that mice had to be withdrawn early from the experiment (5-7 days post-challenge, Figure

6.8B), an observation not seen in mice infected with either the wild-type line or the Rm-GM3 clones.

Growth of the Rm-GM clones was also compared to growth of a monomorphic line of GUTat 7.2, in the presence of a pre-existing chronic infection (Figures 6.9A and B). As previously described, the R-mGM13 clones were more effective in overcoming growth inhibition compared to the R-mGM3 clones. However, the monomorphic line also showed complete recovery from inhibition, reaching high parasitaemia levels in all infected mice and as such mice had to be withdrawn from the study on days 5-6 post-challenge. This observation has also been made with another monomorphic line, ILTat 1.61 (Turner and Aslam, unpublished results). These data indicate that the cause of high virulence in monomorphic lines is a failure to respond to an external signal modulating the rate of growth and would accord with the observations that mono- and pleomorphic lines do not differ in their intrinsically determined rates of growth (Turner *et al.*, 1995). This study also indicates that passaging the growth mutant clones selected for a more stable phenotype which was able to overcome growth inhibition. Overall, a significant difference in recovery from inhibition was observed between the passaged pleomorphic line and the R-mGM13 clones, suggesting that a mutation or mutations had contributed to the change in phenotype.

As very little is known of the regulation of growth in parasitic infections *in vivo*, it is difficult to say at this stage what factor(s) is/are responsible for growth inhibition in *T. brucei* chronic infections and how a change in phenotype could occur. A change in the rate of growth has been implicated in determining the virulence of a trypanosome infection (Turner *et al.*, 1995). The production of populations that overcame growth inhibition in the present study also increased the virulence of a line (Figure 6.8B and 6.9B), suggesting that the processes of growth and virulence are inextricably linked.

By analogy with other systems, growth regulation in parasitic protozoa (see section 1.4) is clearly controlled by the pleiotropic effects of growth factors. The interaction between growth factors and surface receptors triggers intracellular signalling cascades, which ultimately end in the cell nucleus with proteins that regulate gene expression. It seems highly plausible that the key change in phenotype leading to the production of a growth mutant trypanosome may lie within this signalling network, altering growth rate and virulence of the parasite. When mammalian cells become cancerous, subtle molecular changes enable cancer cells to receive a flood of growth stimulatory signals allowing them to multiply uncontrollably. A number of genes responsible for these changes have been identified e.g. products of the *ras* gene family which are expressed as mutant (oncogenic) forms in cancer cells (Egan and Weinberg, 1993). The identification of such signalling cascades as the Ras pathway, which is central to growth control in a diverse range of eukaryotes e.g. humans, *Drosophila*, nematodes and yeast, provides further vital information on how growth is perhaps similarly regulated in parasites. While many of the required molecular elements in parasites have now been identified, the links that join these elements into functional pathways are yet to be made.

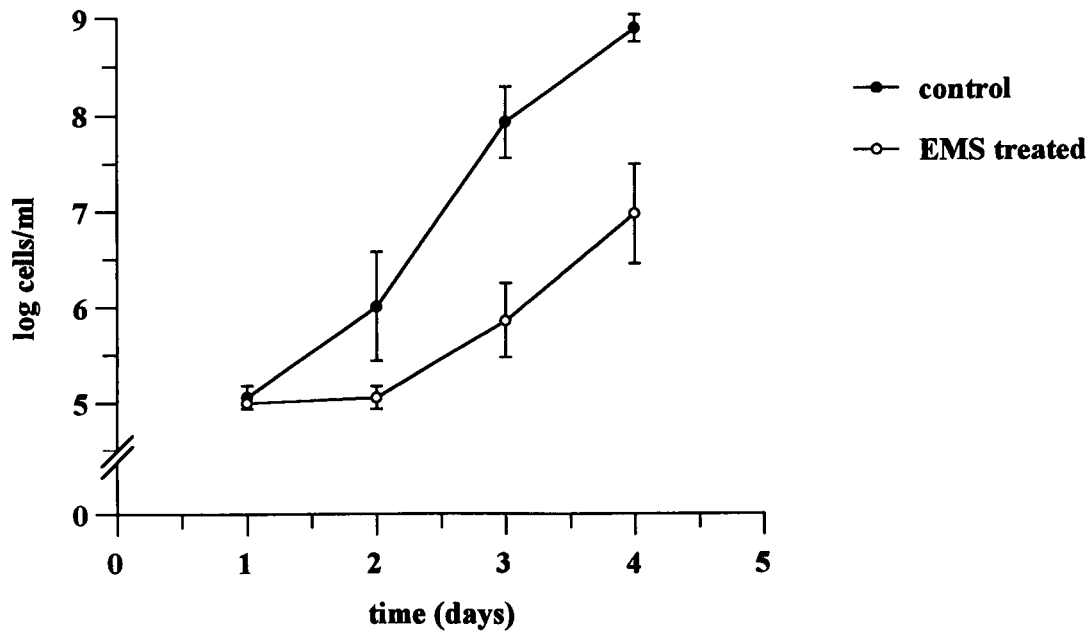


Figure 6.1 Growth of EMS treated GUTat 7.2 monomorphic bloodstream forms in mice.

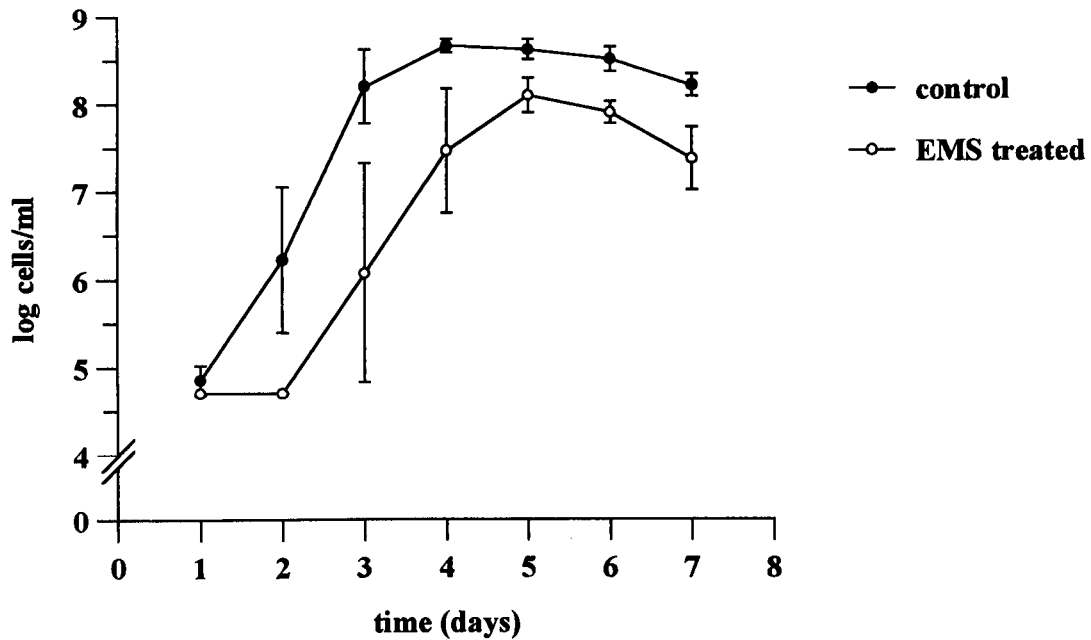


Figure 6.2 Growth of EMS treated GUTat 7.2 pleomorphic bloodstream forms in mice. Data are mean values \pm 2SE (n=5).

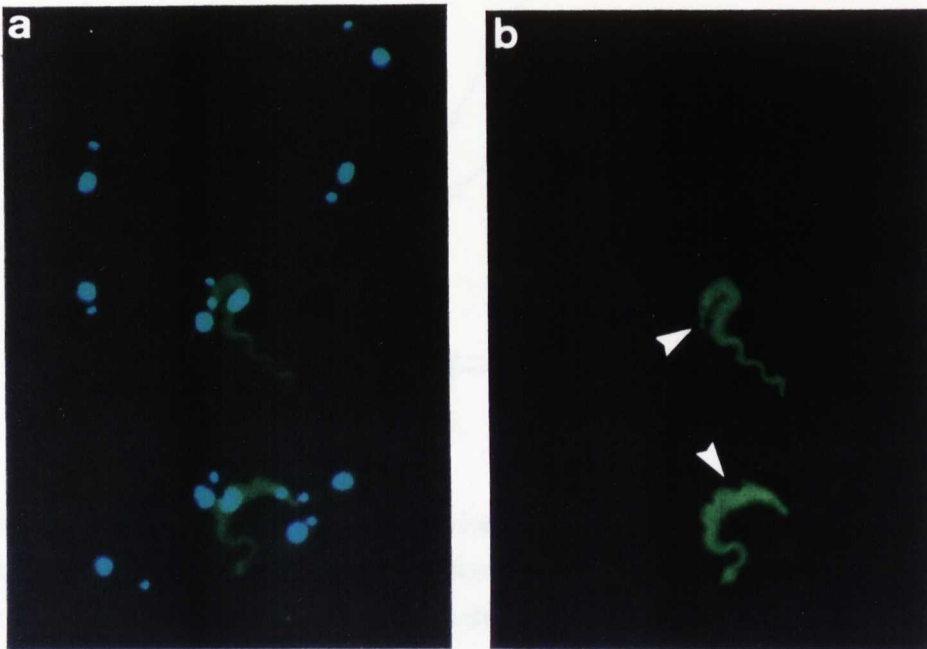


Figure 6.3 Immunofluorescent detection of GUTat 7.2 bloodstream forms in a mixed infection. Mice harbouring an EATRO 2340 chronic infection were challenged with mutagenised GUTat 7.2 bloodstream forms at least 10 days post-infection. The prevalence of GUTat 7.2 in the mixed infection was monitored each day by immunofluorescence. (a) shows a DAPI stained image of a mixed infection and in (b) arrow heads indicate the presence of GUTat 7.2 bloodstream forms.

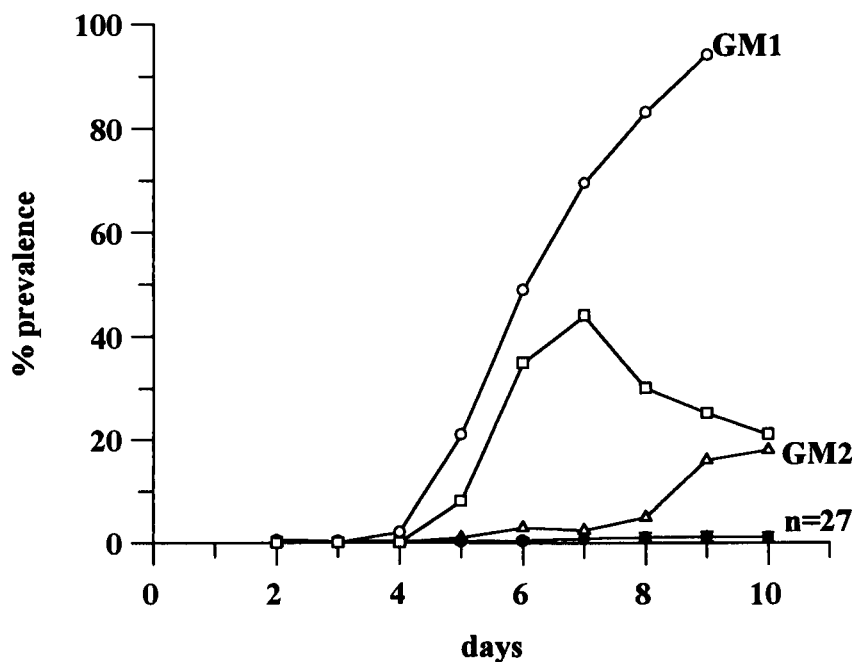


Figure 6.4 % prevalence of mutagenised GUTat 7.2 bloodstream forms in the presence of a pre-existing chronic infection. Of a total of 30 mice, 3 'growth' mutant populations were observed, including GM1 and GM2. The data for 27 mice in which no release from inhibition was observed are presented as mean \pm 2SE, n=27.

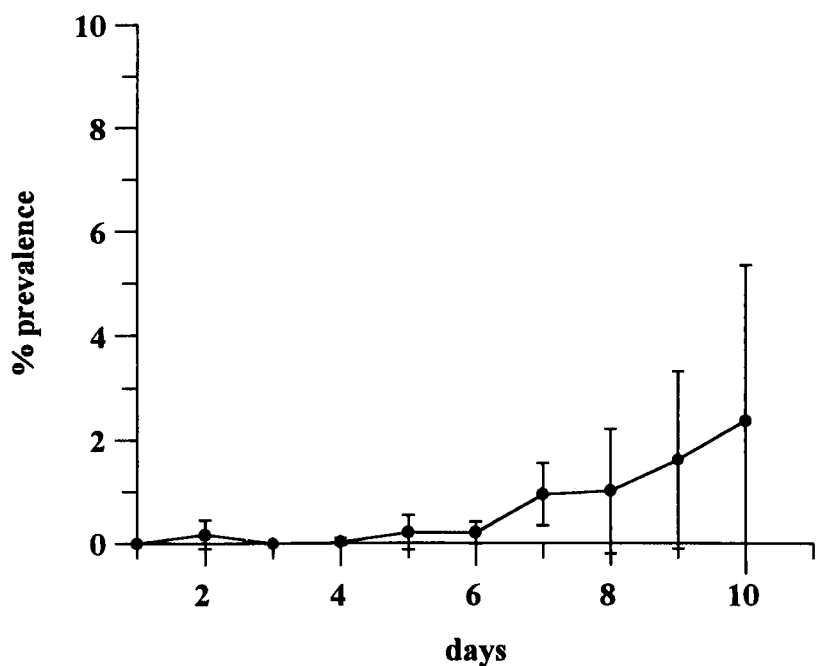


Figure 6.5 % prevalence of non-mutagenised GUTat 7.2 bloodstream forms in the presence of a pre-existing chronic infection. Data are means \pm 2SEs (n=6). Growth of GUTat 7.2 was significantly inhibited in comparison to control experiments (Turner *et al.*, 1996).

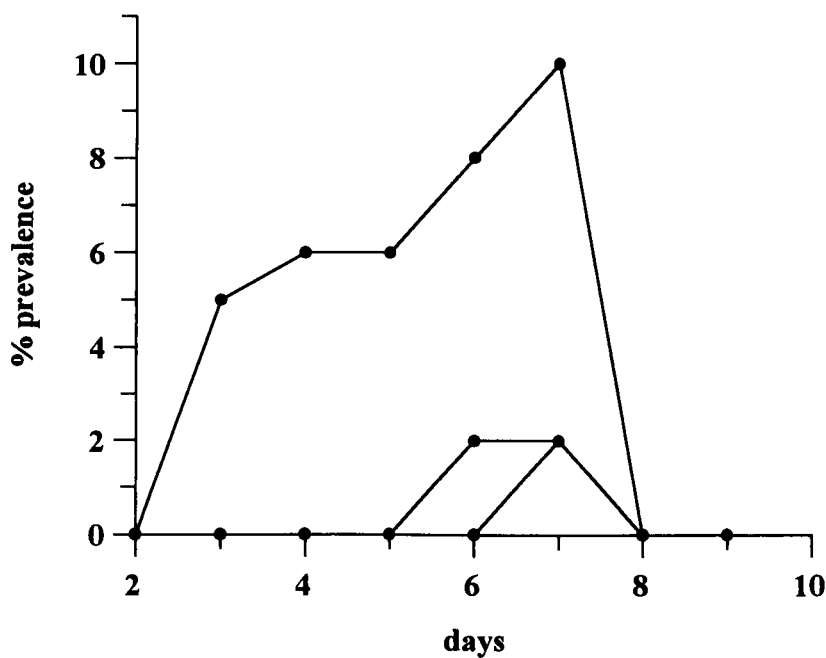


Figure 6.6A Growth of GUTat 7.2 growth mutant clone GM1cl1 in three mice, in the presence of a pre-existing chronic infection.

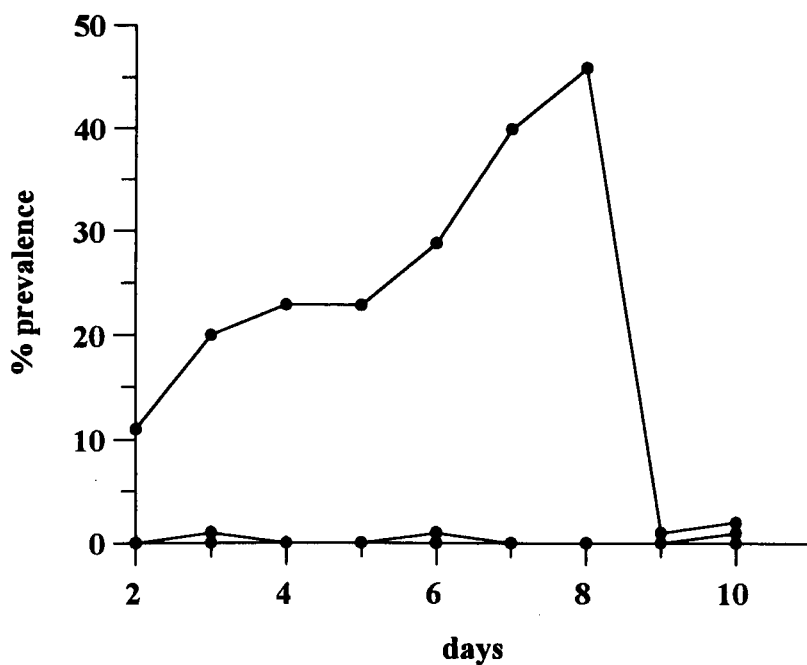


Figure 6.6B Growth of GUTat 7.2 growth mutant clone (GM2cl1) in three mice, in the presence of a pre-existing chronic infection.

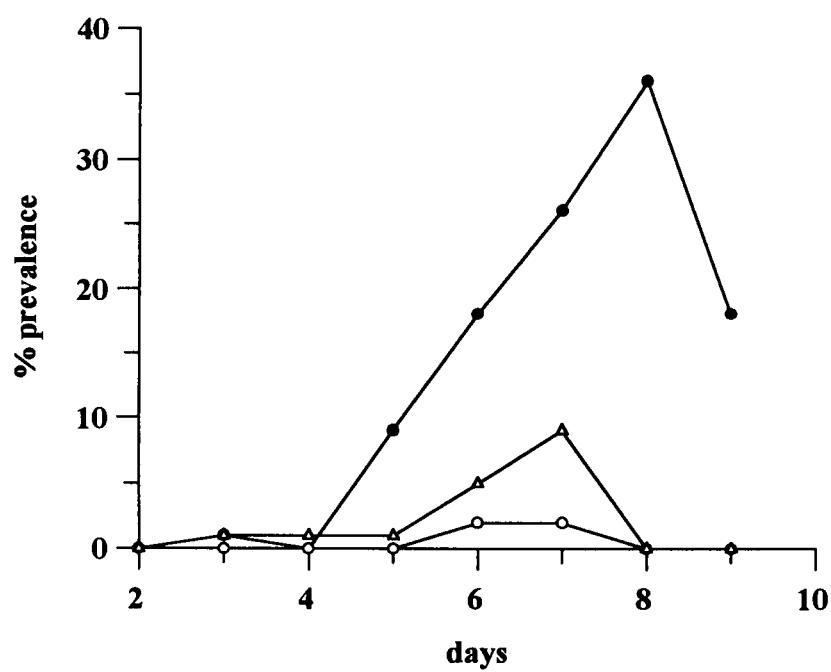


Figure 6.6C Growth of GM1 uncloned population in three mice, in the presence of a pre-existing chronic infection.

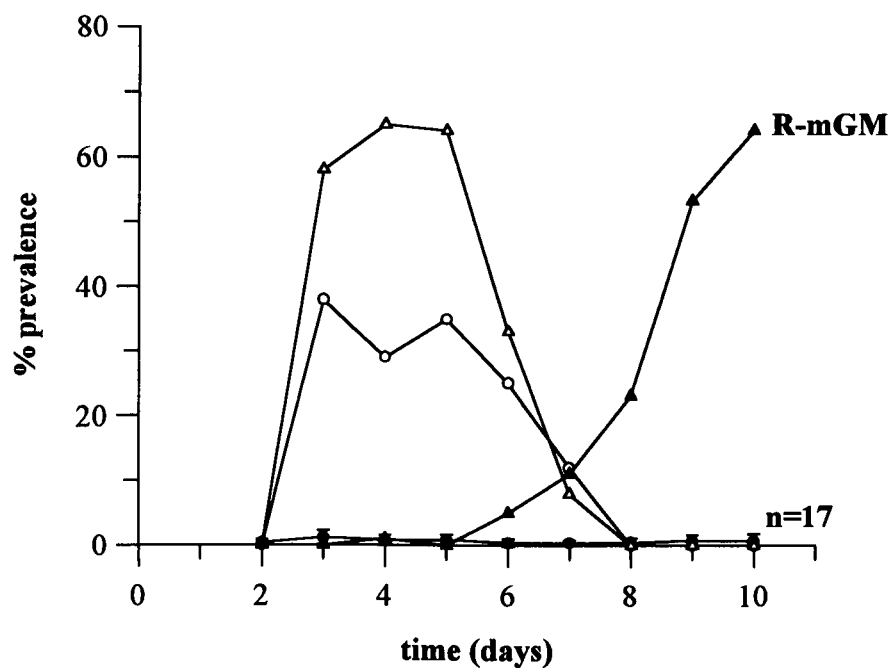


Figure 6.7 % prevalence of re-mutagenised GM1cl1 in the presence of a pre-existing chronic infection. Three mutant populations were identified, one including R-mGM. The data for 17 mice in which no release from inhibition was observed are presented as mean \pm 2SE, n=17.

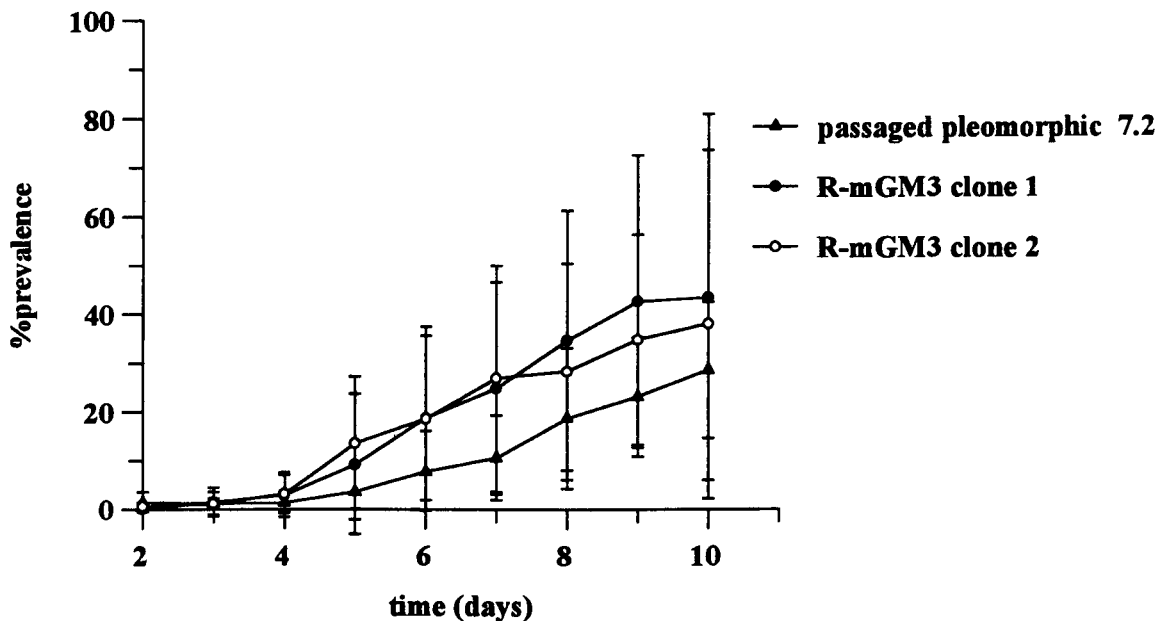


Figure 6.8A % prevalence of R-mGM3 clones 1 and 2 in the presence of a pre-existing chronic infection, compared to the passaged wild-type pleomorphic GUTat 7.2.

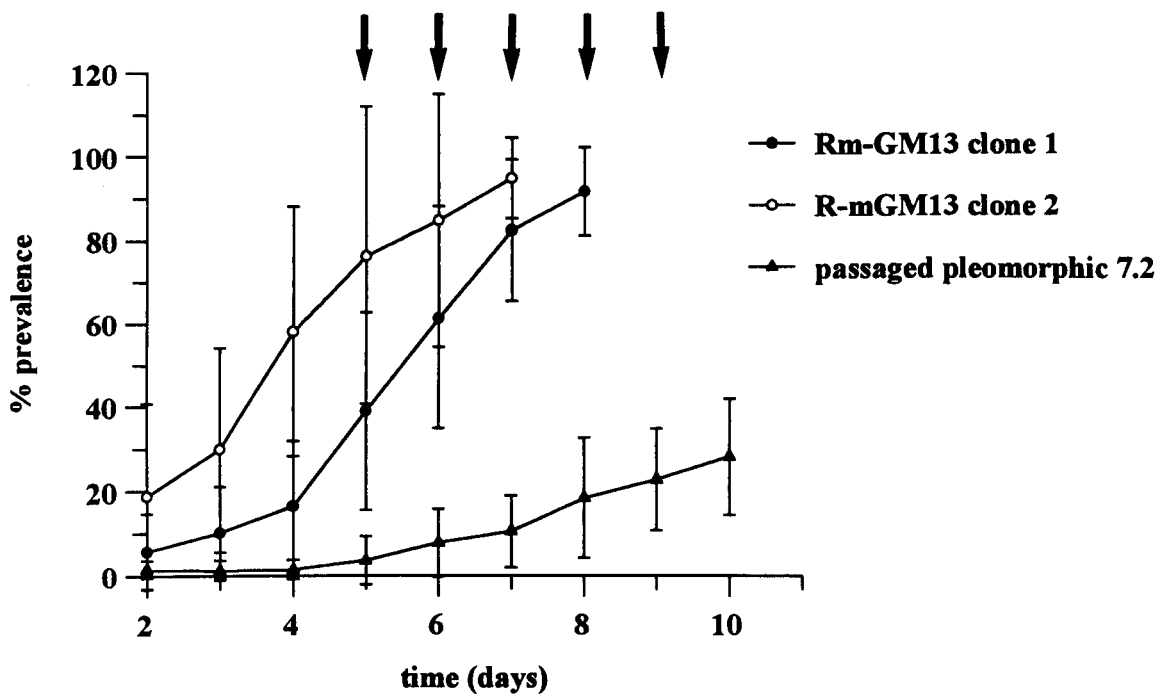


Figure 6.8B % prevalence of R-mGM13 clones 1 and 2 in the presence of a pre-existing chronic infection, compared to passaged wild-type pleomorphic GUTat 7.2. Data for both figures are geometric means \pm 2SE (n=5). Arrows indicate when mice were withdrawn from the study.

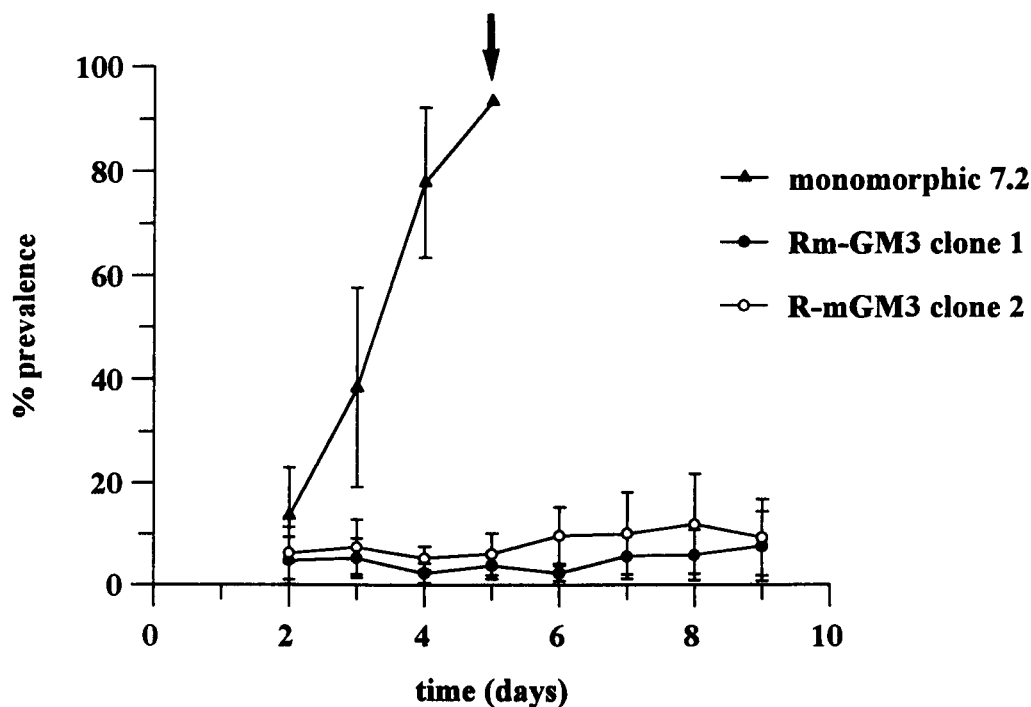


Figure 6.9A % prevalence of R-mGM3 clones 1* and 2 in the presence of a pre-existing chronic infection, compared to monomorphic GUTat 7.2.

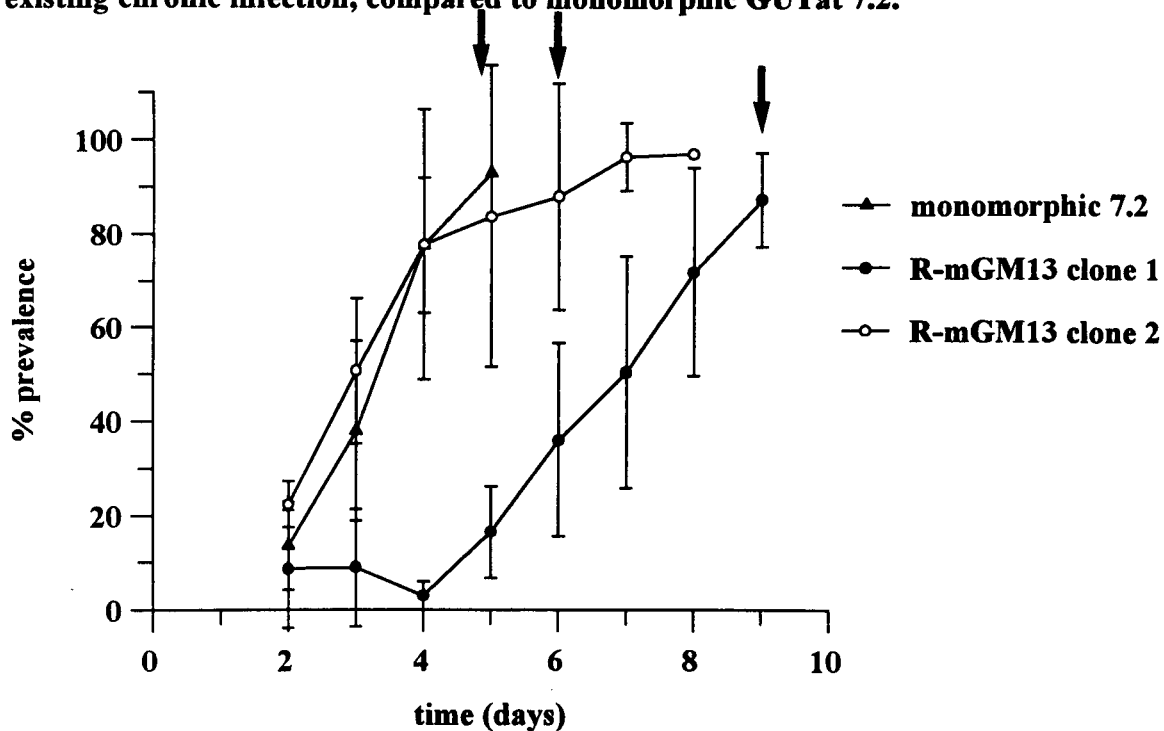
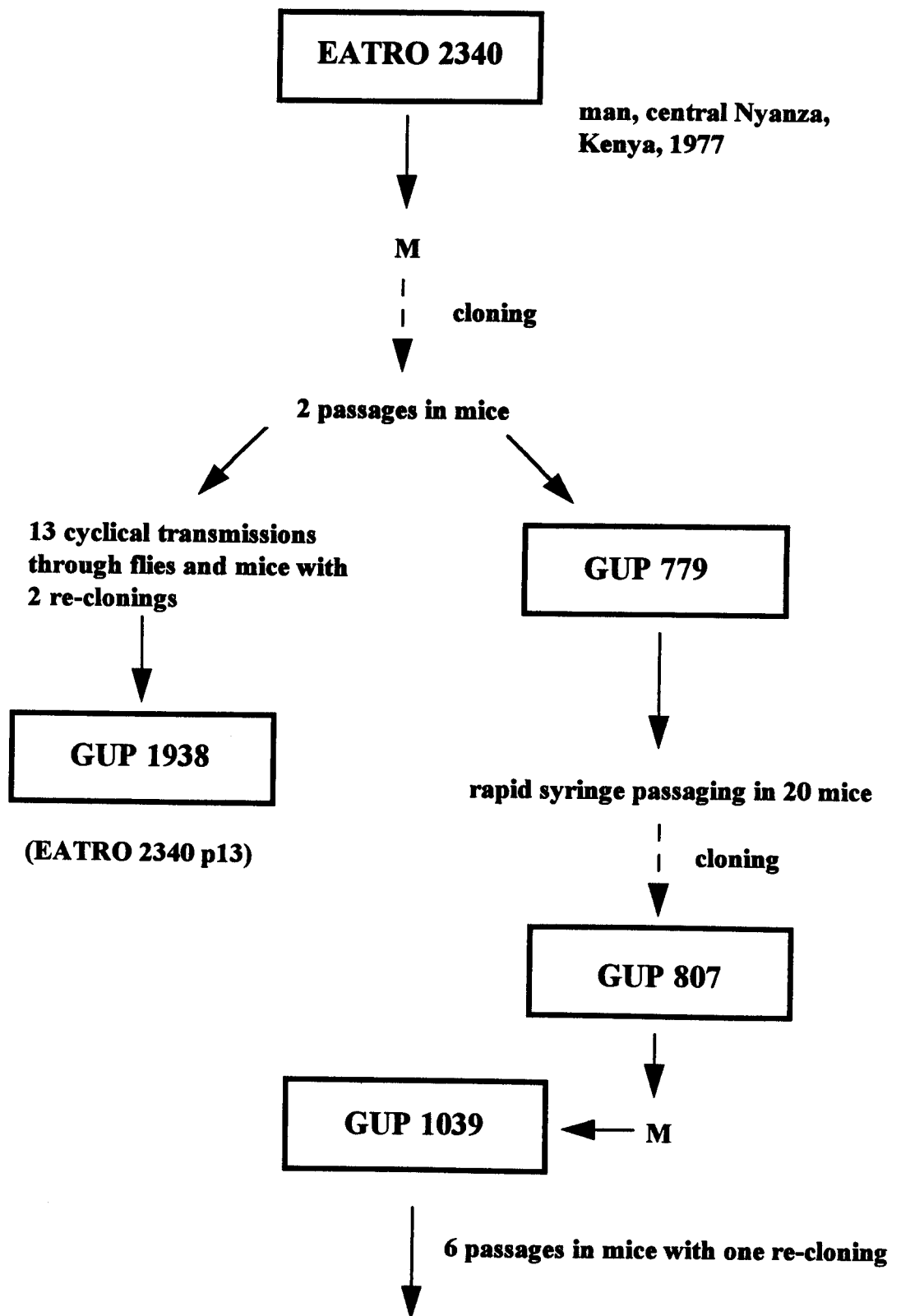
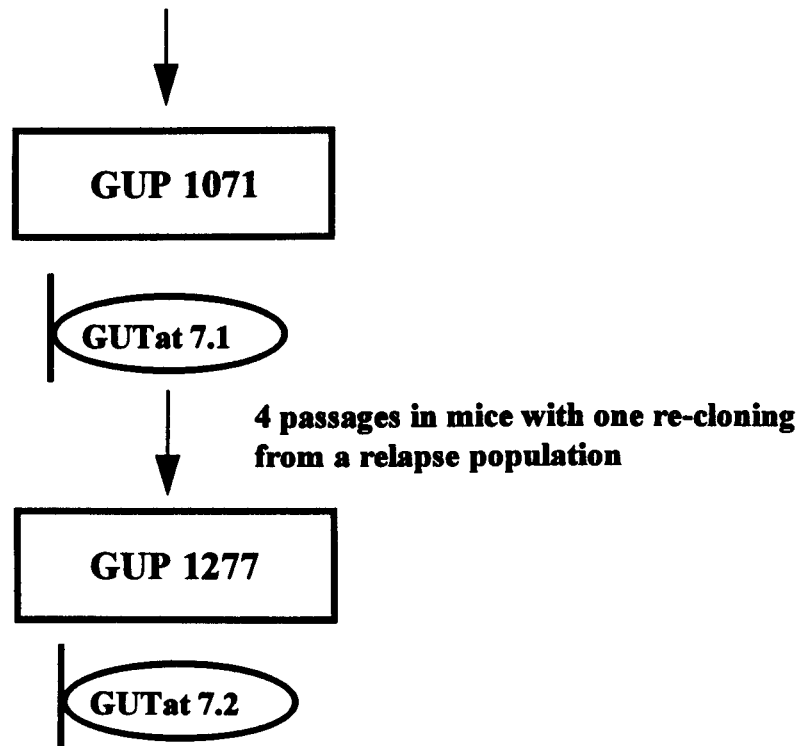


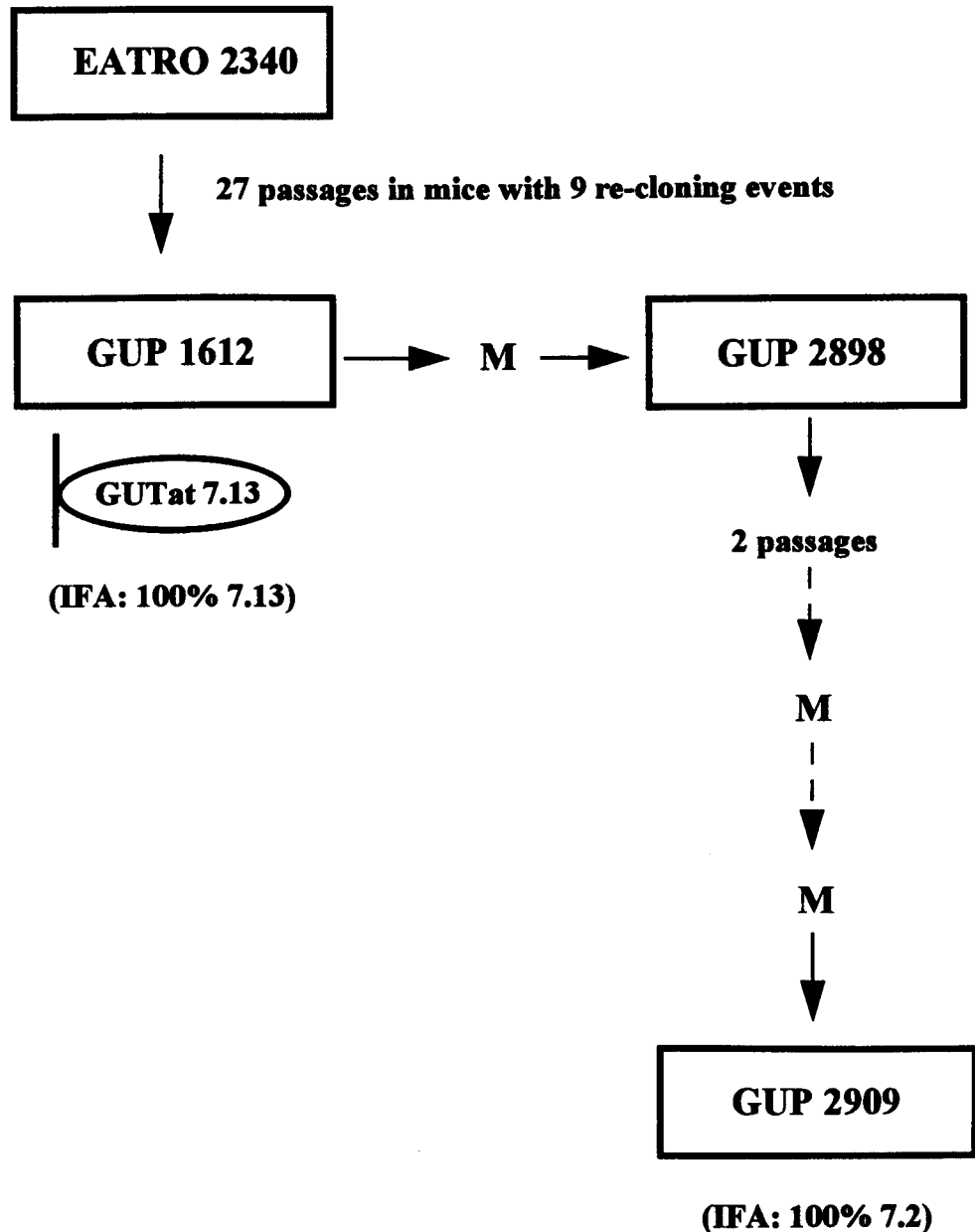
Figure 6.9B % prevalence of R-mGM13 clones 1* and 2 in the presence of a pre-existing chronic infection, compared to monomorphic GUTat 7.2. Data for both figures are geometric means $\pm 2SE$ ($n=5$, except *, $n=4$). Arrows indicate when mice were withdrawn from the study.

Figure 6.10 An abbreviated history of the cloned stock EATRO 2340 and derivation of a cloned monomorphic line GUTat 7.2



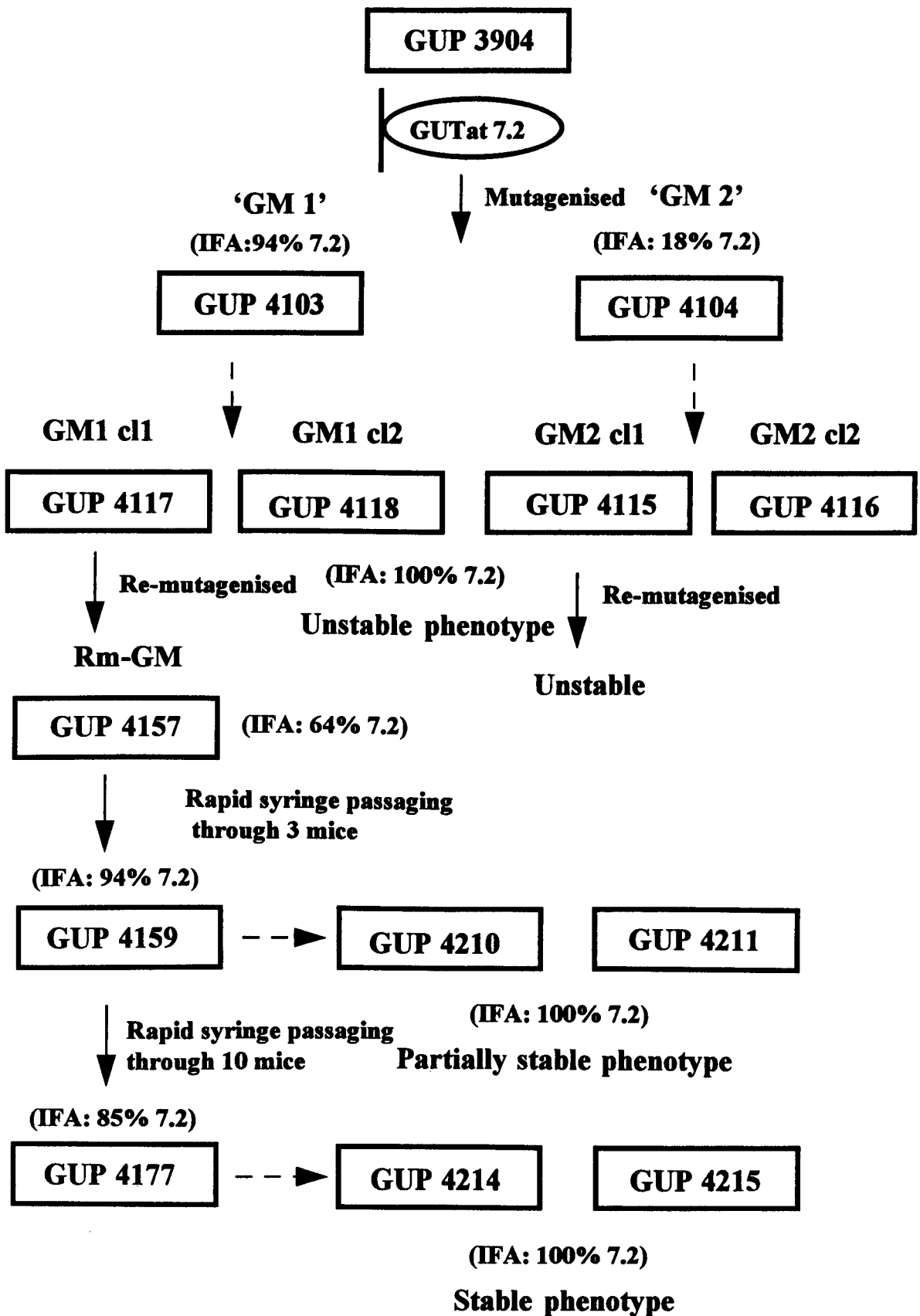


Pedigree diagrams are presented in a simplified format and drawn according to the conventions of Lumsden *et al.* (1973). Stabilate numbers are in boxes; VATs GUTat 7.1 and 7.2 are shown in cartouches; arrows with solid lines represent passage from one mouse to another, whereas dotted lines represent cloning events; M=mouse. EATRO 2340 p13 is the stock used to generate chronic primary infections in all studies described in this chapter.

Figure 6.11 Derivation of a cloned pleomorphic line GUTat 7.2

GUTat 7.13 is a metacyclic clone derived from EATRO 2340 (Cornelissen *et al.*, 1985). A new pleomorphic line that stably expresses GUTat 7.2 was derived from cloning from a relapse population of GUTat 7.13 and re-cloning twice (McLintock, 1990). IFA figures represent the % VAT prevalence determined by indirect immunofluorescence.

Figure 6.12 Generation of growth mutant trypanosomes



Dose of EMS ($\mu\text{g/ml}$)	% dead @ 2 hours	Population size at 48 hours post-mutagenization
0	0	$>10^6$
7.5	0	$>10^6$
15	0	$>10^6$
30	10.2	$>10^6$
60	25.6	ND
150	40.4	$>10^6$
300	32.3	$\cong 10^6$
600	59.2	$<10^6$

Table 6.1 Effect of increasing concentrations of EMS upon the growth of GUTat 7.2 procyclic forms *in vitro*. All cultures were seeded at a density of approximately 10^6 cells/ml. ND=not determined.

Experiment	Inoculum per mouse	Number of mutant populations in mice	Mutation rate/cell/generation
1	3×10^5	3/10	8.24×10^{-7}
2	3×10^5	0/10	$< 2.43 \times 10^{-7}$
3	3×10^5	0/10	$< 2.43 \times 10^{-7}$
Average	3×10^5	3/30	2.43×10^{-7}
4	1.5×10^6	0/20	$< 2.37 \times 10^{-8}$
5 (re-mutagenesis of GM1cl1)	3×10^5	3/20	3.75×10^{-7}

Table 6.2 The mutation rate for each experiment, where mice infected with EATRO 2340 were challenged with mutagenised GUTat 7.2 bloodstream forms and monitored for the presence of mutant populations. Mutation rates were calculated as described in section 6.2.5, after the method of Luria and Delbruck (1943).

Days after challenge	% prevalence of re-mutagenised GM2cl1									
	A					B				
	1	2	3	4	5	1	2	3	4	5
2	0	0	0	0	0	0	0	0	0	1.0
3	3.0	8.0	0	0	0	0	4.0	1.0	1.0	1.0
4	2.0	9.0	0	0	0	1.0	4.0	2.0	0	0
5	0	1.0	0	1.0	0	1.0	2.0	1.0	1.0	3.0
6	1.0	5.0	0	4.0	0	1.0	1.0	2.0	0	1.0
7	1.0	4.0	0	2.0	2.0	1.0	1.0	0	0	2.0
8	3.0	1.0	0	7.0	7.0	0	0	2.0	0	2.0
9	0	0	0	3.0	14.0	1.0	0	0	0	3.0
10	0	1.0	0	8.0	17.0	0	1.0	2.0	0	1.0

Days after challenge	% prevalence of re-mutagenised GM2cl1									
	C					D				
	1	2	3	4	5	1	2	3	4	5
2	0	2.0	0	0	0	2.0	0	0	0	0
3	1.0	2.0	0	6.0	0	6.0	2.0	0	4.0	4.0
4	0	0	0	3.0	0	0	5.0	0	4.0	0
5	2.0	0	1.0	3.0	0	4.0	7.0	0	5.0	0
6	0	0	0	0	0	0	3.0	0	2.0	1.0
7	1.0	3.0	0	0	0	3.0	3.0	2.0	1.0	0
8	8.0	0	0	2.0	0	3.0	7.0	1.0	1.0	1.0
9	5.0	1.0	0	0	1.0	3.0	4.0	2.0	7.0	1.0
10	5.0	0	0	0	0	1.0	0	6.0	20.0	0

Table 6.3 % prevalence of re-mutagenised GM2cl1 in the presence of a pre-existing chronic infection (n=100).

CHAPTER 7 GENERAL DISCUSSION

The main aims of this study were to investigate aspects of the cell biology of *T. brucei* and *Leishmania* species, with particular attention paid to the timing of cell cycle events, growth and differentiation of these parasites. How the processes of cellular growth, division and differentiation are controlled are vital to the parasite sustaining an infection in the host and in promoting transmission to the next stage of its life cycle. This study examined these three aspects, in an attempt to unravel the relationship between cell cycle and life cycle events.

Analysis of the relative timing of cell cycle events was conducted using the method adopted by Woodward and Gull (1990) in their study of *T. brucei* procyclic forms. This method involved constructing a full cell cycle map for events in the nucleus and kinetoplast of two *T. brucei* life cycle stages, procyclic and bloodstream forms and also *L. mexicana* promastigote forms. This analysis allowed comparisons to be made between both species and life cycle stages. A similar pattern of events to the previous study of *T. brucei* procyclic forms (Woodward and Gull, 1990) was observed in that events in the kinetoplast both started and ended before corresponding events in the nucleus. However, a true picture of cell cycle events could not be established due to a bias in the classification of dividing organelles and highlighted a conceptual weakness in the approach whereby it was difficult to compare timing of events between organelles. To overcome this difficulty a simpler approach was adopted which did not require the construction of a full cell cycle map and enabled direct comparisons to be made between organelles. The relative lengths and timing of the periods of S-phase were found to be similar in three of the cell types examined, the exception being *L. mexicana* amastigote forms. Greater differences between *T. brucei* and *L. mexicana* were observed, however, in terms of the relative timing of the periods of mitosis/division and cytokinesis. While different mechanisms of cell cycle control may be operating in each species, particularly with regard to the difference in the pattern of

the division periods, the duration of the cytokinesis periods indicated that the morphology of each cell type is a more likely candidate for the requirements for organelle re-positioning and segregation. Organelle re-positioning has been shown to be microtubule-dependent during the differentiation of *T. brucei* bloodstream to procyclic forms and is co-incident with DNA synthesis of transforming cells as they re-enter the cell cycle (Matthews *et al.*, 1995). The re-positioning of organelles to their correct locations in the cell is vital to the fidelity of organelle segregation. The relatively complex cellular architecture of the African trypanosomes necessitates extensive organelle re-assortment before cell cleavage takes place, as demonstrated by the extended phase of cytokinesis, whereas in *Leishmania* parasites there is much less of a requirement for extensive re-arrangements, resulting in a much reduced phase of cytokinesis.

This method of analysing the relative timing of key cell cycle events could be applied to other kinetoplastids, to determine whether or not the features identified in this study apply to kinetoplastids as a whole. The timing of other key cell cycle events, such as basal body replication and paraflagellar outgrowth, might also prove informative but could prove difficult. These events were temporally mapped in the cell cycle of *T. brucei* procyclic forms (Woodward and Gull, 1990) but the antibodies employed are species-specific for *T. brucei* (unpublished results). A more productive interspecies comparison might be to use inhibitors to investigate the link between the basal body and the kinetoplast previously identified in trypanosomes (Robinson and Gull, 1991). The role of microtubules in cell division and organelle re-positioning and segregation in *Leishmania* and other species also needs to be fully determined. How the timing of kinetoplastid cell cycles is ultimately controlled, however, is highly likely to rely upon regulatory proteins functionally homologous to the CDKs identified in higher eukaryotes, including yeast and mammals (Morgan, 1995). The identification of *cdc2* sequence homologues (Mottram, 1994) and other cell cycle-regulated protein kinases, e.g. the serine-threonine protein kinase SPK89 (Gale *et al.*, 1994), in

trypanosomatids indicates that similar mechanisms of cell cycle control may exist in these primitive eukaryotes.

The proposed link between antigenic switching and the cell cycle could not be properly addressed due to the failure to detect double expressors in the cloned lines examined. Limitations in the detection system employed were more than likely responsible for the failure to detect the weaker levels of labelling on double-labelled trypanosomes in comparison to single-labelled cells. Optimising the microscope system, either by an improved light source or image enhancement would provide one solution or alternatively the use of other immunocytochemical and/or immunofluorescence methods for the enhancement of the antibody signal. While the switch from one VSG to another requires DNA recombination, it seems that one round of DNA replication is required such that only slender forms are capable of antigenic switching whereas non-dividing stumpy forms are not (Matthews and Gull, 1994b). Evidence of a link between antigenic switching and the cell cycle, however, remains indirect and therefore requires direct confirmation.

Examination of the differentiation step from *L. major* promastigotes to metacyclic forms was enabled by the availability of suitable metacyclic-specific markers, a key factor which has to date severely hindered attempts to study equivalent differentiation steps in other kinetoplastids, e.g. the differentiation from *T. brucei* bloodstream forms to stumpy forms. These cell surface markers permitted the examination of metacyclic production in *in vitro* culture as well as production at the cellular level. Differentiation from promastigote to metacyclic forms was observed as being intrinsically programmed, as indicated by the exponential increase in the number of metacyclic forms through time in culture. Comparison of the growth data for the metacyclic and promastigote populations with mathematical models indicated that the total population was heterogeneous consisting of sub-populations that replicate and differentiate at different rates, as observed also in *T. brucei* slender to stumpy

differentiation (Turner *et al.*, 1995). The heterogeneous model therefore appears to be a model which could be applied generally to kinetoplastid replication and differentiation but would not rule out other suitable models.

The heterogeneous model also assumes that metacyclic forms are non-dividing and are also incapable of de-differentiating to promastigote forms. Each of these two possibilities were tested experimentally in this study and confirmed, although not unequivocally, that metacyclics are indeed non-dividing forms, but are also capable of de-differentiation. De-differentiation appeared to occur at a very low rate, however, this aspect needs further investigation to assess its effect upon the heterogeneous model and how the model could be modified to incorporate this further dimension to *Leishmania* replication and differentiation. It is possible that de-differentiation only occurs in *in vitro* culture and is of no obvious benefit to *Leishmania* development in the sandfly. Studying the capability of metacyclic forms to de-differentiate in *in vitro* culture also revealed the heterogeneity of stationary phase populations with respect to the growth status of its sub-populations and their capacity to undergo differentiation. While this evidence would appear to further validate the heterogeneous model, the model's suitability to differentiation *in vivo* also requires confirmation. The implications of this model for the development of *Leishmania* in the sandfly vector is that 'altruism' (*sensu* Vickerman, 1989) could play a major role within the parasite population, where sub-populations which replicate at high rates but differentiate at low rates sustain dense infections, which are often observed in the sandfly midgut (Walters *et al.*, 1987) and yet allow other sub-populations which differentiate at higher rates to migrate forwards and promote transmission to the mammalian host. This idea, however, is only at present a matter for speculation and would require greater validation.

The genetic basis for intrinsic programming also needs to be determined. Differential screening of clonal populations which replicate and differentiate at different rates

would perhaps indicate which genes are involved in the intrinsic control of differentiation. Induction of differentiation was also observed in this study as the total population reached stationary phase in *in vitro* culture but this extrinsic effect was not investigated. The role of putative induction factors would therefore be a prime area for investigation, but would also require parallel studies of promastigote development towards metacyclic forms *in vivo*. Regulators of promastigote differentiation such as haemoglobin concentration and pH have been identified but the mechanisms of their actions remain to be resolved. How these factors affect the outcome of the heterogeneous model would be another matter to consider by, for example, monitoring metacyclic production in *in vitro* culture at a lower pH, 5.5, culture conditions known to induce metacyclogenesis (Bates and Tetley, 1993). As the developmental biology of *Leishmania* becomes clearer, the collective evidence points to a combination of intrinsic programming and/or selectional pressure creating suitable conditions for the production of an infective metacyclic population, as the parasite population migrates within the sandfly vector.

As the differentiation from promastigotes to metacyclic forms involves release from the cell cycle and entry into a quiescent or G₀/G₁-phase, it seems likely that a link exists between the two processes of cell cycle and life cycle progression. Examination of metacyclic production at the cellular level indicated that the commitment to differentiate occurs before cell division, arising in symmetrical production of two daughter metacyclic forms. Metacyclic production therefore complies with the "decide and divide" model as proposed by Matthews and Gull (1994b). Whether or not the commitment to differentiate occurs at a particular point in the cell cycle could not be determined in this study, but the use of cell cycle phase-specific inhibitors would perhaps indicate when the expression of metacyclic-specific genes is likely to occur. It is possible, however, that more than one cell division is required for the production of two non-dividing metacyclic forms and that the expression of metacyclic-specific LPG or the Gene B protein does not necessarily represent fully

differentiated metacyclic forms. It is also unknown whether an irreversible point of commitment to differentiation exists as described in other systems e.g. in the differentiation of *Theileria annulata* macroschizonts to the merozoite stage (Shiels *et al.*, 1994). The differentiating macroschizont stage passes through a reversible phase, during which there is a low level expression of merozoite-specific genes which are fully expressed following the commitment point leading to irreversible differentiation.

Symmetrical production of metacyclics also differs from mechanisms which give rise to new cell types in other eukaryotes. Asymmetric cell divisions or the interaction of two cell types producing a third cell type are observed in animal development (Wolpert, 1988, Gurdon, 1992). Asymmetric cell divisions are also observed in the differentiation of bacteria (Newton and Ohta, 1990). The mechanism responsible for symmetrical division in *Leishmania* is unknown. The availability of cell surface markers for equivalent differentiation steps in other kinetoplastids would determine whether symmetrical cell divisions are a general feature of the production of new cell types/life cycle stages in these organisms.

Manipulation of a method used to assess growth in *T. brucei* chronic infections led to the generation of 'growth' mutant trypanosomes. Growth mutants expressed an altered growth phenotype i.e. they could overcome growth inhibition, a phenomenon identified in chronic infections (Turner *et al.*, 1996). A combination of chemical mutagenesis and rapid-syringe passaging of mutagenised populations in mice led to the selection of mutant populations which expressed a stable phenotype. The nature of this altered phenotype, however, is as yet unknown. Determination of the genetic lesion involved in comparison to wild-type lines would therefore be a natural progression to this work, focusing particularly upon the control of growth by external factors and how external signals are transduced within the parasite. Comparisons at this stage can only be made with growth regulation and signal transduction in other

eukaryotic systems, although enormous progress has been made in determining how growth is similarly regulated in protozoan parasites (Turco, 1995).

In conclusion, this study has examined cell cycle timing, growth and differentiation in kinetoplastids and attempted to address how these three processes may be inter-linked. The requirements for cell cycle co-ordination and differentiation leading to safe passage to the next stage of the parasite's life cycle have been emphasised. The availability of a number of tools to examine *Leishmania* differentiation, as demonstrated in this study, as well as in other differentiation systems e.g. *T. brucei* bloodstream to procyclic differentiation (Matthews and Gull, 1994a and b) will permit future studies to investigate more fully both the cellular and molecular basis for cell cycle and life cycle progression.

REFERENCES

- Adler, S. (1964) *Leishmania*. *Advances in Parasitology* 2, 35-96
- Affranchino, J.L., Gonzalez, S.A. & Pays, E. (1993) Isolation of a mitotic-like cyclin homologue from the protozoan *Trypanosoma brucei*. *Gene* 132, 75-82
- Alexander, J. & Vickerman, K. (1975) Fusion of host cell secondary lysosomes with the parasitophorous vacuoles of *Leishmania mexicana*-infected macrophages. *Journal of Protozoology* 22(4), 502-508
- Bahouth, S. & Malbon, C.C. (1994) Genetic (transcriptional and post-transcriptional) regulation of G-protein linked receptor expression. In: *Regulation of cellular signal transduction pathways by desensitization and amplification*. Sibley, D.R. & Houslay, M.D. (Editors) Wiley, Chichester chapter 4, 99-112
- Balber, A.E. (1972) *Trypanosoma brucei*: fluxes of the morphological variants in intact and X-irradiated mice. *Experimental Parasitology* 31, 307-319
- Baltz, T., Baltz, D., Giroud, C. & Crockett, J. (1985) Cultivation in a semi-defined medium of animal infective forms of *Trypanosoma brucei*, *T. equiperdum*, *T. evansi*, *T. rhodesiense* & *T. gambiense*. *EMBO Journal* 4, 1273-1277
- Baltz, T., Giroud, C., Baltz, D., Roth, C., Raibaud, A. & Eisen, H. (1986) Stable expression of two variable surface glycoproteins by cloned *Trypanosoma equiperdum*. *Nature* 319, 602-604
- Banerjee, C. & Sarkar, D. (1990) Partial purification and characterisation of a soluble protein kinase from *Leishmania donovani* promastigotes. *Journal of General Microbiology* 136, 1051-1057
- Barcinski, M.A., Schechtman, D., Quintao, L.G., Costa, D.D.D., Soares, L.R.B., Moreira, M.E.C. & Charlab, R. (1992) Granulocyte-macrophage colony-stimulating factor increases the infectivity of *Leishmania amazonensis* by protecting promastigotes from heat-induced death. *Infection and Immunity* 60, 3523-3527
- Barcinski, M.A. & Costa-Moreira, M.E. (1994) Cellular response of protozoan parasites to host-derived cytokines. *Parasitology Today* 10(9), 352-355

- Barry, J.D. & Turner, C.M.R.** (1991) The dynamics of antigenic variation and growth of African trypanosomes. *Parasitology Today* **7**(8), 207-211
- Basegra, R.** (1989) Measuring parameters of growth. In: *Cell Growth and Division, A Practical Approach*. Basegra, R. (Editor) University Press
- Bastin, P. Coppens, I., Saint-Remy, J.-M., Baudhuin, P., Opperdoes, F.R. & Courtoy, P.J.** (1994) Identification of a specific epitope on the extracellular domain of the LDL-receptor of *Trypanosoma brucei brucei*. *Molecular and Biochemical Parasitology* **63**, 193-202
- Bates P.A.** (1994) Complete developmental cycle of *Leishmania mexicana* in axenic culture. *Parasitology* **108**, 1-9
- Bates, P.A.** (1995) The lipophosphoglycan-associated molecules of *Leishmania*. *Parasitology Today* **11**(9), 317-318
- Bates., P.A., Robertson, C.D., Tetley, L. & Coombs, G.H.** (1992) Axenic cultivation and characterisation of *Leishmania* amastigote-like forms. *Parasitology* **105**, 193-202
- Bates, P.A. & Tetley, L.** (1993) *Leishmania mexicana*: induction of metacyclogenesis by cultivation of promastigotes at an acidic pH. *Experimental Parasitology* **76**, 412-423
- Berens, R.L., Brun, R. & Krassner, S.M.** (1976) A simple monophasic medium for axenic culture of hemoflagellates. *Journal of Parasitology* **62**, 360-365
- Black, S.J., Sendashonga, C.N., O'Brien, C., Borowy, N.K., Naessens, M., Webster, P. & Murray, M.** (1985) Regulation of parasitaemia in mice infected with *Trypanosoma brucei*. *Current Topics in Microbiology and Immunology* **117**, 93-118
- Bogenhagen, D. & Clayton, D.A.** (1977) Mouse L cell mitochondrial DNA molecules are selected randomly for replication throughout the cell cycle. *Cell* **11**, 719-727

- Borst, P. & Rudenko, G. (1994)** Antigenic variation in African trypanosomes. *Science* **264**, 1872-1873
- Bray, R.S. & Alexander, J. (1987)** *Leishmania* and the macrophage. In: *The Leishmaniases in Biology and Medicine*. Peters, W. & Killick-Kendrick, R. (Editors) Academic Press, London **1**, 211-233
- Brodin, T.N., Heath, S. & Sacks, D.L. (1992)** Genes selectively expressed in the infectious (metacyclic) stage of *Leishmania major* promastigotes encode a potential basic-zipper structural motif. *Molecular and Biochemical Parasitology* **52**, 241-250
- Brown, K.G., Bates, P.A. & Coombs, G.H. (1994a)** Developmental stages of *Leishmania panamensis* grown *in vitro*. *Journal of Eukaryotic Microbiology* **41**, Abstract 54
- Brown, K.G., Bates, P.A. & Coombs, G.H. (1994b)** Preliminary characterisation of the developmental stages of *L. panamensis*. *Transactions of the Royal Society of Tropical Medicine and Hygiene* **88**, 20
- Brun, R. & Schonenberger, M. (1979)** Cultivation and *in vitro* cloning of procyclic culture forms of *Trypanosoma brucei* in a semi-defined medium. *Acta Tropica* **36**, 289-292
- Brun, R. & Schonenberger, M. (1981)** Stimulating effect of citrate and cis-aconitate on the transformation of *Trypanosoma brucei* bloodstream forms to procyclic forms *in vitro*. *Zeitschrift Fur Parasitenkunde* **66**, 17-24
- Bulow, R., Overath, P. Davoust, J. (1988)** Rapid lateral diffusion of the variant surface glycoprotein in the coat of *Trypanosoma brucei*. *Biochemistry* **27**, 2384-2388
- Capburn, A., Giroud, C., Baltz, T. & Mattern, P. (1977)** *Trypanosoma equiperdum*: Etude des variation antigeniques au cours de la trypanosomose experimentale du lapin. *Experimental Parasitology* **42**, 23-42
- Cassel, D., Shoubi, S., Glusman, G., Cukierman, E., Rotman, M. & Zilberstein, D. (1991)** *Leishmania donovani*: characterisation of a 38kDa membrane protein that

cross-reacts with mammalian G-protein transducin. *Experimental Parasitology* **72**, 411-417

Chang, K.-P., Fong, D. & Bray, R.S. (1985) Biology of *Leishmania* and leishmaniasis. In: *Leishmaniasis* Chang, K.-P. & Bray, R.S. (Editors) Human Parasitic Diseases series Ruitenberg, E.J. & MacInnis, A.J. (Editors) Elsevier **1**, 2-27

Charlab, R., Blaineau, C., Schechtman, D. & Barcinski, M.A. (1990) Granulocyte-macrophage colony stimulating factor is a growth-factor for promastigotes of *Leishmania mexicana amazonensis*. *Journal of Protozoology* **37**, 352-357

Charlab, R. & Ribeiro, J.M.C. (1993) Cytostatic effect of *Lutzomyia longipalpis* salivary gland homogenates on *Leishmania* parasites. *The American Journal of Tropical Medicine and Hygiene* **48**, 831-838

Charlab, R., Tesh, R.B., Rowton, E.D. & Ribeiro, J.M.C. (1995) *Leishmania amazonensis*: sensitivity of different promastigote morphotypes to salivary gland homogenates of the sand fly *Lutzomyia longipalpis*. *Experimental Parasitology* **80**, 167-175

Christophers, S.R., Shortt, H.E. & Barraud, P.J. (1926) The morphology and life cycle of the parasite of Indian kala-azar in culture. *Indian Medical Research Memoirs*, **4**, 19-53

Clayton, D.A. (1982) Replication of animal mitochondrial DNA. *Cell* **28**, 693-705

Cooper, J.A., Bowen-Pope, D.F., Raines, E., Ross, R. & Hunter, T. (1982) Similar effects of platelet-derived growth factor and epidermal growth factor on the phosphorylation of tyrosine in cellular proteins. *Cell*, **31**, 263-273

Coppens, I., Baudhuin, P., Oppendoes, F.R. & Courtoy, P.J. (1988) Receptors for the host low-density lipoproteins on the hemoflagellate *Trypanosoma brucei brucei*: purification and involvement in the growth of the parasite. *Proceedings of the National Academy of Sciences USA* **85**, 6753-6757

Coppens, I., Bastin, P., Oppendoes, F.R., Baudhuin, P. & Courtoy, P.J. (1992) *Trypanosoma brucei brucei*: antigenic stability of its LDL-receptor and

immunological cross-reactivity with the LDL-receptor of the mammalian host. *Experimental Parasitology* 74, 77-86

Cornelissen, A.W.C.A., Bakkeren, G.A.M., Barry, J.D., Michels, P.A.M. & Borst, P. (1985) Characteristics of trypanosome variant antigen genes active in the tsetse fly. *Nucleic Acids Research* 13(13), 4661-4676

Cosgrove, W.B. & Skeen, M.J. (1970) The cell cycle in *Crithidia fasciculata*. Temporal relationships between synthesis of deoxyribonucleic acid in the nucleus and the kinetoplast. *Journal of Protozoology* 17(2), 172-177

Coulson, R.M.R. & Smith, D.F. (1990) Isolation of genes showing increased or unique expression in the infective promastigotes of *Leishmania major*. *Molecular and Biochemical Parasitology* 40, 63-75

Da Silva, R. & Sacks, D.L. (1987) Metacyclogenesis is a major determinant of *Leishmania* promastigote virulence and attenuation. *Infection and Immunity* 55, 2802-2807

Davis, C.E., Colmerauer, M.E.M., Kim, C.-H., Matthews, B. & Guiney, D. (1989) *myc*-related proteins and DNA sequences in *Trypanosoma brucei*. *Microbial Pathogenesis* 7, 45-53

Davies, C.R., Cooper, A.M., Peacock, C., Lane, R.P. & Blackwell, J.M. (1990) Expression of LPG and GP63 by different developmental stages of *Leishmania major* in the sandfly *Phlebotomus papatasi*. *Parasitology* 101, 337-343

De Waele, M., De Mey, J., Renmans, W., Labeur, C., Jochmans, K. & Van Camp, B. (1986) Potential of immunogold-silver staining for the study of leukocyte subpopulations as defined by monoclonal antibodies. *Journal of Histochemistry and Cytochemistry* 34(10), 1257-1263

Descoteaux, A. & Turco, S.J. (1993) The lipophosphoglycan of *Leishmania* and macrophage protein kinase C. *Parasitology Today* 9, 468-471

Egan, S.E. & Weinberg, R.A. (1993) The pathway to signal achievement. *Nature* 365, 781-783

- Eperon, S. & McMahon-Pratt, D. (1989) Extracellular cultivation and morphological characterisation of amastigote-like forms of *Leishmania panamensis* and *L. braziliensis*. *Journal of Protozoology* **36**, 502-510
- Esko, J.D. & Raetz, C.R.H. (1978) Replica plating and *in situ* enzymatic assay of animal cell colonies established on filter paper. *Proceedings of the National Academy of Sciences USA* **75**(3), 1190-1193
- Esser, K.M. & Schoenbechler, M.J. (1985) Expression of two variant surface glycoproteins on individual African trypanosomes during antigenic switching. *Science* **229**, 190-193
- Evans, T.E. (1966) Synthesis of a cytoplasmic DNA during the G₂ interphase of *Physarum polycephalum*. *Biochemical & Biophysical Research Communications* **22**, 678
- Fairlamb, A.H., Carter, N.S., Cunningham, M. & Smith, K. (1992) Characterisation of melarsen-resistant *Trypanosoma brucei brucei* with respect to cross-resistance to other drugs and trypanothione metabolism. *Molecular and Biochemical Parasitology* **53**, 213-222
- Farzaneh, F., Shall, S., Michel, P. & Borst, P. (1985) ADP-ribosyl transferase activity in *Trypanosoma brucei*. *Molecular and Biochemical Parasitology* **14**, 251-259
- Feder, D. & Bishop, J.M. (1990) Purification and enzymatic characterisation of pp60-src from human platelets. *Journal of Biological Chemistry* **265**, 8205-8211
- Ferguson, M.A.J. & Homans, S.W. (1989) The membrane attachment of the variant surface glycoprotein coat of *Trypanosoma brucei*. In: *New Strategies in Parasitology* McAdam, K.P.W.J. (Editor) Churchill Livingstone, Edinburgh **chapter 7**, 121-143
- Fertig, G., Kloppinger, M. & Miltenburger, H.G. (1990) Cell cycle kinetics of insect cell cultures compared to mammalian cell cultures. *Experimental Cell Research* **189**, 208-212

- Flinn, H.M. & Smith, D.F. (1992) Genomic organisation and expression of a differentially-regulated gene family from *Leishmania major*. *Nucleic Acids Research* **20**, 755-762
- Flinn, H.M., Rangarajin, D. & Smith, D.F. (1994) Expression of a hydrophilic surface protein in infective stages of *Leishmania major*. *Molecular and Biochemical Parasitology* **65**, 259-270
- Gale, M., Carter, V. & Parsons, M. (1994) Cell cycle-specific induction of an 89kDa serine/threonine protein kinase activity in *Trypanosoma brucei*. *Journal of Cell Science* **107**, 1825-1832
- Giannini, M.S. (1974) Effects of promastigote growth phase, frequency of subculture and host age on promastigote-initiated infections in *Leishmania donovani* in the golden hamster. *Journal of Protozoology* **21**, 521-527
- Gillet, M.P.T. & Owen, J.S. (1992) Characteristics of the binding of human and bovine high-density lipoproteins by bloodstream forms of the African trypanosome, *Trypanosoma brucei brucei*. *Biochimica et Biophysica Acta* **1123**, 239-248
- Glaser, T.A., Moody, S.F., Handman, E., Bacic, A. & Spithill, T.W. (1991) An antigenically distinct lipophosphoglycan on amastigotes of *Leishmania major*. *Molecular and Biochemical Parasitology* **45**, 337-344
- Gomez, M.L. Erijman, L., Arauzo, S., Torres, H.N. & Tellez-Inon, M.T. (1989) Protein kinase C in *T. cruzi* epimastigote forms: partial purification and characterisation. *Molecular and Biochemical Parasitology* **36**, 101-108
- Gonzalez-Perdomo, M., Romero, P. & Goldenberg, S. (1988) Cyclic AMP and adenylate cyclase activators stimulate *Trypanosoma cruzi* differentiation. *Experimental Parasitology* **66**, 205-212
- Gratzner, H.G. (1982) Monoclonal antibody to 5-Bromo- and 5-Iododeoxyuridine: A new reagent for detection of DNA replication. *Science* **218**, 474-475
- Gull, K., Birkett, C., Gerke-Bonet, R., Parma, A., Robinson, D., Sherwin, T. & Woodward, R. (1990) The cell cycle and cytoskeletal morphogenesis in *Trypanosoma brucei*. *Biochemical Society Transactions* **5**, 720-722

- Gurdon, J.B.** (1992) The generation of diversity and pattern in animal development. *Cell* **68**, 185-199
- Haber, J.E.** (1992) Mating-type gene switching in *Saccharomyces cerevisiae*. *Trends in Genetics* **8**(12), 446-452
- Hajduk, S.L. & Vickerman, K.** (1981) Antigenic variation in cyclically transmitted *Trypanosoma brucei*. Variable antigen composition of the first parasitaemia in mice bitten by trypanosome-infected *Glossina morsitans*. *Parasitology* **83**, 609-621
- Hajduk, S.L., Moore, D.R., Vasudevacharya, J., Siqueira, H., Torri, A.F., Tytler, E.M. & Esko, J.D.** (1989) Lysis of *Trypanosoma brucei* by a toxic subspecies of human high density lipoprotein. *Journal of Biological Chemistry* **264**(9), 5210-5217
- Hamm, B., Schindler, A., Mecke, D. & Duszenco, M.** (1990) Differentiation of *Trypanosoma brucei* bloodstream trypomastigotes from long slender to short stumpy-like forms in axenic culture. *Molecular and Biochemical Parasitology* **40**, 13-22
- Hart, D.T. & Coombs, G.H.** (1980) Morphological and biochemical studies of the *in vitro* transformation of *Leishmania mexicana mexicana* amastigotes to promastigotes. *Journal of Protozoology* **27**, 63A
- Hart, D.T., Vickerman, K. & Coombs, G.H.** (1981a) A quick simple method for purifying *Leishmania mexicana* amastigotes in large numbers. *Parasitology* **82**, 345-355
- Hart, D.T., Vickerman, K. & Coombs, G.H.** (1981b) Transformation *in vitro* of *Leishmania mexicana* amastigotes to promastigotes: nutritional requirements and the effects of drugs. *Parasitology* **83**, 529-541
- Heimer, G.V. & Taylor, C.E.D.** (1974) Improved mountant for immunofluorescence preparations. *Journal of Clinical Pathology* **27**, 254-256
- Herbert, W.J., Mucklow, M.G. & Lennox, B.** (1975) The cause of death in murine trypanosomiasis. *Transactions of the Royal Society of Tropical Medicine and Hygiene* **69**, 4

Hide, G., Tait, A. & Keith, K. (1990) Characterization of *Trypanosoma brucei* protein kinases and a growth factor receptor. *Biochemical Society Transactions* **18**, 733-735

Hide, G., Gray, A., Harrison, C.M. & Tait, A. (1989) Identification of an epidermal growth factor receptor homologue in trypanosomes. *Molecular and Biochemical Parasitology* **36**, 51-60

Hide, G., Graham, T., Buchanan, N., Tait, A. & Keith, K. (1994) *Trypanosoma brucei*: characterisation of protein kinases that are capable of autophosphorylation *in vitro*. *Parasitology* **108**, 161-166

Hirata, J., Nakagoshi, H., Nabeshima, Y. & Matsuzaki, F. (1995) Asymmetric segregation of the homeodomain protein Prospero during *Drosophila* development. *Nature* **377**, 627-630

Hoare, C.A. (1972) *The Trypanosomes of Mammals*. Blackwell Scientific Publications, Oxford

Horvitz, H.R. & Herskovitz, I. (1992) Mechanisms of asymmetric cell division: two Bs or not two Bs, that is the question. *Cell* **68**, 237-255

Howard, A. & Pelc, S.R. (1953) Synthesis of deoxyribonucleic acid in normal and irradiated cells and its relation to chromosome breakage. *Heredity* **6 suppl.**, 261-263

Howard, M.K., Sayers, G. & Miles, M.A. (1987) *Leishmania donovani* metacyclic promastigotes: transformation *in vitro*, lectin agglutination, complement resistance and infectivity. *Experimental Parasitology* **64**, 147-156

Hughes, D.E., Schneider, C.A. & Simpson, L. (1982) Isolation and characterization of drug resistant mutants of *Crithidia fasciculata*. *Journal of Parasitology* **68(4)**, 642-649

Jackson, D.G., Owen, M.J. & Voorheis, H.P. (1985) A new method for the rapid purification of both the membrane-bound and released forms of the variant surface glycoprotein from *Trypanosoma brucei*. *Biochemical Journal* **230**, 195-202

- Jacobson, R.L.** (1995) *Leishmania*, LPG and the sandfly connection. *Parasitology Today* 11(6), 203-204
- Karp, C.L., Turco, S.J. & Sacks, D.L.** (1991) Lipophosphoglycan masks recognition of *Leishmania donovani* promastigote surface by human Kala-azar serum. *Journal of Immunology* 147, 680-684
- Keith, K., Hide, G. & Tait, A.** (1990) Characterisation of protein kinase C like activities in *Trypanosoma brucei*. *Molecular and Biochemical Parasitology* 43, 107-116
- Kelleher, M., Curtis, J.M., Sacks, D.L., Handman, E. & Bacic, A.** (1994) Epitope mapping of monoclonal antibodies directed against lipophosphoglycan of *Leishmania major* promastigotes. *Molecular and Biochemical Parasitology* 66, 187-200
- Killick-Kendrick, R.** (1979) Biology of *Leishmania* in phlebotomine sandflies. In: *Biology of the Kinetoplastida*. Lumsden, W.H.R. & Evans, D.A. (Editors) Academic Press, London 2, 396-460
- Klar, A.J.S.** (1992) Developmental choices in mating-type interconversion in fission yeast. *Trends in Genetics* 8(6), 208-213
- Knoblich, J.A., Jan, L.Y. & Jan, Y.N.** (1995) Asymmetric segregation of Numb and Prospero during cell division. *Nature* 377, 624-627
- Koch, J. & Stokstad, E.** (1967) Incorporation of [³H] thymidine into nuclear and mitochondrial DNA in synchronized mammalian cells. *European Journal of Biochemistry* 3, 1-6
- Kuo, J.F., Anderson, R.G.G., Wise, B.C., Mackerlova, L., Salomonsson, I., Brackett, N.L., Katoh, N., Shoji, M. & Wrenin, R.W.** (1980) Calcium-dependent protein kinase: widespread occurrence in various tissues and phyla of the animal kingdom and comparison of effects of phospholipid, calmodulin and trifluoperazine. *Proceedings of the National Academy of Sciences, USA* 77(12), 7039-7043
- Lainson, R. & Shaw, J.J.** (1987) Evolution, classification and geographical distribution. In: *The Leishmaniasis in Biology and Medicine*. Peters, W. & Killick-Kendrick, R. (Editors) Academic Press, London 1, 1-120

- Lamont, G.S., Tucker, R.S. & Cross, G.A.M.** (1986) Analysis of antigenic switching rates in *Trypanosoma brucei*. *Parasitology* **92**, 355-367
- Lawyer, P.G., Young, D.G., Butler, J.F. & Akin, D.E.** (1987) Development of *Leishmania mexicana* in *Lutzomyia diabolica* and *Lutzomyia shannoni* (Diptera (Psychodidae)). *Journal of Medical Entomology* **24**, 347-355
- Liew, F.Y. & Cox, F.E.G.** (1991) Non-specific defence mechanism: the role of nitric oxide. *Immunology Today* **12**, A17-A21
- Lloyd, D., Poole, R.K. & Edwards, S.W.** (1982) *The Cell Division Cycle: temporal organization and control of cellular growth and reproduction*. Academic Press, London
- Lodish, H., Baltimore, D., Berk, A., Zipursky, S.L., Matsudaira, P. & Darnell, J.** (1995) Regulation of the eukaryotic cell cycle. In: *Molecular Cell Biology*. Scientific American Books (3rd Edition) 1201-1245
- Lorenz, P., Betschart, B. & Owen, J.S.** (1995) *Trypanosoma brucei brucei* and high-density lipoproteins: old and new thoughts on the identity and mechanism of the trypanocidal factor in human serum. *Parasitology Today* **11**(9), 348-352
- Lumsden, W.H.R., Herbert, W.H. & McNeillage, G.J.C.** (1973) *Techniques with trypanosomes*. Churchill Livingstone, Edinburgh
- Lund, K.A. & Wiley, H.S.** (1994) Regulation of the epidermal growth factor receptor by phosphorylation. In: *Regulation of cellular signal transduction pathways by desensitization and amplification*. Sibley, D.R. & Houslay, M.D. (Editors) Wiley, Chichester chapter 12, 277-303
- Luria, S.E. & Delbruck, M.** (1943) Mutations of bacteria from virus sensitivity to virus resistance. *Genetics* **28**, 491-511
- Mallinson, D.J. & Coombs, G.H.** (1989) Biochemical characteristics of the metacyclic forms of *Leishmania major* and *L. mexicana mexicana*. *Parasitology* **98**, 7-15

- Marr, J.J.** (1980) Carbohydrate metabolism in *Leishmania*. In: *Biochemistry and Physiology of Protozoa*. Levandowsky, M. & Hutner, S.H. (Editors) Academic Press, London 3, 313-340
- Marsden, P.D.** (1984) Selective primary health care: Strategies for control of disease in the developing world XIV Leishmaniasis. *Review of Infectious Diseases* 6(5), 736-744
- Matthews, K.R. & Gull, K.** (1994a) Evidence for an interplay between cell cycle progression and the initiation of differentiation between life cycle forms of African trypanosomes. *Journal of Cell Biology* 125(5), 1147-1156
- Matthews, K.R. & Gull, K.** (1994b) Cycles within Cycles: The interplay between differentiation and cell division in *Trypanosoma brucei*. *Parasitology Today* 10(12), 473-476
- Matthews, K. R., Sherwin, T. & Gull, K.** (1995) Mitochondrial genome repositioning during the differentiation of the African trypanosome between life cycle forms is microtubule mediated. *Journal of Cell Science* 108, 2231-2239
- Mazingue, C., Cottrez-Detouef, F., Louis, J., Kweider, M., Auriault, C. & Capron, A.** (1989) *In vitro* and *in vivo* effects of interleukin 2 on the protozoan parasite *leishmania*. *European Journal of Immunology* 19, 487-491
- McConnell, J., Turner, M. & Rovis, L.** (1983) Biosynthesis of *Trypanosoma brucei* variant surface glycoproteins-analysis of carbohydrate heterogeneity and timing of post-translational modifications. *Molecular and Biochemical Parasitology* 8, 119-135
- McConville, M., Thomas-Oates, T., Ferguson, M.A. & Homans, S.W.** (1990) Structure of the lipophosphoglycan from *Leishmania major*. *Journal of Biological Chemistry* 265, 19611-19623
- McConville, M., Turco, S.J., Ferguson, M.A. & Sacks, D.L.** (1992) Developmental modification of lipophosphoglycan during the differentiation of *L. major* promastigotes to an infectious stage. *EMBO Journal* 11, 3593-3600

- McLintock, L.M.L.** (1990) The regulation of pleomorphic *Trypanosoma brucei* infections in immunocompetent hosts. *PhD Thesis*, Unpublished, University of Glasgow
- McLintock, L.M.L., Turner, C.M.R. & Vickerman, K.** (1993) Comparison of the effects of immune killing mechanisms on *Trypanosoma brucei* parasites of slender and stumpy morphology. *Parasite Immunology* **15**, 475-480
- Metcalf, D.** (1989) The molecular control of cell division, differentiation commitment and maturation in haemopoietic cells. *Nature* **339**, 27-30
- Metcalf, D. & Burgess, A.W.** (1982) Clonal analysis of progenitor cell commitment to granulocyte or macrophage production. *Journal of Cellular Physiology* **111**, 275-283
- Mitchison, J.M. & Creanor, J.** (1971) Further measurements of DNA synthesis and enzyme potential during cell cycle of fission yeast *Schizosaccharomyces pombe*. *Experimental Cell Research* **69**, 244-247
- Molyneux, D.H. & Killick-Kendrick, R.** (1987) Morphology, ultrastructure and life-cycles. In: *The Leishmaniases in Biology and Medicine*. Peters, W. & Killick-Kendrick, R. (Editors) Academic Press, London 1, 121-176
- Moreno, S.N.J., Docampo, R. & Vercesi, A.E.** (1992) Calcium homeostasis in procyclic and bloodstream forms of *Trypanosoma brucei*. *Journal of Biological Chemistry* **267**(9), 6020-6026
- Morgan, D.O.** (1995) Principles of CDK regulation. *Nature* **374**, 131-134
- Mottram, J.C.** (1994) cdc2-related protein kinases and cell cycle control in trypanosomatids. *Parasitology Today* **10**(7), 253-257
- Mottram, J.C., Kinnaird, J.H., Shiels, B.R., Tait, A. & Barry, J.D.** (1993) A novel CDC2-related protein kinase from *Leishmania mexicana* LmmCRK1, is post-translationally regulated during the life cycle. *The Journal Of Biological Chemistry* **268** (28), 21044-21052

- Mottram, J.C. & Smith, G. (1995)** A family of trypanosome cdc2-related protein kinases. *Gene* **162**, 147-152
- Murray, A.W. & Kirschner, M.W. (1991)** What controls the cell cycle. *Scientific American*, **264**(3), 56-63
- Newton, A. & Ohta, N. (1990)** Regulation of the cell division cycle and differentiation in bacteria. *Annual Review of Microbiology* **44**, 689-719
- Nurse, P. (1990)** Universal control mechanism regulating onset of M-phase. *Nature* **344**, 503-508
- Nurse, P., Thuriaux, P. & Nasmyth, K. (1976)** Genetic control of the cell division cycle in the fission yeast *Schizosaccharomyces pombe*. *Molecular & General Genetics* **146**, 167-178
- Olsson, T., Bakheit, M., Edlund, C., Hojeberg, B., Van Der Meide, P.H. & Kristensson, K. (1991)** Bi-directional activating signals between *Trypanosoma brucei* and CD8⁺ T cells: a trypanosome-released factor triggers interferon- γ production that stimulates parasite growth. *European Journal of Immunology* **21**, 2447-2454
- Oppenheimer, F.R. (1985)** Biochemical peculiarities of trypanosomes, African and South American. *British Medical Bulletin* **41**(2), 130-136
- Orkin, S.H., Harosi, F.I. & Leder, P. (1975)** Differentiation in erythroleukemic cells and their somatic hybrids. *Proceedings of the National Academy of Sciences USA* **72**(1), 98-102
- Orrenius, S. & Bellomo, G. (1986)** In: *Calcium and Cell Function*. Cheung, W.Y. (Editor) Academic Press, New York **VI**, 185-207
- Paindavoine, P., Rolin, S., Van Assel, S., Geuskens, M., Jauniaux, J.C., Dinsart, C., Huet, G. & Pays, E. (1992)** A gene from the variant surface glycoprotein expression site encodes one of several transmembrane adenylate cyclases located on the flagellum of *Trypanosoma brucei*. *Molecular and Cellular Biology* **12**, 1218-1225

- Parsons, J.A.** (1965) Mitochondrial incorporation of tritiated thymidine in *Tetrahymena pyriformis*. *Journal of Cell Biology* **25**, 641-646
- Parsons, J.A. & Rustad, R.C.** (1968) The distribution of DNA among dividing mitochondria of *Tetrahymena pyriformis*. *Journal of Cell Biology* **37**, 683-693
- Parsons, M., Valentine, M. & Carter, V.** (1993) Protein kinases in divergent eukaryotes: identification of protein kinase activities regulated during trypanosome development. *Proceedings of the National Academy of Sciences USA* **90**, 2656-2660
- Pays, E., Vanhamme, L. & Berberof, M.** (1994) Genetic controls for the expression of surface antigens in African trypanosomes. *Annual Review of Microbiology* **48**, 25-52
- Philosoph, H. & Zilberstein, D.** (1989) Regulation of intracellular calcium in promastigotes of the human protozoan parasite *Leishmania donovani*. *Journal of Biological Chemistry* **264**(18), 10420-10424
- Pimenta, P., Turco, S., McConville, M., Lawyer, P., Perkins, P. & Sacks, D.** (1992) Stage-specific adhesion of *Leishmania* promastigotes to the sandfly midgut. *Science* **256**, 1812-1815
- Pimenta, P.F.P., Pinto Da Silva, P., Rangarajan, D., Smith, D.F. & Sacks, D.L.** (1994) *Leishmania major*: Association of the differentially expressed Gene B protein and the surface lipophosphoglycan as revealed by membrane capping. *Experimental Parasitology* **79**, 468-479
- Prescott, D.M.** (1976) *Reproduction of Eukaryotic Cells*. Academic Press, London
- Puentas, S.M., Da Silva, R.P., Sacks, D.L., Hammer, C.H. & Joiner, K.A.** (1991) Serum resistance of metacyclic stage *Leishmania major* promastigotes is due to release of C5b-9. *Journal of Immunology* **145**, 4311-4316
- Ready, P.D. & Smith, D.F.** (1988) Peanut lectin agglutination and isolation of infective forms of *Leishmania major*. *Transactions of the Royal Society of Tropical Medicine and Hygiene* **82**, 418

- Robinson, D.R. & Gull, K.** (1991) Basal body movements as a mechanism for mitochondrial genome segregation in the trypanosome cell cycle. *Nature* **352**, 731-733
- Roditi, I., Schwartz, H., Pearson, T.W., Beecroft, R.P., Liu, M.K., Richardson, J.P., Burhing, H.J., Pleiss, J., Bulow, R., Williams, R.O. & Overath, P.** (1989) Procyclin gene expression and loss of the variant surface glycoprotein during the differentiation of *Trypanosoma brucei*. *Journal of Cell Biology* **108**, 737-746
- Rolin, S., Paindavoine, P., Hanocq-Quertier, J., Hanocq, F., Claes, Y., Le Ray, D., Overath, P. & Pays, E.** (1993) Transient adenylate cyclase activation accompanies differentiation of *Trypanosoma brucei* from bloodstream to procyclic forms. *Molecular and Biochemical Parasitology* **61**, 115-126
- Ross, D.T., Raibaud, A., Florent, I.C., Sather, S., Gross, M.K., Storm, D.R. & Eisen, H.** (1991) The trypanosome VSG expression site encodes adenylate cyclase and a leucine-rich putative regulatory gene. *EMBO Journal* **10**, 2047-2057
- Russell, P.J.** (1992) Extensions of Mendelian genetic analysis. In: *Genetics* 3rd Edition Harper Collins, New York
- Russell, D. G., Xu, S. & Chakraborty, P.** (1992) Intracellular trafficking and the parasitophorous vacuole of *Leishmania mexicana*-infected macrophages. *Journal of Cell Science* **103**, 1193-1210
- Sacks, D.L.** (1989) Metacyclogenesis in *Leishmania* promastigotes. *Experimental Parasitology* **69**, 100-103
- Sacks, D.L.** (1992) The structure and function of the surface lipophosphoglycan on different developmental stages of *Leishmania* promastigotes. *Infectious Agents and Disease* **1**, 200-206
- Sacks, D.L. & Perkins, P.V.** (1984) Identification of an infective stage of *Leishmania* promastigotes. *Science* **223**, 1417-1419
- Sacks, D.L. & Perkins, P.** (1985) Development of infective stage *Leishmania* promastigotes within phlebotomine sandflies. *American Journal of Tropical Medicine and Hygiene* **34**, 456-459

- Sacks, D.L., Hieny, S. & Sher, A. (1985) Identification of cell surface carbohydrate and antigenic changes between non-infective and infective developmental stages of *Leishmania major* promastigotes. *Journal of Immunology* **135**, 456-459
- Sacks, D.L. & Da Silva, R. (1987) The generation of infective stage *Leishmania major* promastigotes is associated with the cell-surface expression and release of a developmentally regulated glycolipid. *Journal of Immunology* **139**, 3099-3106
- Saraiva, E.M.B., Pimenta, P.F.P., Brodin, T.N., Rowton, E., Modi, G.B. & Sacks, D.L. (in press) Changes in lipophosphoglycan and gene expression associated with the development of *Leishmania major* in *Phlebotomus papatasi*.
- Schell, D., Evers, R., Preis, D., Ziegelbauer, K., Kiefer, H., Lottspeich, F., Cornelissen, A.W.C.A. & Overath, P. (1991) A transferrin-binding protein of *Trypanosoma brucei* is encoded by one of the genes in the variant surface glycoprotein gene expression site. *EMBO Journal* **10**(5), 1061-1066
- Schlein, Y., Jacobson, R.L. & Shlomai, J. (1991) Chitinase secreted by *Leishmania* functions in the sandfly vector. *Proceedings of the Royal Society of London B* **245**, 121-126
- Schlein, Y., Jacobson, R.L. & Messer, G. (1992) *Leishmania* infections damage the feeding mechanism of the sandfly vector and implement parasite transmission by bite. *Proceedings of the National Academy of Sciences USA* **89**, 9944-9948
- Schlein, Y. & Jacobson, R.L. (1994) Haemoglobin inhibits the development of infective promastigotes and chitinase secretion in *Leishmania major* cultures. *Parasitology* **109**, 23-28
- Schmidt, G.D. & Roberts, L.S. (1989) Order Kinetoplastida: Trypanosomes and their kin. In: *Foundations of Parasitology* Times Mirror/Mosby, St. Louis (4th Edition), 55-80
- Schneider, P., Rosat, J.-P., Bouvier, J., Louis, J. & Bordier, C. (1992) *Leishmania major*: differential regulation of the surface metalloprotease in amastigote and promastigote stages. *Experimental Parasitology* **75**, 196-206

- Shapiro, S. Z., Naessens, J., Liesegang, B., Moloo, S. K., Magondou, J. (1984) Analysis by flow cytometry of DNA synthesis during the life-cycle of African trypanosomes. *Acta Tropica* **41**, 313-323
- Sher, A. & Snary, D. (1982) Specific inhibition of the morphogenesis of *Trypanosoma cruzi* by a monoclonal antibody. *Nature* **300**, 639-640
- Sherwin, T., Schneider, A., Sasse, R., Seebeck, T. & Gull, K. (1987) Distinct localization and cell cycle dependence of COOH terminally tyrosinolated α -tubulin in the microtubules of *Trypanosoma brucei brucei*. *Journal of Cell Biology* **104**, 439-446
- Sherwin, T. & Gull, K. (1989) The cell division cycle of *Trypanosoma brucei brucei*: timing of event markers and cytoskeletal modulations. *Philosophical Transactions of the Royal Society of London B* **323**, 573-588
- Shiels, B.R., Smyth, A., Dickson, J., McKellar, S., Tetley, L., Fujisaki, K., Hutchison, B. & Kinnaird, J.H. (1994) A stoichiometric model of stage differentiation in the protozoan parasite *Theileria annulata*. *Molecular and Cellular Differentiation* **2**(2), 101-125
- Simpson, L. (1968) The leishmania-leptomonad transformation of *Leishmania donovani*: nutritional requirements, respiration changes and antigenic changes. *Journal of Protozoology* **15**, 201-207
- Simpson, L. (1972) The kinetoplast of the hemoflagellates. *International Review of Cytology* **32**, 139-207
- Simpson, L. & Braly, P. (1970) Synchronization of *Leishmania tarentolae* by hydroxyurea. *Journal of Protozoology* **17**(4), 511-517
- Smith, D.F., Ready, P.D., Coulson, R.M.R., Searle, S. & Campos, A.J.R. (1988) Gene expression in the infective promastigotes of *Leishmania major*. In: *NATO-ASI Monograph on Leishmaniasis* Hart, D.T. (Editor) Plenum Press, New York **163**, 567-580

- Smith, D.F. & Ready, P.D. (1989) Gene expression in the infective promastigotes of *Leishmania major*. In: *Leishmaniasis: The current status and new strategies for control*. Hart, D.T. (Editor) NATO 563-573
- Snedecor, G.W. & Cochran, W.G. (1967) *Statistical Methods* (6th Edition) Iowa State University Press, Ames IA
- Stanners, C.P. & Till, J.E. (1960) DNA synthesis in individual L-strain mouse cells. *Biochimica et Biophysica Acta* 37, 406-419
- Steel, G. G. (1986) Autoradiographic analysis of the cell cycle: Howard and Pelc to the present day. *International Journal of Radiation Biology* 49(2), 227-235
- Steinert, M. & Steinert, G. (1962) La synthese de l'acide desoxyribonucleique au cours du cycle de division de *Trypanosoma mega*. *Journal of Protozoology* 9(2), 203-211
- Sternberg, J.M. & McGuigan, F. (1994) *Trypanosoma brucei*: Mammalian epidermal growth factor promotes the growth of the African trypanosome bloodstream form. *Experimental Parasitology* 78, 422-424
- Tarella, C., Ferrero, D., Gallo, E., Pagliardi, G. L. & Ruscetti, F.W. (1982) Induction of differentiation of HL-60 cells by dimethyl sulfoxide: evidence of a stochastic model not linked to the cell division cycle. *Cancer Research* 42, 445-449
- Taylor, D.R. & Williams, G.T. (1988) *Leishmania mexicana amazonensis*: ADP-ribosyltransferase antagonists specifically inhibit amastigote to promastigote differentiation. *Experimental Parasitology* 66, 189-196
- Tetley, L., Turner, C.M.R., Barry, J.D., Crowe, J.S. & Vickerman, K. (1987) Onset of expression of the variant surface glycoproteins of *Trypanosoma brucei* in the tsetse fly using immunoelectron microscopy. *Journal of Cell Science* 87, 363-372
- Tournier, F. & Bornens, M. (1994) Cell cycle regulation of centrosome function. In: *Microtubules*. Hyams, J.S. & Lloyd, C.W. (Editors) Wiley-Liss, New York 303-324

- Turco, S.J.** (1995) Surface constituents of kinetoplastid parasites. In: *Biochemistry and Molecular Biology of Parasites*. Marr, J.J. & Muller (Editors) Academic Press, London chapter 11, 177-202
- Turner, C.M.R.** (1990) The use of experimental artefacts in African Trypanosome research. *Parasitology Today* 6(1), 14-17
- Turner, C.M.R.** (1992a) Antigenic variation in parasitic protozoa. In: *Recombinant DNA vaccines: Rationale and Strategy*. Isaacson, R.E. (Editor) Marcel Dekker, New York, 115-146
- Turner, C.M.R.** (1992b) Cell cycle co-ordination in trypanosomes. *Parasitology Today* 8(1), 3-4
- Turner, C.M.R., Barry, J.D., Maudlin, I. & Vickerman, K.** (1988) An estimate of the size of the metacyclic variable antigen repertoire of *Trypanosoma brucei rhodesiense*. *Parasitology* 97, 269-276
- Turner, C.M.R. & Barry, J.D.** (1989) High frequency of antigenic variation in *Trypanosoma brucei rhodesiense* infections. *Parasitology* 99, 67-75
- Turner, C.M.R., Aslam, N. & Dye, C.** (1995) Replication, differentiation, growth and the virulence of *Trypanosoma brucei* infections. *Parasitology* 111, 289-300
- Turner, C.M.R., Aslam, N. & Angus, S.D.** (1996) Inhibition of growth of *Trypanosoma brucei* parasites in chronic infections. *Parasitology Research* 82, 61-66
- Vaessin, H., Grell, E., Wolff, E., Bier, E., Jan, L.Y. & Jan, Y.N.** (1991) *prospero* is expressed in neuronal precursors and encodes a nuclear protein that is involved in the control of axonal outgrowth in *Drosophila*. *Cell* 67, 941-953
- Van Assel, S. & Steinert, M.** (1971) Nuclear and kinetoplastic DNA replication cycles in normal and synchronously dividing *Crithidia luciliae*. *Experimental Cell Research* 65, 353-358
- Van Meirvenne, N., Janssens, P.G. & Magnus, E.** (1975) Antigenic variation in syringe passaged populations of *Trypanosoma (Trypanozoon) brucei*. Rationalization

of the experimental approach. *Annales de la Societe belge de Medicine tropicale* **55**, 1-23

Vickerman, K. (1985) Developmental cycles and biology of pathogenic trypanosomes. *British Medical Bulletin* **41**(2), 105-114

Vickerman, K. (1989) Trypanosome sociology and antigenic variation. *Parasitology* **99**, S37-S47

Vickerman, K. & Preston, T.M. (1976) Comparative cell biology of the kinetoplastid flagellates. In: *Biology of the Kinetoplastida*. Lumsden, W.H.R. & Evans, D.A. (Editors) Academic Press, London **1**, 35-130

Vickerman, K., Myler, P.J. & Stuart, K.D. (1991) African Trypanosomiasis. In: *Immunology and Molecular Biology of Parasitic Infections* Warren, K.S. (Editor) Blackwell Scientific Publications, Oxford (3rd Edition) 170-212

Walters, L.L. (1993) *Leishmania* differentiation in natural and unnatural sand fly hosts. *Journal of Eukaryotic Microbiology* **40**(2), 196-206

Walters, L.L., Modi, G.B., Tesh, R.B. & Burrage, T. (1987) Host-parasite relationship of *Leishmania mexicana mexicana* and *Lutzomyia abonnenci* (Diptera:Psychodidae). *American Journal of Tropical Medicine and Hygiene* **36**, 294-314

Walters, L.L., Modi, G.B., Chaplin, G.L., & Tesh, R.B. (1989) Ultrastructural development of *Leishmania chagasi* in its vector, *Lutzomyia longipalpis* (Diptera: Psychodidae). *American Journal of Tropical Medicine and Hygiene* **41**, 295-317

Webster, P. & Grab, D.J. (1988) Intracellular colocalization of variant surface glycoprotein and transferrin-gold in *Trypanosoma brucei*. *Journal of Cell Biology* **106**, 279-288

Williams, F.M. (1971) Dynamics of microbial populations. In: *Systems Analysis and Simulation Ecology*. Patten, B. (Editor) Academic Press, New York **1**, 247-262

- Williams, G.T.** (1983) *Trypanosoma cruzi*: inhibition by ADP-ribosyl transferase antagonists of intracellular and extracellular differentiation. *Experimental Parasitology* **56**, 409-415
- Williams, G.T.** (1984) Specific inhibition of the differentiation of *Trypanosoma cruzi*. *Journal of Cell Biology* **99**, 79-82
- Williams, G.T.** (1985) Control of differentiation in *Trypanosoma cruzi*. *Current Topics in Microbiology and Immunology* **117**, 1-22
- Williams, G.T. & Johnstone, A.P.** (1983) ADP-ribosyltransferase, rearrangement of DNA and cell differentiation. *Bioscience Reports* **3**, 815-830
- Williamson, K., Halliday, I., Hamilton, P., Ruddell, J., Varma, M., Maxwell, P., Crockard, A. & Rowlands, B.** (1993) *In vitro* BrdUrd incorporation of colorectal tumour tissue. *Cell Proliferation* **26**, 115-124
- Wolpert, L.** (1988) Stem cells: a problem with asymmetry. *Journal of Cell Science* Suppl. **10**, 1-9
- Woodward, R. & Gull, K.** (1990) Timing of nuclear and kinetoplast DNA replication and early morphological events in the cell cycle of *Trypanosoma brucei*. *Journal of Cell Science* **95**, 49-57
- World Health Organisation** (1986) Epidemiology and control of African trypanosomiasis. *Report of a WHO Expert Committee, Technical Report Series* **739**, 1-125
- Ziegelbauer, K., Quinten, M., Schwartz, H., Pearson, T.W. & Overath, P.** (1990) Synchronous differentiation of *Trypanosoma brucei* bloodstream forms to procyclic forms *in vitro*. *European Journal of Biochemistry* **192**, 373-378
- Ziegelbauer, K., Stahl, B., Karas, M., Steirhof, Y.-D. & Overath, P.** (1993) Proteolytic release of cell surface proteins during differentiation of *Trypanosoma brucei*. *Biochemistry* **32**, 3737-3742
- Zilberstein, D. & Shapira, M.** (1994) The role of pH and the temperature in the development of *Leishmania* parasites. *Annual Review of Microbiology* **48**, 449-470

Zoeller, R.A. & Raetz, C.R.H. (1992) Strategies for isolating somatic cell mutants defective in lipid biosynthesis. *Methods in Enzymology* **209**, 34-51